

CRANFIELD UNIVERSITY

JOANA MANUEL SILVA DIAS

THE IMPACT OF CARRIER MEDIA PHYSICAL PROPERTIES ON  
MOVING ATTACHED GROWTH SYSTEMS

School of Water, Environment and Energy  
Research Degree

PhD  
Academic Year: 2014 - 2018

Supervisor: Dr Ana Soares and Prof Tom Stephenson  
February 2018

CRANFIELD UNIVERSITY

School of Water, Environment and Energy  
Research Degree

PhD

Academic Year 2014- 2018

JOANA MANUEL SILVA DIAS

The impact of carrier media physical properties on moving attached  
growth systems

Supervisor: Dr Ana Soares and Prof Tom Stephenson  
February 2018

This thesis is submitted in partial fulfilment of the requirements for  
the degree of PhD

© Cranfield University 2018. All rights reserved. No part of this  
publication may be reproduced without the written permission of the  
copyright owner.

## ABSTRACT

Moving attached growth processes are commonly used for the effective removal of organic pollutants and nitrogen in wastewater treatment plants. In these processes, biofilm grows attached to plastic media. Moving attached growth systems, such as submerged aerated filters (SAF), moving bed biofilm reactors (MBBR) and integrated fixed film activated sludge (IFAS), are traditionally designed and operated based on the carrier media protected surface area (PSA). Therefore, much attention has been given to maximising carrier PSA, neglecting other carrier media physical properties, such as geometry, size, shape and voidage.

This thesis investigated the influence of carrier media physical properties on moving attached growth systems, contributing to improved reactor performance. A pilot plant treating municipal wastewater was operated with five media that varied in shape (cylindrical and spherical), size, voidage and protected surface area ( $112\text{-}610\text{ m}^2/\text{m}^3$ ). Hydrodynamic and aeration tests revealed that carrier media enhanced the overall oxygen transfer and hydraulic efficiency (HE) by 23-45% and 41-53%, respectively. A weak correlation was identified between these parameters and carrier media PSA, the variable traditionally selected to design biofilm processes. However strong correlations were identified when considering a combination of carrier media physical parameters; specifically, dimensionality ( $D_i$ ) and voidage ( $V_{oi}$ ) ( $R^2= 0.88\text{-}0.92$ ). When the pilot plant was operated under the same organic ( $7.52\pm 0.81\text{ g COD}/\text{m}^2\cdot\text{day}$ ) and ammonia loading rates ( $0.94\pm 0.10\text{ g NH}_4^+\text{-N}/\text{m}^2\cdot\text{day}$ ), start-up studies indicated that spherical and lower PSA ( $112\text{-}220\text{ m}^2/\text{m}^3$ ) carrier media achieved faster biofilm formation rates and shorter start-up periods (15-30 days) compared with cylindrical and higher PSA ( $348\text{-}610\text{ m}^2/\text{m}^3$ ) carrier media (23-47 days). During steady state, obtainable COD removal and ammonia removal was  $87\pm 1.4$  and  $74\pm 6.1\%$  with spherical media and  $85.5\pm 0.5$  and  $38\pm 5.0\%$  with cylindrical shape media. Heterotrophic and nitrifiers' activity tests demonstrated that spherical media presented the highest organic removals ( $19.2\text{-}34.8\text{ mg sCOD}/\text{g TS}\cdot\text{h}$ ) while smaller spherical shape media achieved the highest nitrification removals ( $5.2\text{-}7.2\text{ mg NH}_4^+\text{-N}/\text{g}$

TS.h) compared to cylindrical shape media (13.4 mg sCOD/g TS.h and 4.9-5.2 mg NH<sub>4</sub><sup>+</sup>-N/g TS.h). Strong correlations were achieved between biofilm formation rates, maximum COD utilisation rate and ammonia removal rate and the association of parameters (Di x Voi)/HE (R<sup>2</sup>= 0.92-0.95).

Studies on boundary layer thickness (geometry) and external mass transfer helped with the interpretation of these results. The mass transfer boundary layer (MTBL) thickness values were smaller in the spherical media and high voidage media (low PSA) (71.4, 15.5 µm) in comparison with cylindrical media and low voidage media (high PSA) (122.9 µm). Hence, media voidage and shape impacted on MTLB and played a role in reducing mass transfer limitations. Media with high PSA was greatly affected by mass transfer limitations. Poor correlation was observed between PSA and MTBL thickness (R<sup>2</sup>= 0.27) and stronger correlations were verified with the combination of parameters: (Di x Voi)/HE (R<sup>2</sup>= 0.86). This thesis showed that the traditional indicator used to design and model biofilm processes, PSA, was insufficient to explain the behaviour of moving attached growth systems. Media physical parameters (such as shape, Di and Voi) should be considered when evaluating existing process hydraulic efficiency, oxygen mass transfer, start-up, performance, modelling as well as during the development of new carrier media and design of biofilm processes.

**Keywords:**

Biofilm, biofilm formation rate, biofilm thickness, biofilm activity, boundary layer thickness, carrier media, dimensionality, hydraulic efficiency, moving attached growth systems, oxygen transfer efficiency, protected surface area, start-up, voidage.

## **ACKNOWLEDGEMENTS**

Now that I am at the end of this long journey, I can finally thank the people who made this PhD possible.

First, I would like to express my special gratitude to Dr Ana Soares, my main supervisor, for the opportunity, knowledgeable guidance and constructive suggestions. I really appreciated your enthusiasm, trust and confidence in me and my capabilities; your help during this PhD has been precious.

I am very grateful to Prof. Tom Stephenson, my second supervisor, for his support, trust and expert contributions.

To my sponsor Warden Biomedica; more specifically Mel Bellingham, Junaid Hassan and Mark Barrett, I am much appreciative of the opportunity to conduct this work, your encouragement and support throughout these past four years. Thank you for your interest during our meetings, conferences and also the good laughs and enjoyable lunches; I really felt part of Warden Biomedica family.

I thank my colleagues at Cranfield Water Science Institute for all your kindness and support in the office.

I want to thank Kanming Wang, my pilot plant neighbour and good friend, who was of vital importance during my daily work at the pilot plant and lab. For all the heavy winters, hot “summers” and the happy moments we have shared; and all our research discussions.

Thanks to Anjani Parsotamo and Luciano Biasi for the great help in the laboratory. Thanks to Nigel Janes, the pilot plant guardian, for always being there taking care of our “babies”.

Thank you to my friends Judith, Edwina, Eleanor and André, for all your emotional support, patience, many laughs and tears, and endless research conversations. To Carlos, for his good laughs, Brazilian conversations and Python expertise. I will be forever grateful to every single one of you.

To Eleanor, André, Drew and Edwina, I will always be thankful for all your help and support, especially with proof-reading and last-minute corrections. Thanks to Sonita and Sabrina for the good laughs and endless coffees.

My final thank goes to my family. Muito obrigada mãezinha por todo o apoio que me deste ao longo deste tempo, por estares sempre ao meu lado nos bons e maus momentos e, acima de tudo, por acreditares em mim. Agradeço também ao meu pai, irmã, cunhado, tio Lando e Gi por estarem sempre disponíveis para me apoiarem e ajudarem nesta etapa da minha vida. Um xi muito especial à minha sobrinha do coração Margarida, ao meu primo Gil e à Alice por trazerem fantasia e alegria ao meu dia a dia. Agradeço ainda aos meus amigos de longa data, Vaninha, Catia, Juliana, Daniela e Filipe por estarem presentes nesta minha jornada.

# TABLE OF CONTENTS

ABSTRACT .....	i
ACKNOWLEDGEMENTS.....	iii
LIST OF FIGURES.....	viii
LIST OF TABLES .....	xi
Chapters.....	xi
Appendices.....	xii
LIST OF EQUATIONS.....	xiii
Chapter .....	xiii
Appendices.....	xiv
LIST OF ABBREVIATIONS .....	xv
1 INTRODUCTION.....	1
1.1 Background.....	1
1.2 Aim and objectives.....	3
1.3 Thesis plan .....	3
1.4 References .....	2
2 CARRIER MEDIA PROPERTIES IN A MOVING ATTACHED GROWTH SYSTEM– A REVIEW .....	5
2.1 Introduction .....	6
2.1.1 Type and properties of the support material.....	8
2.1.2 Carrier surface properties.....	16
2.2 Discussion .....	34
2.3 Conclusions .....	36
2.4 References .....	37
3 IMPACT OF CARRIER MEDIA ON OXYGEN TRANSFER AND WASTEWATER HYDRODYNAMICS ON A MOVING ATTACHED GROWTH SYSTEM.....	51
3.1 Introduction .....	52
3.2 Material and methods .....	55
3.2.1 Experimental setup.....	55
3.2.2 Tracer studies .....	56
3.2.3 Clean water oxygen mass transfer tests .....	58
3.2.4 Oxygen mass transfer and hydrodynamic behaviour under operational conditions .....	60
3.3 Results and discussion .....	61
3.3.1 Hydrodynamic behaviour without biofilm growth .....	61
3.3.2 Hydrodynamic behaviour under operational conditions (with biofilm growth) .....	64
3.3.3 Clean water oxygen mass transfer .....	66
3.3.4 Oxygen mass transfer under operational conditions (with biofilm growth) .....	68

3.3.5 Influence of media physical properties on hydrodynamics and oxygen mass transfer.....	69
3.4 Conclusions .....	74
3.5 References .....	75
4 INFLUENCE OF CARRIER MEDIA PHYSICAL PROPERTIES ON START-UP OF MOVING ATTACHED GROWTH SYSTEMS .....	83
4.1 Introduction .....	84
4.2 Material and methods .....	86
4.2.1 Pilot plant setup and operation conditions.....	86
4.2.2 Analytical methods .....	87
4.3 Results and discussion .....	89
4.3.1 Performance of moving attached growth system during start-up .....	89
4.3.2 Biofilm formation and start-up .....	92
4.4 Influence of the media physical properties on start-up duration.....	98
4.5 Conclusions .....	101
4.6 References .....	102
5 IMPACT OF CARRIER MEDIA PHYSICAL PROPERTIES ON THE PERFORMANCE OF MOVING ATTACHED GROWTH SYSTEMS .....	107
5.1 Introduction .....	108
5.2 Material and methods .....	110
5.2.1 Pilot plant setup and operation conditions.....	110
5.2.2 Attached biofilm.....	113
5.2.3 Biofilm activity tests .....	114
5.2.4 Analytical methods .....	115
5.3 Results and discussion .....	115
5.3.1 Biofilm accumulation .....	115
5.3.2 COD and ammonia removal performance.....	116
5.3.3 Biofilm activity tests .....	121
5.3.4 Physical carrier media properties and operation performance .....	123
5.4 Conclusions .....	126
5.5 References .....	127
6 IMPACT OF CARRIER MEDIA PHYSICAL PROPERTIES ON BOUNDARY LAYER THICKNESS AND EXTERNAL MASS TRANSFER ON MOVING ATTACHED GROWTH SYSTEMS.....	135
6.1 Introduction .....	136
6.2 Material and methods .....	138
6.2.1 Lab scale reactor configuration and experimental process .....	138
6.2.2 Determination of the external mass transfer.....	140
6.2.3 Analytical methods .....	142
6.3 Results and discussion .....	142
6.3.1 Attached biofilm and thickness .....	142
6.3.2 External mass transfer .....	143



6.3.3 Physical carrier media properties and MTBL thickness.....	150
6.4 Conclusions .....	152
6.5 References .....	153
7 DISCUSSION .....	157
7.1 The effect of carrier media on oxygen mass transfer and wastewater hydrodynamics.....	158
7.2 Influence of carrier media on start-up .....	158
7.3 Effect of carrier media on process performance .....	159
7.4 Boundary layer thickness, external mass transfer and carrier media....	160
7.5 Impact of media physical properties on moving attached growth systems.....	161
7.6 Contribution to knowledge .....	166
7.7 References .....	171
8 CONCLUSIONS .....	175
9 FUTURE WORK.....	179
<b>APPENDICES</b> .....	180
Appendix A Correlation between SOTE and HE (with and without biofilm growth) with different carrier media physical properties.....	180
Appendix B Correlation between rate of biofilm with different carrier media physical properties during COD and ammonia removal start-up.....	183
Appendix C Correlation between $U_m$ and ammonia removal rate with different carrier media physical properties. ....	185
Appendix D Correlation between MTBL thickness and media physical properties.....	187

## LIST OF FIGURES

Figure 1-1 PhD thesis structure and interaction between chapters. ....	1
Figure 2-1 Schematic representation of the factors influencing moving attached growth systems performance efficiency.....	7
Figure 2-2 Relation between SFE of adhesion $\Delta G_{\text{wi}}$ (open circles, $R^2= 0.83$ ) and zeta potential (filled circles, $R^2= 0.96$ ) alongside with attached biofilm (Teixeira and Oliveira, 1999) (a) relation between SFE and attached biofilm ( $R^2= 0.88$ ) (Khan et al., 2013) (b). ....	20
Figure 2-3 Biofilm attached against adhesion forces for the different plastic supports, ( $R^2= 0.12$ ) (Stephenson et al., 2013) (a) and ( $R^2=0.09$ ) (Rodriguez, 2012) (b).....	21
Figure 2-4 Biofilm attached against COD removal rates for the different plastic supports $R^2= 0.39$ .....	22
Figure 2-5 Biofilm attached against nitrification removal rates for the different plastic supports, ( $R^2= 0.05$ ) (Stephenson et al., 2013) (a) and ( $R^2= 0.05$ ) (Rodriguez, 2012)(b). ....	22
Figure 2-6 Nitrification removal rates against SFE ( $R^2= 0.96$ ) (a) and against biofilm attached ( $R^2= 0.91$ ) (b) for the different plastic supports (Khan et al., 2013). ....	23
Figure 2-7 Relation between biofilm attached (a) and contact angle (b) with ammonia removal rate of different support material ( $\circ$ Khan et al., 2013 $\bullet$ Rodriguez et al., 2013). ....	24
Figure 2-8 Specific nitrification activity ( $\text{mg NH}_4^+\text{-N/g TS.h}$ ) ( $\circ$ Khan et al., 2013 $\bullet$ Rodriguez et al., 2013). ....	24
Figure 2-9 Ratio between plastic carrier length and diameter with PSA (a) and biofilm surface area reduction with increased biofilm thickness (b) (Goode, 2010). ....	29
Figure 3-1 Schematic side view of the pilot-plant used to study hydrodynamic behaviour and aeration efficiency of 5 carrier media. ....	56
Figure 3-2 $k_La$ (a) and SOTE (%/m) (b) measurements in clean water and with 5 different media at three air flow velocities. Media 1 (Biofil), Media 2 (Bioball), Media 3 (Biomarble), Media 4 (Biopipe) and Media 5 (Biotube). Media was supplied by Warden Biomedica ( <a href="http://www.wardenbiomedica.com/">http://www.wardenbiomedica.com/</a> ). ....	67
Figure 3-3 Correlation between hydraulic efficiency (a) and SOTE (%/m) (b) with the media protected surface area ( $\text{m}^2/\text{m}^3$ ). Media 1 (Biofil), Media 2 (Bioball), Media 3 (Biomarble), Media 4 (Biopipe) and Media 5 (Biotube). Media was supplied by Warden Biomedica ( <a href="http://www.wardenbiomedica.com/">http://www.wardenbiomedica.com/</a> ). ....	70

Figure 3-4 Correlation between hydraulic efficiency and $D_i \times V_{oi}$ (a) and correlation between SOTE (%/m) and hydraulic efficiency (b) without biofilm growth. Media 1 (Biofil), Media 2 (Bioball), Media 3 (Biomarble), Media 4 (Biopipe) and Media 5 (Biotube). Media was supplied by Warden Biomedica ( <a href="http://www.wardenbiomedica.com/">http://www.wardenbiomedica.com/</a> ). .....	72
Figure 3-5 Correlation between hydraulic efficiency (a) and $\alpha$ SOTE (b) with biofilm developed on the carrier at steady state. Media 1 (Biofil), Media 2 (Bioball), Media 3 (Biomarble), Media 4 (Biopipe) and Media 5 (Biotube). Media was supplied by Warden Biomedica ( <a href="http://www.wardenbiomedica.com/">http://www.wardenbiomedica.com/</a> ). .....	73
Figure 4-1 Schematic of the moving attached growth pilot plant and schematic representation of media used during the study. ....	87
Figure 4-2 Removal efficiencies for obtainable COD (a) and ammonia (b) during start-up during operation with Media 1, 2, 3, 4 and 5, respectively. ....	91
Figure 4-3 Biofilm attachment during 60 days of operation in Cell 1 (COD removal) (a) and fitting of a trendline to calculate the slope corresponding to the biofilm formation rate (b) during start-up. ....	93
Figure 4-4 Biofilm attached during the 60 days of operation in Cell 3 (ammonia removal) (a) and fitting of a trendline to calculate the slope corresponding to the biofilm formation rate (b) during start-up. ....	94
Figure 4-5 Biofilm thickness during 60 days of operation Cell 1 (a) and Cell 3 (b). .....	95
Figure 4-6 Images captured during OCT measurements on different media. ....	96
Figure 4-7 Total EPS values registered in Cell 1 (a) and Cell 3 (b) during 60 days of operation. ....	97
Figure 4-8 Biofilm yield (a) and biofilm detachment rate (b) calculated for the five media during COD start-up. ....	98
Figure 4-9 The correlation between rate of biofilm formation and protected surface area (a) and combination of parameters ( $D_i \times V_{oi}$ )/HE (b) during COD (-) and ammonia removal start-up (--). ....	99
Figure 5-1 Schematic representation of the moving attached growth system pilot plant. ....	111
Figure 5-2 Obtainable removal COD (a) and ammonia removal (b) as a function of loading rates for the five media studied. ....	118
Figure 5-3 Correlation between $U_m$ and protected surface area (a) and the combination of parameters ( $D_i \times V_{oi}$ )/HE (b). ....	124
Figure 5-4 Correlation between ammonia removal rate and protected surface area (a) and the combination of parameters ( $D_i \times V_{oi}$ )/HE (b). ....	125

Figure 6-1 Schematic of lab scale reactor and media studied (a) cylindrical, dimensionality 4.27 media on the lab scale reactor (b).....	139
Figure 6-2 Biofilm attached to the carrier media: spherical, dimensionality 2.68 (left), spherical, dimensionality 2.78 (centre) and cylindrical, dimensionality 4.27 (right). .....	143
Figure 6-3 Soluble COD removed at different mixing intensities (L/L.min) for spherical, dimensionality 2.68 (a), spherical, dimensionality 2.78 (b) and cylindrical, dimensionality 4.27 (c) as a function of time. ....	144
Figure 6-4 Soluble COD removal rates at different mixing intensities. ....	146
Figure 6-5 External mass transfer coefficients for spherical, dimensionality 2.68, spherical, dimensionality 2.78 and cylindrical, dimensionality 4.27 media. ....	147
Figure 6-6 MTBL thickness as a function of mixing intensity obtained in the different media tested (a) and comparison between MTBL thickness at different energy dissipation rates identified in this study and in Nogueira et al. (2015) (b). ....	149
Figure 6-7 Correlation between MTBL thickness and protected surface area (a) and combination of parameters $(D_i \times V_{oi})/HE$ (b) at 0.21 L/L.min.....	150
Figure 7-1 Schematic representation of the PhD main results. ....	165

# LIST OF TABLES

## Chapters

Table 2-1 Information on typical biofilm carriers used in moving attached growth systems. ....	10
Table 2-2 Contact angle, SFE, zeta potential and roughness of common materials used to manufacture carrier media. ....	18
Table 3-1 Characteristics of the carrier media tests in the moving attached growth systems. Media 1 (Biofil), Media 2 (Bioball), Media 3 (Biomarble), Media 4 (Biopipe) and Media 5 (Biotube). Media was supplied by Warden Biomedia ( <a href="http://www.wardenbiomedia.com/">http://www.wardenbiomedia.com/</a> ). ....	56
Table 3-2 Summary of the hydraulic parameters determined based on two wastewater flow rates (4 m <sup>3</sup> /day and 9 m <sup>3</sup> /day). Media 1 (Biofil), Media 2 (Bioball), Media 3 (Biomarble), Media 4 (Biopipe) and Media 5 (Biotube). Media was supplied by Warden Biomedia ( <a href="http://www.wardenbiomedia.com/">http://www.wardenbiomedia.com/</a> ). ....	63
Table 3-3 Summary of the hydraulic parameters and aeration efficiency at operation conditions with biofilm attached. Media 1 (Biofil), Media 2 (Bioball), Media 3 (Biomarble), Media 4 (Biopipe) and Media 5 (Biotube). Media was supplied by Warden Biomedia ( <a href="http://www.wardenbiomedia.com/">http://www.wardenbiomedia.com/</a> ). ....	65
Table 4-1 Media characteristics used in this study. Media 1 (Biofil), Media 2 (Bioball), Media 3 (Biomarble), Media 4 (Biopipe) and Media 5 (Biotube). Media was supplied by Warden Biomedia ( <a href="http://www.wardenbiomedia.com/">http://www.wardenbiomedia.com/</a> ). ....	87
Table 4-2 Characterisation of the wastewater fed to the pilot plant operated with different media during start up. ....	90
Table 5-1 Characteristics of the carrier media tested: Media 1 (Biofil), Media 2 (Bioball), Media 3 (Biomarble), Media 4 (Biopipe) and Media 5 (Biotube). Media was supplied by Warden Biomedia ( <a href="http://www.wardenbiomedia.com/">http://www.wardenbiomedia.com/</a> ). ....	111
Table 5-2 Influent settled wastewater characterisation for different carrier media (average values measured after star-up until steady state). Media 1 (Biofil), Media 2 (Bioball), Media 3 (Biomarble), Media 4 (Biopipe) and Media 5 (Biotube). Media was supplied by Warden Biomedia ( <a href="http://www.wardenbiomedia.com/">http://www.wardenbiomedia.com/</a> ). ....	111
Table 5-3 Summary of the pilot plant temperature, DO, influent loadings and removals, for the 5 carrier media studied. Media 1 (Biofil), Media 2 (Bioball), Media 3 (Biomarble), Media 4 (Biopipe) and Media 5 (Biotube). Media was supplied by Warden Biomedia ( <a href="http://www.wardenbiomedia.com/">http://www.wardenbiomedia.com/</a> ). ....	117

Table 5-4 Specific organic and nitrification rates obtained during batch tests with the five carrier media studied.....	122
Table 6-1 Media characteristics and reactor operation conditions. Spherical, dimensionality 2.68 (Biofil), spherical, dimensionality 2.78 (Biomarble), cylindrical, dimensionality 4.27 (Biopipe). Media was supplied by Warden Biomedia ( <a href="http://www.wardenbiomedia.com/">http://www.wardenbiomedia.com/</a> ).....	140
Table 6-2 Soluble COD removal rates obtained at different mixing intensities for spherical, dimensionality 2.68, spherical, dimensionality 2.78 and cylindrical, dimensionality 4.27 media. ....	145
Table 7-1 Sensitivity analysis for spherical media with a $D_i \times V_{oi}$ of 2.4. ....	163
Table 7-2 Thesis contribution to the current state of knowledge. ....	167

## Appendices

Table A-1 Correlation between SOTE and HE (with and without biofilm growth) with different carrier media physical properties.....	180
Table B-1 Correlation between rate of biofilm with different carrier media physical properties during COD and ammonia removal start-up .....	183
Table C-1 Correlation between $U_m$ and ammonia removal rate with different carrier media physical properties.....	185
Table D-1 Correlation between MTBL thickness and physical properties. ....	187

# LIST OF EQUATIONS

## Chapter

(3-1).....	56
(3-2).....	57
(3-3).....	58
(3-4).....	58
(3-5).....	58
(3-6).....	58
(3-7).....	58
(3-8).....	58
(3-9).....	58
(3-10).....	59
(3-11).....	59
(3-12).....	59
(3-13).....	59
(3-14).....	59
(3-15).....	59
(3-16).....	60
(3-17).....	60
(3-18).....	60
(3-19).....	60
(3-20).....	69
(3-21).....	69
(3-22).....	72
(3-23).....	72
(3-24).....	72
(4-1).....	88
(4-2).....	89
(5-1).....	112

(5-2).....	112
(5-3).....	113
(6-1).....	141
(6-2).....	141
(6-3).....	141

## **Appendices**

(A-1) .....	181
(A-2) .....	181
(A-3) .....	181
(A-4) .....	181
(A-5) .....	181
(A-6) .....	181
(A-7) .....	181



## LIST OF ABBREVIATIONS

ABS	Acrylonitrile butadiene styrene
AOB	Ammonia oxidizing bacteria
ASP	Activated sludge plants
BOD	Biochemical oxygen demand
BOD <sub>5</sub>	Five-day biochemical oxygen demand
BSA	Bovine serum albumin
C/N	Carbon: nitrogen ratio
COD	Chemical oxygen demand
CPAM	Cationicpolyacrylamides
D	Diameter
Di	Dimensionality
DO	Dissolved oxygen
EPS	Extracellular polymeric substances
HDPE	High density polyethylene
HDPS	high density polystyrene
HE	Hydraulic efficiency
HRT	Hydraulic retention time
IFAS	Integrated fixed-film activated sludge
L	Length
L <sub>f</sub>	Biofilm thickness
MBBR	Moving bed biofilm reactor
MLSS	Mixed liquid suspended solids
MTBL	Mass transfer boundary layer thickness
NH <sub>4</sub> <sup>+</sup> -N	Ammonium-nitrogen
NO <sub>3</sub> <sup>-</sup> -N	Nitrate-nitrogen
NOB	nitrogen oxidizing bacteria
NPDES	National Pollutant Discharge Elimination System
OCT	Optical coherence tomography
OTE	Oxygen transfer efficiency
OUR	Oxygen utilization rates
PAC	Powdered activated carbon
PAO	Phosphorus accumulating microorganisms

PC	Polycarbonate
PCL	Polycaprolactone
pCOD	Particulate chemical oxygen demand
Pe	Peclet number
PE	Polyethylene
PEG	Poly(ethyleneglycol)
PET	Polyethylene terephthalate
PETG	Polyethylene Terephthalate Glycol
PEVA	Polyethylenvinylacetate
PMMA	Poly(methyl methacrylate)
PNA	Partial nitrification and anammox
POM	Polyoxymethylene
PP	Polypropylene
PQAS-10	Polyquaternium-10
PS	Polystyrene
PSA	Protected surface area
PTFE	Polytetrafluoroethylene
PVA	Polyvinyl alcohol
PVC	Polyvinyl chloride
PVDF	Poly(vinylidene fluoride)
RTD	Residence time distribution
SAE	Standard aeration efficiency
SAF	Submerged aerated filter
SAMs	Self-assembled monolayers
sBOD <sub>5</sub>	Soluble five-day biochemical oxygen demand
sCOD	Soluble chemical oxygen demand
SFE	Surface free energy
SLR	Surface area loading rate
SND	Simultaneous nitrification and denitrification
SOTE	Standard oxygen transfer efficiency
SOTR	Standard oxygen transfer rate
SS	Suspended solids
tCOD	Total chemical oxygen demand

TN	Total nitrogen
TP	Total phosphorus
TS	Total solids
TSA	Total surface area
TSS	Total suspended solids
UK	United Kingdom
US	United States
VLR	Volumetric loading rate
Voi	Voidage
VSS	volatile suspended solids
VTS	Volatile total solids
W	Width
WWTP	Wastewater Treatment Plant



# 1 INTRODUCTION

## 1.1 Background

The increasingly stringent discharge limits set by the European Union regulations (e.g. *Water Framework Directive 2000/60/EC* and *Urban Wastewater Treatment Directive 91/271/EC* (European Parliament. Council of the European Union, 1991, 2009)) have driven the installation of new and the retrofitting and upgrading of wastewater treatment plants (WWTPs). For more than two decades, moving attached growth systems have been increasingly used for the treatment of both municipal wastewater and complex industrial effluents as they provide a robust, reliable and cost effective treatment solution for the removal of organic matter and nitrogen in both secondary and tertiary applications (Daigger and Boltz, 2017).

Moving attached growth systems, such as submerged aerated filters (SAF), moving bed biofilm reactors (MBBR) and integrated fixed film activated sludge (IFAS) are biological attached growth systems that use media as a biofilm growth support material (WEF, 2011). The media is fully submerged in the wastewater promoting the attachment and growth of microorganisms (comprised of heterotrophic and autotrophic bacteria) that form an active biofilm promoting high biomass concentration allowing for a very compact system (Lewandowski and Boltz, 2011). The media is held in suspension and thoroughly mixed with the wastewater by the aeration system or mechanical mixing. Thus, in aerobic MBBRs sufficient air needs to be provided to meet bacterial oxygen requirements and keeping the media in suspension (McQuarrie and Boltz, 2011). This mode of operation enhances biofilm/bulk liquid mass transfer, reducing biofilm diffusion limitations and accelerates biochemical reactions, therefore improving treatment performance (Boltz and Daigger, 2010).

The high demand for moving attached growth systems has led to an increase in the number of carrier media manufacturers and a wide variety are currently on offer. Protected surface area (PSA), has been the main focus of carrier media development (Piculell, Welander and Joñsson, 2014). Hence, an increase in PSA is directly linked with an increased biofilm concentration, treatment capacity and

performance. Therefore, biofilm reactors' design and performance are commonly based on the carrier media protected surface area (Ødegaard, 2006).

The selection of appropriate material properties on the adhesion and growth of biofilm is also subject of considerable importance in moving attached growth systems. Different kind of media have been used, including plastic, polyurethane foam, woven, ceramic, glass, etc. and chemical modified polymer) (Deng et al., 2016; Eldyasti, Nakhla and Zhu, 2012). Among the commercial media, plastic has been selected as an excellent biofilm support media owing to its attractive attributes such as longevity, resistance to decay, hydrophobicity and low-surface energy (Chu and Wang, 2011). Therefore, polyethylene (PE), polypropylene (PP) and high-density polyethylene are commonly used as carrier media material (Mao et al., 2017).

To date, current studies fail to consider the influence of the carriers' physical properties (shape, size and voidage) on the biofilm community structure and activity, as well as mass transfer and process hydrodynamics, on the process performance. Although, knowledge and research on biofilm processes involving media carriers is extensive, most of the studies are focussed on reactor performance i.e. by varying organic and volumetric loadings, media filling ratios and aeration loadings, with little focus on the impact of carrier media physical properties. Nevertheless, carrier media physical properties can influence internal hydrodynamic conditions with an impact on oxygen and substrate mass transfer (Herrling et al., 2015) and biofilm dynamics including growth, thickness and detachment (Rusten et al., 2006) that can have a considerable effect on the overall process performance. Consequently, there is a need to improve the understanding of carrier media physical properties (shape, size and voidage) on moving attached growth systems, to assist in process design and optimisation, providing opportunities for capital and operational cost savings, thereby, making moving attached growth systems more competitive with alternative technologies. Thus, in this study one of the most commercially successful polymeric materials, PP, with the same density, are compared whilst varying other physical carrier media properties.

## **1.2 Aim and objectives**

This research aims to understand the key media physical properties (e.g.: geometry, surface area, voidage, shape, size, etc) that govern oxygen mass transfer, hydrodynamics, biofilm formation rates, biofilm mass transfer limitations and overall treatment efficiency in attached growth systems treating municipal wastewater.

The key project objectives are to:

1. Review scientific literature on the different carrier media designs used at full-scale, pilot-scale and lab-scale studies in moving attached growth systems. Identify the role of carrier shape, size and material surface physical and chemical properties on microorganisms' adhesion, growth and biofilm activity.
2. Identify the key carrier media physical properties that impact oxygen mass transfer and hydraulic efficiency in a moving attached growth system through an understanding of gas-liquid mass transfer, flow hydrodynamics and mixing characteristics with and without biofilm.
3. Understand how carrier media physical properties can accelerate bacteria adhesion and biofilm formation rates during wastewater treatment in a moving attached growth system and how they can also influence subsequent reactor performance towards delivering improved effluent quality.
4. Measure the influence of the carrier media physical properties on organic carbon removal and nitrification through the investigation of biofilm activity and substrate utilisation rates.
5. Measure the boundary layer thickness to understand the impact of carrier media with different physical properties on biofilm mass transfer limitations, further influencing substrate availability and removal.

## **1.3 Thesis plan**

The thesis is presented and organised as a series of papers for publication and divided into chapters addressing each objective. Figure 1-1 illustrates a flow

diagram of thesis structure. Each chapter was written by the first author Joana Manuel Silva Dias and supervisor's comments were provided by Dr Ana Soares and Prof Tom Stephenson.

Pilot plant design, and experimental work methodology was developed by the first author Joana Manuel Silva Dias supervised by Dr Ana Soares. Pilot-plant and lab-scale reactors were operated by Joana Manuel Silva Dias and the laboratory work was undertaken by Joana Manuel Silva Dias. Pilot plant operation and laboratory support was received in Chapter 4 and 6 from Anjani Parsotamo (placement student) under supervision of Joana Manuel Silva Dias.

Chapter 2 constitutes a literature review on the current knowledge of different types of carrier media (surface area, shape, size, voidage and physical and chemical surface properties) used in moving attached growth systems and linked with biofilm (attachment, viability and metabolic activity). Chapter 2 has been submitted to Environmental Technology Reviews.

Chapter 3 aims to complement the limited numbers of studies found in the literature on the impact of carrier media physical properties on: oxygen transfer efficiency, hydraulic flow patterns and mixing conditions in clean media and with biofilm attached. Results from this chapter were partially presented during the 9<sup>th</sup> European Waste Water Management Conference (2015), the 3<sup>rd</sup> IWA Specialized International Conference Ecotechnologies for Wastewater Treatment (ecoSTP) (2016) and the 10<sup>th</sup> International Conference on Biofilm Reactors (2017). Chapter 3 - *Dias, J., Stephenson, T., Bellingham, M., Hassan, J., Barrett, M. and Soares, A. (2018) 'Impact of carrier media on oxygen transfer and wastewater hydrodynamics on a moving attached growth system', Chemical Engineering Journal, 351, pp. 399–408. Published in Chemical Engineering Journal.*

Chapter 4 describes the influence of carrier media physical properties on start-up of moving attached growth systems. It therefore provides a better understanding on how physical properties can increase biofilm formation ability and accelerated start-up enabling faster commissioning periods and treatment robustness during steady state. The outcomes of this paper can provide guidance for design and start-up of full-scale moving attached growth systems. Chapter 4 - *Dias, J.,*



*Bellingham, M., Hassan, J., Barrett, M., Stephenson, T. and Soares, A. (2018) 'Influence of carrier media physical properties on start-up of moving attached growth systems', Bioresource Technology, 266, pp. 463–471. Published in Bioresource Technology.*

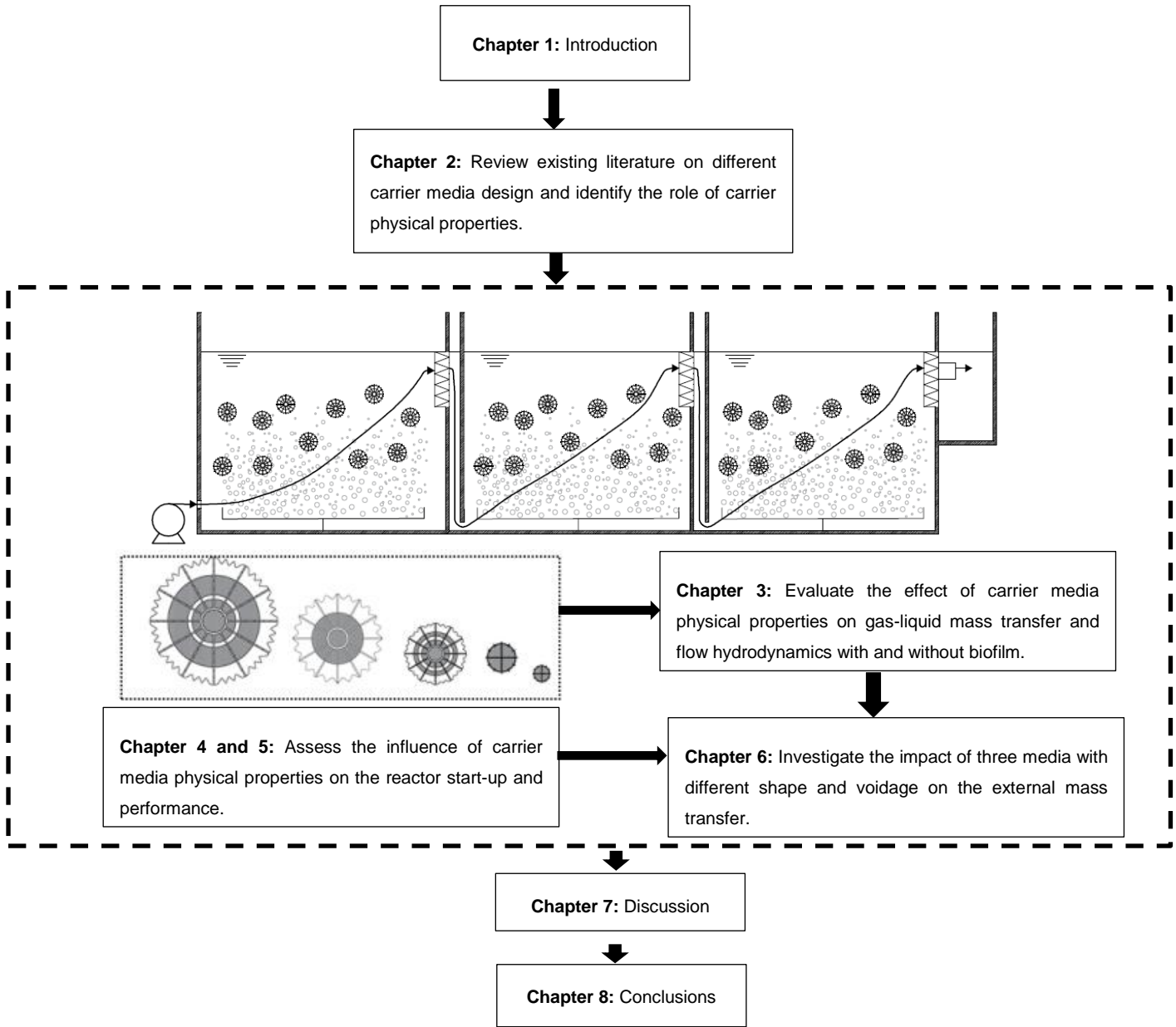
Chapter 5 focuses on the impact of media physical properties on biofilm dynamics and activity, that further influences performance of moving attached growth systems used for combined organic removal and nitrification. Chapter 5 was in part, presented at the 10<sup>th</sup> International Conference on Biofilm Reactors (2017). Chapter 5 was written up to be submitted to Water Research.

Chapter 6 examines the impact of carrier media physical properties on boundary layer thickness and external mass transfer on a lab-scale moving attached growth system performing COD removal. This chapter complements the key findings of previous chapters. Chapter 6 has been submitted to Water Research.

Chapter 7 presents the overall discussion of the research outputs. Consolidating the key findings on the importance of carrier media physical properties on carrier and moving attached growth systems optimisation. This chapter also states the PhD thesis contributions to knowledge and areas for future work.

Chapter 8 concludes this PhD research study with synthesis of the whole thesis in regards to the established research objectives.





**Figure 1-1 PhD thesis structure and interaction between chapters.**

## 1.4 References

Boltz, J.P. and Daigger, G.T. (2010) 'Uncertainty in bulk-liquid hydrodynamics and biofilm dynamics creates uncertainties in biofilm reactor design', *Water Science and Technology*, 61(2), pp. 307–316.

Chu, L. and Wang, J. (2011) 'Comparison of polyurethane foam and biodegradable polymer as carriers in moving bed biofilm reactor for treating wastewater with a low C/N ratio', *Chemosphere*, 83(1), pp. 63–68.

Daigger, G.T. and Boltz, J.P. (2017) 'Oxygen Transfer in Moving Bed Biofilm Reactors and Integrated Fixed Film Activated Sludge Processes', *Water Environment Research*

Deng, L., Guo, W., Ngo, H.H., Zhang, X., Wang, X.C., Zhang, Q. and Chen, R. (2016) 'New functional biocarriers for enhancing the performance of a hybrid moving bed biofilm reactor-membrane bioreactor system', *Bioresource Technology*, 208, pp. 87–93.

Eldyasti, A., Nakhla, G. and Zhu, J. (2012) 'Influence of particles properties on biofilm structure and energy consumption in denitrifying fluidized bed bioreactors (DFBBRs)', *Bioresource Technology*, 126, pp. 162–171.

European Parliament. Council of the European Union (1991) Council Directive concerning urban waste-water treatment (91/271/EEC). Available at: <http://eur-lex.europa.eu/legal-content/EN/TXT/?uri=celex%3A31991L0271> (Accessed: 4 October 2015).

European Parliament. Council of the European Union (2009) Common Implementation Strategy For The Water Framework Directive (2000/60/EC). Available at: <http://eur-lex.europa.eu/legal-content/EN/TXT/?uri=CELEX:32000L0060> (Accessed: 4 October 2015).

Herrling, M.P., Guthausen, G., Wagner, M., Lackner, S. and Horn, H. (2015) 'Determining the flow regime in a biofilm carrier by means of magnetic resonance imaging', *Biotechnology and Bioengineering*, 112(5), pp. 1023–1032.

Lewandowski, Z. and Boltz, J.P. (2011) 'Biofilms in Water and Wastewater Treatment', in Peter Wilderer (ed.) *Treatise on Water Science*. Oxford: Academic Press, pp. 529–570.

Mao, Y., Quan, X., Zhao, H., Zhang, Y., Chen, S., Liu, T. and Quan, W. (2017) 'Accelerated startup of moving bed biofilm process with novel electrophilic suspended biofilm carriers', *Chemical Engineering Journal*, 315, pp. 364–372.

McQuarrie, J.P. and Boltz, J.P. (2011) 'Moving Bed Biofilm Reactor Technology: Process Applications, Design, and Performance', *Water Environment Research*, 83(6), pp. 560–575.

Ødegaard, H. (2006) 'Innovations in wastewater treatment: The moving bed biofilm process', *Water Science and Technology*, 53(9), pp. 17–33.

Piculell, M., Welander, T. and Joñsson, K. (2014) 'Organic removal activity in biofilm and suspended biomass fractions of MBBR systems', *Water Science and Technology*, 69(1), pp. 55–61.

Rusten, B., Eikebrokk, B., Ulgenes, Y. and Lygren, E. (2006) 'Design and operations of the Kaldnes moving bed biofilm reactors', *Aquacultural Engineering*, 34(3), pp. 322–331.

WEF (2011) 'Moving-Bed Biofilm Reactors', in McGraw-Hill (ed.) *Biofilm Reactors - WEF MoP 35*. New York: WEF Press.



## 2 CARRIER MEDIA PROPERTIES IN A MOVING ATTACHED GROWTH SYSTEM– A REVIEW

J. Dias<sup>a</sup>, M. Bellingham<sup>b</sup>, J. Hassan<sup>b</sup>, M. Barrett<sup>b</sup>, T. Stephenson<sup>a</sup>, A. Soares<sup>a</sup>

<sup>a</sup> *Cranfield University Water Sciences Institute, Cranfield, MK43 0AL, UK.*

<sup>b</sup> *Warden Biomedica, 31 Sundon Industrial Estate, Dencora Way, Luton, Bedford, LU3 3HP, UK.*

### Abstract

Moving attached growth systems, such as moving bed biofilm reactors (MBBRs), integrated fixed film activated sludge (IFAS) and submerged aerated filters (SAF), are increasingly popular due to their reliability to produce high quality effluents in municipal and industrial wastewater treatment plants (WWTPs). The carrier media plays a fundamental role in microbial adhesion and biofilm growth allowing for substantially greater quantities of microorganisms inside the reactor, up to 10-60 g/L, in comparison to trickling filters (1-3 g/L) and rotating biological contactors (2.5-4 g/L). Moving biological attached growth systems are mainly designed based on organic and nutrient loading per carrier media surface and less commonly on volumetric organic loading. Consequently, much attention has been given to the increase of the carrier media protected surface area to maximise substrate removal efficiency. Less attention, however, has been given to the carrier media design (geometry, size, shape and voidage) and material that may affect initial adhesion, biofilm development, microbial activity, reactor hydrodynamics and substrate removal. This review is focused on the role of the carrier media in moving attached growth systems and attempts to associate the carrier's physical and chemical properties with the biofilm attachment, viability, and metabolic activity. The link between these parameters can contribute to a better understanding of the role of carrier media on moving attached growth systems and ultimately contribute to carrier media optimisation and improved process performance.

**Keywords:** Biofilm, physical and chemical properties, protected surface area, shape and size.

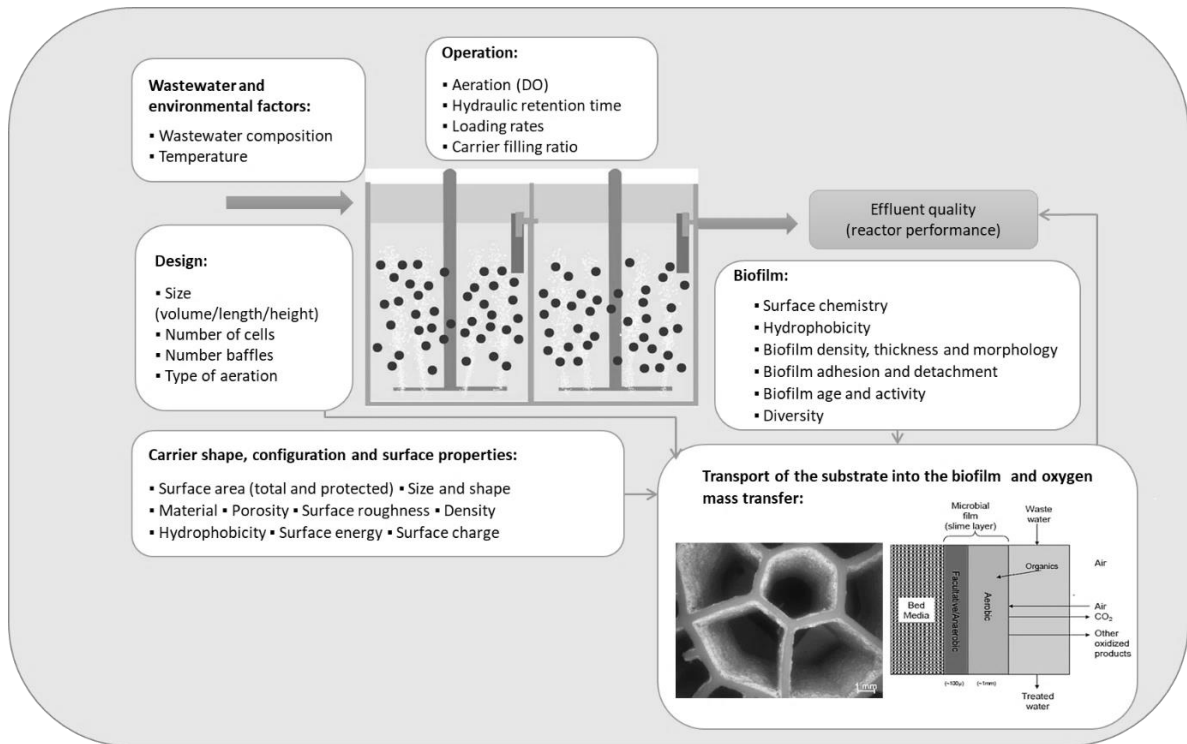
## 2.1 Introduction

Biological processes are often applied to removed, dissolved and particulate pollutants from wastewater prior to reuse, or discharge into the environment (Tchobanoglous, Burton and Stensel, 2003). There has been extensive development in both scientific knowledge and technologies to treat wastewater by biological means (UN Water, 2015). Among the suspended growth type of technologies, activated sludge processes (ASPs) are the most common and widely used (Borkar, Gulhane and Kotangale, 2013). However, the tightened standard limits implemented by the European Union Regulations (e.g. *Water Framework Directive 2000/60/EC* and *Urban Wastewater Treatment Directive 91/271/EC* (European Parliament. Council of the European Union, 1991, 2009)) has led to construction of new wastewater treatment plants, and the expansion, upgrade and refurbishment of many of the existing ones. Attached growth processes such as moving bed biofilm reactors (MBBR), integrated fixed film activated sludge (IFAS), and submerged aerated filters (SAF), are being widely utilised as add-on or an alternative to the conventional ASPs, due to the greater microbial concentration (10-60 g of volatile suspended solids) (VSS)/L compared to the concentration expected in suspended growth systems (1-8 g VSS/L) (Lewandowski and Boltz, 2011; WEF, 2011). The higher microbial concentration allows higher loads to be treated, leading to more compact systems and reduced sensitivity to toxicity and shock loadings (Dezotti, Lippel and Bassin, 2017). In moving attached growth systems an inert solid support, also referred to as carrier media, is incorporated into the process providing a large volumetric protected surface area for biologically active microorganisms to attach and grow. The movement of the carrier media is promoted by aeration in aerobic conditions, and mechanical mixers in anoxic/anaerobic conditions (McQuarrie and Boltz, 2011). The continuous motion of carrier media inside the reactor has improved benefits such as the reduction of mass transfer at the biofilm-liquid interface, reducing biofilm diffusion limitations and accelerating biochemical reactions resulting in a specialised and active biofilm (Lewandowski and Boltz, 2011). The presence of carrier media also promotes the retention of slow growing bacteria such as nitrifying bacteria and anammox bacteria (Kermani et al., 2008; WEF, 2011). Due



to the interaction between the biofilm matrix and the surrounding bulk wastewater, the structure and activity of biofilms is highly dependent on environmental factors (e.g.: influent wastewater composition and temperature), design and operation procedures, carrier media, oxygen supply and nutrient mass transport within the biofilm (Figure 2-1). Hence, it is difficult to discuss each of the factors individually once they interact with each other in numerous ways.

There are a significant number of scientific reviews on moving attached growth systems reporting process design, development, application, performance and optimisation (Barwal and Chaudhary, 2014; Borkar, Gulhane and Kotangale, 2013; Dezotti, Lippel and Bassin, 2017; Lariyah et al., 2016; McQuarrie and Boltz, 2011; Ødegaard, 2016; Qiqi, Qiang and Husham, 2012). This review focuses on factors related with carrier media, paying special attention to shape, size and material surface physical and chemical properties that ultimately link with biofilm properties (attachment, viability and metabolic activity). These factors can ultimately contribute to carrier media optimisation and consequently improve moving attached growth systems efficiency and stability.



**Figure 2-1 Schematic representation of the factors influencing moving attached growth systems performance efficiency.**







### 2.1.1 Type and properties of the support material



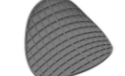


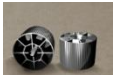




The key component of moving attached growth systems is the carrier media. Carrier media plays a fundamental role in microbial adhesion and biofilm growth while also needing to be light enough so mixing and mass transfer are not compromised. Existing studies that are focused on carrier media development mainly document the impact of protected surface area (PSA) and filling ratios on process loading rates. Few recent studies report the impact of different materials on bacteria adhesion. However, little attention has been given to the carrier media design (geometry, size, shape and voidage).











Table 2-1 lists media manufacturers and types of carrier media currently available on the market. There are more than 20 different carrier suppliers offering a wide variety of carrier media, with different physical properties including materials, voidage, shape, size and PSA (200-3000 m<sup>2</sup>/m<sup>3</sup>) (Table 2-1). Among the commercial media, plastic has been found to be an excellent scaffold for biofilm colonisation, owing to its attractive attributes such as longevity, resistance to decay, hydrophobicity and low-surface energy (Chu and Wang, 2011). The most commonly used plastic is polyethylene or polypropylene with a density ranging from 0.94 to 1.02 g/cm<sup>3</sup>, allowing sufficient buoyancy and enabling good mixing (Table 2-1) (WEF, 2011). Carrier suppliers offer media with a wide variety of shapes: flat, spherical, square, honeycomb, saddle and chip (Table 2-1). The most commonly used carrier media, AnoxKaldnes™ K1, has a cylindrical shape with an internal space divided by a cross longitudinal fin, with a length of approximately 7 mm, 10 mm diameter and a PSA of 500 m<sup>2</sup>/m<sup>3</sup> (Table 2-1). Variants of cylindrical shape carrier are popular. Many incorporate internal walls, transverse ridges and grooves to increase the surface areas, including the Bioflo<sup>+</sup> and Biotube commercialised by Warden Biomedica, with 800 and 1000 m<sup>2</sup>/m<sup>3</sup>, respectively, Biosphere produced by Evoqua Water Technologies with 630 m<sup>2</sup>/m<sup>3</sup>, BMX 2 produced by Vinci Environment (1200 m<sup>2</sup>/m<sup>3</sup>) and MB3 media manufactured by Water Management Technologies, Inc. with a PSA of 604 m<sup>2</sup>/m<sup>3</sup> (Table 2-1). Other companies also offer different shapes at increased PSA. For example Veolia Water Technologies has commercialised at least 5 alternative shapes: a flat shape media with larger diameters (30-48 mm) and internal dividing



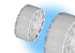











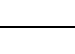
walls (Chip P and Chip M, 900-1200 m<sup>2</sup>/m<sup>3</sup>); a cylindrical shape with honeycomb shaped apertures, K3 and K5 (500-800 m<sup>2</sup>/m<sup>3</sup>). Alternatively, a square shaped media, with different dimensions, is commercialised by Biowater Technology BTW (PSA of 650-828 m<sup>2</sup>/m<sup>3</sup>). Aqwise created a “hollow square spiral” divided internally by a cross fin with a PSA of 600-650 m<sup>2</sup>/m<sup>3</sup>. Nevertheless, other new and established carrier suppliers are determined to design innovative carrier media to answer to an increasingly competitive market and emerging wastewater treatment technologies. Warden Biomedia offers media with spherical shape with feature triangular fins with a total surface area that varied from 135-310 m<sup>2</sup>/m<sup>3</sup> and high voidage (90-95%). A chip paraboloid carrier media with fine porous surface was developed by Mutag Umwelttechnologie AG offering the highest PSA in the carrier media market (3000 m<sup>2</sup>/m<sup>3</sup>) (Table 2-1). The most recent carrier media design from Veolia Water Technologies is a saddle shaped media (Z-carrier), that is aimed at improving and controlling biofilm thickness (Piculell et al., 2016b). Recently, complex geometries and high PSA carrier media have been fabricated using 3D printing (Fullerene-type carrier media, spindle shape, spherical gyroid) (Dong et al., 2015; Elliott, 2017; Tang et al., 2017b). However, when designing alternative carrier media, manufacturers need to identify the optimum compromise between production complexity and costs (Martínez-Huerta et al., 2009).












**Table 2-1 Information on typical biofilm carriers used in moving attached growth systems.**

Supplier	Media type	Surface area (m <sup>2</sup> /m <sup>3</sup> )		Dimensions (mm)		Voidage (%)	Specific gravity/weight (kg/m <sup>3</sup> )	Carriers /m <sup>3</sup>	Material	Carrier description	Application/FR (%)	Carrier Photograph	References	
		TSA*	PSA*	L	D									
Kruger Inc. (Veolia Water System)	AnoxKaldnes™ K1	700	500	7	10	95	0.96-0.98/ 145-159	975,000	HDPE	Small cylindrical shape with two cross pieces on the inside and longitudinal fins on the outside.	BOD/COD removal, nitrification and denitrification 50-70%		(Salveti et al., 2006)	
	AnoxKaldnes™ K3	600	500	12	25		0.95/95	144 000	HDPE	Cylindrical shape with internal multiple honeycomb shape passages.	BOD/COD removal, nitrification Partial Nitritation/ Anammox 35-66%		(Falletti, Conte and Maestri, 2014; Hoang et al., 2014)	
	AnoxKaldnes™ Biofilm Chip (M)	1400	1200	2.2	48		0.96-1.02 234	160 000	HDPE	Flat Circular plate with square apertures forming a plurality of passages, 1.7 mm x 1.7 mm compartment size	Nitrification Partial Nitritation/ Anammox 30-40%		(Gilbert et al., 2015)	
	Biofilm Chip (P)	990	900	3	45		0.96-1.02 173	132 000	HDPE	Flat Circular plate with square apertures forming a plurality of passages.	Nitrification Partial Nitritation/ Anammox 30-40%		(Mašić, Bengtsson and Christensson, 2010)	
	MiniChip™			1931	2	30			707 326	HDPE	Flat Circular plate with square apertures forming a plurality of passages (121 and 314).	Nitritation- Anammox		(Almstrand et al., 2014)
				1933	3	30			471 463	HDPE				
	AnoxKaldnes™ K5			800	4	25		0.96	331 000	HDPE	Cylinder hollow carrier with plurality honeycomb apertures	BOD/COD removal, 50-60%		(Piculell, Welander and Jofisson, 2014)

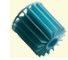



Supplier	Media type	Surface area (m <sup>2</sup> /m <sup>3</sup> )		Dimensions (mm)		Voidage (%)	Specific gravity/weight (kg/m <sup>3</sup> )	Carriers /m <sup>3</sup>	Material	Carrier description	Application/FR (%)	Carrier Photograph	References
		TSA*	PSA*	L	D								
Kruger Inc. (Veolia Water System)	Z-50	1270	1120 <sup>+</sup>	50 <sup>±</sup>	32				HDPE	Coin shaped carrier 1.5 x 1.5 mm compartment size	Nitrification 30%		(Piculell et al., 2016b)
	Z200	1740	1280	200 <sup>±</sup>	30				HDPE				(Piculell et al., 2016c)
	Z300	1960	1280	300 <sup>±</sup>	30				HDPE	Saddle-shaped carrier with 2.3 x 2.3 mm compartment size	BOD/COD removal, nitrification		
	Z400	2190	1280	400 <sup>±</sup>	30				HDPE		Nitrification 30-66%		
	Z500	2420	1280	500 <sup>±</sup>	30				HDPE				
	Natrix C2	265	220	30	36				HDPE				
	Natrix F3	230	200	50	64		1.02-1.04	24800	HDPE	Each carrier is built up of 12 walls arranged radially to form a cylindrical body	Nitrification 30-70%		(Gapes and Keller, 2009; Münch et al., 2000)
Natrix C10/10		310	32	31-36									
Headworks BIO	ActiveCell™	450	402	15	22		0.96/134		HDPE	Small cylindrical shape with 8 internal walls	BOD removal		(Maas, Parker and Legge, 2007)
		515	485				0.96/144			Small cylindrical shape with 12 internal walls			
		920	680							Small square shape with 9 internal walls			
Water Management Technologie, Inc.	MB3		604	15.8	20.5		0.96/126				Nitrification <70%		(Pfeiffer and Wills, 2011)
AqWise	ABC4™		600	14	12		0.94-0.96						(Martín-Pascual et al., 2012)
	ABC5™		650	14	12		150	308,000	HDPE	Hollow square spiral with inner cross-shaped cut out	COD removal Nitrification 20-50%		

Supplier	Media type	Surface area (m <sup>2</sup> /m <sup>3</sup> )		Dimensions (mm)		Voidage (%)	Specific gravity/weight (kg/m <sup>3</sup> )	Carriers /m <sup>3</sup>	Material	Carrier description	Application/FR (%)	Carrier Photograph	References	
		TSA*	PSA*	L	D									
Entex Technologies Inc.	Bioportz™		589	14	18	96					COD removal Nitrification 50%		(Kim et al., 2009)	
	BioSphere		800	5-9	13			PE						
	BioSphere N		800	9	13									
Evoqua Water technologies	BWT15™		840	14.5	14.5 W x 5 H				HDPE	Square with rounded corners with internal dividing walls with 25 apertures.				
	BWT X™		650	14.5	14.5 W x 8.2 H				HDPE	Square with rounded corners with internal dividing walls with 9 apertures.				
	BWT S™		650	14.5	18.5 W x 7.3 H				HDPE	Inclined rectangular shaped with rounded corners with internal dividing walls with 9 apertures.				
USF Italia	RMP-HPS®		277	18.2	20.5				PP	Plastic corrugated tube with a cross piece on the inside				
Henderson Plastics Ltd	Flocor RS	230		35	35	96	1.4/52					Plastic corrugated tube		
	Flocor RM	400		25	20	88	1.4/63					Plastic corrugated tube		
Warden Biomedica	Biofil	135	112	65	95	95	0.97/45	2500	rPP	Spherical design Serrated edges	COD removal Nitrification		(Dias et al., 2018)	
	Bioball	220	148	53	65	92	0.97/50	5833	rPP	Spherical design Serrated edges	60%			

Supplier	Media type	Surface area (m <sup>2</sup> /m <sup>3</sup> )		Dimensions (mm)		Voidage (%)	Specific gravity/weight (kg/m <sup>3</sup> )	Carriers /m <sup>3</sup>	Material	Carrier description	Application/FR (%)	Carrier Photograph	References
		TSA*	PSA*	L	D								
Warden Biomedia	Biomarble	310	220	36	46	90	0.97/76	17833	rPP	Spherical design Serrated edges	COD removal		(Dias et al., 2018)
	Biopipe	600	348	13	21.5	82.5	0.97/150	163,000	rPP	Pipe shaped filter media with internal and external fins	Nitrification 60%		
	Biopipe+		500	10	25	83	1.05/105		rPP				
	Bioflo+	1036	800	10.5	16.7 5	63	0.97/210		rPP	Tubular shaped filter media with internal and external fins	COD removal Nitrification 60%		
	Biotube	1000	610	8	12	80	0.97/217	727,000	rPP	Pipe shaped filter media with internal and external fins			
GEA 2H Water Technologies Ltd	Random media 2H-BCP 750	750	635	15	15		0.93/158 1.20/210	255,000	PP	An inner ring and tall fins and a ring on the outer diameter	Nitrification		(Tangkitjawsut et al., 2016)
	2H-BCC 011	1180	890	10	11		1.42/260		PVC	Large number of tall fins on the pipe wall.			
	2H-BCC 020	640	530	20	20		1.42/190						
	2H-BCN 012 LKLL	859	704				150		HDPE				
Brightwater F.L. I	BMax® media	700							rHDPE				
Suez environment Degremont technologies		450			22								
	Meteor	515											
		660											
Multi Umwelttechnologie AG	Mutag Biochip™	3000	1.1	20-22			0.96/70		PE	Chip paraboloid shaped carrier with fine pore structure	COD removal Nitrification 8%		(Bassin et al., 2016)
Yuhuan Water Treatment Group Co.			230	25	20		1.0		PE	Oblique cylinder, with longitudinal fins that divide the cylinder into six sectors	Nitrification 30-70%		(Zhang et al., 2013)

Supplier	Media type	Surface area (m <sup>2</sup> /m <sup>3</sup> )		Dimensions (mm)		Voidage (%)	Specific gravity/weight (kg/m <sup>3</sup> )	Carriers /m <sup>3</sup>	Material	Carrier description	Application/FR (%)	Carrier Photograph	References
		TSA*	PSA*	L	D								
Pfleiderer Water Systems GmbH	Newfloat carrier	700	500		20		1.1/250		HDPE	Irregular spherical shape	COD removal Nitrification 10%		(Podedworna, Zubrowska-Sudoł and Grabińska-Łoniewska, 2009)
	COOLFloat CD-BF22		450	20	22	80	0.90-0.95/300		PP	Ring shape with cross inside			(Barwal and Chaudhary, 2016)
COOLDECK Industries Pvt Ltd	CD-BF30		250			90	0.93-0.98	400	PP	Trapezoidal cylinder			(Barwal and Chaudhary, 2016)
	CD-BF25		650			82	0.93-0.96	170	PHDPE	Disc shape			
	CD-BF1K		1000			76	0.93-0.96	135	HDPE	Disc shape			
Vinci environment	BMX 1	500	431	7	9		0.96		HDPE	Cylindrical shape	BOD/COD removal, nitrification 44-60%		(Barry et al., 2017)
	BMX 2	1200	1000	7	4.5				HDPE	Cylindrical shape	BOD/COD removal 60%		
	BMJ 40	1700	960	39	3W				HDPE	Square shape	Nitrification 35%		
AMITEC srl	Biomaster		680	15	15	83			HDPE	Cylindrical shape with an open structure on the outside surface	BOD/COD removal 50%		(Siciliano and De Rosa, 2016)
UPM Waste Technology Centre	Cosmoball™		160		85	85	0.9/75	>2000	PE	Spherical shape with 4 holes on each surface and fins across			(Hussain, Tan and Idris, 2010)
RVT Process Equipment GmbH Company	Bioflow 9		800	7	9		145		PE	Small cylindrical shape with internal and external fins	BOD/COD removal, nitrification 50-60%		(Huang et al., 2017; Shao et al., 2017)



Supplier	Media type	Surface area (m <sup>2</sup> /m <sup>3</sup> )		Dimensions (mm)		Voidage (%)	Specific gravity/weight (kg/m <sup>3</sup> )	Carriers /m <sup>3</sup>	Material	Carrier description	Application/FR (%)	Carrier Photograph	References
		TSA*	PSA*	L	D								
RKPlast	RK Bioelements	750	750				0.93/158 1.00/172 1.20/210		PP	Ring shape asymmetrical design	Nitrification 50%		(Pedersen, Oosterveld and Pedersen, 2015)
EvU Ltd	Kielce EvU Perl	700	600	8	8		0.92-0.94/250		rPVA	Ring shape corrugated in and outside	BOD/COD removal, nitrification/denitrification 25%		(Kopec, Drewnowski and Kopec, 2016)
		460			25	90	0.95	85,000	PP	Polyhedron empty ball	COD removal Nitrification 35%		(Tang et al., 2016)
KSK Aqua	Saddle-chips		700				1.0-1.2			Saddle shape	Nitrification		(KSK, 2017)

PSA- Protected surface area, TSA- Total surface area, L-length, W-width, D-diameter, H-height, FR-Filling ratio, PP- Polypropylene, rPP-Recycled polypropylene, HDPE- High density polyethylene, PHDPE- Porous high density polyethylene, PVC- Polyvinyl chloride, rPVA- recycled polyvinyl alcohol

\*Based on 100% FR † Grid height (µm)

## **2.1.2 Carrier surface properties**

### **2.1.2.1 Physical and chemical surface properties**

The physical and chemical surface properties of the carrier media, such as surface charge, surface topography, roughness, surface hydrophobicity and surface free energy (SFE) have a significant impact on initial bacterial attachment and biofilm formation (Habimana, Semião and Casey, 2014; Siegismund et al., 2014). However, the impact of physical properties of carrier media surfaces on biofilm adhesion is still poorly documented. Flat shaped support plates or coupons have been used in experimental tests to study the impact of different material on bacteria attachment and development. Table 2-2 details the contact angle, SFE, surface charge and roughness of common polymers. High density polyethylene (HDPE), polypropylene (PP) and polyethylene (PE) have been widely used as materials of MBBR carrier construction, presenting relatively low SFE (30-39.5 mJ/m<sup>2</sup>), high hydrophobicity (85-94.3°) and negative charge (-20.4 and -45 mV). Fluorinated polymer, such as polytetrafluoroethylene (PTFE) presents the most hydrophobic surface, with a contact angle of 120° and a negative charge of -68 mV.

Surface topography and roughness plays an important role on bacteria adhesion and biofilm development. as surface irregularities can increase surface area and protect biofilms from shear stress (Alnnasouri et al., 2011; Ammar et al., 2015). However, few studies have reported a positive correlation between roughness and microbial adhesion. In a study completed by Habouzit et al. (2011) low correlation between bacterial adhesion and surface roughness was shown when five plastic materials were studied, polypropylene (PP), polyethylene (PE), polyvinyl chloride (PVC), acrylonitrile butadiene styrene (ABS) and polycarbonate (PC) ( $R^2 < 0.50$ , with surface roughness of 41, 132, 49, 20 and 38 nm, for PP, PE, ABS, PC and PVC, respectively) (Table 2-2). Higher bacterial adhesion was reported in PP and PE, with 1.37% and 1.29% of the surface covered in comparison with 0.79, 0.68 and 0.19% achieved for ABS, PC and PVC, respectively. These results are corroborated by studies from Rodriguez (2012)

and Stephenson et al. (2013) where no correlation between material surface roughness and biofilm growth was found ( $R^2 < 0.05$ ).

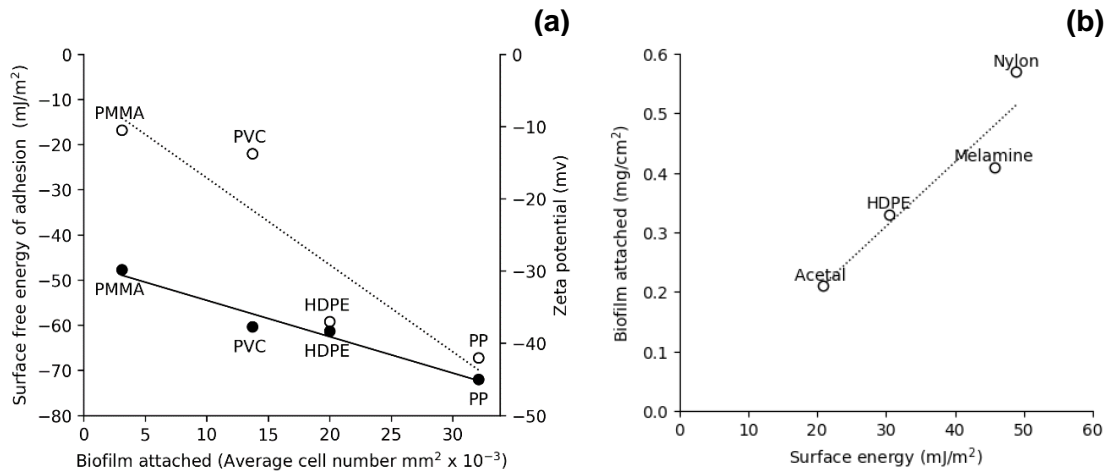
Habouzit et al. (2011) demonstrated a strong negative correlation between total SFE and microbial adhesion ( $R^2 = -0.92$ ). Carrier materials with high SFE such as PVC ( $51.2 \pm 1.9$  mJ/m<sup>2</sup>), PC ( $52.0 \pm 1.3$  mJ/m<sup>2</sup>) and ABS ( $45.3 \pm 2.5$  mJ/m<sup>2</sup>) achieved the lowest microbial adhesion in comparison with PP ( $35.6 \pm 1.7$  mJ/m<sup>2</sup>) and PE ( $39.8 \pm 1.7$  mJ/m<sup>2</sup>). Recent studies from Saur et al. (2017) confirmed these results where lower SFE, PP was associated with higher adhesion in comparison with PVC (Table 2-2).

**Table 2-2 Contact angle, SFE, zeta potential and roughness of common materials used to manufacture carrier media.**

Material	Chemical structure	Contact angle (degrees)	Surface free energy (mJ/m <sup>2</sup> )	Free energy of adhesion ( $\Delta G_{iwi}$ ) <sub>water</sub>	Density g/cm <sup>3</sup>	Zeta potential (mV) pH=7	Roughness (R <sub>a</sub> nm)	References
PVA	[CH <sub>2</sub> CH(OH)] <sub>n</sub>	10	37					(Levstek and Plazl, 2009)
Nylon	~[CO(CH <sub>2</sub> ) <sub>4</sub> CO-NH(CH <sub>2</sub> ) <sub>6</sub> NH] <sub>n</sub> ~	53	49				107	(Khan et al., 2013; Stephenson et al., 2013)
PS	~[CH <sub>2</sub> -CH(C <sub>6</sub> H <sub>5</sub> )] <sub>n</sub> ~	66.9	47.2	-70.18	1.05	-30/-59	1.3	(Dimitrov, Hadjiev and Nikov, 2007; Lee, Ong and Ng, 2004)
PVC	~(CH <sub>2</sub> -CHCl) <sub>n</sub> ~	72.2	35/51.2	-22.0		-37.7	75/38	(Hadjiev et al., 2007; Nguyen et al., 2016; Saur et al., 2017)
PMMA	~[CH <sub>2</sub> -C(CH <sub>3</sub> )CO <sub>2</sub> CH <sub>3</sub> ] <sub>n</sub> ~	74.3	40/43.5	-16.01		-28.8	0.4	(Hadjiev et al., 2007)
PETG		76.1	43.5			-11.31		(Nguyen et al., 2016; Rodriguez, 2012)
PCL	(C <sub>6</sub> H <sub>10</sub> O <sub>2</sub> ) <sub>n</sub>	76.6	57.6					(Hadjiev et al., 2007)
PVDF	~(C <sub>2</sub> H <sub>2</sub> F <sub>2</sub> ) <sub>n</sub> ~	77.4	33.8/37.3			-39.3	18	(Nguyen et al., 2016; Rodriguez, 2012)
PC	C <sub>15</sub> H <sub>16</sub> O <sub>2</sub>	82	44/52.0			-78	6/20	(Habouzit et al., 2011; Stephenson et al., 2013)
ABS	(C <sub>8</sub> H <sub>8</sub> ·C <sub>4</sub> H <sub>6</sub> ·C <sub>3</sub> H <sub>3</sub> N) <sub>n</sub>	82	35/45.3				34/49	(Habouzit et al., 2011)
Melamine	C <sub>3</sub> H <sub>6</sub> N <sub>6</sub>	84	45.7					(Khan et al., 2013)
PE	(C <sub>2</sub> H <sub>4</sub> ) <sub>n</sub>	84.8	39.5			-20.4	132	(Hadjiev et al., 2007)
PEVA	(C <sub>2</sub> H <sub>4</sub> ) <sub>n</sub> (C <sub>4</sub> H <sub>6</sub> O <sub>2</sub> ) <sub>m</sub>	86.3	41.2	-2.56				(Hadjiev et al., 2007; Nguyen et al., 2016)
PP	~[CH <sub>2</sub> -CH(CH <sub>3</sub> )] <sub>n</sub> ~	89	39.1	-67.2	0.9	-45	25/41	(Hadjiev et al., 2007; Nguyen et al., 2016; Saur et al., 2017)
HDPE	~(CH <sub>2</sub> -CH <sub>2</sub> ) <sub>n</sub> ~	94.3	30.4/39.5	-59.2	0.952	-38.3	11.1	(Khan et al., 2013; Mao et al., 2017)
POM	(CH <sub>2</sub> O) <sub>n</sub>	98	21					(Khan et al., 2013)
PET	(C <sub>10</sub> H <sub>8</sub> O <sub>4</sub> ) <sub>n</sub>	101	47.8	19.11	1.3	-54	6.91	(Hadjiev et al., 2007)
PTFE	~(CF <sub>2</sub> -CF <sub>2</sub> ) <sub>n</sub> ~	120	19/27	-98.39	2.2	-68/-48	162/47	(Ammar et al., 2015; Lee, Ong and Ng, 2004; Nguyen et al., 2016)

Polyvinyl alcohol (PVA), Polystyrene (PS), Poly(methyl methacrylate) (PMMA), Polyethylene Terephthalate Glycol (PETG), Polycaprolactone (PCL), Poly(vinylidene fluoride) (PVDF), Polycarbonate (PC), P Acrylonitrile butadiene styrene (ABS), Polyethylene (PE), Poly ethylenvinylacetate (PEVA), Poly (ethylene terephthalate) (PET), Polypropylene (PP), poly(vinyl chloride) (PVC), High-density polyethylene (HDPE), Polyoxymethylene - acetal (POM), Polyethylene terephthalate (PET), Fluoroethylene Propylene-teflon (PTFE).

Sousa et al. (1997) studied nitrifying bacteria adhesion to five different polymeric materials; high density polystyrene (HDPS), HDPE, PP, PVC and PMMA. Polypropylene was the material that achieved the highest ammonia oxidation with a linear correlation attained between bacterial adhesion and surface hydrophobicity. Moreover, attachment was favoured on higher contact angles ( $79^\circ$ ). Teixeira and Oliveira (1999) studied effects of four types of polymeric material (HDPE, PP, PVC and PMMA) on *Staphylococcus epidermidis* adhesion. Results were reported as a function of the SFE of interaction between two surfaces ( $\Delta G_{wi}$ ). Polypropylene was reported to promote higher bacteria adhesion, followed by PVC, HDPE and PMMA. Polypropylene presented the lowest SFE of adhesion ( $-67.2 \text{ mJ/m}^2$ ) and an average number of adhered cells of  $32.1 \text{ mm}^2 \times 10^{-3}$  (Figure 2-2a) in comparison to  $20.0 \pm 1.1$ ,  $13.7 \pm 1.0$  and  $3.1 \pm 0.1 \text{ mm}^2 \times 10^{-3}$  registered with HDPE ( $-59.2 \text{ mJ/m}^2$ ), PVC ( $-22.0 \text{ mJ/m}^2$ ) and PMMA ( $-16.8 \text{ mJ/m}^2$ ), respectively. Additionally, the material surface charge was also correlated with cell adhesion ( $R^2 = 0.96$ ); a larger number of cells adhered to the greatest negatively charged surface material PP ( $-45 \text{ mV}$ ) (Figure 2-2a). At a typical pH range (6-9) bacteria and material presented negative zeta potential values. Thus, the electrostatic forces were expected to be repulsive. Nevertheless, the adhesion still occurred possibly due to charge rearrangement, by small molecules, ions and proteins and the repulsion was then inhibited by the layer of extracellular organelles that promote the adhesion to the plastic surface (Harimawan, Rajasekar and Ting, 2011).

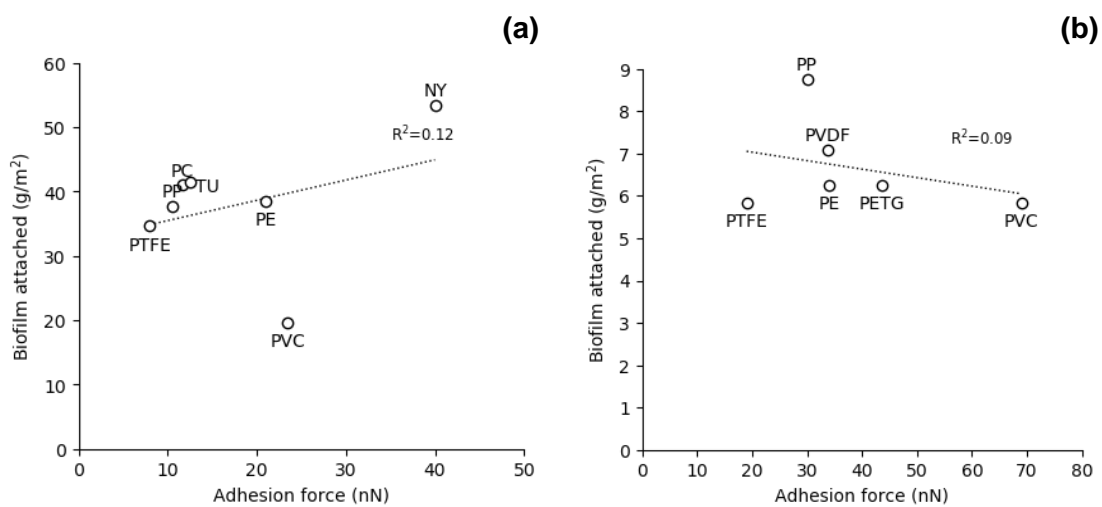


**Figure 2-2 Relation between SFE of adhesion  $\Delta G_{iwi}$  (open circles,  $R^2= 0.83$ ) and zeta potential (filled circles,  $R^2= 0.96$ ) alongside with attached biofilm (Teixeira and Oliveira, 1999) (a) relation between SFE and attached biofilm ( $R^2= 0.88$ ) (Khan et al., 2013) (b).**

Khan et al. (2013) studied the effect of the surface properties of four plastic sheets' surfaces, acetal polymer plastic, HDPE, melamine and nylon on biofilm attachment and nitrification treatment performance for a full scale nitrifying activated sludge process. The results revealed a linear correlation between attached biomass with SFE ( $R^2= 0.88$ ) and an inverse correlation with attached surface hydrophobicity ( $R^2= 0.95$ ) (Figure 2-2b). These results contradicted the findings of Sousa et al. (1997), which stated that the most hydrophobic surface had the highest adhesion. Higher values of surface energy (48.9 mJ/m<sup>2</sup>) and the total biomass (5.7 g/m<sup>2</sup>) were obtained in nylon and the lowest in acetal (20.9 mJ/m<sup>2</sup> and 2.1 g/m<sup>2</sup> respectively). Dimitrov, Hadjiev and Nikov (2007) presented results consistent with Khan et al. (2013). An improvement in biofilm growth was observed whenever the surface energy increased and contact angle decreased. Dimitrov, Hadjiev and Nikov (2007) also studied the effect of initial colonisation on biofilm formation. The first deposited cells modified the initial surface energy having influenced the adhesion process.

Rodriguez (2012) and Stephenson et al. (2013) studied the influence of media surface properties on the adhesion and colonisation of bacteria using settled wastewater. Stephenson et al. (2013) focused on a nitrifying biofilm, whilst,

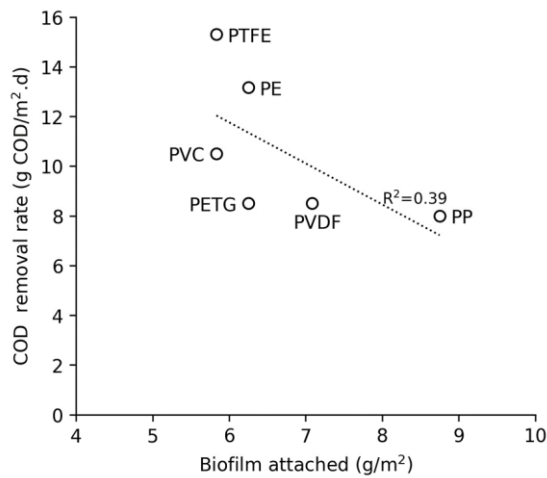
Rodriguez (2012) focused on heterotrophs and nitrifying biofilms. Stephenson et al. (2013) found no evident correlation between adhesion forces and attached biomass (Figure 2-3a), however, nylon, with the highest adhesion force (40 nN), achieved the highest attached biomass (56.4 g/m<sup>2</sup>). Rodriguez (2013) observed that PP was not the most hydrophobic material (89° and 30 mJ/m<sup>2</sup>) but presented the highest biofilm attachment (8.75 g/m<sup>2</sup>). PTFE, a fluorinated material that presents large contact angles (120°) and low SFE (19 mJ/m<sup>2</sup>), achieved lower bacteria adhesion (5.83 g/m<sup>2</sup>), confirming the preference of bacteria for less hydrophobic surfaces (lower contact angles) (Figure 2-3b).



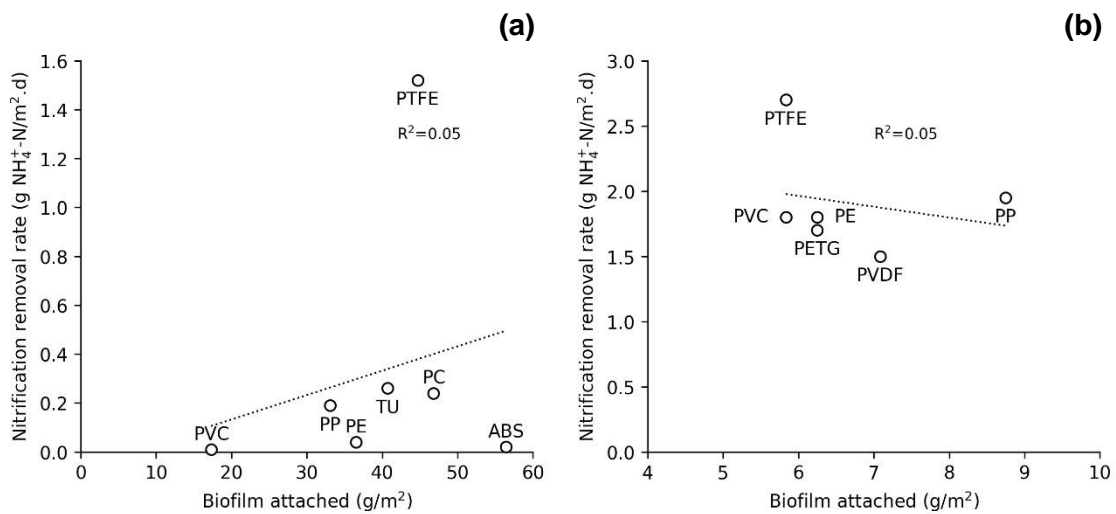
**Figure 2-3 Biofilm attached against adhesion forces for the different plastic supports, ( $R^2= 0.12$ ) (Stephenson et al., 2013) (a) and ( $R^2= 0.09$ ) (Rodriguez, 2012) (b).**

Rodriguez (2012) studied the influence of physicochemical material surface properties, surface energy and roughness on biofilm attachment and treatment performance. The results demonstrated that PTFE resulted in the highest organic removal (15.3 g COD/m<sup>2</sup>.d), however, it did not present the highest amount of attached biomass (5.83 g/m<sup>2</sup>). Despite the higher biofilm attached obtained on PP (8.75 g/m<sup>2</sup>), PP achieved the lowest organic removal (8 g COD/m<sup>2</sup>.d) (Figure 2-4). Additionally, no correlation was observed between the attached growth and nitrification removal rate  $R^2= 0.05$ . PTFE and PP obtained the highest nitrification removal rate of 2.7 and 1.95 g NH<sub>4</sub><sup>+</sup>-N/m<sup>2</sup>.d with attached biomass of 5.83 and

8.75 g/m<sup>2</sup>. A thinner biofilm obtained on PTFE may have promoted the greatest nitrification achieved (Figure 2-5 ).



**Figure 2-4 Biofilm attached against COD removal rates for the different plastic supports  $R^2= 0.39$ .**

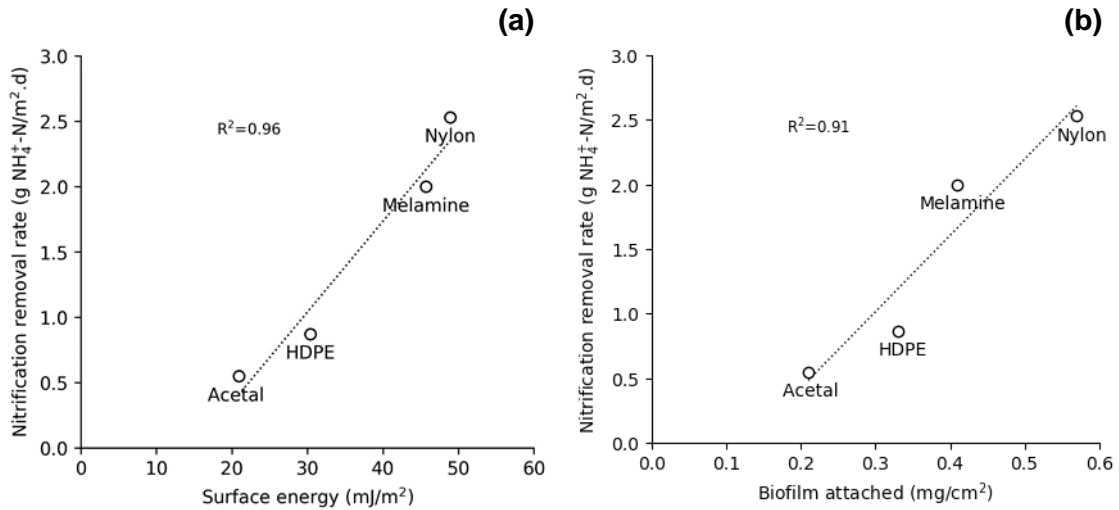


**Figure 2-5 Biofilm attached against nitrification removal rates for the different plastic supports, ( $R^2= 0.05$ ) (Stephenson et al., 2013) (a) and ( $R^2=0.05$ ) (Rodriguez, 2012)(b).**

Khan et al. (2013) demonstrated a correlation between surface energy and nitrification removal rates, showing an increase in nitrifying activity with the surface energy ( $R^2= 0.96$ ) (Figure 2-6a) and with the attached biomass ( $R^2= 0.91$ ) (Figure 2-6b). Nitrification removal rate values ranged from 0.55 to 2.53 g/m<sup>2</sup>.d, for acetal and nylon respectively. Nitrifiers preference for higher surface energy

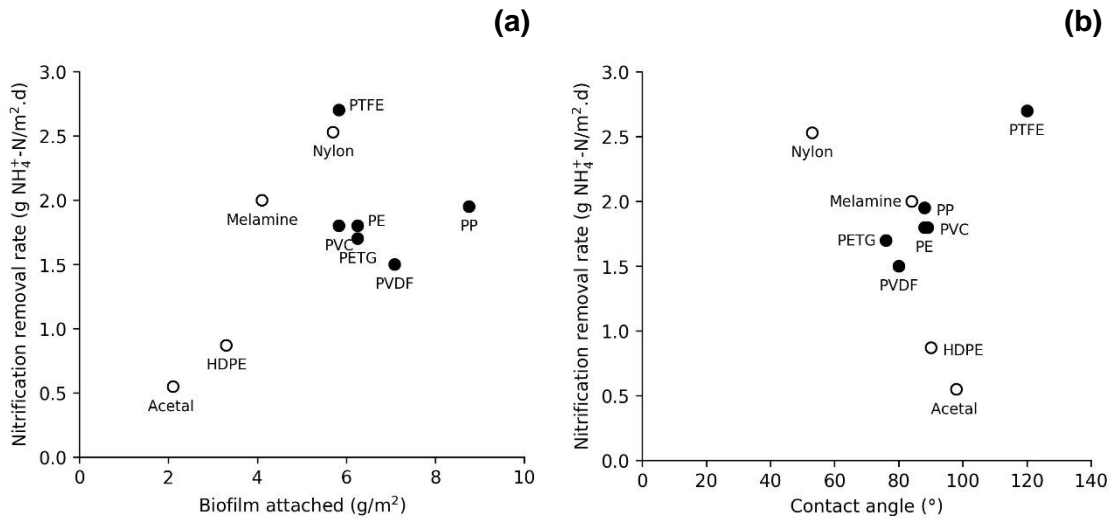


material was therefore demonstrated. In this study the author concluded that surface energy is better correlated with attached biomass than hydrophobicity (Khan et al., 2013).

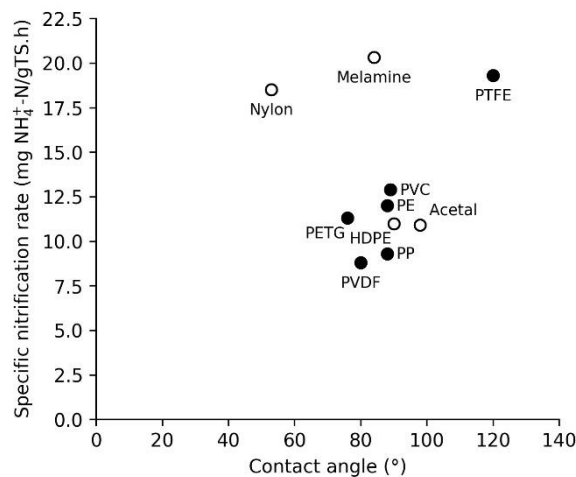


**Figure 2-6 Nitrification removal rates against SFE ( $R^2=0.96$ ) (a) and against biofilm attached ( $R^2=0.91$ ) (b) for the different plastic supports (Khan et al., 2013).**

When comparing the results of different studies the different conditions of each experimental work e.g. COD/N ratios, ratio of heterotrophs/nitrifiers or biofilm development and test duration should be considered. PTFE was the most hydrophobic surface found ( $120^\circ$ ), with the lowest surface energy ( $19 \text{ mJ/m}^2$ ) and highest ammonia removal ( $2.7 \text{ g/m}^2\cdot\text{d}$ ) and one of the lowest biofilm attachments ( $5.83 \text{ g/m}^2$ ). PP exhibited the highest value of attached biomass ( $8.75 \text{ g/m}^2$ ) but not the best ammonia removal ( $1.95 \text{ g/m}^2\cdot\text{d}$ ). HDPE, commonly used as carrier media, was the third most hydrophobic material ( $90^\circ$ ) with a surface energy of  $30 \text{ mJ/m}^2$  but it had the second lowest ammonia removal ( $0.87 \text{ g/m}^2\cdot\text{d}$ ) (Figure 2-7). Regarding the specific nitrification activity, there was no clear correlation with contact angle, and higher specific nitrification was achieved for melamine, Nylon and PTFE ( $21.2, 18.5$  and  $19.3 \text{ mg NH}_4^+\text{-N}/(\text{g TS}\cdot\text{h})$ , respectively) (Figure 2-8).



**Figure 2-7 Relation between biofilm attached (a) and contact angle (b) with ammonia removal rate of different support material (○ Khan et al., 2013 ● Rodriguez et al., 2013).**



**Figure 2-8 Specific nitrification activity (mg NH<sub>4</sub><sup>+</sup>-N/g TS.h) (○ Khan et al., 2013 ● Rodriguez et al., 2013).**

Other studies demonstrated that the nitrifier biomass appeared to attach better to high surface energy material, and values were better correlated than with hydrophobicity (Dimitrov, Hadjiev and Nikov, 2007; Khan et al., 2013). It is therefore important to study the different surface energy components and other physicochemical factors which may be involved. The studies presented above were based on experimental works carried out in fixed flat sheets and not in floating carrier media, commonly used in SAFs, MBBRs and IFAs. Therefore

more experiments are required to verify the effect of carrier surface properties on biofilm attachment and treatment performance.

### **2.1.2.2 Carrier media surface chemistry**

The chemical properties of carrier media surface has a significant influence on the initial bacterial attachment, subsequent biofilm formation and ultimately a quick start-up leading to stable process performance (Dimitrov, Hadjiev and Nikov, 2007; Mao et al., 2017). Carrier media surface modifications such as hydrophobicity, surface charge, topography and roughness can lead to improved microbial attachment and therefore enhance bacterial adhesion and biofilm formation.

Many developments have been made to manipulate surface chemistry, including the development of chemically modified polymer coating using self-assembled monolayers (SAMs) by chemical grafting. The use of SAMs contributes to attaining desired plastic carrier surface properties, with high affinity/selectivity for certain bacterial groups (Khan et al., 2011, 2013).

Hadjiev et al. (2007) studied a conditioning film of polymethyl methacrylate and powdered activated carbon (PMMA/PAC) on poly ethylenvinylacetate (PEVA) and PE coated with PAC. The results showed that for surfaces conditioned by PMMA/PAC the biofilm colonisation was higher compared to non-conditioned material. Furthermore the coating considerably increased the surface roughness (approximately 10 fold) (Hadjiev et al., 2007). The attached biofilm was higher in PE/PAC ( $3 \times 10^5$  cells/mm<sup>2</sup>) than PMMA/PAC coated PEVA ( $0.99 \times 10^5$  cells/mm<sup>2</sup>) and PEVA ( $0.45 \times 10^5$  cells/mm<sup>2</sup>). However, higher COD removal rates were achieved using PMMA/PAC coated PEVA (41.7 g/m<sup>3</sup>.h) compared with PE/PAC (28.7 g/m<sup>3</sup>.h) (Hadjiev et al., 2007). In another study, enhanced biofilm formation was observed when a poly(ethylene glycol) associated with amino groups (PEG–NH<sub>2</sub>) modification was used on PP ( $15.1 \pm 0.9 \mu\text{m}^3/\mu\text{m}^2$ ) and PE ( $6.4 \pm 1.0 \mu\text{m}^3/\mu\text{m}^2$ ) surface in comparison with limited growth on non-modified membrane PP ( $2.8 \pm 4.3 \mu\text{m}^3/\mu\text{m}^2$ ) and PE ( $2.7 \pm 0.6 \mu\text{m}^3/\mu\text{m}^2$ ) (Lackner et al., 2009). Poor biofilm formation was registered when PP and PE were modified with PEG grafted with a functional group (-CH<sub>3</sub>),  $1.1 \pm 0.2$  and  $0.1 \pm 0.05 \mu\text{m}^3/\mu\text{m}^2$ , respectively (Lackner

et al., 2009). Another study has shown that adding ferric ions and gelatine on PE carrier media surface, modified the contact angle from 77° to 65° and 45°, respectively. A 37.5 and 60% improvement on biofilm formation rate was achieved compared to unmodified carrier, shortening the start-up in 37.5% and 60%, respectively (Zhu and Chen, 2002). In a study by Ma et al. (2014) foam, calcium carbonate and plasma surface treatment were added to a HDPE carrier to modify surface properties such as: roughness, hydrophobicity and surface energy. The original HDPE media with roughness of 336 nm and contact angle of 73.1° achieved lower attached biofilm 5.77 mg/carrier, compared with foam addition (7.73 mg/carrier) with higher roughness and contact angle (1360 nm, 76.4°). The foam porous structure increased carrier media roughness and surface area for bacteria to attach, achieving 34% higher attached biofilm when compared with unmodified media. While plasma treatment (270 nm, 49.2°) and calcium carbonate (526 nm, 99.0°) had the lowest quantity of biofilm, 5.79 and 4.61 mg/carrier, respectively (Ma et al., 2014).

Another study assessed treatment performance and biofilm characteristics of a commercial non-porous carrier and a home-made porous carrier, by placing a porous layer on the internal and external walls of a PE ring shaped carrier media (Chen et al., 2015). In terms of substrate consumption rates and nitrification rate, high porous media had much higher removal compared to the other media, essentially due to the large PSA for attachment. Almost 100% COD removal when compared with 67% was achieved by the non-porous media after 7 days of operation. Ammonia removal efficiencies of 94% were also achieved on the 7<sup>th</sup> day compared with 33% of the non-porous media (Chen et al., 2015). Sponges have also been added to a cylindrical carrier media in Deng et al. (2016) studies. Results showed that higher attached biofilm was found on the modified carrier's (0.14 g MLSS/g carrier) compared with unmodified carrier (0.07 g MLSS/g carrier). The sponge's high porosity offered larger spaces for biofilm to attach. Modified carriers at steady state achieved better effluent quality, 93.3±2.8, 83.8±4.1, 75.3±2.2% of COD, NH<sub>4</sub><sup>+</sup>-N and total nitrogen (TN) removal compared with 92.0±3.2, 74.9±5.2 and 59.9±6.3 %. The foam modified carriers promoted the

adhesion of slow growing organisms enhancing ammonia removal and simultaneous nitrification and denitrification (SND).

Moreover, various studies, suggested the use of electrophilic materials polyquaternium-10 (PQAS-10) and cationic polyacrylamides (CPAM), to modify surface charge of a conventional negatively charged HDPE carrier media to improve biofilm development and start-up (Mao et al., 2017). Surface charge was increased from  $-39\pm 0.7$  mV (HDPE) to  $12.9\pm 1.4$  (PQAS-10) and  $10.8\pm 1.7$ (CPAM), while contact angles decreased, from  $94.3\pm 3.2^\circ$  (HDPE) to  $59.8\pm 4.2^\circ$  (PQAS-10) and  $58.8\pm 2.8^\circ$  (CPAM). Higher biofilm growth rates were achieved with modified PQAS-10 (0.222 1/h) compared to 0.165 and 0.099 1/h achieved in CPAM and unmodified carrier, respectively. Reactor start-up times were longer on the unmodified carrier (27 days), when compared with 13 and 19 days of PQAS-10 and CPAM, respectively (Mao et al., 2017). Bacteria are commonly negatively charged at neutral pH, therefore positive charge surfaces attracted bacteria cells, whereas, in the unmodified surface repulsive forces were experienced. The same modified carriers (PQAS-10 and CPAM) were used on the start-up of a partial nitrification (PN) process in a study by Liu et al. (2017). A faster growth of ammonia oxidizing bacteria (AOBs) promoted a quicker start-up when compared with unmodified carriers.

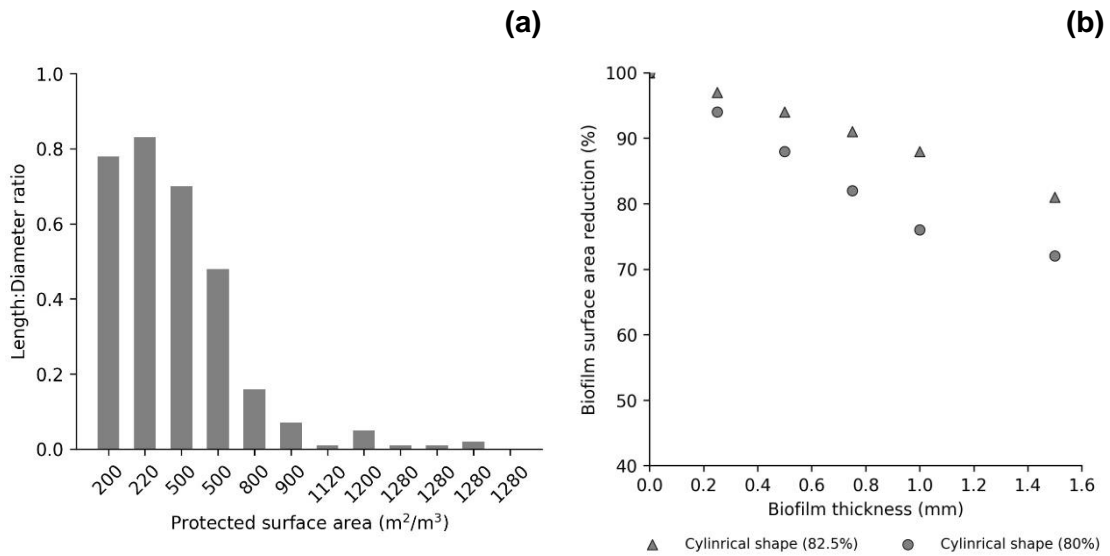
The use of bio coated carrier media (preliminary heterotrophic bacteria layer) has been recently proven to positively affect the start-up of deammonification processes. An increase in 400% was verified during specific anammox activity tests ( $250 \text{ mg NH}_4^+\text{-N/g VSS/L.d}$ ) using the bio coated in comparison with seeded reactor values ( $50 \text{ mg NH}_4^+\text{-N/g VSS/L.d}$ ). Whereas, a coated granular-activated carbon (GAC) carrier media only increased annamox activity by 50% in comparison with seeded reactor (Kowalski, Devlin and Oleszkiewicz, 2017). This result corroborates Klaus et al. (2016) studies, where anammox activity was increased in the presence of a preliminary biofilm. This study also tested other carrier media surface modifications; Fenton's reagent and potassium permanganate resulted in higher anammox activity.

### 2.1.2.3 Protected surface area, shape and voidage

Protected surface area is generally referred as the surface area available for the biofilm to grow protected from carrier collision and shear force and is commonly used as a design and operational parameter in moving attached growth systems (Ødegaard, Gisvold and Strickland, 2000). Comparison studies among carrier shape and size identified correlations between removal rates and media PSA (Barwal and Chaudhary, 2014; Bolton et al., 2006; Ødegaard, Gisvold and Strickland, 2000; Welander, Henrysson and Welander, 1998), therefore, much attention has been given to maximising the carrier media PSA, independently of carrier design (Piculell et al., 2016c).

Figure 2-9a illustrates the length to diameter ratio (L/D ratio) in function of protected surface area. As the PSA increases (200-1200 m<sup>2</sup>/m<sup>3</sup>), L:D ratio decreases (0.83-0.01), and carrier media shape tends to thin down with larger diameters (flat shaped). Higher PSA >1200 m<sup>2</sup>/m<sup>3</sup> leads to a chip shape carrier media with smaller internal dividing walls (reduced diameter of the grid meshes) that generally limit the space for biofilm growth (Table 2-1) (Goode, 2010). Small internal surfaces can have detrimental effects on wastewater flow through the carrier and biofilm control (i.e. detachment and clogging) negatively impacting the overall treatment performance (Bassin et al., 2016). Boltz and Daigger (2010) indicated that an increased biofilm thickness promoted a reduction in carrier media protected surface area, while Goode (2010) suggested a PSA correction for carrier media with cylindrical shape following mature biofilm development (Figure 2-9b). An increase in thickness up to 1000 µm reduced the PSA of a cylindrical shaped carrier by 60% (180 m<sup>2</sup>/m<sup>3</sup>) and at 700 µm a reduction of 22% in PSA, respectively (Goode, 2010). Protected surface carrier correction seems to be an important factor to consider, with special significance for higher PSA carriers that tend to have smaller internal voids. A similar observation was registered in another study, where an increased biofilm thickness from 250 to 1000 µm reduced the PSA by 33% (Sen et al., 2007). Bjornberg, Lin and Zimmerman (2010) suggested the use of active biofilm surface area together with specific surface perimeter (active biofilm thickness). Recent studies have emphasised the importance of biofilm active thickness on PSA definition

suggesting the use of active surface area as the area of biofilm that is exposed to the bulk-liquid (Piculell et al., 2016c).



**Figure 2-9 Ratio between plastic carrier length and diameter with PSA (a) and biofilm surface area reduction with increased biofilm thickness (b) (Goode, 2010).**

### 2.1.2.4 Carrier media functionality

#### 2.1.2.4.1 Filling fraction and carrier media fluidisation

Media filling ratio is an important parameter on MBBR design affecting investment cost, energy consumption and treatment performance (Feng et al., 2012). Despite, an increase in the filling ratio being of benefit to the increased biofilm available, increased energy (aeration and/ or mechanical mixing) needs to be provided to maintain carrier media in suspension (McQuarrie and Boltz, 2011). Moreover, an increase in carrier media filling ratio can also lead to carrier to carrier collision encouraging biofilm detachment (Gu et al., 2014). Values of 65% media filling ratio have been recommended in most of the literature (Ødegaard, 2016). However, different filling ratios have been used by different researchers. Studies on the performance of two carriers under different filling ratios (20, 35 and 50%), K1 (500 m<sup>2</sup>/m<sup>3</sup>) ABC5 (650 m<sup>2</sup>/m<sup>3</sup>) stated that the highest COD removal obtained was realised at 35 and 50% filling ratio, of 59±7% and 57±6%, for K1 and ABC5, respectively (Martín-Pascual et al., 2012). Studies on the impact of media filling ratio using cylindrical shaped media (10-70%) on oxygen

uptake rates (OUR), showed higher OUR at 40% filling ratio ( $1.65 \pm 0.49$  mg O<sub>2</sub>/L.h), decreasing when filling ratio was increased up to 70% ( $1.31 \pm 0.59$  mg O<sub>2</sub>/L.h). Additionally, optimal mixing intensities were indicated at 40% filling ratio (Barwal and Chaudhary, 2015). Studies using a polyvinyl chloride carrier (PVC) demonstrated that with an increase in carrier media filling ratio from 10% to 75%, the COD removal efficiency improved by 17%. An optimal filling ratio of 50% for COD removal and 70% for nitrification was suggested (Wang, Wen and Qian, 2005). Other studies on the impact of media filling ratio showed that a 50% filling ratio presented optimal conditions for BOD<sub>5</sub> removal, whereas a 100% filling ratio was beneficial for ammonia removal (Holloway and Soares, 2018). Furthermore, internal hydrodynamic experiments showed that 100% carrier media filling ratio achieved the lowest internal recirculation rate, while 50% and 25% registered a moderate and complete fluidisation, respectively (Holloway and Soares, 2018).

Other aspects to consider regarding carrier media fluidisation, are the effect of mixing intensities and carrier media on mass transfer boundary layer thickness (MTBL) and external mass transfer (Prehn et al., 2012). The transfer of substrate, and oxygen from the bulk liquid to the interior of the biofilm occurs mainly by diffusion and is often separated by a stagnant liquid layer commonly designated as MTBL (Boltz, Morgenroth and Sen, 2010; Herrling et al., 2015). An increase in flow velocities and mixing intensity can significantly reduce MTBL thickness, promoting fast movement of the carrier media, increasing oxygen transfer within the biofilm, enhancing bacteria activity and overall substrate conversion rate (WEF, 2011). Mixing intensities' influence on MTBL thickness has been proven in many studies (Gapes and Keller, 2009; Hem, Rusten and Odegaard, 1994; Mašić, Bengtsson and Christensson, 2010; Melcer and Schuler, 2014; Nogueira et al., 2015). Within the mixing intensities studies using *in-situ* methodologies and carrier media, Nogueira et al. (2015) achieved ranges of external mass transfer coefficients and MTBL thickness of 0.68-13.50 m/d and 2.9-22.4 m/d, and 12.9-256.6 µm and 7.8-61.1 µm for nitrification and COD removal, respectively. However, no clear evidence of the impact on carrier media of different physical properties (e.g.; voidage, shape and size) has been demonstrated to date.



#### **2.1.2.4.2 Carrier media properties: oxygen transfer**

Different studies have demonstrated the positive impact of plastic carrier media on the standard oxygen transfer efficiency (SOTE) in coarse bubble aeration (Collignon, 2006; Jing, Feng and Li, 2009). It is proposed that the contact of air bubbles with the carrier media and tank's surface causes bubble break-up, increasing the time for oxygen to transfer and enhancing gas-liquid interface area renewal (Jing, Feng and Li, 2009). An increase of 20 to 40% on SOTE in the presence of carrier media was reported when a coarse bubble aeration was used (Pham, Viswanathan and Kelly, 2008). Another study reported a 50% increase on SOTE when a cylindrical carrier media was used at 50% filling ratio (Sander, Behnisch and Wagner, 2017). Values of mass transfer coefficient ( $k_La$ ) with a 40% carrier media filling ratio were nearly three times higher compared with no media in Barwal and Chaudhary (2015) studies. In the same study a further increase on carrier media filling ratio decreased oxygen mass transfer.

Contrasting results were observed for fine bubble aeration, where the addition of media decreased SOTE substantially and promoted fine bubbles coalescence (Collignon, 2006; Hodkinson, 1997). The only studies found in the literature that compared the impact of carrier media shape and size on oxygen mass transfer, stated an improvement of 6-22% using a coarse bubble aeration when the ring-shaped carrier media was used while flat shaped media caused bubbles to coalesce, thus reducing oxygen mass transfer (Collignon, 2006). Very few studies were found in the literature regarding pilot and full-scale operation. Pham, Viswanathan and Kelly (2008) using off-gas techniques observed that the presence of media had negligible effect on a fine-bubble aeration process at full scale. Similar results were observed at pilot scale under operational conditions for fine bubble aeration. However, an increase in  $\alpha$ SOTE (2.4 to 3.7 %/m) was reported when a coarse bubble aeration and 50% media filling ratio was applied (Sander, Behnisch and Wagner, 2017).

#### **2.1.2.4.3 Operating conditions and biofilm function**

The use of different media alongside process operation/reactor configurations can potentially favour the adhesion and growth of specific bacteria such as

heterotrophs, autotrophs (ammonia oxidizing bacteria - AOB - and nitrogen oxidizing bacteria - NOB), heterotrophs denitrifying species, phosphorus accumulating microorganisms (PAO) and anammox (Haandel and Lubbe, 2012). The variety of carrier media, have contributed to the wide range of specific applications such as: simultaneous nitrification and denitrification (SND), partial nitrification and anammox (PNA), where redox and anoxic layers are required within the same media (McQuarrie and Boltz, 2011) and micropollutants removal (Torresi et al., 2017).

In a SND-MBBR process using two differently shaped carrier media, the ring corrugated shaped media showed better TN removal than a cylindrical shaped carrier media, where anoxic conditions were favoured due to carrier structure (Zinatizadeh and Ghaytooli, 2015). Christensson et al. (2013) studied the impact of different carrier media design on PNA process performance. The results obtained indicate that cylindrical shaped carrier media ( $500 \text{ m}^2/\text{m}^3$ ) developed more biomass per surface area than the carriers with a PSA higher than  $1000 \text{ m}^2/\text{m}^3$  with chip format, due to their high voidage and cavities that allowed an inner thicker biofilm to be formed (Christensson et al., 2013). The chip design revealed a denser and more compact biofilm when compared with cylindrical shape media. Nitrogen removal rate was higher when cylindrical shaped media ( $3.8 \text{ g N}/\text{m}^2\cdot\text{d}$ ) was used in *ex-situ* anoxic batch tests compared to chip design ( $1.5 \text{ g N}/\text{m}^2\cdot\text{d}$ ). Similar results were found in Gilbert et al. (2015) studies where, a cylindrical shaped media ( $500 \text{ m}^2/\text{m}^3$ ) with 10 mm thickness had the best performance when compared with a chip-shaped carrier media ( $1200 \text{ m}^2/\text{m}^3$ ) with 2 mm thickness which provided more anaerobic conditions for anammox activity (Gilbert et al., 2015). New saddle shaped carrier with predefined biofilm thickness of  $200 \text{ }\mu\text{m}$  (Z carrier, AnoxKaldnes™) has been successfully applied in a nitrification stage achieving 75-85% of nitrite accumulation (Piculell et al., 2016a). The positive effect of having a thin biofilm was complemented in another study, where a greater nitrite production was achieved in a predefined carrier grid of  $50 \text{ }\mu\text{m}$  (Z50) compared with a predefined grid carrier of  $400 \text{ }\mu\text{m}$  (Z400) (Piculell et al., 2016b). Further studies demonstrate that complete nitrification was achieved in a thin biofilm developed on the Z50 ( $50 \text{ }\mu\text{m}$ ) saddle shaped carriers in

comparison with Z200, Z300, Z400, and Z500. With nitrification rates of 0.75, 0.2 and 0.18 gN-NH<sub>4</sub><sup>+</sup>/gTSS.d for Z50, Z200 and Z500, respectively (Torresi et al., 2016). While thicker biofilms developed in Z500 (500 µm) promoted higher removals of 60% of the target micropollutants (Torresi et al., 2016, 2017). In Falås et al. (2012, 2013) studies, no differences were identified between cylindrical and chip shaped carrier media on the removal of micropollutants, however carrier media promoted higher removals in comparison to activated sludge (Falås et al., 2012, 2013). Two different shape and size media were applied for the removal of micropollutants, the chip shaped with a porous surface media (PSA, 3000 m<sup>2</sup>/m<sup>3</sup>) achieved higher removal efficiencies (85±10%) when compared with a cylindrical shaped carrier media (74±22%) with PSA of 500 m<sup>2</sup>/m<sup>3</sup> (Zupanc et al., 2013).

#### **2.1.2.4.4 Biofilm distribution and specific activity**

Biofilm activity is commonly used to quantify and monitor biofilm substrate utilisation rates in MBBR. Biological growth kinetic studies are of greatest interest once biofilm activity is not directly proportional to the quantity of biomass attached to the carrier media or biofilm thickness. To some extent kinetics increases with biofilm attachment and thickness, beyond the optimal thickness (“active thickness”), the nutrient and oxygen diffusion decrease becoming a limiting factor (Lazarova and Manem, 1995). Different activity tests have been applied to compare carrier media, using batch tests, including substrate utilisation rates (Siciliano and De Rosa, 2016), oxygen utilisation rates (OUR) (Dong et al., 2015), ammonia and nitrate utilisation rates (Hoang et al., 2014; Regmi et al., 2011). Hoang et al. (2014), Forrest, Delatolla and Kennedy (2016) and Young et al. (2016) studied the “nitrification kinetics normalised to biofilm and biomass” by means of relating ammonia removal rate with average biofilm thickness and viable cell coverage (% of viable cell coverage). At high loading conditions, cylindrical shaped carrier media (500 m<sup>2</sup>/m<sup>3</sup>) achieved higher levels of cellular activity 17.2±2.0 g N/m<sup>3</sup>.d.% viable cells compared to the flat shaped carrier media (900 m<sup>2</sup>/m<sup>3</sup> and 1200 m<sup>2</sup>/m<sup>3</sup>) with activity of 10.9±1.8 and 7.6±1.6 g N/m<sup>3</sup>.d.%viable cells, respectively. Under normal loading conditions, higher cellular activity was still achieved with the lowest surface area media 500 m<sup>2</sup>/m<sup>3</sup> (7.5±1.7 g N/m<sup>3</sup>.d.% viable cells) compared to 3.9±0.7 and 4.8±0.4 g N/m<sup>3</sup>.d.%

viable cells reached by 900 and 1200 m<sup>2</sup>/m<sup>3</sup> (Young et al., 2016). The increased biofilm thickness measured on the flat shaped media, decreased nitrification efficiency due to reduced pore space and changes to flow hydrodynamics reducing the substrate mass transfer within the biofilm. A cylindrical shape carrier (800 m<sup>2</sup>/m<sup>3</sup>) was compared with three fullerene-type carriers with spherical shape (437-600 m<sup>2</sup>/m<sup>3</sup>) and activities were 8.7-27.6% higher in the spherical media than the cylindrical media (Dong et al., 2015). Other studies observed higher attached biomass on a cylindrical shape media 500 m<sup>2</sup>/m<sup>3</sup> compared with a 3000 m<sup>2</sup>/m<sup>3</sup> chip shaped carrier. Bassin et al. (2016) proposed that there was no positive correlation between the amount of attached biofilm and carrier media surface area, and that other media characteristics should be considered (shape, size and surface) (Bassin et al., 2016).

## **2.2 Discussion**

Moving attached growth systems, such as MBBR, have been implemented worldwide, and there are more than 1200 full scale operating plants (Boltz et al., 2017). However, the increased restriction in the wastewater discharge legislation together with the increased load and diversity of wastewater sources, has resulted in the crucial need for the further development and optimisation of MBBR processes. Despite the considerable amount of research carried out on MBBR process optimisation, most of the work assumed carrier media PSA as the key parameter for MBBR design, modelling and operational control. This is based on the knowledge that the greater the carrier media PSA the greater the biomass attached and substrate removal capacity. However, studies have started to question the fundamental use of PSA and give importance to other carrier characteristics, such as carrier media shape and structure (Herrling et al., 2015; Melcer and Schuler, 2014; Piculell et al., 2016c). These properties have been shown to affect the bacterial distributions and biofilm formation over the carrier shielding biofilm from hydrodynamic conditions. Carrier media physical properties help to control biofilm thickness enhancing oxygen and substrate penetration. Carrier media physical properties enabled the generation of microhabitats: aerobic, anoxic and anaerobic layers within the biofilm that can expand the range

of MBBR applications, as integrated technology or on its own. Carrier media properties have been shown to increase oxygen transfer efficiency with greater energy efficiencies. Improved mixing conditions prevent clogging and increase hydraulic diameter for wastewater to flow ensuring good oxygen and substrate mass transfer. Evidently, the available area for biofilm growth is one of the essential parameters that guarantee a compact and robust process. However, more research is needed to better understand the carrier media physical properties. MBBR research and carrier optimisation needs to look beyond the use of conventional carriers (cylinder-shaped) produced by established manufacturers and other carrier shapes and sizes should be compared.

Overall, the selection of a suitable media continues to be a difficult task due to the different types of media existent in the market (Table 2-1). Carrier media exhibit different behaviours according to application, and future research should link carrier geometry with treatment purposes. Manipulating carrier physical properties that can create macro and microenvironment arrangements (aerobic anoxic and anaerobic), generating different environments that can simultaneously promote aerobic and anaerobic processes seems to be an interesting topic. Thus, to treat a broad range of wastewaters and follow different removal process pathways, carrier media needs to be continually modified.

Future developments can pass from exploring the use of chemical modification of the carrier media surface to enhancing bacteria adhesion and biofilm formation. Where plastic is mixed with positively charged polymers, plastic hydrophilicity and electrophilicity is altered (Mao et al., 2017), or through the incorporating of open macro-porous structures (graphene, carbon based materials reticulated carbon foam) onto carrier media surface or other foam type surfaces. Use of existent by-products, such as aluminium by products from water treatment to remove phosphorus, have been used in wetlands and other suggestions within the phosphorus removal will be to cultivate microalgae onto the carriers or polymeric hydrogels.

It is expected that carrier media optimisation will result in increased costs (materials and manufacture), which may be justified by the improved treatment

performance, a more compact process and operational cost savings making this process more competitive with alternative technologies.

## **2.3 Conclusions**

Little value has been given to carrier physical properties on moving attached growth systems. Thus, the key outcome of this review was to challenge the PSA as the sole efficiency/optimisation parameter and consider others, namely physical properties and carrier functionality in the overall removal efficiency of the process. Besides, carrier protected surface area:

- Surface material, roughness and hydrophobicity play a vital role on biofilm formation. A weak correlation was found between roughness and adhesion. Adhesion appears to be higher on high SFE material and lower hydrophobicity (lower contact angles).
- Surface modification by chemical additives or foam addition has proved to be a potential solution to improve bacteria adhesion and accelerate start-up.
- Protected surface carrier correction appears to be an important factor to consider, with special significance for higher PSA carriers that tend to have smaller internal voids.
- Optimal carrier media design requires a balance between carrier media surface area and open spaces to allow free flow and enhance mass transfer and substrate penetration.
- Carrier functionality represents an important parameter; thus, carriers should be linked with treatment application as a way to create distinctive zones for specific biofilm formation and stratification.

The need to revise WWTPs associated with high energy demand, resources and energy recovery gives a high potential to apply technologies that involve the use of carrier media.

## 2.4 References

Almstrand, R., Persson, F., Daims, H., Ekenberg, M., Christensson, M., Wilén, B.M., Sörensson, F. and Hermansson, M. (2014) 'Three-dimensional stratification of bacterial biofilm populations in a moving bed biofilm reactor for nitrification-anammox', *International Journal of Molecular Sciences*, 15(2), pp. 2191–2206.

Alnnasouri, M., Lemaitre, C., Gentric, C., Dagot, C. and Pons, M.N. (2011) 'Influence of surface topography on biofilm development: Experiment and modeling', *Biochemical Engineering Journal*, 57(1), pp. 38–45.

Ammar, Y., Swailes, D., Bridgens, B. and Chen, J. (2015) 'Influence of surface roughness on the initial formation of biofilm', *Surface and Coatings Technology*, 284, pp. 410–416.

Barry, U., Choubert, J.M., Canler, J.P., Pétrimaux, O., Héduit, A. and Lessard, P. (2017) 'A one dimensional moving bed biofilm reactor model for nitrification of municipal wastewaters', *Bioprocess and Biosystems Engineering*, 40(8), pp. 1141–1149.

Barwal, A. and Chaudhary, R. (2014) 'To study the performance of biocarriers in moving bed biofilm reactor (MBBR) technology and kinetics of biofilm for retrofitting the existing aerobic treatment systems: A review', *Reviews in Environmental Science and Biotechnology*, 13(3), pp. 285–299.

Barwal, A. and Chaudhary, R. (2016) 'Feasibility study for the treatment of municipal wastewater by using a hybrid bio-solar process', *Journal of Environmental Management*, 177, pp. 271–277.

Barwal, A. and Chaudhary, R. (2015) 'Impact of carrier filling ratio on oxygen uptake & transfer rate, volumetric oxygen transfer coefficient and energy saving potential in a lab-scale MBBR', *Journal of Water Process Engineering*, 8, pp. 202–208.

Bassin, J.P., Dias, I.N., Cao, S.M.S., Senra, E., Laranjeira, Y. and Dezotti, M. (2016) 'Effect of increasing organic loading rates on the performance of moving-bed biofilm reactors filled with different support media: Assessing the activity of

suspended and attached biomass fractions', *Process Safety and Environmental Protection*, 100, pp. 131–141.

Bjornberg, C., Lin, W. and Zimmerman, R. (2010) 'Kinetic evaluation and model simulation of temperature impact on biofilm growth and nitrification in a full scale MBBR system', *WEFTEC 2010*. New Orleans: Water Environment Federation, pp. 4146–4171.

Bolton, J., Tummala, A., Kapadia, C., Dandamudi, M. and Belovich, J.M. (2006) 'Procedure to quantify biofilm activity on carriers used in wastewater treatment systems', *Journal of Environmental Engineering*, 132(11), pp. 1422–1430.

Boltz, J.P. and Daigger, G.T. (2010) 'Uncertainty in bulk-liquid hydrodynamics and biofilm dynamics creates uncertainties in biofilm reactor design', *Water Science and Technology*, 61(2), pp. 307–316.

Boltz, J.P., Morgenroth, E. and Sen, D. (2010) 'Mathematical modelling of biofilms and biofilm reactors for engineering design', *Water Science and Technology*, 62(8), pp. 1821–1836.

Boltz, J.P., Smets, B.F., Rittmann, B.E., Van Loosdrecht, M.C.M., Morgenroth, E. and Daigger, G.T. (2017) 'From biofilm ecology to reactors: A focused review', *Water Science and Technology*, 75(8), pp. 1753–1760.

Borkar, R.P., Gulhane, M.L. and Kotangale, A.J. (2013) 'Moving Bed Biofilm Reactor – A New Perspective in Wastewater Treatment', *IOSR Journal Of Environmental Science Toxicology And Food Technology*, 6(6), pp. 2319–2399.

Chen, X., Kong, L., Wang, X., Tian, S. and Xiong, Y. (2015) 'Accelerated start-up of moving bed biofilm reactor by using a novel suspended carrier with porous surface', *Bioprocess and Biosystems Engineering*, 38(2), pp. 273–285.

Christensson, M., Ekström, S., Chan, A.A., Le Vaillant, E. and Lemaire, R. (2013) 'Experience from start-ups of the first ANITA Mox Plants', *Water Science and Technology*, 67(12), pp. 2677–2684.

Chu, L. and Wang, J. (2011) 'Comparison of polyurethane foam and



biodegradable polymer as carriers in moving bed biofilm reactor for treating wastewater with a low C/N ratio', *Chemosphere*, 83(1), pp. 63–68.

Collignon, D. (2006) *Insight into oxygen transfer in IFAS processes*. MSc thesis. Cranfield University. Available at: <http://cclibweb-3.central.cranfield.ac.uk/handle/1826.1/2750> (Accessed: 26 August 2015).

Deng, L., Guo, W., Ngo, H.H., Zhang, X., Wang, X.C., Zhang, Q. and Chen, R. (2016) 'New functional biocarriers for enhancing the performance of a hybrid moving bed biofilm reactor-membrane bioreactor system', *Bioresource Technology*, 208, pp. 87–93.

Dezotti, M., Lippel, G. and Bassin, J.P. (2017) 'Moving Bed Biofilm Reactor (MBBR)', in *Advanced Biological Processes for Wastewater Treatment: Emerging, Consolidated Technologies and Introduction to Molecular Techniques*. Springer, pp. 37–74.

Dias, J., Stephenson, T., Bellingham, M., Hassan, J., Barrett, M. and Soares, A. (2018) 'Impact of carrier media on oxygen transfer and wastewater hydrodynamics on a moving attached growth system', *Chemical Engineering Journal*, 351, pp. 399–408.

Dimitrov, D., Hadjiev, D. and Nikov, I. (2007) 'Optimisation of support medium for particle-based biofilm reactors', *Biochemical Engineering Journal*, 37(3), pp. 238–245.

Dong, Y., Fan, S.-Q., Shen, Y., Yang, J.-X., Yan, P., Chen, Y.-P., Li, J., Guo, J.-S., Duan, X.-M., Fang, F. and Liu, S.-Y. (2015) 'A Novel bio-carrier fabricated using 3D printing technique for wastewater treatment', *Scientific Reports*, 5(1), pp. 1–10.

Elliott, O. et al. (2017) 'Design and Manufacturing of High Surface Area 3D-Printed Media for Moving Bed Bioreactors for Wastewater Treatment', *Journal of Contemporary Water Research & Education*, (160), pp. 144–156.

European Parliament. Council of the European Union (2009) *Common Implementation Strategy For The Water Framework Directive (2000/60/EC)*.

Available at: <http://eur-lex.europa.eu/legal-content/EN/TXT/?uri=CELEX:32000L0060> (Accessed: 4 October 2015).

European Parliament. Council of the European Union (1991) *Council Directive concerning urban waste-water treatment (91/271/EEC)*. Available at: <http://eur-lex.europa.eu/legal-content/EN/TXT/?uri=celex%3A31991L0271> (Accessed: 4 October 2015).

Falås, P., Baillon-Dhumez, A., Andersen, H.R., Ledin, A. and La Cour Jansen, J. (2012) 'Suspended biofilm carrier and activated sludge removal of acidic pharmaceuticals', *Water Research*, 46(4), pp. 1167–1175.

Falås, P., Longrée, P., La Cour Jansen, J., Siegrist, H., Hollender, J. and Joss, A. (2013) 'Micropollutant removal by attached and suspended growth in a hybrid biofilm-activated sludge process', *Water Research*, 47(13), pp. 4498–4506.

Falletti, L., Conte, L. and Maestri, A. (2014) 'Upgrading of a wastewater treatment plant with a hybrid moving bed biofilm reactor (MBBR)', *AIMS Environmental Science*, 1(2), pp. 45–52.

Feng, Q., Wang, Y., Wang, T., Zheng, H., Chu, L., Zhang, C., Chen, H., Kong, X. and Xing, X.H. (2012) 'Effects of packing rates of cubic-shaped polyurethane foam carriers on the microbial community and the removal of organics and nitrogen in moving bed biofilm reactors', *Bioresource Technology*, 117, pp. 201–207.

Forrest, D., Delatolla, R. and Kennedy, K. (2016) 'Carrier effects on tertiary nitrifying moving bed biofilm reactor: An examination of performance, biofilm and biologically produced solids', *Environmental Technology*, 37(6), pp. 662–671.

Gapes, D.J. and Keller, J. (2009) 'Impact of oxygen mass transfer on nitrification reactions in suspended carrier reactor biofilms', *Process Biochemistry*, 44(1), pp. 43–53.

Gilbert, E.M., Agrawal, S., Schwartz, T., Horn, H. and Lackner, S. (2015) 'Comparing different reactor configurations for Partial Nitritation/Anammox at low temperatures', *Water Research*, 81, pp. 92–100.

Goode, C. (2010) *Understanding biosolids dynamics in a moving bed biofilm reactor*. PhD thesis. University of Toronto. Available at: [https://tspace.library.utoronto.ca/bitstream/1807/24758/6/Goode\\_Christopher\\_J\\_201006\\_PhD\\_Thesis.pdf](https://tspace.library.utoronto.ca/bitstream/1807/24758/6/Goode_Christopher_J_201006_PhD_Thesis.pdf) (Accessed: 18 November 2014).

Gu, Q., Sun, T., Wu, G., Li, M. and Qiu, W. (2014) 'Influence of carrier filling ratio on the performance of moving bed biofilm reactor in treating coking wastewater', *Bioresource Technology*, 166, pp. 72–78.

Haandel, A. van and Lubbe, J. van der (2012) 'Moving Bed Biofilm Reactors', in *Handbook of Biological Wastewater Treatment*. 2nd edn. IWA Publishing.

Habimana, O., Semião, A.J.C. and Casey, E. (2014) 'The role of cell-surface interactions in bacterial initial adhesion and consequent biofilm formation on nanofiltration/reverse osmosis membranes', *Journal of Membrane Science*, 454, pp. 82–96.

Habouzit, F., Gévaudan, G., Hamelin, J., Steyer, J.P. and Bernet, N. (2011) 'Influence of support material properties on the potential selection of Archaea during initial adhesion of a methanogenic consortium', *Bioresource Technology*, 102(5), pp. 4054–4060.

Hadjiev, D., Dimitrov, D., Martinov, M. and Sire, O. (2007) 'Enhancement of the biofilm formation on polymeric supports by surface conditioning', *Enzyme and Microbial Technology*, 40(4), pp. 840–848.

Harimawan, A., Rajasekar, A. and Ting, Y.P. (2011) 'Bacteria attachment to surfaces - AFM force spectroscopy and physicochemical analyses', *Journal of Colloid and Interface Science*, 364(1), pp. 213–218.

Hem, L.J., Rusten, B. and Odegaard, H. (1994) 'Nitrification in a moving bed biofilm reactor', *Water Research*, 28(6), pp. 1425–1433.

Herrling, M.P., Guthausen, G., Wagner, M., Lackner, S. and Horn, H. (2015) 'Determining the flow regime in a biofilm carrier by means of magnetic resonance imaging', *Biotechnology and Bioengineering*, 112(5), pp. 1023–1032.

Hoang, V., Delatolla, R., T, A., Mottawea, W., Gadbois, A., Laflamme, E. and Stintzi, A. (2014) 'Nitrifying moving bed biofilm reactor (MBBR) biofilm and biomass response to long term exposure to 1 C', *Water Environment Research*, 9(49), pp. 215–224.

Hodkinson, B.J. (1997) *The sewage treatment capability of non-backwash biological aerated filter systems for small communities*. PhD thesis. University of Portsmouth.

Holloway, T.G. and Soares, A. (2018) 'Influence of internal fluid velocities and media fill ratio on submerged aerated filter hydrodynamics and process performance for municipal wastewater treatment', *Process Safety and Environmental Protection*, 114, pp. 179–191.

Huang, C., Shi, Y., Gamal El-Din, M. and Liu, Y. (2017) 'Performance of flocs and biofilms in integrated fixed-film activated sludge (IFAS) systems for the treatment of oil sands process-affected water (OSPW)', *Chemical Engineering Journal*, 314, pp. 368–377.

Hussain, S.A., Tan, H.T. and Idris, A. (2010) 'Numerical studies of fluid flow across a cosmo ball by using CFD', *Journal of Applied Sciences*, 10(24), pp. 3384–3387.

Jing, J.Y., Feng, J. and Li, W.Y. (2009) 'Carrier effects on oxygen mass transfer behavior in a moving bed biofilm reactor', *Asia-Pacific Journal of Chemical Engineering*, 4, pp. 618–623.

Kermani, M., Bina, B., Movahedian, H., Amin, M.M. and Nikaein, M. (2008) 'Application of moving bed biofilm process for biological organics and nutrients removal from municipal wastewater', *American Journal of Environmental Sciences*, 6(4), pp. 675–682.

Khan, M.M.T., Chapman, T., Cochran, K. and Schuler, A.J. (2013) 'Attachment surface energy effects on nitrification and estrogen removal rates by biofilms for improved wastewater treatment', *Water Research*, 47(7), pp. 2190–2198.

Khan, M.M.T., Ista, L.K., Lopez, G.P. and Schuler, A.J. (2011) 'Experimental and

theoretical examination of surface energy and adhesion of nitrifying and heterotrophic bacteria using self-assembled monolayers.', *Environmental science & technology*, 45(3), pp. 1055–1060.

Kim, H., Pei, R., Boltz, J.P., Gunsch, C., Gellner, J., Dodson, R. and Schuler, A.J. (2009) 'How does IFAS affect distributions of AOB and NOB communities? Population measurements and modelling of pilot scale systems', *WEFTEC 2009*. Orlando: Water Environment Federation, pp. 2349–2358.

Kopec, L., Drewnowski, J. and Kopec, A. (2016) 'The application of moving bed biofilm reactor to denitrification process after trickling filters', *Water Science and Technology*, 74(12), pp. 2909–2916.

Kowalski, M.S., Devlin, T.R. and Oleszkiewicz, J.A. (2017) 'Attachment of anaerobic ammonium-oxidizing bacteria to augmented carrier material', *Environmental Technology (United Kingdom)*, , pp. 1–8.

KSK, A.A. (2017) *Saddle-Chips*. Available at: [http://www.ksk-aqua.dk/downloads/KSKAqua\\_A4Flyer\\_UK\\_K3.pdf](http://www.ksk-aqua.dk/downloads/KSKAqua_A4Flyer_UK_K3.pdf) (Accessed: 4 October 2017).

Lackner, S., Holmberg, M., Terada, A., Kingshott, P. and Smets, B.F. (2009) 'Enhancing the formation and shear resistance of nitrifying biofilms on membranes by surface modification', *Water Research*, 43(14), pp. 3469–3478.

Lariyah, M.S., Mohiyaden, H.A., Hayder, G., Hayder, G., Hussein, A., Basri, H., Sabri, A.F. and Noh, M.N. (2016) 'Application of Moving Bed Biofilm Reactor (MBBR) and Integrated Fixed Activated Sludge (IFAS) for Biological River Water Purification System: A Short Review', *IOP Conference Series: Earth and Environmental Science*, 32(1), pp. 1–15.

Lazarova, V. and Manem, J. (1995) 'Biofilm characterization and activity analysis in water and wastewater treatment', *Water Research*, 29(10), pp. 2227–2245.

Lee, L.Y., Ong, S.L. and Ng, W.J. (2004) 'Biofilm morphology and nitrification activities: Recovery of nitrifying biofilm particles covered with heterotrophic outgrowth', *Bioresource Technology*, 95(2), pp. 209–214.

Levstek, M. and Plazl, I. (2009) 'Influence of carrier type on nitrification in the moving-bed biofilm process', *Water Science and Technology*, 59(5), pp. 875–882.

Lewandowski, Z. and Boltz, J.P. (2011) 'Biofilms in Water and Wastewater Treatment', in Peter Wilderer (ed.) *Treatise on Water Science*. Oxford: Academic Press, pp. 529–570.

Liu, T., Mao, Y., Shi, Y. and Quan, X. (2017) 'Start-up and bacterial community compositions of partial nitrification in moving bed biofilm reactor', *Applied Microbiology and Biotechnology*, 101(6), pp. 2563–2574.

Ma, A., Tang, D., Zhai, L. and Chan, O. (2014) 'DSD International Conference', *New MBBR Carriers for High Loading Applications*. Hong Kong.

Maas, C.L.A., Parker, W.J. and Legge, R.L. (2007) 'Detachment of solids and nitrifiers in IFAS systems', *WEFTEC 2007*. California: Water Environment Federation, pp. 1429–1449.

Mao, Y., Quan, X., Zhao, H., Zhang, Y., Chen, S., Liu, T. and Quan, W. (2017) 'Accelerated startup of moving bed biofilm process with novel electrophilic suspended biofilm carriers', *Chemical Engineering Journal*, 315, pp. 364–372.

Martín-Pascual, J., López-López, C., Cerdá, A., González-López, J., Hontoria, E. and Poyatos, J.M. (2012) 'Comparative kinetic study of carrier type in a moving bed system applied to organic matter removal in urban wastewater treatment', *Water, Air, and Soil Pollution*, 223(4), pp. 1699–1712.

Martínez-Huerta, G., Prendes-Gero, B., Ortega-Fernández, F. and Mesa-Fernández, J.M. (2009) 'Design of a carrier for wastewater treatment using moving bed bioreactor', *Proceedings of the 2nd International Conference on Environmental and Geological Science and Engineering*. Brasov, Romania, pp. 44–49.

Mašić, A., Bengtsson, J. and Christensson, M. (2010) 'Measuring and modeling the oxygen profile in a nitrifying Moving Bed Biofilm Reactor', *Mathematical Biosciences*, 227(1), pp. 1–11.

McQuarrie, J.P. and Boltz, J.P. (2011) 'Moving Bed Biofilm Reactor Technology: Process Applications, Design, and Performance', *Water Environment Research*, 83(6), pp. 560–575.

Melcer, H. and Schuler, A.J. (2014) *Mass Transfer Characteristics of Floating Media in MBBR and IFAS Fixed-Film Systems*. London, United Kingdom.

Münch, E. V., Barr, K., Watts, S. and Keller, J. (2000) 'Suspended carrier technology allows upgrading high-rate activated sludge plants for nitrogen removal via process intensification', *Water Science and Technology*, 41(4–5), pp. 5–12.

Nguyen, V., Karunakaran, E., Collins, G. and Biggs, C.A. (2016) 'Biointerfaces Physicochemical analysis of initial adhesion and biofilm formation of *Methanosarcina barkeri* on polymer support material', *Colloids and Surfaces B: Biointerfaces*, 143, pp. 518–525.

Nogueira, B.L., Pérez, J., van Loosdrecht, M.C.M., Secchi, A.R., Dezotti, M. and Biscaia, E.C. (2015) 'Determination of the external mass transfer coefficient and influence of mixing intensity in moving bed biofilm reactors for wastewater treatment', *Water Research*, 80, pp. 90–98.

Ødegaard, H. (2016) 'A road-map for energy-neutral wastewater treatment plants of the future based on compact technologies (including MBBR)', *Frontiers of Environmental Science and Engineering*, 10(4), pp. 1–17.

Ødegaard, H., Gisvold, B. and Strickland, J. (2000) 'The influence of carrier size and shape in the moving bed biofilm process', *Water Science and Technology*, 41(4–5), pp. 383–391.

Pedersen, L.F., Oosterveld, R. and Pedersen, P.B. (2015) 'Nitrification performance and robustness of fixed and moving bed biofilters having identical carrier elements', *Aquacultural Engineering*, 65, pp. 37–45.

Pfeiffer, T.J. and Wills, P.S. (2011) 'Evaluation of three types of structured floating plastic media in moving bed biofilters for total ammonia nitrogen removal in a low salinity hatchery recirculating aquaculture system', *Aquacultural Engineering*,

45(2), pp. 51–59.

Pham, H., Viswanathan, S. and Kelly, R.F. (2008) 'Evaluation of Plastic Carrier Media Impact on Oxygen Transfer Efficiency with Coarse and Fine Bubble Diffusers', *WEFTEC 2008*. New Orleans: Water Environment Federation, p. 5069–5079(11).

Piculell, M., Christensson, M., Jönsson, K. and Welander, T. (2016a) 'Partial nitrification in MBBRs for mainstream deammonification with thin biofilms and alternating feed supply', *Water Science and Technology*, 73(6), pp. 1253–1260.

Piculell, M., Suarez, C., Li, C., Christensson, M., Persson, F., Wagner, M., Hermansson, M., Jönsson, K. and Welander, T. (2016b) 'The inhibitory effects of reject water on nitrifying populations grown at different biofilm thickness', *Water Research*, 104, pp. 292–302.

Piculell, M., Welander, P., Jönsson, K. and Welander, T. (2016c) 'Evaluating the effect of biofilm thickness on nitrification in moving bed biofilm reactors', *Environmental Technology (United Kingdom)*, 37(6), pp. 732–743.

Piculell, M., Welander, T. and Jönsson, K. (2014) 'Organic removal activity in biofilm and suspended biomass fractions of MBBR systems', *Water Science and Technology*, 69(1), pp. 55–61.

Podedworna, J., Zubrowska-Sudoł, M. and Grabińska-Łoniewska, A. (2009) 'Assessment of the propensity of biofilm growth on newfloat carrier media through process and biological experiments', *Water Science and Technology*, 60(11), pp. 2781–2789.

Prehn, J., Waul, C.K., Pedersen, L.F. and Arvin, E. (2012) 'Impact of water boundary layer diffusion on the nitrification rate of submerged biofilter elements from a recirculating aquaculture system', *Water Research*, 46(11), pp. 3516–3524.

Qiqi, Y., Qiang, H. and Husham, T.I. (2012) 'Review on Moving Bed Biofilm Process', *Pakistan Journal of Nutrition*, 11(9), pp. 706–713.



Regmi, P., Thomas, W., Schafran, G., Bott, C., Rutherford, B. and Waltrip, D. (2011) 'Nitrogen removal assessment through nitrification rates and media biofilm accumulation in an IFAS process demonstration study', *Water Research*, 45(20), pp. 6699–6708.

Rodriguez, A. (2012) *Media performance for rotating biological contactors (RBCs)*. MSc thesis. Cranfield University. Available at: <http://cclibweb-3.central.cranfield.ac.uk/handle/1826.1/6015> (Accessed: 16 November 2014).

Salveti, R., Azzellino, A., Canziani, R. and Bonomo, L. (2006) 'Effects of temperature on tertiary nitrification in moving-bed biofilm reactors', *Water Research*, 40(15), pp. 2981–2993.

Sander, S., Behnisch, J. and Wagner, M. (2017) 'Energy, cost and design aspects of coarse and fine bubble aeration systems in the MBBR IFAS process', *Water Science and Technology*, 75(4), pp. 890–897.

Saur, T., Morin, E., Habouzit, F., Bernet, N. and Escudié, R. (2017) 'Impact of wall shear stress on initial bacterial adhesion in rotating annular reactor', *PLoS ONE*, 12(2), pp. 1–19.

Sen, D., Randall, C.W., Brink, W., Farren, G., Pehrson, D., Flournoy, W. and Copithorn, R.R. (2007) 'Understanding the importance of aerobic mixing, biofilm thickness control and modeling on the success or failure of ifas systems for biological nutrient removal', *Nutrient Removal 2007*. Water Environment Federation, Vol.29, pp. 1098–1126.

Shao, Y., Shi, Y., Mohammed, A. and Liu, Y. (2017) 'Wastewater ammonia removal using an integrated fixed-film activated sludge-sequencing batch biofilm reactor (IFAS-SBR): Comparison of suspended flocs and attached biofilm', *International Biodeterioration & Biodegradation*, 116, pp. 38–47.

Siciliano, A. and De Rosa, S. (2016) 'An experimental model of COD abatement in MBBR based on biofilm growth dynamic and on substrates' removal kinetics', *Environmental Technology (United Kingdom)*, 37(16), pp. 2058–2071.

Siegismund, D., Undisz, A., Germerodt, S., Schuster, S. and Rettenmayr, M.

(2014) 'Quantification of the interaction between biomaterial surfaces and bacteria by 3-D modeling', *Acta Biomaterialia*, 10(1), pp. 267–275.

Sousa, M., Azeredo, J., Feijo, J. and Oliveira, R. (1997) 'Polymeric supports for the adhesion of a consortium of autotrophic nitrifying bacteria', *Biotechnology Techniques*, 11(10), pp. 751–754.

Stephenson, T., Reid, E., Avery, L.M. and Jefferson, B. (2013) 'Media surface properties and the development of nitrifying biofilms in mixed cultures for wastewater treatment', *Process Safety and Environmental Protection*, 91(4), pp. 321–324.

Tang, B., Yu, C., Bin, L., Zhao, Y., Feng, X., Huang, S., Fu, F., Ding, J., Chen, C., Li, P. and Chen, Q. (2016) 'Essential factors of an integrated moving bed biofilm reactor-membrane bioreactor: Adhesion characteristics and microbial community of the biofilm', *Bioresource Technology*, 211, pp. 574–583.

Tang, B., Zhao, Y., Bin, L., Huang, S. and Fu, F. (2017) 'Variation of the characteristics of biofilm on the semi-suspended bio-carrier produced by a 3D printing technique: Investigation of a whole growing cycle', *Bioresource Technology*, 244, pp. 40–47.

Tangkitjawisut, W., Limpiyakorn, T., Powtongsook, S., Pornkulwat, P. and Suwannasilp, B.B. (2016) 'Differences in nitrite-oxidizing communities and kinetics in a brackish environment after enrichment at low and high nitrite concentrations', *Journal of Environmental Sciences (China)*, 42, pp. 41–49.

Tchobanoglous, G., Burton, F.L. and Stensel, H.D. (2003) *Wastewater engineering: treatment and reuse*. 4th edn. Boston: McGraw-Hill.

Teixeira, P. and Oliveira, R. (1999) 'Influence of surface characteristics on the adhesion of *Alcaligenes denitrificans* to polymeric substrates', *Journal of Adhesion Science and Technology*, 13(11), pp. 1287–1294.

Torresi, E., Fowler, S.J., Polesel, F., Bester, K., Andersen, H.R., Smets, B.F., Plósz, B.G. and Christensson, M. (2016) 'Biofilm thickness influences biodiversity in nitrifying MBBRs - Implications on micropollutant removal', *Environmental*

*Science and Technology*, 50(17), pp. 9279–9288.

Torresi, E., Polesel, F., Bester, K., Christensson, M., Smets, B.F., Trapp, S., Andersen, H.R. and Plósz, B.G. (2017) 'Diffusion and sorption of organic micropollutants in biofilms with varying thicknesses', *Water Research*, 123, pp. 388–400.

UN Water (2015) *Wastewater Management A UN-Water Analytical Brief*. Available at: <http://www.unwater.org/publications/wastewater-management-un-water-analytical-brief/> (Accessed: 2 February 2017).

Wang, R.C., Wen, X.H. and Qian, Y. (2005) 'Influence of carrier concentration on the performance and microbial characteristics of a suspended carrier biofilm reactor', *Process Biochemistry*, 40(9), pp. 2992–3001.

WEF (2011) 'Moving-Bed Biofilm Reactors', in McGraw-Hill (ed.) *Biofilm Reactors - WEF MoP 35*. New York: WEF Press.

Welander, U., Henrysson, T. and Welander, T. (1998) 'Biological nitrogen removal from municipal landfill leachate in a pilot scale suspended carrier biofilm process', *Water Research*, 32(5), pp. 1564–1570.

Zhang, S., Wang, Y., He, W., Wu, M., Xing, M., Yang, J., Gao, N. and Yin, D. (2013) 'Responses of biofilm characteristics to variations in temperature and NH<sub>4</sub><sup>+</sup>-N loading in a moving-bed biofilm reactor treating micro-polluted raw water', *Bioresource Technology*, 131, pp. 365–373.

Zhu, S. and Chen, S. (2002) 'The impact of temperature on nitrification rate in fixed biofilters', *Aquacultural Engineering*, 26(4), pp. 221–237.

Zinatizadeh, A.A.L. and Ghaytooli, E. (2015) 'Simultaneous nitrogen and carbon removal from wastewater at different operating conditions in a moving bed biofilm reactor (MBBR): Process modeling and optimization', *Journal of the Taiwan Institute of Chemical Engineers*, 53, pp. 98–111.

Zupanc, M., Kosjek, T., Petkovšek, M., Dular, M., Kompare, B., Širok, B., Blažeka, Ž. and Heath, E. (2013) 'Removal of pharmaceuticals from wastewater

by biological processes, hydrodynamic cavitation and UV treatment', *Ultrasonics Sonochemistry*, 20(4), pp. 1104–1112.

### 3 IMPACT OF CARRIER MEDIA ON OXYGEN TRANSFER AND WASTEWATER HYDRODYNAMICS ON A MOVING ATTACHED GROWTH SYSTEM

J. Dias<sup>a</sup>, M. Bellingham<sup>b</sup>, J. Hassan<sup>b</sup>, M. Barrett<sup>b</sup>, T. Stephenson<sup>a</sup>, A. Soares<sup>a</sup>

<sup>a</sup> Cranfield University Water Sciences Institute, Cranfield, MK43 0AL, UK.

<sup>b</sup> Warden Biomedica, 31 Sundon Industrial Estate, Dencora Way, Luton, Bedford, LU3 3HP, UK.

#### Abstract

This study investigated the impact of five different carrier media on oxygen mass transfer efficiency and flow mixing in a 2 m<sup>3</sup> moving attached growth system pilot-plant. The five media studied varied in shape (cylindrical and spherical), size, voidage and protected surface area (112-610 m<sup>2</sup>/m<sup>3</sup>). In clean water tests, the media enhanced the overall oxygen transfer efficiency by 23-45% and hydraulic efficiency (HE) by 41-53%, compared with operation with no media. When using spherical media (Media 1, 2 and 3), the presence of biofilm increased the HE to 89, 93 and 100%, respectively. Conversely, Media 4 and 5 with biofilm contributed to a reduction in HE to 74 and 63%, respectively. The media protected surface area, the parameter traditionally selected to design biofilm processes, did not correlate with HE or with oxygen mass transfer efficiency in clean water tests. This study provides clear evidence that other media physical properties play a role in the mixing and oxygen mass transfer in moving attached growth systems. A correlation ( $R^2$ ) of 0.89 and 0.90 was obtained between the media dimensionality times voidage ( $D_i \times V_{oi}$ ) and HE, with and without biofilm development, respectively. The combination of parameters ( $D_i \times V_{oi} / HE$ ) also correlated well with oxygen mass transfer efficiency in clean water ( $R^2$  of 0.92 without biofilm and  $R^2$  of 0.88 with biofilm). Dimensionality and voidage should be utilised to design and optimise media size and shape, to enhance mixing and oxygen mass transfer, ultimately contributing to energy savings and higher removal efficiencies.

**Keywords:** Aeration efficiency, carrier media, dimensionality, hydraulic efficiency, voidage.

### 3.1 Introduction

Aeration of secondary processes requires high energy consumption in wastewater treatment plants (WWTPs), which can account for 20-60% of the total energy demand, depending on the plant configuration (Longo et al., 2016). The energy requirements to operate activated sludge processes (ASPs) are estimated to be in the order of 0.18-0.8 kWh/m<sup>3</sup> in the UK (Longo et al., 2016), 0.16-0.45 kWh/m<sup>3</sup> in the United States (US), 0.46 kWh/m<sup>3</sup> in Australia, and 0.43-2.07 kWh/m<sup>3</sup> in Japan (Bodik and Kubaska, 2013). The increasing cost of energy in the UK, and worldwide, have made ASP less attractive to the water industry. Furthermore, in Europe, the *Urban Wastewater Treatment Directive 91/271/EEC*, is tightening the ammonium-nitrogen (mg NH<sub>4</sub><sup>+</sup>-N/L) discharge consent level from 5 mg NH<sub>4</sub><sup>+</sup>-N/L to 3 mg NH<sub>4</sub><sup>+</sup>-N/L, and in certain sensitive areas down to 1 mg N-NH<sub>4</sub><sup>+</sup>/L (European Parliament. Council of the European Union, 1991). In the US, as authorised by the Clean Water Act, the National Pollutant Discharge Elimination System (NPDES) effluent limit for mg NH<sub>4</sub><sup>+</sup>-N/L ranges from 0.1 to 1.0 mg NH<sub>4</sub><sup>+</sup>-N/L. The energy requirements to treat the wastewater to this level are expected to increase, as the oxygen requirement for nitrification is 4.6 kg O<sub>2</sub>/kg NH<sub>4</sub><sup>+</sup>-N (Jenkins, D. and J. Wanner, 2014).

Moving attached growth system, such as submerged aerated filters (SAF) moving bed biofilm reactors (MBBR) and integrated fixed film activated sludge (IFAS), have been increasingly used as cost effective processes and alternatives to ASP, to meet the more-stringent nutrient/ammonia consents (Rusten, Ødegaard and Lundar, 1992; Sen and Randall, 1996). Moving attached growth systems make use of buoyant carrier media, which support and allow biofilms to grow promoting high biomass concentrations. The use of carrier media promotes the development of slow growing bacteria such as nitrifiers, preventing wash out and enhancing the nitrification efficiency (Rusten et al., 2006). The constant movement of the carrier media increases biofilm/bulk liquid oxygen levels and substrate mass transfer, compared with fixed media processes. Moving attached growth systems maximise the loading capacity and efficiency of the conventional biological processes at reduced footprints due to high biomass retention (McQuarrie and Boltz, 2011). Sufficient air needs to be provided for the

degradation of organic matter, endogenous respiration, nitrification as well as mixing and scouring of the biofilm (McQuarrie and Boltz, 2011). In moving attached growth systems, dissolved oxygen (DO) set points are usually high (3-5 mg/L), compared to conventional ASP (1-2 mg/L) (Jenkins, D. and J. Wanner, 2014). Owing to the increased oxygen demand associated with greater microbial concentration and to overcome the resistance to mass transfer and higher diffusional resistances, higher DO set point are needed in biofilm systems. Thus, it is important to optimise aeration efficiency, thereby minimising energy consumption and operational costs, while ensuring good process performance (Rosso et al., 2011).

Different studies have investigated the impact of plastic carrier media on oxygen transfer efficiency and have demonstrated consistent results on the enhancement of oxygen mass transfer with different media and filling ratios (Jing, Feng and Li, 2009; Pham, Viswanathan and Kelly, 2008; Sander, Behnisch and Wagner, 2017; Sun et al., 2016). An increase of 15-32% in standard oxygen transfer efficiency (SOTE) has been described when the media filling ratio was 25% (Pham, Viswanathan and Kelly, 2008), and an increase in SOTE of 50% was observed with a media filling ratio of 50% (Sander, Behnisch and Wagner, 2017). A 48-61% enhancement on the volumetric mass transfer coefficient ( $k_{La}$ ) was reached using a lab scale reactor filled with 40% of media (Jing, Feng and Li, 2009). Other studies stated a 10% increase with a 50% filling ratio (Sun et al., 2016). Results generated indicated that air bubbles were sheared into small bubbles through contact with the carriers, thereby increasing the gas-liquid interfacial area. Carrier media also promoted bubble dispersion increasing bubble retention time within the reactor. Nevertheless, only a small number of studies compared different sizes and shapes of carriers. Two media with ring shape (500 and 650  $m^2/m^3$  of protected surface area) and a plane surface (1200  $m^2/m^3$ ) were studied by Collignon (2006). Results generated indicated that little difference was observed in standard oxygen transfer efficiency (SOTE) using fine bubble aeration with and without media. A more pronounced impact was observed using coarse bubble aeration. With regards to size, shape and density of the media, the ring shape media helped the break-up of coarse bubbles. This in turn increased  $k_{La}$  by 6-

22% at a 40% filling ratio and the circular flat shape encouraged bubble coalescence (Collignon, 2006).

The hydraulic characteristics of moving attached growth systems have a significant impact on system performance. Hence, different size and shape carriers can influence flow pathways and hydraulic velocities with an impact on oxygen and substrate mass transfer (Herrling et al., 2015) and biofilm dynamics including growth, thickness and detachment (Rusten et al., 2006). Little is known about the impact of plastic carrier media on hydraulic flow patterns and mixing conditions. Tracer studies are frequently used to characterise hydraulic profiles and mixing behaviour in reactors. These studies help to identify hydraulic limitations, such as inactive volume (stagnant flow), hydraulic short circuiting and preferential flow paths, channelling (Holloway and Soares, 2018). Dead volume or stagnant zones reduce the actual volume available for chemical and biochemical reactions, reducing the treatment capacity (Sharma and Kazmi, 2015). Tracer analyses are also vital in illustrating the influence of aeration in a reactor. Often, well aerated reactors have a maximum use volume for biological treatment (Mann, 1997).

Although there are different studies on the effect of plastic carriers on oxygen mass transfer and a few studies on moving attached growth systems hydrodynamics, physical media properties appear to have been overlooked. To the best of the authors' knowledge, no studies have correlated media physical properties with oxygen mass transfer and moving attached growth systems hydrodynamics. Therefore, in this study, five media with different physical properties (surface area, voidage, shape and size) were used to study their impact on reactor hydrodynamics and oxygen mass transfer efficiency in a moving attached growth systems pilot plant. The study was performed with and without biofilm, from which correlations between physical properties of the media and hydrodynamic and oxygen mass transfer parameters were obtained.

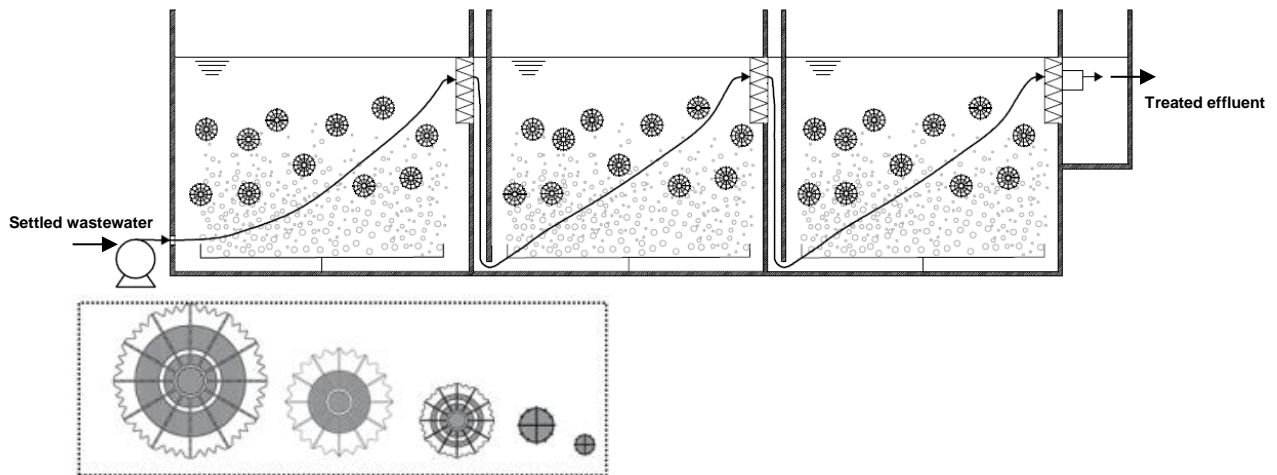


## 3.2 Material and methods

### 3.2.1 Experimental setup

The experimental tests were conducted at Cranfield University WWTP (Cranfield, UK), treating 600 m<sup>3</sup>/day of municipal wastewater. The pilot plant consisted of a reactor divided into three aerobic cells of equal volume with a total volume of 2 m<sup>3</sup> (1.0 m width x 1.5 m length and 1.30 m height) (Figure 3-1). The wastewater was introduced at the bottom of the tank and exited at the top, with narrow vertical baffles included to improve wastewater distribution to all of the cells. The media was retained within each cell by flat perforated sieves with 6 mm openings. A medium bubble aeration grid made of a 25 mm diameter PVC pipe drilled with 4 mm diameter holes, was fitted into each section of the tank. Air distribution was adjusted and controlled using three individual air flow rotameters installed in each of the cells and flow regulated by valves. Three recycled polypropylene spherical shape carrier media (Media 1, 2 and 3) with a protected surface area of 112, 148, 220 m<sup>2</sup>/m<sup>3</sup> and two recycled polypropylene cylindrical shape media (Media 4 and 5) with a protected surface area of 348 and 610 m<sup>2</sup>/m<sup>3</sup> were tested (Table 3-1). Protected surface area was defined in this study as the surface area available for the biofilm to grow protected from carrier collision and shear force (Ødegaard, Gisvold and Strickland, 2000). The five carrier media were provided by Warden Biomedia (Luton, UK). Organic and nutrient loading rates was based on surface area and calculated using equation (3-1). Where, *SLR* is the surface area loading rate (g COD/m<sup>2</sup>.d or N-NH<sub>4</sub><sup>+</sup>/m<sup>2</sup>.d), *C* is the pollutant concentration (g/m<sup>3</sup>), *Q* is the influent flow rate (m<sup>3</sup>/day), *V* is the reactor volume (m<sup>3</sup>), *A<sub>sc</sub>* surface area to volume ratio (m<sup>2</sup>/m<sup>3</sup>) and *α* is the media filling ratio (%). The organic and nutrient loading per surface area was kept constant by fixing the media filling ratio at 60%, within the values recommended in the literature (McQuarrie and Boltz, 2011). The feeding loading rates were 6.1±0.2 g COD/m<sup>2</sup>.day, 3.0±0.4 g BOD/m<sup>2</sup>.day and 0.6±0.1 g NH<sub>4</sub><sup>+</sup>-N/m<sup>2</sup>.day. The pilot-plant was designed to deliver variable air flow velocities (between 3.6-18.7 m<sup>3</sup>/m<sup>2</sup>.h) and variable wastewater flow (between 2.5-18.0 m<sup>3</sup>/day).

$$SLR = \frac{(C \times Q)}{V \times A_{sc} \times \alpha} \quad (3-1)$$



**Figure 3-1 Schematic side view of the pilot-plant used to study hydrodynamic behaviour and aeration efficiency of 5 carrier media.**

**Table 3-1 Characteristics of the carrier media tests in the moving attached growth systems. Media 1 (Biofil), Media 2 (Bioball), Media 3 (Biomarble), Media 4 (Biopipe) and Media 5 (Biotube). Media was supplied by Warden Biomedia (<http://www.wardenbiomedia.com/>).**

Media	Total surface (m <sup>2</sup> /m <sup>3</sup> )	Protected surface area (m <sup>2</sup> /m <sup>3</sup> )	Shape	Dimensions		Voidage (%)	Material	Density (g/cm <sup>3</sup> )
				Length (mm)	Diameter (mm)			
1	135	112	Spherical	65	95	95	Recycled polypropylene (PP)	0.97
2	220	148	Spherical	53	65	92		
3	310	220	Spherical	36	46	90		
4	600	348	Cylindrical	13	21.5	82.5		
5	1000	610	Cylindrical	8	12	80		

### 3.2.2 Tracer studies

Tracer studies were performed using Rhodamine (Rhodamine WT 20%; Fisher Scientific, Loughborough, UK). The tracer was injected in the reactor by the “pulse input technique” as described by Levenspiel (1999). A volume of 5 ml of Rhodamine was injected instantaneously into the inlet of the reactor. The Rhodamine concentration was then monitored in the effluent using a submersible fluorometer (Cyclops-7; RS Aqua Ltd, Hampshire, UK) and data collected was

recorded on a data logger (Databank Handheld Dataloggers; RS Aqua Ltd, Hampshire, UK). Measurements were taken every 30 seconds over a period equivalent to 3 to 4 hydraulic retention times (HRT) equation (3-2). Tracer mass recovered was calculated directly from the measured flowrate and concentration data. A tracer mass recovered within 80-100% was considered to be acceptable. An initial set of tests was completed without media and with and without aeration. A second set of tests included media with and without aeration at a wastewater flow of 4 and 9 m<sup>3</sup>/day (at HRT of 11.8 and 5.30h) and two air flow velocities of 2.2 and 9 m<sup>3</sup>/m<sup>2</sup>.h (a total of 72 tracer studies). All tests were carried out in triplicate.

$$HRT = V/Q \quad (3-2)$$

### 3.2.2.1 Determination of the residence time distribution (RTD) curves

Residence time distribution ( $E(t)$ ) curves were obtained from the tracer concentrations measured at the outlet of the reactor ( $C(t_i)$ ) as function of time ( $t_i$ ) and calculated using equation (3-3) as described by Levenspiel (1999).

Based on the  $E(t)$ , the average time that the tracer remained in the reactor (mean residence time -  $t_m$ ), and the distribution variance ( $\sigma^2$ ) were calculated using equation (3-4) and equation (3-5). To allow for a comparison between RTD profiles, tracer concentration  $E(\theta)$  and time ( $\theta$ ) were normalised, where  $\theta$  is the ratio between  $t_i$  and  $HRT$ .

An analytical dispersion model was used to represent non-ideal flows (between Plug Flow and Mixed Flow) as described by Levenspiel (1999). Dispersion number ( $\delta = D/uL$ ) and variance ( $\sigma\theta^2$ ) were calculated based on iterative calculations and used as mixing indicators, where  $D$  is the axial dispersion coefficient (m<sup>2</sup>/s),  $L$  is the axial distance of the reactor (m) and  $u$  is the velocity (m/s) equation (3-6). Dimensionless Peclet is defined to be the ratio of the rate of transport by convection and the rate of transport by diffusion or dispersion and it is used to describe the back-mixing behaviour using the axial dispersion model (3-6). Thus, Peclet number, can be calculated as the inverse of dispersion number ( $Pe=1/\delta$ ), and a threshold value of 5 ( $Pe \leq 1/0.2$ ) was predicted by the

dispersion model in Levenspiel (1999) and Tomlinson and Chambers (1979) has the criterion of greater back mixing.

RTD curves can be interpreted and quantified in different ways. Brannock et al. (2010) stated a number of relationships commonly used to evaluate RTD curves, such as dead zones, or short-circuiting flow. Dead zones ( $V_d$ ) and hydraulic efficiency (HE) were calculated according to equation (3-7) and (3-8) (Li et al., 2015b; Li, Nan and Gao, 2016). Hydraulic efficiency (HE) was used to measure the hydraulic behaviour of the reactor (wastewater flow distribution and mixing) and calculated based on the ratio between mean residence time and hydraulic retention time ( $t_m/HRT$ ). The effective volume was calculated based on total volume correction ( $V_t$ ), considering the HE and bed voidage ( $V_{oi}$ ) and equation (3-9).

$$E(t) = C(t_i) / \sum_0^{\infty} C(t_i) \cdot d(t_i) \quad (3-3)$$

$$t_m = \sum_0^{\infty} t_i C(t_i) \cdot \Delta t_i / \sum_0^{\infty} C(t_i) \cdot \Delta t_i \quad (3-4)$$

$$\sigma^2 \cong \sum_0^{\infty} (t_i - t_m)^2 C(t_i) \cdot \Delta t_i / \sum_0^{\infty} C(t_i) \cdot \Delta t_i \quad (3-5)$$

$$\sigma_{\theta}^2 = 2(D/uL) - 2(D/uL)^2 [1 - e^{-uL/D}] \quad (3-6)$$

$$HE (\%) = t_m / HRT \quad (3-7)$$

$$V_d (m^3) = (1 - (t_m / HRT)) \quad (3-8)$$

$$V_{\text{effective}} = V_t \cdot V_{oi} \cdot HE \quad (3-9)$$

### 3.2.3 Clean water oxygen mass transfer tests

Oxygen mass transfer was assessed using the procedure described in the standard methods "Measurement of Oxygen Transfer Capacity in Clean Water" (ASCE, 2007). Batch trials were performed in one of the three reactor cells at three air flow velocities: 2.2, 9.0 and 16.2  $m^3/m^2 \cdot h$ . A first set of tests was completed without media, then with media at a 60% filling ratio. The DO concentrations were measured using two DO portable metres (HACH HQ40d;

Camlab, Cambridge, UK). The DO probes were placed at two fixed positions in the tank 0.2 m and 0.8 m below the water level. All tests were completed in triplicate to assess reproducibility.

### 3.2.3.1 Determination of the oxygen mass transfer parameters

Measurements of the increasing DO concentrations were taken during the aeration period, at time intervals of 10s ( $t_p$ ). Following Gourich et al. (2008) and Garcia-Ochoa and Gomez (2009) the dynamics of the oxygen sensor can be neglected only if the characteristic time of mass transfer,  $t_f = 1/K_L a$ , is higher than  $10t_p \approx 100$  s. The volumetric oxygen mass transfer coefficient ( $k_L a$ ) (1/h), was calculated based on equation (3-10) and equation (3-11), where  $C_0$  is the initial dissolved oxygen concentration,  $C_t$  bulk oxygen concentration at time  $t$  and  $C_\infty^*$  the oxygen saturation concentration (mg/L). All the values collected were adjusted to standard conditions (zero DO, 20 °C, and 1 atm) (ASCE, 2007). The standard oxygen transfer rate (SOTR, kgO<sub>2</sub>/h) and the standard oxygen transfer efficiency (SOTE, %/m) were also determined in equation (3-12) to (3-15), where  $W_{O_2}$  is calculated based on the mass fraction of oxygen into dry air, the flow rate ( $Q$ ) and  $\rho$  air density.

$$C_t = C_\infty^* - (C_\infty^* - C_0) \cdot e^{(-k_L a \cdot (t-t_0))} \quad (3-10)$$

$$\ln(C_\infty^* - C_0) = K_L a_{20} \cdot t + \ln(C_\infty^* - C_0) \quad (3-11)$$

$$SOTR = K_L a_{20} \cdot V \cdot C_{20}^* \quad (3-12)$$

$$K_L a_{(T)} = K_L a_{20} \cdot \theta^{T-20} \quad (3-13)$$

$$w_{O_2} = \rho Q \quad (3-14)$$

$$SOTE = \frac{SOTR}{W_{O_2}} = \frac{SOTR}{h_D \times Q \times 0.299} \quad (3-15)$$

Standard aeration efficiency (SAE, kgO<sub>2</sub>/kWh) for each media was also calculated based on the power requirements ( $P_w$ ) from air flow rates (2.2, 9.0 and 16.2 m<sup>3</sup>/m<sup>2</sup>.h) and on compressor efficiency ( $e=60\%$ ), where  $R$  is the gas

constant for air,  $P_2$  and  $P_1$  absolute inlet and outlet pressure, respectively (equation (3-16) and (3-17)).

$$P_w = wRT/29.7 n. e [(P_2/P_1)^{0.283} - 1] \quad (3-16)$$

$$SAE = SOTR/P_w \quad (3-17)$$

### 3.2.4 Oxygen mass transfer and hydrodynamic behaviour under operational conditions

To study the effect of biofilm development in the hydrodynamic behaviour, tracer studies were conducted when the operation reached steady state and the biofilm was fully attached to each media. Oxygen transfer efficiency during operation was measured using off-gas techniques according to the ASCE (1997). A plastic cover with two layers was used to cover each cell, a sealed hose was used to collect the off-gas released (gas flow rates were measured using rotameters and DO). Temperature, and COD at inlet and outlet were also measured. A portable gas analyser (Geotech's BIOGAS 5000, Leamington Spa, UK) was used to measure the percentage of  $O_2$  (0-25%) and  $CO_2$  (0-100%) from the off-gas with an accuracy of  $\pm 1\%$ . The oxygen transfer efficiency was calculated based on a mass balance between the gas feeding and the off-gas equation (3-18). The operation standard oxygen transfer efficiency ( $\alpha SOTE$ ) was then calculated using equation (3-19), where,  $\theta$  is the temperature correction factor ( $\theta=1.024$ ) for wastewater temperature ( $T_w$ ),  $\beta$  beta factor,  $C_{s,20}$  concentration of oxygen at 20 degrees (mg/L), DO concentration of dissolved oxygen (mg/L), and  $C_{s,T}$  oxygen concentration under operational conditions. The  $\alpha$  value was determined by the ratio between  $\alpha SOTE$  and the clean  $SOTE$  (ASCE, 1997).

$$OTE = (Oxygen\ air, \%) - (Oxygen\ off - gas, \%) / (Oxygen\ air, \%) \quad (3-18)$$

$$\alpha SOTE = C_{s,20} \cdot OTE \cdot \theta^{(20-T_w)} / \beta \cdot C_{s,T} - DO \quad (3-19)$$

### 3.3 Results and discussion

#### 3.3.1 Hydrodynamic behaviour without biofilm growth

Residence time distribution (RTD) curves were investigated in clean media (without biofilm) and wastewater. Hydraulic efficiency ( $t_m/HRT$ ) was calculated for each condition studied, with and without media (with and without aeration) at a wastewater flow rate of 4 and 9 m<sup>3</sup>/day and two air flow velocities of 2.2 and 9 m<sup>3</sup>/m<sup>2</sup>.h (Table 3-2).

Differences between HRT and  $t_m$  indicated that the reactor deviated from the ideal plug-flow behaviour. The results obtained (with and without media) demonstrated that the hydraulic efficiency was always inferior to 100%. When aeration was off, the mean residence time varied from 3.15-5.85, 3.32-7.51, 3.92-7.66, 3.40-8.07, 3.45-7.61, 3.39-7.43 h, without media and with Media 1, 2, 3, 4 and 5, respectively, for a theoretical value of 5.30-11.80 h. When aeration was on, the mean residence time varied from 3.22-9.00, 4.00-9.51, 4.85-10.07, 4.83-10.09, 3.58-10.23, 3.60-10.94 h without media and with Media 1, 2, 3, 4 and 5, respectively (Table 3-2). The mean residence time was always shorter than the theoretical value. These results indicated that the occurrence of hydraulic short circuits or dead zones, reduced the effective volume of the reactor.

The average hydraulic efficiency was found to improve by 5-28% when the results obtained were compared for when the aeration was off and in the presence of media. Without media, values of hydraulic efficiency varied from 40-52% compared with 63-64% with Media 1, 66-74% with Media 2, 64-68% with Media 3, 64-65% with Media 4 and 63-64% with Media 5, for the two HRTs studied (Table 3-2). Once aeration was introduced, hydraulic efficiency increased from 25-38% without media compared with 14-25% with Media 1, 19-24% with Media 2, 8-30% with Media 3, 4-27% with Media 4 and 6-32% with Media 5. Other studies also observed the positive effect of aeration and media on hydraulic efficiency. This is because the reactor behaviour tended to be completely mixed due to agitation promoted by the air (Holloway and Soares, 2018; Morgan-Sagastume and Noyola, 2008). Morgan-Sagastume and Noyola (2008) demonstrated that the presence of media (volcanic scoria media) increased the

hydraulic efficiency by 72% when compared with the aerated filter without media. Other studies revealed that the introduction of 100% media filling ratio in a submerged aerated filter, improved the hydraulic efficiency by 48% (Holloway and Soares, 2018).

Comparing the hydraulic efficiency results statistically, using paired *t* tests, was verified that hydraulic efficiency for Media 1 was statistically different ( $p < 0.05$ ) from all the other media. Between Media 2 and 3 and between Media 4 and 5 there was no statistical difference in the hydraulic efficiency results. However, there was a statistical difference between the spherical (1, 2 and 3) and the cylindrical (4 and 5).



**Table 3-2 Summary of the hydraulic parameters determined based on two wastewater flow rates (4 m<sup>3</sup>/day and 9 m<sup>3</sup>/day). Media 1 (Biofil), Media 2 (Bioball), Media 3 (Biomarble), Media 4 (Biopipe) and Media 5 (Biotube). Media was supplied by Warden Biomedia (<http://www.wardenbiomedia.com/>).**

Air Flow velocities	No air						Air flow rate 2.2 m <sup>3</sup> /m <sup>2</sup> .h						Air flow rate 9 m <sup>3</sup> /m <sup>2</sup> .h					
	Clean		Media 1		Media 2		Clean		Media 1		Media 2		Clean		Media 1		Media 2	
HRT (h)	11.8	5.30	11.8	5.30	11.8	5.30	11.8	5.30	11.8	5.30	11.8	5.30	11.8	5.30	11.8	5.30	11.8	5.30
t <sub>m</sub> (h)	5.8 ±0.5	3.2± 0.2	7.5± 0.2	3.3± 0.3	7.7± 0.3	3.9± 0.9	8.2±0.1	3.2± 0.1	9.5± 0.2	4.4± 0.1	9.4± 0.6	4.8± 0.1	9.0± 0.3	3.5± 0.1	8.7± 0.1	4.0± 0.2	10.1± 0.4	4.9± 0.3
V <sub>d</sub> (m <sup>3</sup> )	0.44± 0.01	0.59± 0.04	0.58± 0.03	0.60± 0.05	0.55± 0.02	0.41± 0.02	0.36± 0.02	0.37± 0.00	0.31± 0.02	0.27± 0.01	0.31 ±0.05	0.092 ±0.04	0.16± 0.3	0.272 ±0.01	0.43± 0.96	0.4± 0.03	0.35± 0.03	0.17± 0.04
HE (%)	52	40	64	63	64	77	69	61	81	83	79	92	76	65	73	75	77	94
Dispersion δ	0.21± 0.12	0.20± 0.08	0.22± 0.03	0.18± 0.01	0.22± 0.04	0.23± 0.04	0.18± 0.01	0.17± 0.01	0.22± 0.04	0.21± 0.01	0.19 ±0.0	0.21± 0.00	0.18± 0.02	0.20± 0.03	0.20± 0.01	0.21± 0.02	0.20± 0.01	0.198 ±0.01
N-CSTR	3.4± 0.1	2.3± 0.4	3.2± 0.1	3.4± 0.1	3.2± 0.5	2.9± 0.3	3.4±0.1	3.4± 0.14	2.9± 0.4	2.1± 0.1	3.2 ±0.2	3.0± 0.1	3.5± 0.3	3.2± 0.3	3.1± 0.1	3.0± 0.2	3.1± 0.1	3.0± 0.2

Air Flow velocities	No air						Air flow rate 2.2 (m <sup>3</sup> /m <sup>2</sup> .h)						Air flow rate 9 m <sup>3</sup> /m <sup>2</sup> .h					
	Media 3		Media 4		Media 5		Media 3		Media 4		Media 5		Media 3		Media 4		Media 5	
HRT (h)	11.8	5.30	11.8	5.30	11.8	5.30	11.8	5.30	11.8	5.30	11.8	5.30	11.8	5.30	11.8	5.30	11.8	5.30
t <sub>m</sub> (h)	8.1± 0.6	3.4± 0.2	7.6± 0.3	3.5± 0.7	7.3± 0.6	3.4± 0.6	10.1±0.2	4.8± 0.4	10.2± 0.1	3.6± 0.1	10.9 ±0.1	3.6± 0.7	8.8± 0.5	4.9± 0.1	8.9± 0.1	4.7± 0.3	7.4± 0.6	4.7± 0.3
V <sub>d</sub> (m <sup>3</sup> )	0.49± 0.01	0.56± 0.04	0.52± 0.01	0.51± 0.05	0.54± 0.02	0.54± 0.02	0.23± 0.01	0.19± 0.01	0.20± 0.02	0.34± 0.01	0.11 ±0.05	0.36 ±0.01	0.40± 0.02	0.07± 0.01	0.36± 0.01	0.05± 0.03	0.05± 0.03	1.50± 0.04
HE (%)	66	62	59	60	57	58	83	91	80	71	84	68	72	92	76	89	63	89
Dispersion δ	0.18± 0.12	0.18± 0.08	0.16± 0.03	0.16± 0.01	0.22± 0.02	0.22± 0.01	0.18± 0.01	0.20± 0.01	0.18± 0.04	0.20± 0.01	0.19 ±0.01	0.21± 0.00	0.19± 0.02	0.20± 0.03	0.21± 0.01	0.25± 0.02	0.19± 0.01	0.188 ±0.01
N-CSTR	3.2± 0.3	3.1± 0.2	3.5± 0.3	3.0± 0.1	3.4± 0.5	2.8± 0.2	3.2±0.1	3.1± 0.1	3.4± 0.3	3.1± 0.2	3.3± 0.1	3.1± 0.2	3.3± 0.2	3.1± 0.3	3.0± 0.1	2.8± 0.2	3.0± 0.2	3.0±0 2

HRT theoretical retention time, t<sub>m</sub> mean residence time, V<sub>d</sub> volume of dead zones, HE hydraulic efficiency, δ dispersion number, N-CSTR number of Continuous Stirred Tank Reactors

Results indicated a decrease of dead zones from 28 to 77% for both air flow rates and with media. In this study, the dead volume percentages varied from 17-26%, 8-20%, 8-26%, 11-32% and 7-37% with Media 1, 2, 3, 4 and 5, respectively (Table 3-2). Aeration has been shown to have a greater impact on mixing. The presence of media and aeration held the tracer for a longer period inside the reactor, reducing dead zones. Similar results were obtained by Morgan-Sagastume and Noyola (2008) demonstrating that dead zones were decreased by 53% when aeration and media were used.

Mixing patterns (back-mixing) were analysed based on dispersion number ( $D/\mu L$ ). Tomlinson and Chambers (1979) defined a low degree of mixing when  $D/\mu L \leq 0.02$  and a large degree of mixing when  $D/\mu L \geq 0.2$ . For an ideal plug-flow reactor, the dispersion coefficient  $D/\mu L = 0$ , whereas  $D/\mu L = \infty$ , is expected in a perfectly mixed reactor. The values of dispersion coefficient (Table 3-2) varied from 0.16 to 0.25 suggesting a moderate to high degree of mixing. An average Peclet number, the inverse of dispersion number ( $1/\delta$ ), of  $5.1 \pm 0.4$  also confirmed the large degree of dispersion  $Pe < 5$ , as stated by Fogler (2006). The presence of media did not increase the dispersion coefficient values, rather, the same results were verified in the studies by Morgan-Sagastume and Noyola (2008). Back mixing can also be characterised by the value of  $N$ -CSTR, with an  $N \leq 3$  indicating higher back mixing (Fogler, 2006). The values varied from 2.11 and 3.53 within the media.

### **3.3.2 Hydrodynamic behaviour under operational conditions (with biofilm growth)**

To study the impact of biofilm growth in the hydrodynamic behaviour of the reactor, tracer studies were conducted after biofilm development. Values of mean residence time of  $16.90 \pm 0.29$ h,  $11.20 \pm 0.65$ h,  $8.69 \pm 0.29$ h,  $5.25 \pm 0.34$ h and  $3.02 \pm 0.65$ h were obtained at operation conditions for Media 1, 2, 3, 4 and 5, respectively (Table 3-3). The hydraulic efficiency achieved with Media 1 and 2 was  $89 \pm 2\%$  and  $93 \pm 5\%$ , respectively. With Media 3 the mean residence time exceeded the theoretical value of 8h,  $8.69 \pm 0.29$ h (tracer retention within the biofilm). The same observation was verified in Holloway and Soares (2018),

where  $t_m$  exceeded by 27-40% the HRT. The presence of biofilm in Media 1, 2 and 3 led to an increase in the residence time, reducing channelling, increasing reactor effective volume and back mixing. Effective volume of  $1.34\pm 0.02$ ,  $1.33\pm 0.05$  and  $1.68 \pm 0.02$  m<sup>3</sup> were registered with Media 1, 2 and 3. The same effect was observed in Holloway and Soares (2018) where biofilm growth increased tracer retention and back mixing by 33%, at 50% media filling ratio. A 5% increase on tracer retention was also reported by Morgan-Sagastume and Noyola (2008). For Media 4 and 5, the biofilm contributed to a reduction in mean residence time,  $5.25\pm 0.34$ h and  $3.02\pm 0.65$ h compared to theoretical values of 6.8 and 4h. Hydraulic efficiency of  $74\pm 1$  and  $63\pm 2\%$  were registered for Media 4 and 5, respectively, with effective volumes of  $1.14\pm 0.02$  and  $1.10\pm 0.05$  m<sup>3</sup> (Table 3-3). Dispersion coefficient values were very similar within the media value of 0.22; this value was indicative of intermediate to high dispersion. The parameter, N-CSTR, also exhibited similarities within the media, with values of  $2.81\pm 0.05$  were calculated for Media 1,  $2.98\pm 0.01$  for Media 2 and  $2.78\pm 0.05$  for Media 3. Media 4 and 5 shifted the flow behaviour towards a plug flow with values of N-CSTR of  $3.0\pm 0.23$  for Media 4 and  $3.0\pm 0.01$  for Media 5.

**Table 3-3 Summary of the hydraulic parameters and aeration efficiency at operation conditions with biofilm attached. Media 1 (Biofil), Media 2 (Bioball), Media 3 (Biomarble), Media 4 (Biopipe) and Media 5 (Biotube). Media was supplied by Warden Biomedica (<http://www.wardenbiomedica.com/>).**

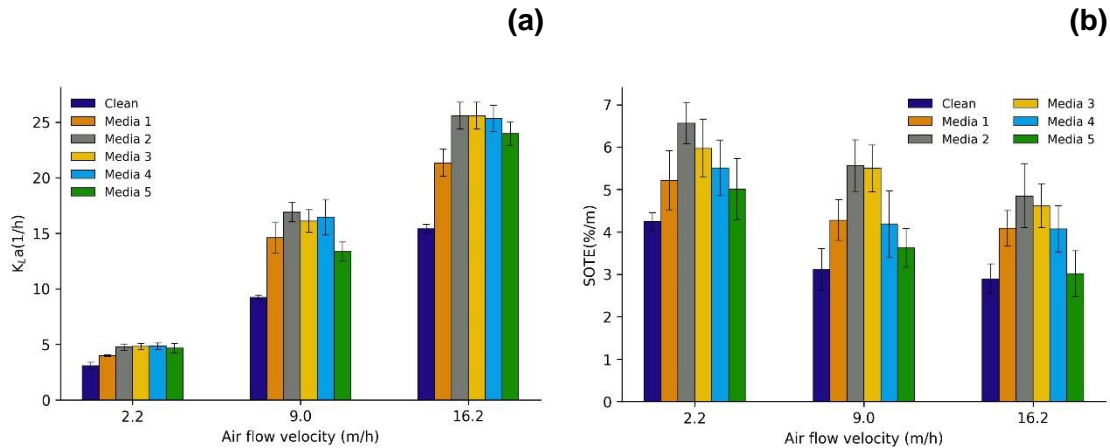
	Media 1	Media 2	Media 3	Media 4	Media 5
$t_m$ (h)	16.9±0.3	11.2±0.6	8.7±0.3	5.2±0.3	3.0±0.6
$\delta$	0.22±0.03	0.22±0.04	0.22±0.03	0.21±0.04	0.22±0.04
N-CSTR	2.81±0.05	2.98±0.01	2.78±0.05	3.0±0.23	3.0±0.01
$V_e$ (m <sup>3</sup> )	1.34±0.02	1.33±0.05	1.68 ±0.02	1.14±0.02	1.10±0.05
HE (%)	89±2	93±5	100±2	74±1	63±2
$\alpha$ factor	0.80±0.10	0.59±0.17	0.63±0.17	0.62±0.20	0.63±0.03
$\alpha$ SOTE (%/m)	3.98±0.10	3.65±0.17	3.50±0.17	2.72±0.20	1.58±0.03
$\alpha$ K <sub>la</sub> (1/h)	4.71	5.94	8.64	11.02	12.82
$\alpha$ SAE (kgO <sub>2</sub> /kWh)	3.65	2.85	2.75	2.28	1.70
kWh/kgO <sub>2</sub> consumed	0.6	0.6	0.5	0.5	0.4
kWh/m <sup>3</sup> wastewater	0.23	0.19	0.19	0.17	0.14

### 3.3.3 Clean water oxygen mass transfer

The results obtained for  $k_{LA}$  for each media are presented in Figure 3-2a. The results demonstrated that aeration mass transfer in clean water was enhanced by the presence of the media. The  $k_{LA}$  values without media varied from 3.07, 9.53 and 15.44 1/h at aeration rates of 2.2, 9.0 and 16.2  $m^3/m^2.h$ , respectively. When the media was introduced the  $k_{LA}$  increased from 3.97 and 25.57 1/h. The  $k_{LA}$  in clean water was significantly different for all the media ( $p < 0.05$ ). Media 1 improved  $k_{LA}$  from 23-37%, Media 2 from 35-45%, Media 3 from 36-45%, Media 4 from 37-44% and Media 5 from 31-36%, when compared with clean water. Comparing the results obtained within the media, statistical analysis using the paired  $t$  tests was performed and this demonstrated that  $k_{LA}$  for Media 1 and 5 were statistically different ( $p < 0.05$ ) from Media 2, 3 and 4.

A  $k_{LA}$  increase from 21-55% has been reported by different authors that studied the influence of carrier media on aeration (Collignon, 2006; Jing, Feng and Li, 2009). The presence of carrier media had been shown to influence bubble break-up, decreasing bubble size, increasing gas hold-up and hence the contact time between the gas and liquid. Limited studies have been conducted on the impact of media physical properties on oxygen mass transfer in moving attached growth systems. Using different packing material properties (size, density and shape), Fujie et al. (1992), found that physical properties play an important role in gas-liquid oxygen mass transfer, by bubble hold up and dispersion. Among the materials studied, smaller material promoted bubble coalescence, reducing  $k_{LA}$ , while larger materials increased  $k_{LA}$  by bubble hold-up. Three plastic carrier media, two cylindrical and a circular flat shaped, were studied by Collignon (2006) using coarse bubble aeration. The results confirmed an improvement in oxygen transfer by 6-22% in the presence of cylindrical media at a 40% filling ratio, whereas the addition of circular flat shaped media affected the  $k_{LA}$  negatively. The different reactor designs (water depth), type of dispersed air system, media carrier and filling ratios used, make comparisons between studies challenging. Considering the clean water  $k_{LA}$  data in more detail, and comparing against other studies, the values registered in this study were higher. However, when the influence of water depth was considered, the values were lower (15.67 g

$O_2/m^3.m$ ) than the ones obtained by Collignon (2006)  $21.18 g O_2/m^3.m$ . The aeration efficiency ( $g O_2/m^3$  water per meter of submergence) was calculated following Al-Ahmady (2011); considering the air flow velocity and the oxygen transfer capacity of the system ( $g O_2/m^3.hr$ ). Ødegaard (2015) presented values of  $10 g O_2/m^3$  water per meter of submergence in clean water, 13 and 15  $g O_2/m^3.m$  when a  $500 m^2/m^3$  media was used at 30 and 50% filling ratio.



**Figure 3-2  $k_L a$  (a) and SOTE (%/m) (b) measurements in clean water and with 5 different media at three air flow velocities. Media 1 (Biofil), Media 2 (Bioball), Media 3 (Biomarble), Media 4 (Biopipe) and Media 5 (Biotube). Media was supplied by Warden Biomedia (<http://www.wardenbiomedia.com/>).**

The SOTE (%/m) with media at  $2.2 m^3/m^2.h$  ranged from 5.01-6.56 %/m, 3.62-5.56 %/m at 9.0 m/h and 3.02-4.85 %/m at  $16.2 m^3/m^2.h$  (Figure 3-2b). Lower values were registered by Collignon (2006) at a 40% media filling ratio and  $17 m^3/m^2.h$ , 2.27 and 2.41%/m and Pham et al. (2008) at a 50% filling ratio registered values of SOTE of 2.6 %/m at an air flow velocity of  $9.9 m^3/m^2.h$ . The values of SOTE obtained were also slightly higher compared to the theoretical design values used in MBBRs with coarse bubble diffusers that are usually around 2.5 to 3.5 %/m (McQuarrie and Boltz, 2011). The addition of media improved the SOTE (%/m) by 10 to 44%. SOTE enhancement in Collignon (2006) was 22% compared to the results achieved without media. In Sander, Behnisch and Wagner (2017) the addition of carrier media increased SOTE from 2.9%/m (without media) to 5.6%/m (at 50% filling ratio) using a coarse bubble aeration.

### 3.3.4 Oxygen mass transfer under operational conditions (with biofilm growth)

To estimate the impact of the media with biofilm on oxygen transfer efficiency (OTE), off-gas tests were conducted under steady-state conditions. Values of  $\alpha$  factor of  $0.80\pm 0.10$ ,  $0.59\pm 0.17$ ,  $0.63\pm 0.17$ ,  $0.62\pm 0.20$  and  $0.63\pm 0.03$  were attained with Media 1, 2, 3, 4 and 5, respectively (Table 3-3). The  $\alpha$  factors obtained were within the typical values for coarse bubble aeration, 0.55 and 0.94 (Groves et al., 1992) and consistent with an  $\alpha$  factor of 0.63 calculated in Sander, Behnisch and Wagner (2017). A high variability in  $\alpha$  factors was registered during the sampling. This was mainly due to the natural variability of the influent and operation limitations such as reactor depth and operation with no defined DO set point. The  $\alpha$ SOTE obtained were  $3.98\pm 0.10$ ,  $3.65\pm 0.17$ ,  $2.83\pm 0.17$ ,  $2.72\pm 0.20$ , and  $1.58\pm 0.03\%/m$  for Media 1, 2, 3, 4 and 5, respectively (Table 3-3). These values are consistent with the ones achieved by Pham et al. (2008) of 2.9%/m and  $\alpha$  value of 0.6 with plastic carrier media and fine bubble aeration. A  $\alpha$ SOTE in the range of 3.79 and 3.88 %/m using fine bubble aeration was achieved in a full scale IFAS, with flat shaped carrier media with  $\alpha$  values varying from 0.57 up to 0.85 (Kappel, 2009). An  $\alpha$ SOTE of 3.72 %/m with coarse bubble aeration was also reported by Sander, Behnisch and Wagner (2017), respectively.

The energy efficiency values at operation conditions were 3.65, 2.85, 2.75, 2.28 and 1.7 kg O<sub>2</sub>/kWh for Media 1, 2, 3, 4 and 5, respectively. The values were higher than the ones described for coarse bubble 0.6-1.5 kg O<sub>2</sub>/kWh in Stenstrom and Rosso (2008) and similar to the ones specified by Kappel (2009) for an IFAS within 1.5-3.6 kg O<sub>2</sub>/kWh using fine bubble aeration. The values of oxygen consumption per cubic metre of wastewater treated ranged from 0.14-0.23 kWh/m<sup>3</sup>, the lower range values were registered with Media 5 and the higher value in Media 1. Compared with the literature, the aeration energy consumption registered by Belloir et al. (2015) in two oxidation ditches was 0.95 kWh/m<sup>3</sup> and 0.64 kWh/m<sup>3</sup>. Values in the order of 0.15-0.7 kWh/m<sup>3</sup> were estimated for ASP in Bodik and Kubaska (2013). An MBBR operated with oxygen had been supplied continuously registered a 0.25 kWh/m<sup>3</sup> (Amatya, 2015). Other studies presented values of 0.17 kWh/m<sup>3</sup> (Rusten and Paulsrud, 2009).

### 3.3.5 Influence of media physical properties on hydrodynamics and oxygen mass transfer

#### 3.3.5.1 Without biofilm growth

The results obtained on HE and on oxygen mass transfer efficiency (SOTE) were correlated with the carrier media protected surface area (Figure 3-3). A linear fitting of  $R^2= 0.67$  and  $R^2= 0.48$  suggested that the protected surface area does not correlate with hydraulic efficiency and SOTE.

Other physical parameters, such as porosity, have been mentioned in the literature as more suitable, compared to the specific surface area, to describe hydraulic behaviour and performance on an upflow biofilter (Show and Tay, 1999). Others suggested that additional media properties should be considered and not only surface area, such as voidage (Dupla et al., 2006). Physical properties (length to diameter ratio) were indicated as an influential parameter on the fluidization velocity (Zhong et al. 2008).

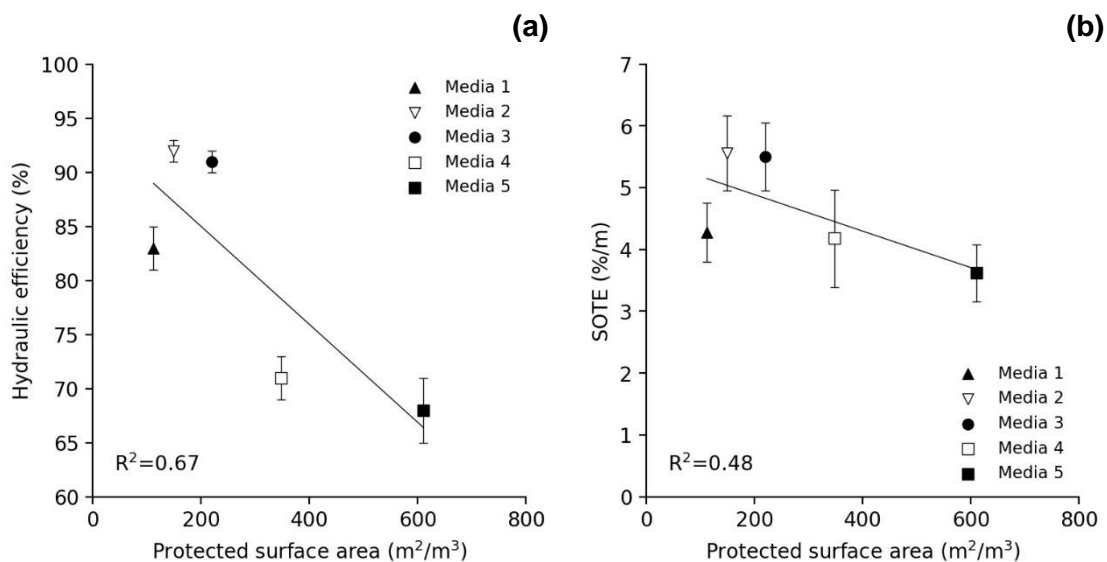
To gain a better understanding, other physical properties of the five media studied were investigated and correlated with HE and SOTE. Parameters such as: diameter, length to diameter ratio (L:D), sphericity, Sauter mean diameter, shape factor and voidage were considered and correlated with HE and on oxygen mass transfer efficiency SOTE (Appendix A). Due to the three-dimensional geometric shapes of the carrier media other geometric properties were used to normalise the carrier media shape. Dimensionality ( $D_i$ ) was used and was defined by Jones (2011) as the “maximum-dimension-normalised sum” and calculated using equation (3-20) for a sphere and equation (3-21) for a cylinder. Where  $D$ ,  $r$  and  $L$  are the radius and side/edge lengths, respectively.

$$D_i = (L_x + L_y + L_z) / \max(L_x, L_y, L_z) \quad (3-20)$$

$$D_i = 1 + (4 \cdot r \cdot L / [2r^2 + L^2]) + \left( 2r / \left[ \sqrt{4r^2 + L^2} \right] \right) \quad (3-21)$$

A strong correlation was given between the combination of  $D_i$  and  $V_{oi}$  with HE ( $R^2$  of 0.89) (Figure 3-4a). A relationship between dimensionality and voidage influenced the wastewater flow and mixing impacting the reactor hydraulic efficiency. The spherical shape media with high voidage (90-95%) promoted a

better use of the reactor effective volume (1.33-1.44 m<sup>3</sup>) compared with the cylindrical shape media, with lower voidage (80-82.5%) (reactor effective volume of 0.93-0.96 m<sup>3</sup>). The lower voidage (80-82.5%) and the smaller size of the cylindrical media (Ø21.5 and 12 mm) compared with larger spherical size media (Ø95, 65 and 46 mm) influenced the flow path when the air flow velocity was 2.2 m<sup>3</sup>/m<sup>2</sup>.h, and this later improved the reactor effective volume by 29%. At higher air flow velocity (9 m<sup>3</sup>/m<sup>2</sup>.h) the difference between media was not significant, effective volume in spherical media was 5% higher than cylindrical media. Increasing aeration velocity from 2.2 to 9 m<sup>3</sup>/m<sup>2</sup>.h promoted greater turbulence that had a positive effect on the hydraulic efficiency when cylindrical media was used 87±7% compared to 68±1%.

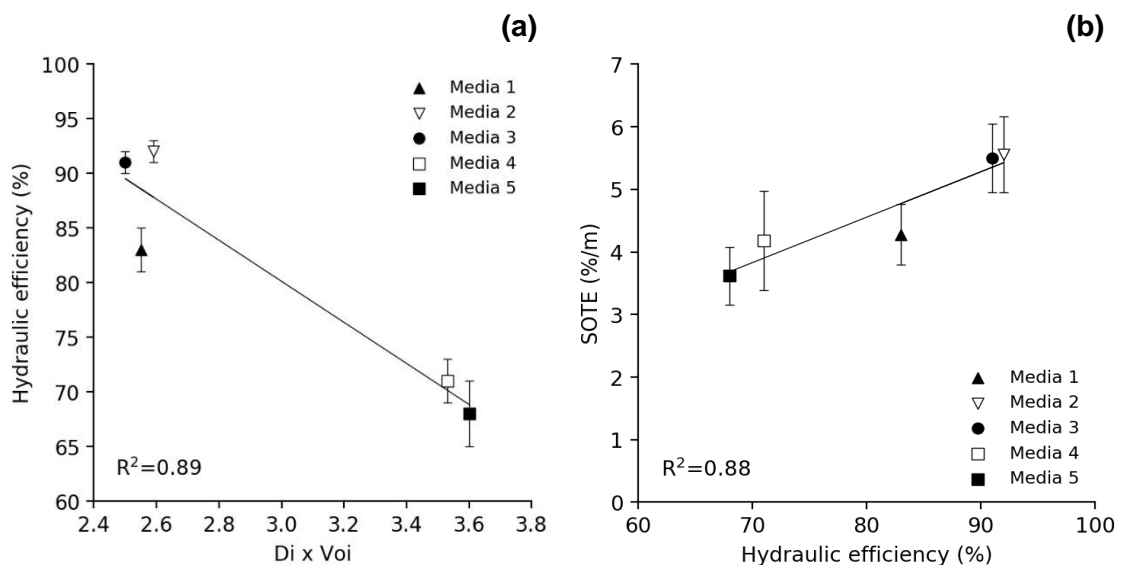


**Figure 3-3 Correlation between hydraulic efficiency (a) and SOTE (%/m) (b) with the media protected surface area (m<sup>2</sup>/m<sup>3</sup>). Media 1 (Biofil), Media 2 (Bioball), Media 3 (Biomarble), Media 4 (Biopipe) and Media 5 (Biotube). Media was supplied by Warden Biomedica (<http://www.wardenbiomedica.com/>).**

Regarding the results achieved during the oxygen mass transfer tests in clean media, a strong correlation was attained when comparing SOTE with HE (R<sup>2</sup>=0.88) (Figure 3 4b).



When spherical media were added to the reactor, SOTE improved by  $38\pm 10\%$  compared with cylindrical shape media;  $16\pm 6\%$ . Large voidage and the shape of Media 1 appeared to break up the bubbles enhancing the SOTE by 27% when compared with no media in the reactor. However, the shearing effect and bubble hold up was insufficient to promote greater oxygen mass transfer when compared with 44% and 43% enhancement obtained with Media 2 and 3, respectively. Once the larger number of media inside the tank was coupled with the smaller voidage they appear to break up the bubbles, retaining them for longer in the tank. A smaller improvement on SOTE was registered when using the cylindrical shape and lower voidage media (Media 4 and 5), 20 and 12%, respectively. Although gas bubble visualisation experiments were not completed in this study, it was hypothesised that, the increased number of media promoted higher collision within the bubbles and bubble entrainment, hindering the oxygen mass transfer by aggregating the smaller bubbles into larger bubbles reducing the contact between the gas and the liquid. A similar effect was reported in Dean and Webb (1986) where a solid fraction up to 0.10 (1-Voi) increased the oxygen mass transfer, however a further increase in solid, decreased the oxygen mass transfer due to the bubble coalescing effect. Negative influence in  $k_L a$  was also observed by Ferreira et al. (2010) and Freitas and Teixeira (2001) when an increase in solids concentration promoted bubble collision and subsequent coalescence and reduction of specific interfacial area.



**Figure 3-4 Correlation between hydraulic efficiency and  $Di \times Voi$  (a) and correlation between SOTE (%/m) and hydraulic efficiency (b) without biofilm growth. Media 1 (Biofil), Media 2 (Bioball), Media 3 (Biomarble), Media 4 (Biopipe) and Media 5 (Biotube). Media was supplied by Warden Biomedia (<http://www.wardenbiomedia.com/>).**

### 3.3.5.2 Operational conditions with biofilm growth

The same data analysis was performed when biofilm was developed in the media. Considering the same combination of parameters, as in clean conditions, dimensionality and voidage. Nevertheless, voidage reduction was considered and calculated based on the biofilm growth (thickness) and total surface area correction. For the spherical media, Alonso et al. (1997) and Dumont, Woudberg and Van Jaarsveld (2016) equation was used (3-22). Where  $Voi$  is the voidage with biofilm,  $L_f$  is the biofilm thickness,  $Voi_0$  is the initial voidage, without biofilm,  $r$  is the radius and  $n$ , a coordination number calculated based on equation (3-23), as described by Dullien (1992). For the cylindrical shape media, the equation presented in Goode (2010), was used (3-24).

$$Voi = 1 - (1 - Voi_0) \left[ \left(1 + \frac{L_f}{r}\right)^3 - \frac{n}{4} \left(\frac{L_f}{r}\right)^2 \left(2 \frac{L_f}{r} + 3\right) \right] \quad (3-22)$$

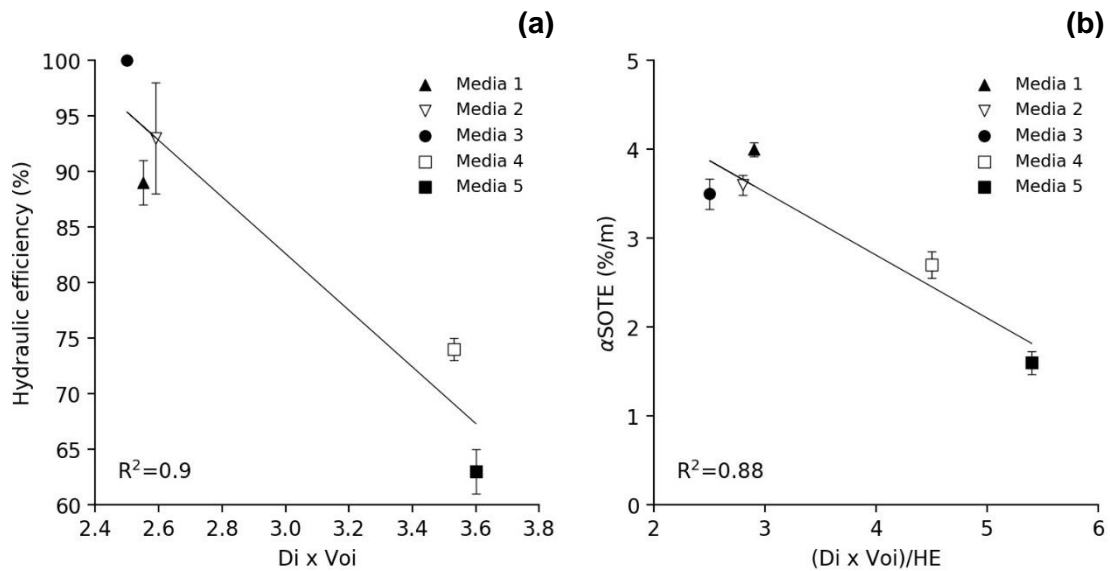
$$Voi_0 = 1.072 - 0.1193n + 0.004312n^2 \quad (3-23)$$

$$a = \left(8(r - 2L_f) + 2\pi(r - 2L_f)\right)h + \left(\pi r^2 - \pi(r - 2L_f)^2\right) \quad (3-24)$$

Thickness values when the biofilm was fully developed were considered. For the spherical media, Media 1, 2 and 3 the thickness was of  $426 \pm 88$ ,  $375 \pm 45$  and  $328 \pm 70$   $\mu\text{m}$ , respectively. For the cylindrical media, an average biofilm thickness of  $449 \pm 82$   $\mu\text{m}$  for Media 4 and  $268 \pm 79$   $\mu\text{m}$  for Media 5 were measured. Taking into consideration the voidage reduction, hydraulic efficiency was compared with dimensionality and voidage for each media, and a correlation of  $R^2 = 0.90$  was obtained (Figure 3-5a).

Due to the media physical structure, the biofilm growth (thickness) in Media 1, 2 and 3 did not significantly impact the media voidage. However, for Media 4 and 5, the biofilm thickness led to a reduction in voidage of 6 to 14%, respectively.

Biofilm accumulation in the internal parts of Media 4 and 5, reduced the hydraulic diameter for water to flow through, creating preferential flow paths, accelerating short-circuiting due to media clogging, and therefore decreasing hydraulic efficiency by  $74\pm 1$  and  $63\pm 2\%$ , respectively. It was estimated that voidage could achieve a further 12 and 26% if the biofilm thickness reaches 1000  $\mu\text{m}$ , for example under operation with high organic loads. Regarding the oxygen mass transfer, a higher correlation was achieved when comparing the  $\alpha\text{SOTE}$  with corrected voidage and hydraulic efficiency,  $R^2$  of 0.88 (Figure 3-5b). Furthermore, the SOTE correlated well with protected surface area after biofilm growth ( $R^2= 0.95$ ).



**Figure 3-5 Correlation between hydraulic efficiency (a) and  $\alpha\text{SOTE}$  (b) with biofilm developed on the carrier at steady state. Media 1 (Biofil), Media 2 (Bioball), Media 3 (Biomarble), Media 4 (Biopipe) and Media 5 (Biotube). Media was supplied by Warden Biomedica (<http://www.wardenbiomedica.com/>).**

The strong correlations between hydraulic efficiency, dimensionality and voidage ( $R^2= 0.90$ ) presented within this study demonstrate that carrier physical properties do have an impact in the reactor hydraulic regime. The findings support the importance of shape and voidage on the carrier design, which has been neglected in favour of an increase in surface area of media per volume. The conventional cylindrical shaped media, with smaller open voids are more likely to clog as biofilm thickness increases, thereby not allowing efficient contact between

the biofilm and wastewater. The poor mixing, associated with channelling and short-circuiting make this media less efficient hydraulically. Similar observations were performed in other studies, where a larger and flat shaped media with small pore spaces were also affected by clogging. This is especially when used at high loading conditions due to high biofilm growth, and despite their high specific surface area (Forrest, Delatolla and Kennedy, 2016). These results are also in line with Show and Tay (1999), where a decrease in media voidage, induced clogging and dead spaces, resulting in lower hydrodynamic and treatment performance. The poor mixing and the slightly negative effect on oxygen transfer of large and flat shaped media was also observed by Collignon (2006), by decreasing bubble retention time and increasing bubble coalescence. Information obtained from this work is expected to develop into a useful reference for media size and shape optimisation. These will act to improve process performance providing opportunities for capital and operational cost savings, making this process more competitive with alternative technologies.

### **3.4 Conclusions**

- The presence of media and aeration had a positive impact on the reactor effective volume increasing hydraulic efficiency (HE) by 41-53%, compared with no media, holding the tracer for longer period inside the reactor, and reducing the amount of short-circuiting and dead zones.
- The presence of media had improved aeration performance in comparison to results achieved without media. In clean water tests, the media enhanced the overall oxygen transfer efficiency by 23-45%.
- The biofilm developed on the carrier media increased HE when spherical media (Media 1, 2 and 3) was used by  $89\pm 3$ ,  $93\pm 5$  and 100%, respectively. For Media 4 and 5, the biofilm contributed to a reduction in HE, with values of  $74\pm 1$  and  $63\pm 2$ %, respectively.
- Physical properties, dimensionality and voidage were highly correlated with HE without and with biofilm ( $R^2= 0.89$  and  $0.90$ ), in comparison to

protected surface area ( $R^2= 0.67$ , without biofilm and  $R^2= 0.76$  with biofilm growth).

- Physical properties, dimensionality and voidage, associated with hydraulic efficiency also correlated with oxygen mass transfer efficiency without ( $R^2= 0.92$ ). and with biofilm ( $R^2= 0.88$ ), in comparison to protected surface area ( $R^2= 0.76$ , without biofilm and  $R^2= 0.95$  with biofilm growth).
- The combination of parameters: dimensionality and voidage, can be used to optimise media size and shape, enhancing mixing and oxygen mass transfer; and ultimately contributing towards energy savings and higher removal efficiencies.

### **Acknowledgements**

The authors acknowledge the financial support from Warden Biomedica and Cranfield University.

### **3.5 References**

Al-Ahmady, K.K. (2006) 'Analysis of oxygen transfer performance on sub-surface aeration systems', *International Journal of Environmental Research and Public Health*, 3(3), pp. 301–308.

Alonso, C., Suidan, M.T., Sorial, G.A., Lee Smith, F., Biswas, P., Smith, P.J. and Brenner, R.C. (1997) 'Gas treatment in trickle-bed biofilters: Biomass, how much is enough?', *Biotechnology and Bioengineering*, 54(6), pp. 583–594.

Amatya, A. (2015) Study on Process Performance and Evaluation of Dala Vatten's Two Municipal Wastewater Treatment. Msc thesis. Royal Institute of Technology (KTH). Available at: <http://www.diva-portal.org/smash/record.jsf?pid=diva2%3A952287&dswid=8384> (Accessed: 16 June 2016).

ASCE (2007) ASCE Standard: Measurement of Oxygen Transfer in Clean Water. Virginia: American Society of Civil Engineers.

ASCE (1997) ASCE Standard: Standard Guidelines for In-process Oxygen Transfer Testing. New York: American Society of Civil Engineers.

Belloir, C., Stanford, C. and Soares, A. (2015) 'Energy benchmarking in wastewater treatment plants: The importance of site operation and layout', *Environmental Technology*, 36(2), pp. 260–269.

Bodik, I. and Kubaska, M. (2013) 'Energy and Sustainability of Operation of a Wastewater Treatment Plant', *Environment Protection Engineering*, 39(2), pp. 15–24.

Brannock, M., Wang, Y. and Leslie, G. (2010) 'Mixing characterisation of full-scale membrane bioreactors: CFD modelling with experimental validation', *Water Research*, 44(10), pp. 3181–3191.

Collignon, D. (2006) Insight into oxygen transfer in IFAS processes. MSc thesis. Cranfield University. Available at: <http://cclibweb-3.central.cranfield.ac.uk/handle/1826.1/2750> (Accessed: 26 August 2015).

Dean, J.F. and Webb, C. (1986) 'Oxygen Mass Transfer and Particle Circulation in an Immobilised Cell Bioreactor.', *Applied Biochemistry and Biotechnology*, 15(3), pp. 227–244.

Dullien, F.A.L. (1992) *Porous Media: Fluid Transport and Pore Structure*. 2nd ed. San Diego: Academic Press.

Dumont, E., Woudberg, S. and Van Jaarsveld, J. (2016) 'Assessment of porosity and biofilm thickness in packed beds using porous media models', *Powder Technology*, 303, pp. 76–89.

Dupla, M., Comeau, Y., Parent, S., Villemur, R. and Jolicoeur, M. (2006) 'Design optimization of a self-cleaning moving-bed bioreactor for seawater denitrification', *Water Research*, 40(2), pp. 249–258.

European Parliament. Council of the European Union (1991) Council Directive concerning urban waste-water treatment (91/271/EEC). Available at: <http://eur->

lex.europa.eu/legal-content/EN/TXT/?uri=celex%3A31991L0271 (Accessed: 4 October 2015).

Ferreira, A., Ferreira, C., Teixeira, J.A. and Rocha, F. (2010) 'Temperature and solid properties effects on gas-liquid mass transfer', *Chemical Engineering Journal*, 162(2), pp. 743–752.

Fogler, H.S. (2006) *Elements of Chemical Reaction Engineering*. 4th edn. Pearson and Education (eds.) London.

Forrest, D., Delatolla, R. and Kennedy, K. (2016) 'Carrier effects on tertiary nitrifying moving bed biofilm reactor: An examination of performance, biofilm and biologically produced solids', *Environmental Technology*, 37(6), pp. 662–671.

Freitas, C. and Teixeira, J.A. (2001) 'Oxygen mass transfer in a high solids loading three-phase internal-loop airlift reactor', *Chemical Engineering Journal*, 84(1), pp. 57–61. Available at: 10.1016/S1385-8947(00)00274-6 (Accessed: 25 October 2015).

Fujie, K., Hu, H.-Y., Keda, Y. and Urano, K. (1992) 'Gas-liquid oxygen transfer characteristics in an aerobic submerged biofilter for the wastewater treatment', *Chemical Engineering Science*, 47(13/14), pp. 3745–3752.

Garcia-ochoa, F. and Gomez, E. (2009) 'Bioreactor scale-up and oxygen transfer rate in microbial processes: An overview', *Biotechnology Advances*, 27, pp. 153–176.

Goode, C. (2010) *Understanding biosolids dynamics in a moving bed biofilm reactor*. PhD thesis. University of Toronto. Available at: [https://tspace.library.utoronto.ca/bitstream/1807/24758/6/Goode\\_Christopher\\_J\\_201006\\_PhD\\_Thesis.pdf](https://tspace.library.utoronto.ca/bitstream/1807/24758/6/Goode_Christopher_J_201006_PhD_Thesis.pdf) (Accessed: 18 November 2014).

Gourich, B., Vial, C., Azher, N. El, Soulami, M.B. and Ziyad, M. (2008) 'Influence of hydrodynamics and probe response on oxygen mass transfer measurements in a high aspect ratio bubble column reactor: Effect of the coalescence behaviour of the liquid phase', 39, pp. 1–14.

- Groves, K.P., Daigger, G.T., Simpkin, T.J., Redmon, D.T. and Ewing, L. (1992) 'Evaluation of oxygen transfer efficiency and alpha-factor on a variety of diffused aeration system', *Water Environment Research*, 64(5), pp. 691–698.
- Herrling, M.P., Guthausen, G., Wagner, M., Lackner, S. and Horn, H. (2015) 'Determining the flow regime in a biofilm carrier by means of magnetic resonance imaging', *Biotechnology and Bioengineering*, 112(5), pp. 1023–1032.
- Holloway, T.G. and Soares, A. (2018) 'Influence of internal fluid velocities and media fill ratio on submerged aerated filter hydrodynamics and process performance for municipal wastewater treatment', *Process Safety and Environmental Protection*, 114, pp. 179–191.
- Jenkins, D. and Wanner, J. (eds.) (2014) *Activated Sludge - 100 Years and Counting*. London: IWA Publishing.
- Jing, J.Y., Feng, J. and Li, W.Y. (2009) 'Carrier effects on oxygen mass transfer behavior in a moving bed biofilm reactor', *Asia-Pacific Journal of Chemical Engineering*, 4, pp. 618–623.
- Jones, A. (2011) 'The characterisation of irregularly-shaped particles', *Astronomy & Astrophysics*, 528 (15968), p. A98.
- Kappel, C. (2009) *Simplified Evaluation of the Operational Oxygen Transfer Efficiency of a novel dispersed fixed film activated sludge process*. MSc thesis. Cranfield University. Available at: <http://cclibweb-3.central.cranfield.ac.uk/handle/1826.1/2214> (Accessed: 27 September 2017).
- Levenspiel, O. (1999) *Chemical Reaction Engineering*. 3rd edn. John Wiley & Sons Inc. (ed.) New York.
- Li, S., Nan, J. and Gao, F. (2016) 'Hydraulic characteristics and performance modelling of a modified anaerobic baffled reactor (MABR)', *Chemical Engineering Journal*, 284, pp. 85–92.



Li, S., Nan, J., Li, H. and Yao, M. (2015) 'Comparative analyses of hydraulic characteristics between the different structures of two anaerobic baffled reactors (ABRs)', *Ecological Engineering*, 82, pp. 138–144.

Longo, S., D'Antoni, B.M., Bongards, M., Chaparro, A., Cronrath, A., Fatone, F., Lema, J.M., Mauricio-Iglesias, M., Soares, A. and Hospido, A. (2016) 'Monitoring and diagnosis of energy consumption in wastewater treatment plants. A state of the art and proposals for improvement', *Applied Energy*, 179, pp. 1251–1268.

Mann, A. (1997) *A Comparison of Floating and Sunken Media Biological Aerated Filters (BAF)*. PhD thesis. Cranfield University.

McQuarrie, J.P. and Boltz, J.P. (2011) 'Moving Bed Biofilm Reactor Technology: Process Applications, Design, and Performance', *Water Environment Research*, 83(6), pp. 560–575.

Morgan-Sagastume, J.M. and Noyola, A. (2008) 'Evaluation of an aerobic submerged filter packed with volcanic scoria', *Bioresource Technology*, 99(7), pp. 2528–2536.

Ødegaard, H. (2015) 'Hybrid activated sludge/biofilm processes (IFAS)', *Activated sludge: 100 plus 1 years New trends and perspectives*. Palermo: University of Palermo. Available at: 'Hybrid activated sludge/biofilm processes (IFAS)', *Activated sludge: 100 plus 1 years New trends and perspectives*. (Accessed: 14 May 2016).

Ødegaard, H., Gisvold, B. and Strickland, J. (2000) 'The influence of carrier size and shape in the moving bed biofilm process', *Water Science and Technology*, 41(4–5), pp. 383–391.

Pham, H., Viswanathan, S. and Kelly, R.F. (2008) 'Evaluation of Plastic Carrier Media Impact on Oxygen Transfer Efficiency with Coarse and Fine Bubble Diffusers', *WEFTEC 2008*. New Orleans: Water Environment Federation, p. 5069–5079(11).

Rosso, D., Lothman, S.E., Jeung, M.K., Pitt, P., Gellner, W.J., Stone, A.L. and Howard, D. (2011) 'Oxygen transfer and uptake, nutrient removal, and energy

footprint of parallel full-scale IFAS and activated sludge processes', *Water Research*, 45(18), pp. 5987–5996.

Rusten, B., Eikebrokk, B., Ulgenes, Y. and Lygren, E. (2006) 'Design and operations of the Kaldnes moving bed biofilm reactors', *Aquacultural Engineering*, 34(3), pp. 322–331.

Rusten, B., Ødegaard, H. and Lundar, A. (1992) 'Treatment of dairy wastewater in a novel moving bed biofilm reactor', *Water Science and Technology*, Vol.26, pp. 703–711.

Rusten, B. and Paulsrud, B. (2009) 'Environmental technology verification of a biofilm process for high efficiency nitrogen removal from wastewater', *WEFTEC 2009*. Orlando: Water Environment Federation, pp. 4378–4391.

Sander, S., Behnisch, J. and Wagner, M. (2017) 'Energy, cost and design aspects of coarse and fine bubble aeration systems in the MBBR IFAS process', *Water Science and Technology*, 75(4), pp. 890–897.

Sen, D. and Randall, C.W. (1996) 'Mathematical Model for a Multi-CSTR Integrated Fixed Film Activated Sludge (IFAS) System', *WEFTEC 96*. Dallas, Texas: Water Environment Federation.

Sharma, M.K. and Kazmi, A.A. (2015) 'Effect of physical property of supporting media and variable hydraulic loading on hydraulic characteristics of advanced onsite wastewater treatment system.', *Environmental Technology*, 36(11), pp. 1414–1422.

Show, K.-Y. and Tay, J.H. (1999) 'Influence of support media on biomass growth and retention in anaerobic filters', *Water Research*, 33(6), pp. 1471–1481.

Stenstrom, M.K. and Rosso, D. (2008) 'Aeration and Mixing', in Henze, M., Loosdrecht, M. C. M. van, Ekama, G. A. and Brdjanovic, D. (eds.) *Biological Wastewater Treatment, Principles, Modelling and Design*. London: IWA Publishing.

Sun, L., Zhang, F., Liu, C., Bi, X., Cheng, L., Li, S., Liu, Y. and Qiao, Z. (2016) 'Effect of bio-carrier filling rate on oxygen transfer coefficient of different diffusers in MBBR process', *Desalination and Water Treatment*, 57(39), pp. 18234–18239.

Tomlinson, E.J; Chambers, B. (1979) *Effect of longitudinal mixing on the settleability of activated sludge*. Stevenage, England.

Zhong, W., Jin, B., Zhang, Y., Wang, X. and Xiao, R. (2008) 'Fluidization of Biomass Particles in a Gas -Solid Fluidized Bed', *Energy & Fuels*, 22(12), pp. 4170–4176.



## 4 INFLUENCE OF CARRIER MEDIA PHYSICAL PROPERTIES ON START-UP OF MOVING ATTACHED GROWTH SYSTEMS

J. Dias<sup>a</sup>, M. Bellingham<sup>b</sup>, J. Hassan<sup>b</sup>, M. Barrett<sup>b</sup>, T. Stephenson<sup>a</sup>, A. Soares<sup>a</sup>

<sup>a</sup>*Cranfield University Water Sciences Institute, Cranfield, MK43 0AL, UK.*

<sup>b</sup>*Warden Biomedica, 31 Sundon Industrial Estate, Dencora Way, Luton, Bedford, LU3 3HP, UK.*

### Abstract

The influence of carrier media physical properties on the start-up duration of a moving attached growth system such as a moving bed biofilm reactor (MBBRs) and submerged aerated filters (SAFs) was investigated. Five carrier media with different shapes (spherical and cylindrical), sizes, voidage and protected surface areas ( $112\text{-}610\text{ m}^2/\text{m}^3$ ) were studied. This study aimed to assess start-up duration using the biofilm formation rates, by considering the time required to achieve a constant attached biofilm per unit of carrier media protected surface area ( $\text{g TS}/\text{m}^2$ ). Results indicated that the spherical and lower protected surface area carrier media achieved shorter chemical oxygen demand (COD) removal start-up (18, 15 and 17 days for Media 1, 2 and 3), compared to the 23 and 24 days required by the cylindrical high surface area media (Media 4 and 5). Ammonia removal start-up was also shorter for Media 1, 2 and 3 (30, 22 and 17 days) when compared with Media 4 and 5 (46 and 47 days). During the final days of start-up, the obtainable COD removal efficiencies achieved were similar for all the media ( $88\pm 4$ ,  $81\pm 4$ ,  $85\pm 3$ ,  $80\pm 3$  and  $86\pm 4\%$  for Media 1 to 5). Media 1, 2 and 3 achieved ammonia removal efficiencies of  $50\pm 13$ ,  $64\pm 1$ ,  $63\pm 7\%$  and for Media 4 and 5 the removal efficiencies were  $32\pm 17$  and  $34\pm 5\%$  by the end of start-up. This work demonstrated that the traditional parameter, protected surface area, had weaker correlations with the biofilm formation rate for COD and ammonia removal ( $R^2= 0.83$  and  $0.76$ ). However, good correlations were observed with a combination of physical factors. These were dimensionality ( $D_i$ ) and voidage ( $V_{oi}$ ), and hydraulic efficiency (HE),  $(D_i \times V_{oi})/HE$ , which were strongly correlated with biofilm formation rates ( $R^2= 0.95$  and  $0.92$ ). Hence, this study proposes that physical properties can contribute to enhancing biofilm formation; shortening the

start-up, contributing to improved removal rates and fast commissioning of the moving attached growth system process.

**Keywords:** Biofilm formation rate, dimensionality, moving attached growth, start-up, voidage.

## 4.1 Introduction

The need to meet increasingly stringent discharge limits has made biofilm processes popular for the removal of organic pollutants and nitrogen in wastewater treatment plants (WWTPs) (Barwal and Chaudhary, 2016). Moving attached growth systems, such as submerged aerated filters (SAFs) moving bed biofilm reactor (MBBRs) and integrated fixed film activated sludge (IFAS) use buoyant carrier media as a biofilm growth support material. MBBRs have been established in the past 25 years as robust, versatile and compact solutions and have been successfully implemented in municipal and industrial wastewater treatment (Ødegaard, 2016).

The initial biofilm adhesion plays a crucial role on attached growth systems (Mao et al., 2017; Tang et al., 2017b). Due to the nature of the process the time required to achieve a well-established biofilm can vary considerably from 1 to 6 weeks (Bassin et al., 2016; Dong et al., 2015; Tang et al., 2016). Start-up duration has been a major drawback on full-scale applications especially in nitrification processes (Lackner et al., 2009) due to the slow growth rate of nitrifiers (Habouzit et al., 2014). Bacterial adhesion to support surfaces has been extensively studied, and physical (size, shape, density, roughness) and chemical properties (surface materials: plastic, foam, woven, ceramic, glass, etc. and chemical modified polymer) have been shown to strongly affect early stages of biofilm formation (Deng et al., 2016; Eldyasti, Nakhla and Zhu, 2012).

Biofilm formation occurs after initial cell adhesion to the surface of the carrier media that then leads to bacteria accumulation and extracellular polymeric substances (EPS) production. This helps bacteria bind and form the biofilm (Zhu et al., 2015). However, bacterial adhesion and subsequent biofilm development is a dynamic process that can be affected by external factors such as operating

conditions, organic and nutrient loading and hydrodynamics within the reactor (Liu and Tay, 2002; Pellicer-Nàcher and Smets, 2014). The latter plays a critical role during start-up as it controls biofilm detachment caused by shear forces (superficial air velocity) and abrasion (carrier media concentration) (Goel et al., 2011; Mao et al., 2017). To ensure a fast-start up and stable biofilm formation a balance has to be achieved between biofilm growth and detachment processes (Lackner et al., 2009).

To date, there have been limited studies on start-up of moving attached growth systems. Most studies identified in the literature are performed at the laboratory scale, and focus on strategies to accelerate the adhesion of the microorganisms, to the carrier reducing the start-up duration. Zhu et al. (2015) fed a 9 L laboratory scale reactor with easy biodegradable substrates (synthetic wastewater) inoculated with activated sludge from a secondary clarifier. The reactor was used to describe different start-up stages in biofilm systems with a cylindrical shape carrier media with a protected surface area of  $460 \text{ m}^2/\text{m}^3$ . Stable COD and ammonia removals of 92% and 50% were achieved after 6 and 14 days of start-up respectively. The same strategy was used by Bassin et al. (2016) on the start-up using two different carrier media; a cylindrical and chip shaped media with 500 and  $3000 \text{ m}^2/\text{m}^3$  at 50 and 8.3% filling ratio. Twenty to thirty days were necessary for a constant attached biofilm to be achieved. Seeding sludge and synthetic wastewater was also used in Mao et al. (2017) where start-up was compared using three carriers (two modified and one unmodified), resulting in 13, 19 and 27 days, respectively. Batch feeding and prolonged hydraulic retention times were adopted as a start-up strategy in Tang et al. (2016) using a round polyethylene ball and start-up was achieved in only 6 days. These studies mainly demonstrate the dynamic nature of the process but also highlight the variation of how start-up is interpreted and defined. Start-up in moving attached growth systems has been described in a multitude of parameters, including: biofilm growth, time to form a fully developed biofilm, biofilm activity and reactor performance (i.e. substrate removal efficiencies) (Bassin et al., 2016; Mao et al., 2017; Zhu et al., 2015).

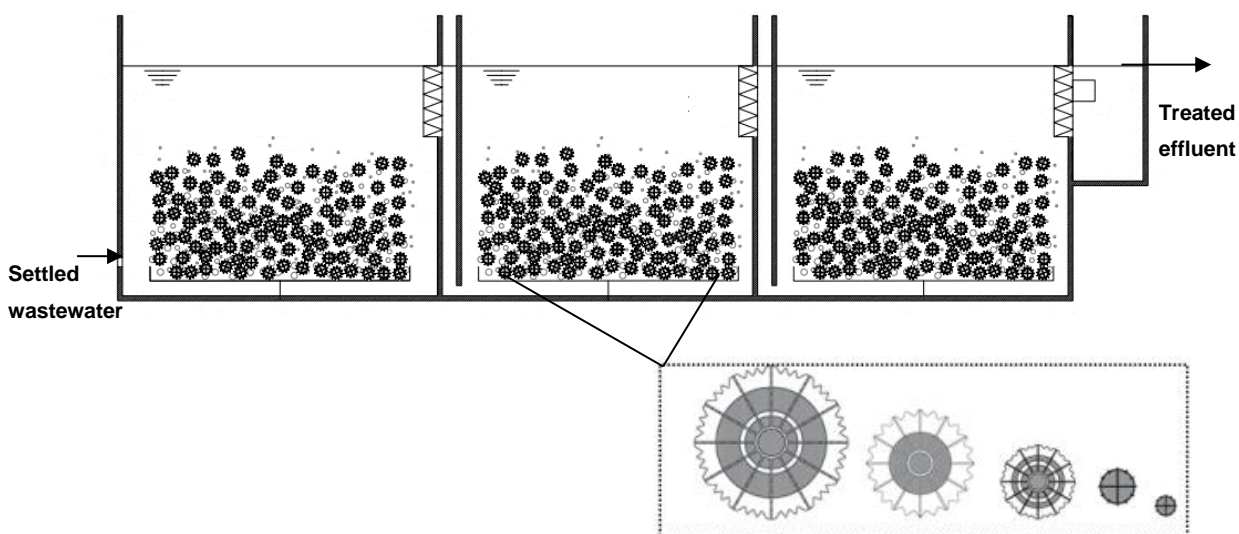
Research on moving attached growth system start-up has been limited so far and to date, no studies have investigated the relationships between carrier media physical properties and start-up. The significance of this is emphasised in the importance of start-up towards achieving low commission periods and treatment robustness during steady state. This in turn can lead to improvement of the economic competitiveness of the moving attached growth system technology. Therefore, this study aims to investigate how carrier media physical properties influence process start-up using real wastewater. The expected outcome of this work is intended to provide guidance for design and start-up of a full-scale moving attached growth system plant. Furthermore, the fast biofilm formation rate, can be of benefit for operation conditions modification (increased flow and organic loading) as well as for upgrade of existing wastewater treatment plants contributing to the extended application of moving attached growth systems.

## **4.2 Material and methods**

### **4.2.1 Pilot plant setup and operation conditions**

A 2 m<sup>3</sup> rectangular shaped pilot plant divided into three separate aerobic cells of equal volume (1.0 m width x 1.5 m length and 1.30 m height), was designed to study process start-up (Figure 4-1). Medium bubble aeration was utilised to supply the required aeration and mixing. The pilot was designed to cope with variable air velocities 3.6-18.7 m<sup>3</sup>/m<sup>2</sup>.h and wastewater flows, ranging from 2.5-18 m<sup>3</sup>/day. Air and wastewater flows were normalised per protected surface area of media. Wastewater distribution was enhanced by the instalment of two baffles on the cells. The five carrier media with different physical properties investigated were supplied by Warden Biomedica (Table 4-1). Media 1, 2 and 3 were spherical media with a protected surface area of 112, 149 and 220 m<sup>2</sup>/m<sup>3</sup> respectively whilst Media 4 and 5 were cylindrical in shape with a protected surface area of 350 and 610 m<sup>2</sup>/m<sup>3</sup> (Table 4-1). The pilot plant was fed with settled wastewater from Cranfield University wastewater treatment plant (Cranfield, UK). The pilot plant was operated at identical surface organic and ammonia loading at a filling ratio of 60% ( $V_{\text{carrier}}/V_{\text{reactor}}$ ) (Table 4-2).





**Figure 4-1 Schematic of the moving attached growth pilot plant and schematic representation of media used during the study.**

**Table 4-1 Media characteristics used in this study. Media 1 (Biofil), Media 2 (Bioball), Media 3 (Biomarble), Media 4 (Biopipe) and Media 5 (Biotube). Media was supplied by Warden Biomedia (<http://www.wardenbiomedia.com>).**

Media	Total surface (m <sup>2</sup> /m <sup>3</sup> )	Protected surface area (m <sup>2</sup> /m <sup>3</sup> )	Shape	Dimensions		Voidage (%)	Material	Density (g/cm <sup>3</sup> )
				Length (mm)	Diameter (mm)			
1	135	112	Spherical	65	95	95	Recycled polypropylene (PP)	0.97
2	220	148	Spherical	53	65	92		
3	310	220	Spherical	36	46	90		
4	600	348	Cylindrical	13	21.5	82.5		
5	1000	610	Cylindrical	8	12	80		

#### **4.2.2 Analytical methods**

The wastewater of the influent and effluent was sampled three times a week during process start-up. Samples were analysed for total 5-day carbonaceous biochemical oxygen demand (BOD<sub>5</sub>) and soluble BOD<sub>5</sub>, total and volatile suspended solids (TSS and VSS) and alkalinity according to standard methods (APHA, 2005). Total and soluble chemical oxygen demand (tCOD and sCOD), ammonium-nitrogen (NH<sub>4</sub><sup>+</sup>-N), and nitrate-nitrogen (NO<sub>3</sub><sup>-</sup>-N) were analysed using Merck cell tests kits (Merck KGaA, Darmstadt, Germany) and measured with a NOVA60 photometer (VWR, UK). Temperature, dissolved oxygen (DO) and pH

were measured onsite daily using portable meters (HACH HQ40d; Camlab, Cambridge, UK).

Attached growth biofilm on the carriers was analysed two to three times a week following the procedure described in Regmi et al. (2011). Carriers were sampled and dried at 105°C overnight and weighed. The biofilm was removed by placing the carriers in a H<sub>2</sub>SO<sub>4</sub> solution (2 N) which was stirred vigorously for 24 hours. The carriers were washed with tap water and then biofilm brushed off and dried at 105°C. The total attached biofilm was calculated based on the difference in media dry weight before and after removing all biofilm attached. The results were expressed as grams of total solids per metre square of protected surface area of carrier media (g TS/m<sup>2</sup>).

Protected surface area was defined in this study as the area of carrier covered with biofilm. The protected surface area was calculated for each media. Individual carriers were cut and separated into small pieces and photographed. Comparisons were made between the area covered with biofilm and the area without biofilm attached. All the images were analysed using ImageJ Software and biofilm coverage area determined.

Organic removal performance was evaluated according to Ødegaard (Ødegaard, 2006). An “obtainable removal rate” was calculated based on 100% solids separation. Influent tCOD and effluent sCOD were compared with flow and protected surface area.

Equation (4-1) was used to fit a curve to the attached biofilm measured (Szilágyi et al., 2013). Where  $m(t)$  is the attached biofilm as a function of time,  $m_{max}$  the maximum amount of biofilm and  $K_m$  coefficient of growth. The curve was fitted by manipulating the  $K_m$  in order to obtain the best fitted curve (Szilágyi et al., 2013).

$$m(t) = m_{max} \frac{t}{K_m + t} \quad (4-1)$$

To enable non-destructive measurements of biofilm thickness, biofilm thickness was measured through Optical Coherence Tomography (OCT) using a Thorlabs Standard (SR-OCT 930nm; Thorlabs. Germany). The obtained signal was multiplied with a factor of 1.33 (refractive index of water) to match the optical

depth with the true depth of the biofilm sample. The media was cut into small pieces with a surgical scalpel and placed on a stage under the OCT probe. Two-dimensional cross-sectional images were acquired from different pieces and locations of the carriers. Biofilm thickness was estimated based on 20 OCT images and the average of 60 measurements.

Extracellular polymeric substances (EPSs) were determined following biofilm detachment from the media using the methodology described by Le-Clech, Chen and Fane (2006). Carbohydrate and protein concentrations were determined according to the Dubois phenol-sulphuric acid method (UV490 nm) with D-glucose (Acros Organics, UK) as the standard (Dubois et al., 1956) and Protein by the Folin method (UV750 nm) with bovine serum albumin (BSA) (Sigma-Aldrich, UK) as the standard (Lowery et al., 1951) respectively.

Observed yields were calculated based on Eldyasti, Nakhla and Zhu (2012) using the linear regression between the cumulative production of volatile suspended solids (VSS) in the effluent and the cumulative COD removed ( $t\text{COD}_{in} - s\text{COD}_{out}$ ).

The detachment coefficient ( $k_{de}$ ) was estimated using the equation described in Patel, Nakhla and Zhu (2005) and Eldyasti, Nakhla and Zhu (2012) (equation (4-2)).

$$k_{de} = \frac{Q \times [VSS_{out}]}{A \times M_t} \quad (4-2)$$

Where,  $VSS_{out}$  is the solids leaving the pilot plant and Q is the flow rate,  $M_t$  is the biofilm attached per protected area of carrier media and A is the media protected surface area.

## 4.3 Results and discussion

### 4.3.1 Performance of moving attached growth system during start-up

The temperature of the wastewater varied from  $18.6 \pm 1.9$ ,  $19.8 \pm 2.3$ ,  $20.2 \pm 0.6$ ,  $13.8 \pm 2.3$  and  $13.1 \pm 1.8^\circ\text{C}$  during operation with Media 1, 2, 3, 4 and 5, respectively (Table 4-2) due to natural annual wastewater temperature fluctuations. The average total COD influent varied  $389 \pm 71$ ,  $257 \pm 44$ ,  $305 \pm 32$ ,  $236 \pm 15$  and  $251 \pm 24$  mg/L for Media 1 to 5, respectively. Ammonia concentration

varied from  $35 \pm 5$ ,  $34 \pm 11$ ,  $36 \pm 3$ ,  $38 \pm 6$  and  $31 \pm 5$  mg  $\text{NH}_4^+\text{-N/L}$  for Media 1 to 5, respectively. Natural wastewater variability resulted in changes in the COD and ammonia concentrations fed to the pilot plant. The average surface organic loading rate varied between  $8.7 \pm 1.6$ ,  $6.8 \pm 1.2$ ,  $8.3 \pm 0.9$ ,  $6.8 \pm 0.4$  and  $7.0 \pm 0.7$  g total COD/ $\text{m}^2\cdot\text{day}$  for Media 1, 2, 3, 4 and 5, respectively (Table 4-2). Nevertheless, the organic loading rates were statistically similar during the operation with the various media (except for Media 1, which demonstrated a difference in the COD loading rate ( $p \leq 0.05$ ), but the total  $\text{BOD}_5$  was comparable and between Media 2 and 4, which showed differences in the total BOD loading rate ( $p \leq 0.05$ ), but the COD was comparable). Ammonia loadings varied from  $0.8 \pm 0.1$ ,  $0.9 \pm 0.3$ ,  $1.0 \pm 0.1$ ,  $1.1 \pm 0.1$  and  $0.9 \pm 0.1$  g  $\text{NH}_4^+\text{-N/m}^2\cdot\text{day}$  for Media 1, 2, 3, 4 and 5 respectively. There was no statistical difference between the five media for ammonia loading. The DO was maintained at  $4.1 \pm 1.03$ ,  $4.0 \pm 1.2$ ,  $3.0 \pm 0.6$ ,  $5.1 \pm 1.6$  and  $3.2 \pm 1.1$  mg  $\text{O}_2/\text{L}$  in Cell 1 and  $5.6 \pm 0.5$ ,  $6.1 \pm 0.9$ ,  $6.9 \pm 1.2$ ,  $5.6 \pm 1.1$  and  $6.6 \pm 1.0$  mg  $\text{O}_2/\text{L}$  in Cell 3.

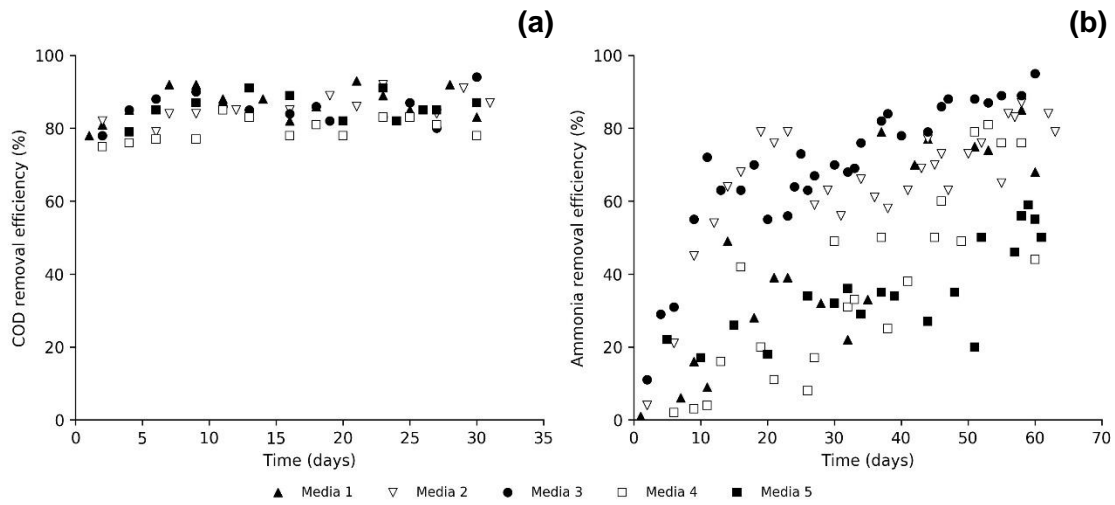
**Table 4-2 Characterisation of the wastewater fed to the pilot plant operated with different media during start up.**

Parameter	Unit	Media 1	Media 2	Media 3	Media 4	Media 5
Temperature	$^{\circ}\text{C}$	$15.1 \pm 2.2$	$19.2 \pm 2.2$	$20.9 \pm 1.7^*$	$13.8 \pm 2.3^*$	$13.1 \pm 1.8$
pH		$7.6 \pm 0.1$	$8.0 \pm 0.2$	$7.7 \pm 0.2$	$7.7 \pm 0.3$	$8.1 \pm 0.2$
Total COD (tCOD)	mg/L	$389 \pm 71$	$257 \pm 44$	$305 \pm 32$	$236 \pm 15$	$251 \pm 24$
Particulate COD (pCOD)	mg/L	$317 \pm 77$	$189 \pm 41$	$234 \pm 30$	$147 \pm 20$	$187 \pm 25$
Soluble COD (sCOD)	mg/L	$72 \pm 7$	$68 \pm 12$	$71 \pm 5$	$89 \pm 11$	$63 \pm 8$
$\text{BOD}_5$	mg/L	$143 \pm 47$	$81 \pm 28$	$125 \pm 27$	$158 \pm 39$	$148 \pm 38$
Soluble $\text{BOD}_5$ (s $\text{BOD}_5$ )	mg/L	$11 \pm 6$	$18 \pm 2$	$22 \pm 4$	$37 \pm 8$	$32 \pm 9$
TSS	mg/L	$225 \pm 54$	$154 \pm 88$	$205 \pm 45$	$162 \pm 33$	$202 \pm 78$
Ammonia ( $\text{NH}_4^+\text{-N}$ )	mg/L	$35 \pm 5$	$34 \pm 11$	$36 \pm 3$	$38 \pm 6$	$31 \pm 5$

\*Due to temperature variability, temperature for Media 4 and 5 were statistically different from Media 1, 2 and 3 ( $p \leq 0.05$ ).

The COD removal efficiency and biofilm formation was tracked during the first 60 days of operation. After 6 days of operation the COD removal was high with values of 78, 82, 78, 75 and 79% with Media 1, 2, 3, 4 and 5, respectively (Figure 4-2a). The COD removal efficiencies reached stable values of  $88 \pm 4\%$  in Media 1 (after day 18),  $81 \pm 4\%$  in Media 2 (after day 15),  $85 \pm 3\%$  in Media 3 (after day 17),

80±3% in Media 4 (after 23 days) and 86±4% in Media 5 (after 24 days) (Figure 4-2a).



**Figure 4-2 Removal efficiencies for obtainable COD (a) and ammonia (b) during start-up during operation with Media 1, 2, 3, 4 and 5, respectively.**

Throughout the first 10 days of operation, ammonia removal efficiencies were low for all media, with values reaching 24±7, 33±17, 31±15, 24±11 and 19±11% for Media 1 to 5, respectively. Media 1, 2 and 3 (spherical shape) achieved ammonia removal efficiencies of 50±13, 64±13, 63±7% after 30, 22 and 17 days, respectively. Media 4 and 5 (cylindrical shape) achieved ammonia removal efficiencies of 32±17% after 46 days and 34±5% after 47 days, respectively (Figure 4-2b).

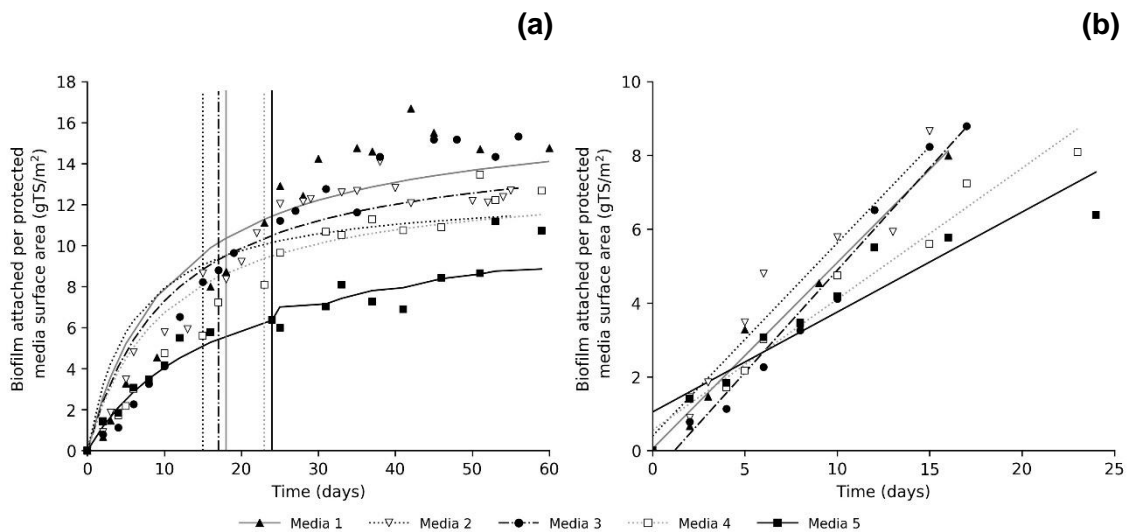
Ammonia removal rates were 0.4±0.1 g NH<sub>4</sub><sup>+</sup>-N/m<sup>2</sup>.day (30 days), 0.5±0.1 g NH<sub>4</sub><sup>+</sup>-N/m<sup>2</sup>.day (22 days), 0.7±0.1 g NH<sub>4</sub><sup>+</sup>-N/m<sup>2</sup>.day (17 days), 0.2±0.1 g NH<sub>4</sub><sup>+</sup>-N/m<sup>2</sup>.day (46 days) and 0.3±0.1 g NH<sub>4</sub><sup>+</sup>-N/m<sup>2</sup>.day (47 days) for Media 1, 2, 3, 4 and 5, respectively. It is likely that low nitrification was impacted by the concentration of organic matter (BOD) reaching the third cell. The third cell organic loading rates was 1.4±0.9, 1.6±0.9, 2.1±1.0, 2.8±0.9 and 2.9±0.7 g BOD<sub>5</sub>/m<sup>2</sup>.day when the reactor was operated with Media 1, 2, 3, 4 and 5 respectively. The values for Media 4 and 5 were slightly higher than those recommended by Hem, Rusten and Odegaard (1994) of approximately < 2 g BOD<sub>5</sub>/m<sup>2</sup>.day. The presence of organics, in the third cell, had promoted growth of heterotrophs and competing nitrifiers slowing down nitrification (Hem, Rusten

and Odegaard, 1994). A similar finding was reported by Zhu et al. (2015), which registered only 50% ammonia removal after 14 days of operation, and the low nitrification was attributed to the high carbon: nitrogen ratio (C/N). From the data reported in the literature, the range of temperatures measured did not indicate nitrification to be impacted by temperature (temperatures in Cell 3 for Media 4 and 5,  $13.8 \pm 2.3$  and  $13.1 \pm 1.8$  °C respectively) (Salvetti et al., 2006). In Zhu and Chen (2002) studies no difference on nitrification rate was registered between 14, 20 and 27 °C.

#### **4.3.2 Biofilm formation and start-up**

In this study, process start-up was defined as the period of time for biofilm formation rates to reach stable values. Bacterial adhesion was observed after the second day of operation, and values of 0.67, 0.90, 1.21, 1.44 and 1.40 g TS/m<sup>2</sup> were measured in Media 1, 2, 3, 4 and 5, respectively (Figure 4-3a). This can be defined as the 1<sup>st</sup> stage of biofilm formation (Zhu et al., 2015). The biofilm continued developing gradually until day 18, 15, 17, 23 and 24 for Media 1, 2, 3, 4 and 5, respectively, when the attached biofilm reached stable values (8.73, 8.66, 8.79, 8.09 and 6.38 g TS/m<sup>2</sup> for Media 1, 2, 3, 4 and 5, respectively) (Figure 4-3a). This corresponds to the 2<sup>nd</sup> and 3<sup>rd</sup> stages of biofilm growth and accumulation respectively. The biofilm formation rate was calculated based on the slope of the biofilm attachment until it reached stable values (Figure 4-3b). The estimated biofilm formation rates during start up were 0.50, 0.52, 0.55, 0.36 and 0.27 g TS/m<sup>2</sup>.day for Media 1, 2, 3, 4 and 5, respectively. The results clearly indicate that the biofilm formation rate was faster on spherical media, with higher voidage and diameter, compared with the cylindrical media. The larger voids and structure of the spherical carrier media, Media 1, 2 and 3, enhanced air and wastewater distribution leading to increased mass transfer encouraging heterotrophic and nitrifying bacteria to attach and form biofilm. In Media 4 and 5 (cylindrical media) much of the area available for bacteria adhesion and biofilm growth is on the outer perimeter surface of the carrier media where exposure to high shear stress from local flow velocities may occur and limit biofilm attachment. Moreover, wastewater and air distribution become very low on the internal narrow

voids hindering biofilm formation rate. Di Trapani et al. (2008), stated that one month was required to reach stable conditions, with an attached biofilm of around 11.57 g TS/m<sup>2</sup> and 15.15 g TS/m<sup>2</sup> at 35 and 65% filling ratio, respectively using a cylindrical shape carrier media. Falletti, Conte and Maestri (2014) observed a visibly fully grown biofilm after five weeks of operation (39.3 g TSS/m<sup>2</sup>) using a cylindrical media. Dong et al. (2015), considered that biofilm was stable and mature in 25 days with a hollow spherical honeycomb and a cylindrical shape carrier media, with attached biofilm of 0.04 g/cm<sup>3</sup>. With pre-settled wastewater, Siciliano and De Rosa (2016) observed that heterotrophic biofilm start up required seven days reaching a 3 g TS/m<sup>2</sup> of attached biofilm in a cylindrical shape carrier media. Bassin et al. (2016) observed, after 20 and 30 days of start-up, a biofilm attached concentration of 13 g TS/m<sup>2</sup> in a 500 m<sup>2</sup>/m<sup>3</sup> cylindrical shape carrier media and 7 g TS/m<sup>2</sup> in a 3000 m<sup>2</sup>/m<sup>3</sup> chip shaped carrier media.

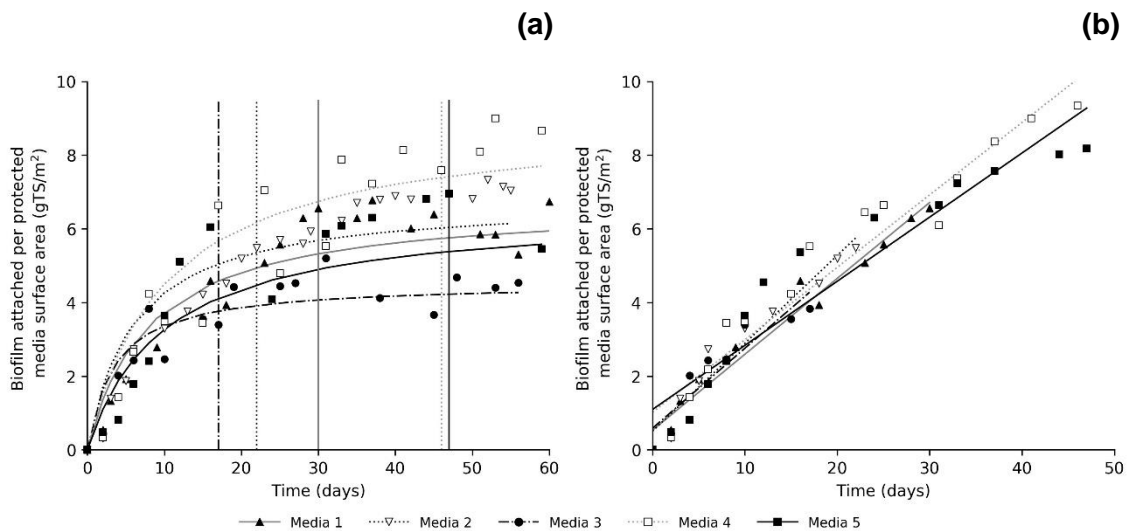


**Figure 4-3 Biofilm attachment during 60 days of operation in Cell 1 (COD removal) (a) and fitting of a trendline to calculate the slope corresponding to the biofilm formation rate (b) during start-up.**

For the nitrification process start-up in Cell 3, bacteria attachment was observed on the second day of operation with 0.54, 0.31, 0.45, 0.33, 0.48 g TS/m<sup>2</sup> for Media 1 to 5, respectively. The biofilm continued to increase until it attained stabilisation around day 30, 22, 17, 46 and 47 for Media 1, 2, 3, 4 and 5, respectively (6.56, 5.48, 3.83, 9.34, 7.57 g TS/m<sup>2</sup>, Media 1 to 5, respectively) (Figure 4-4a). Others

have reported average values of 7 g TSS/m<sup>2</sup> after 1 month on a nitrifying integrated fixed-film activated sludge system (IFAS) start-up using cylindrical shaped carrier media (Regmi et al., 2011). In Bassin et al. (2012) two months were required to start-up a reactor operating under autotrophic conditions using a cylindrical shaped carrier media.

The biofilm formation rate was determined based on the slope of the biofilm attached until stable values were reached, from day 0 to day 30, 22, 17, 46 and 47. These estimated values were 0.21, 0.24, 0.22, 0.18, 0.17 g TS/m<sup>2</sup>.day for Media 1, 2, 3, 4 and 5 respectively (Figure 4-4b). The biofilm formation rate is usually linked with the nitrification rate (Wiesmann, 1994). Spherical shape media achieved higher ammonia removal efficiencies (Figure 4-2b) and thus a higher biofilm formation rate than cylindrical media.



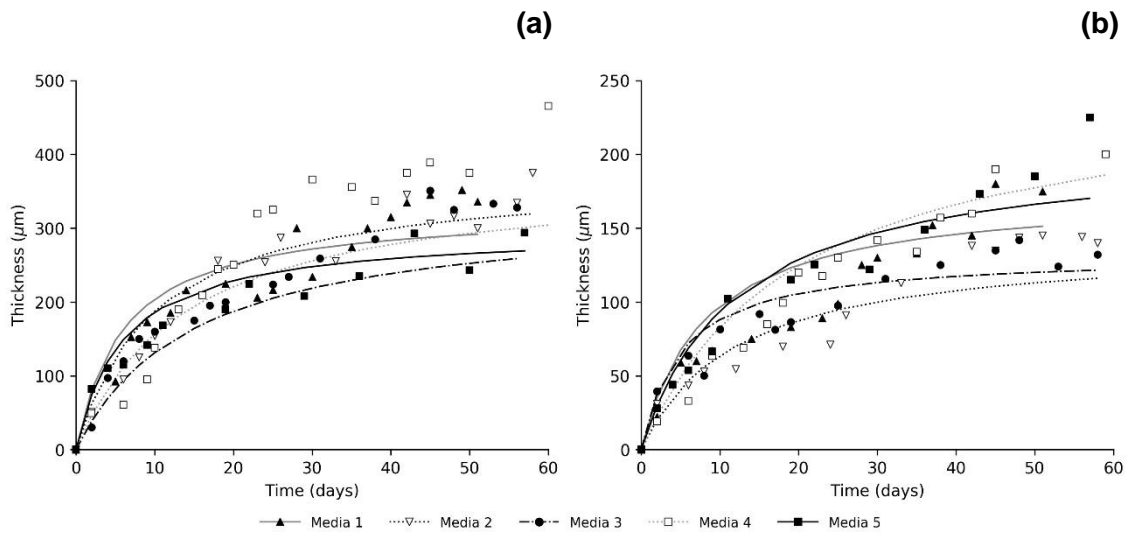
**Figure 4-4 Biofilm attached during the 60 days of operation in Cell 3 (ammonia removal) (a) and fitting of a trendline to calculate the slope corresponding to the biofilm formation rate (b) during start-up.**

The biofilm thicknesses in Cell 1 were 36, 51, 84, 50 and 82  $\mu$ m on the second day, for Media 1 to 5, respectively (Figure 4-5a). The biofilm thickness reached stable values at  $225\pm52$ ,  $172\pm25$ ,  $195\pm35$ ,  $250\pm73$  and  $190\pm63$   $\mu$ m for Media 1, 2, 3, 4 and 5 at day 18, 15, 17, 23 and 24, respectively (Figure 4-5a). For the cylindrical media, the biofilm was mainly situated in the internal fins, in the small ridges of the media and the biofilm thickness attained values between 365-465

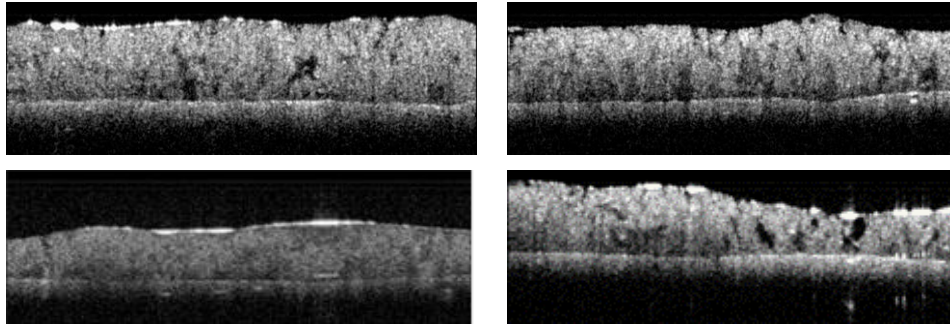


$\mu\text{m}$  and 224-361  $\mu\text{m}$  for Media 4 and 5, respectively, by the end of start-up. The biofilm in Media 1, 2 and 3 was spread uniformly. In Cell 3, aimed at ammonia removal, the initial biofilm thickness was  $22\pm 24$ ,  $31\pm 30$ ,  $39\pm 14$ ,  $19\pm 10$  and  $28\pm 11$   $\mu\text{m}$  for Media 1, 2, 3, 4 and 5, respectively. The thickness increased to values of  $130\pm 25$ ,  $71\pm 22$ ,  $86\pm 29$ ,  $190\pm 50$  and  $149\pm 47$   $\mu\text{m}$  at day 30, 22, 17, 46 and 47, respectively (Figure 4-5b and Figure 4-6).

Protected surface area of each media was estimated at the macroscopic scale with photography. In Media 1 (large spherical shape), the biofilm was distributed evenly over the media. Approximately 83% of the carrier media area was covered with biofilm, giving a protected surface area of  $112 \text{ m}^2/\text{m}^3$ . For Media 2 and 3 (medium and smaller spherical media) the biofilm was mainly situated in the internal fins, covering 68 and 71% of the total area (protected surface area of 148 and  $220 \text{ m}^2/\text{m}^3$ , respectively). In Media 4 and 5 (cylindrical shape) the biofilm was located exclusively on the internal fins. No biofilm attachment was verified on the external surface of Media 4 and 5. As such 58 and 61% of Media 4 and 5 were covered with biofilm, yielding a protected surface area of 348 and  $610 \text{ m}^2/\text{m}^3$ , respectively.



**Figure 4-5 Biofilm thickness during 60 days of operation Cell 1 (a) and Cell 3 (b).**

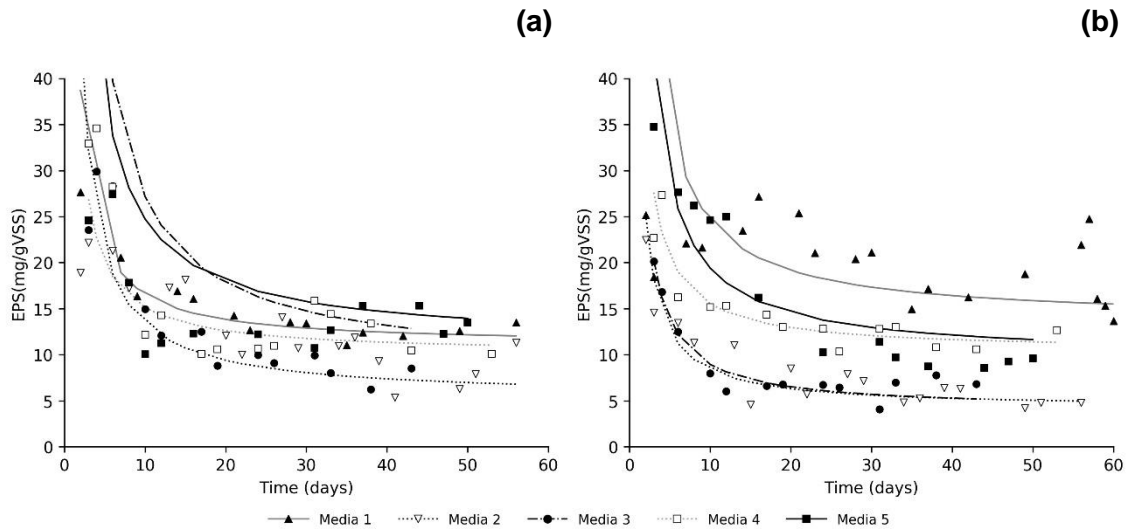


**Figure 4-6 Images captured during OCT measurements on different media.**

During the first days of operation, a similar EPS profile was observed for all the media in Cell 1 (organic removal). The EPS concentration increased, reaching values of  $20.6 \pm 0.4$ ,  $21.3 \pm 0.3$ ,  $28.3 \pm 0.1$ ,  $28.2 \pm 0.75$  and  $27.4 \pm 0.81$  mg tEPS /g VSS for Media 1, 2, 3, 4 and 5, respectively (Figure 4-7a). As expected, the EPS production was higher throughout the first days of operation due to the adhesion phenomena and interaction between the heterotrophic bacteria and the carrier surface (Badireddy et al., 2010). A gradual increase in total EPS was also observed in Tang et al. (2017b) with values of 15, 22, 32.5 and 38 mg tEPS /g VSS measured at the initial stage of biofilm formation (0, 3, 11, 18 and day 25 days). Similar observations, also identified by Tang et al. (2015) demonstrated an increase from 30 mg EPS /g VSS on day 5 up to 250 mg EPS/g VSS on day 27. In Oberoi and Philip (2017) the concentration of EPS increased from 36.8 to 72.2 mg EPS/g VSS at the end of start-up. Total EPS content in an IFAS varied from 44 to 71 mg tEPS/g VSS using different media (Mahendran, Lishman and Liss, 2012).

A gradual decrease in EPS concentration was observed after the first week and values stabilised at  $16.0 \pm 0.4$ ,  $18.2 \pm 0.9$ ,  $9.18 \pm 0.1$ ,  $11.83 \pm 0.9$  and  $12.83 \pm 0.2$  mg tEPS/g VSS on day 16, 15, 19, 17 and 16 for Media 1, 2, 3, 4 and 5, respectively. As predicted the values of EPS decreased after bacteria adhesion and growth. As the biofilm grows in thickness, diffusion becomes critical, and cells start to grow slower reducing EPS production and biofilm cohesion resulting in biofilm detachment (Ahimou et al., 2007). After day 25 a gradual decrease in EPS production was also observed in Tang et al. (2017b) during the maturity and detachment phases.

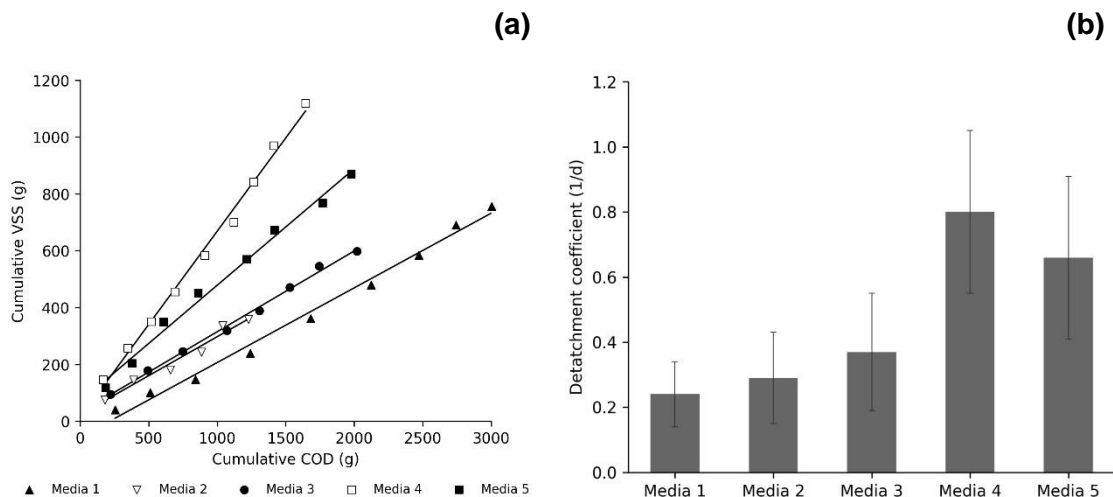
The total EPS associated with the biofilm in Cell 3 of the pilot plant during the first days of operation were  $22.1 \pm 0.5$ ,  $22.5 \pm 0.4$ ,  $20.1 \pm 0.3$ ,  $27.3 \pm 0.6$  and  $34.8 \pm 1.9$  mg tEPS/g VSS for Media 1, 2, 3, 4 and 5, respectively (Figure 4-7b). Similarly, the EPS decreased as operation progressed. After days 30, 22, 17, 46 and 47 days of operation, the EPS were  $17.2 \pm 0.3$ ,  $5.7 \pm 0.3$ ,  $6.6 \pm 0.1$ ,  $10.6 \pm 0.1$  and  $9.7 \pm 0.3$  mg tEPS/g VSS for Media 1, 2, 3, 4 and 5, respectively. Values of EPS were very similar between the first cell and third cell. Nonetheless, nitrifiers are slow growing bacteria with low EPS production compared to heterotrophic bacteria. The high EPS formation in Cell 3, might have been produced by heterotrophic bacteria due to the high COD reaching the third cell during start-up. Bassin et al. (2012) stated that EPS produced by heterotrophic bacteria were utilised by nitrifiers for biofilm formation during start-up.



**Figure 4-7 Total EPS values registered in Cell 1 (a) and Cell 3 (b) during 60 days of operation.**

During start up the biofilm attached on carrier per amount of COD converted was compared between media. Values of 0.26, 0.27, 0.28, 0.65 and 0.41 g VSS/g COD were calculated in Media 1, 2, 3, 4 and 5, respectively (Figure 4-8a). The higher biomass yield achieved in media 4 and 5 correlated well with the lower biofilm formation rate estimated during the start-up period. Values of 0.5 g SS/g filtered COD are reported on the literature (Ødegaard, 2006). An initial detachment rate coefficient was calculated based on a mass balance between the solids leaving the reactor and the biofilm attached per area of carrier media

(Eldyasti, Nakhla and Zhu, 2012). The normalised average detachment rate (1/d) was compared between media, and the attached biofilm considered for COD removal was from Cell 1 of the reactor. Due to the dynamic of biofilm accumulation in moving attached growth systems, detachment rates displayed significant variations during the start-up for all the five media studied. Values of  $0.24 \pm 0.10$ ,  $0.29 \pm 0.14$ ,  $0.37 \pm 0.18$ ,  $0.80 \pm 0.25$  and  $0.66 \pm 0.25$  1/d were measured in Cell 1 for Media 1 to 5, respectively (Figure 4-8b). Media 4 and 5 (cylindrical shape) promoted higher detachment due to interaction with aeration during initial biofilm formation, while the open spherical structure of Media 1, 2 and 3 enhanced initial biofilm formation, protecting the biofilm from shear. Values of 0.12 g VSS/g COD and detachment rates of 0.05 1/d were reported in Eldyasti, Nakhla and Zhu (2012) for a high spherical media compared with 0.19 g VSS/g COD and detachment rates of 0.17 1/d for a low sphericity media.

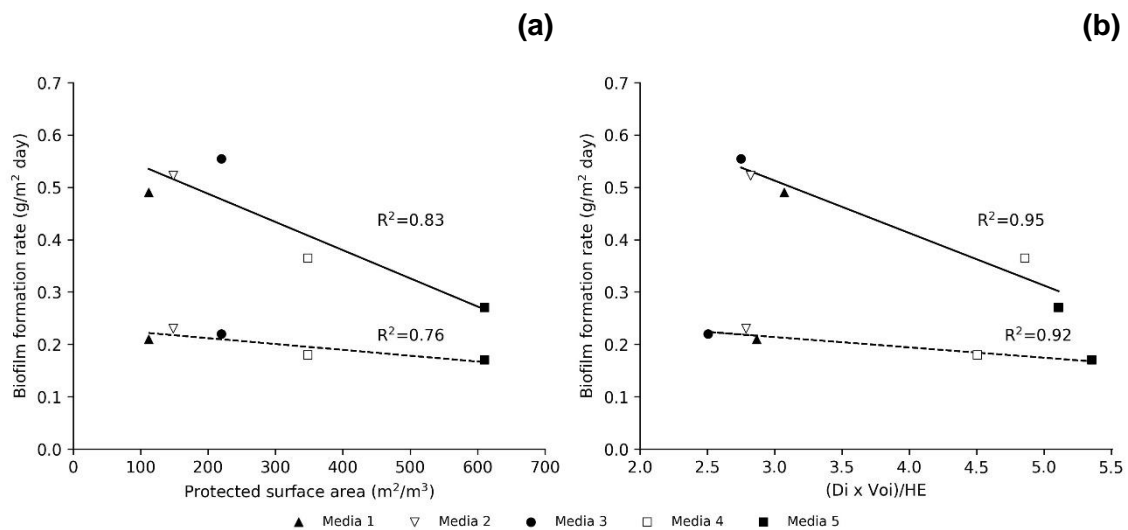


**Figure 4-8 Biofilm yield (a) and biofilm detachment rate (b) calculated for the five media during COD start-up.**

#### 4.4 Influence of the media physical properties on start-up duration

In moving attached growth systems, the main factor assuring a fast start-up is the biofilm development. In this study start-up duration was assessed based on the attached biofilm (g TS/m<sup>2</sup>). In order to study the influence of media physical properties on the pilot plant start-up, the biofilm formation rate was correlated with

media physical properties (Appendix B). The media physical properties were previously identified in Dias et al. (2018b), to correlate with process hydrodynamics and oxygen mass transfer. More specifically, media dimensionality ( $D_i$ ) and voidage ( $V_{oi}$ ) were found to strongly correlate with oxygen mass transfer ( $R^2= 0.89$ ) and pilot plant hydraulic efficiency (HE) ( $R^2= 0.92$ ) both in clean media and with biofilm attached to the media (Dias et al., 2018b). When the rate of biofilm formation in Cell 1 (COD removal) and Cell 3 (ammonia removal) was compared with the media protected surface area, good correlations were achieved ( $R^2$  of 0.83 and  $R^2$  of 0.76, respectively) (Figure 4-9a). A stronger correlation was identified between the combination of parameters  $(D_i \times V_{oi})/HE$ , and the rate of biofilm formation during COD removal start up ( $R^2= 0.95$ ) and an  $R^2$  of 0.92 during ammonia removal start-up (Figure 4-9b).



**Figure 4-9 The correlation between rate of biofilm formation and protected surface area (a) and combination of parameters  $(D_i \times V_{oi})/HE$  (b) during COD (-) and ammonia removal start-up (--).**

The physical media properties and hydraulic efficiency clearly demonstrate the importance of media shape and size on biofilm attachment and start-up. Biofilm formation rates were  $30 \pm 1\%$  higher in the spherical media during organic removal start-up and  $20 \pm 3\%$  higher during ammonia removal start-up, when compared with cylindrical media. The high voidage (95, 92 and 90%) and open structure of spherical media (Media 1, 2 and 3) was associated with higher hydraulic

efficiencies ( $89\pm 2$ ,  $93\pm 5$  and  $100\%$ ) as outlined in Dias et al. (2018b). This led to increased oxygen mass transfer offering better conditions for biofilm to attach, leading to a faster start-up. In turn, this provided improved mass transfer at the bulk/biofilm interface increasing biofilm activity and treatment performance (Tang et al., 2017b). The reduction on hydraulic efficiencies and media voidage, obtained with cylindrical media (Media 4: HE  $74\pm 1\%$  and Voi reduction of  $6\%$ ; Media 5: HE  $63\pm 2\%$  and Voi reduction of  $14\%$ ) (Dias et al., 2018), explained the longer start-up (46 and 47 days).

The diffusion of oxygen is usually limited after a critical biofilm thickness of  $50\text{--}150\ \mu\text{m}$  (Syron and Casey, 2008). Values of biofilm thickness of  $190\pm 50$  and  $149\pm 47\ \mu\text{m}$  were measured in Media 4 and 5 during start-up. Despite the higher protected surface area of Media 4 and 5 the start-up duration and biofilm formation rate were slower compared with the lower protected surface area (Media 1, 2 and 3). This confirms the contribution and the important roles played by other properties in the media. Similar observations were stated in Bassin et al. (2016) where higher attached biofilm concentrations were reached in a smaller protected surface area media compared with higher protected surface area media. In Eldyasti, Nakhla and Zhu (2012) work, surface shape (sphericity), played an important role on biofilm structure with  $70\%$  lower biofilm yield and detachments rate observed on high sphericity media ( $0.9$ ) compared to low sphericity media ( $0.5$ ).

The open spherical structure of Media 1, 2 and 3 notwithstanding the lower protected surface area, favoured wastewater circulation and oxygen distribution within all areas of the media. Therefore, this study highlights the importance of media physical properties on biofilm growth and retention and their impact on the start-up duration on moving attached growth systems. The knowledge gained through this study will challenge current literature knowledge and commercial strategies that appointed the protected surface area as the key factor for the design and operation of moving attached growth system (Ødegaard, Gisvold and Strickland, 2000). Findings highlighted the importance of voidage on biofilm growth and maintenance and thus on treatment performance during start-up.

Hence, considering the importance of start-up to achieve stable operational performance at low commission periods, the economic competitiveness of the moving attached growth system technology can be improved through additional focus on carrier media properties (voidage and shape).

## 4.5 Conclusions

In this study, the influence of carrier media physical properties on the start-up duration of a moving attached growth system was investigated. Five carrier media with different shapes (spherical and cylindrical), size, voidage and protected surface area (112-610 m<sup>2</sup>/m<sup>3</sup>) were studied. Given the data obtained and respective analysis, start-up was monitored using the biofilm formation rate.

- Biofilm formation rates of 0.50, 0.52, 0.55, 0.36 and 0.27 g/m<sup>2</sup>.day were obtained in Cell 1 (COD removal), during 18, 15, 17, 23 and 24 days for Media 1, 2, 3 4 and 5, respectively.
- Biofilm formation rates of 0.21, 0.24, 0.22, 0.18 and 0.17 g/m<sup>2</sup>.day were obtained in Cell 3 (ammonia removal) start up, during 30, 22, 17, 46 and 47 for Media 1, 2, 3, 4 and 5, respectively.
- Correlations (R<sup>2</sup> of 0.83 and 0.76) were identified between carrier media protected surface area and biofilm formation rates for obtained COD and ammonia removal.
- Stronger correlations were observed between the biofilm formation rates and the combination of physical factors and hydraulic efficiency (Di x Voi)/HE for COD and ammonia removal rates (R<sup>2</sup>= 0.95 and 0.92).
- This study demonstrates that moving attached growth systems start-up does not rely solely on protected surface area but also physical properties (shape and voidage) which impacts biofilm development.
- This study highlighted that the conventional way to design moving attached growth systems and estimate substrate removal rates should not be exclusively according to its protected surface area and future moving

attached growth system design and evaluation should focus equally on carrier media physical properties.

## 4.6 References

Ahimou, F., Semmens, M.J., Haugstad, G. and Novak, P.J. (2007) 'Effect of protein, polysaccharide, and oxygen concentration profiles on biofilm cohesiveness', *Applied and Environmental Microbiology*, 73(9), pp. 2905–2910.

APHA (2005) *Standard Methods for the Examination of Water and Wastewater*. 21st edn. Washington, D.C.: American Public Health Association.

Badireddy, A.R., Chellam, S., Gassman, P.L., Engelhard, M.H., Lea, A.S. and Rosso, K.M. (2010) 'Role of extracellular polymeric substances in bioflocculation of activated sludge microorganisms under glucose-controlled conditions', *Water Research*, 44(15), pp. 4505–4516.

Barwal, A. and Chaudhary, R. (2016) 'Feasibility study for the treatment of municipal wastewater by using a hybrid bio-solar process', *Journal of Environmental Management*, 177, pp. 271–277.

Bassin, J.P., Dias, I.N., Cao, S.M.S., Senra, E., Laranjeira, Y. and Dezotti, M. (2016) 'Effect of increasing organic loading rates on the performance of moving-bed biofilm reactors filled with different support media: Assessing the activity of suspended and attached biomass fractions', *Process Safety and Environmental Protection*, 100, pp. 131–141.

Bassin, J.P., Kleerebezem, R., Rosado, A.S., Van Loosdrecht, M.C.M. and Dezotti, M. (2012) 'Effect of different operational conditions on biofilm development, nitrification, and nitrifying microbial population in moving-bed biofilm reactors', *Environmental Science and Technology*, 46(3), pp. 1546–1555.

Deng, L., Guo, W., Ngo, H.H., Zhang, X., Wang, X.C., Zhang, Q. and Chen, R. (2016) 'New functional biocarriers for enhancing the performance of a hybrid moving bed biofilm reactor-membrane bioreactor system', *Bioresource Technology*, 208, pp. 87–93.



Dias, J., Stephenson, T., Bellingham, M., Hassan, J., Barrett, M. and Soares, A. (2018) 'Impact of carrier media on oxygen transfer and wastewater hydrodynamics on a moving attached growth system', *Chemical Engineering Journal*, 351, pp. 399–408.

Dong, Y., Fan, S.-Q., Shen, Y., Yang, J.-X., Yan, P., Chen, Y.-P., Li, J., Guo, J.-S., Duan, X.-M., Fang, F. and Liu, S.-Y. (2015) 'A Novel bio-carrier fabricated using 3D printing technique for wastewater treatment', *Scientific Reports*, 5(1), pp. 1–10.

Dubois, M., Gilles, K.A., Hamilton, J.K., Rebers, P.A. and Smith, F. (1956) 'Colorimetric method for determination of sugars and related substances', *Anal Chem*, 28(3), pp. 350–356.

Eldyasti, A., Nakhla, G. and Zhu, J. (2012) 'Influence of particles properties on biofilm structure and energy consumption in denitrifying fluidized bed bioreactors (DFBBRs)', *Bioresource Technology*, 126, pp. 162–171.

Falletti, L., Conte, L. and Maestri, A. (2014) 'Upgrading of a wastewater treatment plant with a hybrid moving bed biofilm reactor (MBBR)', *AIMS Environmental Science*, 1(2), pp. 45–52.

Goel, R., Kaldate, A., Murthy, S., Schraa, O. and Stinson, B. (2011) 'Examining the phenomenon of self regulation of biofilm density under dynamic conditions using a biofilm model', *WEFTEC 2011*. Los Angeles: Water Environment Federation, pp. 5160–5177. Available at: [10.2175/193864711802765390](https://doi.org/10.2175/193864711802765390) (Accessed: 7 October 2017).

Habouzit, F., Hamelin, J., Santa-Catalina, G., Steyer, J.P. and Bernet, N. (2014) 'Biofilm development during the start-up period of anaerobic biofilm reactors: The biofilm Archaea community is highly dependent on the support material', *Microbial Biotechnology*, 7(3), pp. 257–264.

Hem, L.J., Rusten, B. and Odegaard, H. (1994) 'Nitrification in a moving bed biofilm reactor', *Water Research*, 28(6), pp. 1425–1433.

Lackner, S., Holmberg, M., Terada, A., Kingshott, P. and Smets, B.F. (2009) 'Enhancing the formation and shear resistance of nitrifying biofilms on membranes by surface modification', *Water Research*, 43(14), pp. 3469–3478.

Le-Clech, P., Chen, V. and Fane, T.A.G. (2006) 'Fouling in membrane bioreactors used in wastewater treatment', *Journal of Membrane Science*, 284(1–2), pp. 17–53.

Liu, Y. and Tay, J.H. (2002) 'The essential role of hydrodynamic shear force in the formation of biofilm and granular sludge', *Water Research*, 36(7), pp. 1653–1665.

Lowery, O.H., Rosebrough, N.J., Farr, A.L. and Randall, R.J. (1951) 'Protein measurement with the folin phenol reagent', *The Journal of biological chemistry*, 193, pp. 265–275.

Mahendran, B., Lishman, L. and Liss, S.N. (2012) 'Structural, physicochemical and microbial properties of flocs and biofilms in integrated fixed-film activated sludge (IFFAS) systems', *Water Research*, 46(16), pp. 5085–5101.

Mao, Y., Quan, X., Zhao, H., Zhang, Y., Chen, S., Liu, T. and Quan, W. (2017) 'Accelerated startup of moving bed biofilm process with novel electrophilic suspended biofilm carriers', *Chemical Engineering Journal*, 315, pp. 364–372.

Oberoi, A.S. and Philip, L. (2017) 'Performance evaluation of attached biofilm reactors for the treatment of wastewater contaminated with aromatic hydrocarbons and phenolic compounds', *Journal of Environmental Chemical Engineering*, 5(4), pp. 3852–3864.

Ødegaard, H. (2016) 'A road-map for energy-neutral wastewater treatment plants of the future based on compact technologies (including MBBR)', *Frontiers of Environmental Science and Engineering*, 10(4), pp. 1–17.

Ødegaard, H. (2006) 'Innovations in wastewater treatment: The moving bed biofilm process', *Water Science and Technology*, 53(9), pp. 17–33.

Ødegaard, H., Gisvold, B. and Strickland, J. (2000) 'The influence of carrier size and shape in the moving bed biofilm process', *Water Science and Technology*, 41(4–5), pp. 383–391.

Patel, A., Nakhla, G. and Zhu, J. (2005) 'Detachment of multi species biofilm in circulating fluidized bed bioreactor', *Biotechnology and Bioengineering*, 92(4), pp. 427–437.

Pellicer-Nàcher, C. and Smets, B.F. (2014) 'Structure, composition, and strength of nitrifying membrane-aerated biofilms', *Water Research*, 57, pp. 151–161.

Regmi, P., Thomas, W., Schafran, G., Bott, C., Rutherford, B. and Waltrip, D. (2011) 'Nitrogen removal assessment through nitrification rates and media biofilm accumulation in an IFAS process demonstration study', *Water Research*, 45(20), pp. 6699–6708.

Salveti, R., Azzellino, A., Canziani, R. and Bonomo, L. (2006) 'Effects of temperature on tertiary nitrification in moving-bed biofilm reactors', *Water Research*, 40(15), pp. 2981–2993.

Siciliano, A. and De Rosa, S. (2016) 'An experimental model of COD abatement in MBBR based on biofilm growth dynamic and on substrates' removal kinetics', *Environmental Technology (United Kingdom)*, 37(16), pp. 2058–2071.

Syron, E. and Casey, E. (2008) 'Membrane-aerated biofilms for high rate biotreatment: Performance appraisal, engineering principles, scale-up, and development requirements', *Environmental Science and Technology*, 42(6), pp. 1833–1844.

Szilágyi, N., Kovács, R., Kenyeres, I. and Csikor, Z. (2013) 'Biofilm development in fixed bed biofilm reactors: experiments and simple models for engineering design purposes.', *Water Science & Technology*, 68(6), pp. 1391–1399.

Tang, B., Yu, C., Bin, L., Zhao, Y., Feng, X., Huang, S., Fu, F., Ding, J., Chen, C., Li, P. and Chen, Q. (2016) 'Essential factors of an integrated moving bed biofilm reactor-membrane bioreactor: Adhesion characteristics and microbial community of the biofilm', *Bioresource Technology*, 211, pp. 574–583.

Tang, B., Zhao, Y., Bin, L., Huang, S. and Fu, F. (2017) 'Variation of the characteristics of biofilm on the semi-suspended bio-carrier produced by a 3D printing technique: Investigation of a whole growing cycle', *Bioresource Technology*, 244, pp. 40–47.

Di Trapani, D., Mannina, G., Torregrossa, M. and Viviani, G. (2008) 'Hybrid moving bed biofilm reactors: A pilot plant experiment', *Water Science and Technology*, 57(10), pp. 1539–1545.

Wiesmann, U. (1994) 'Biological nitrogen removal from wastewater', *Advances in Biochemical Engineering/Biotechnology*, 51, pp. 114–153.

Zhu, S. and Chen, S. (2002) 'The impact of temperature on nitrification rate in fixed biofilters', *Aquacultural Engineering*, 26(4), pp. 221–237.

Zhu, Y., Zhang, Y., Ren, H. qiang, Geng, J. ju, Xu, K., Huang, H. and Ding, L. li (2015) 'Physicochemical characteristics and microbial community evolution of biofilms during the start-up period in a moving bed biofilm reactor', *Bioresource Technology*, 180, pp. 345–351.

# 5 IMPACT OF CARRIER MEDIA PHYSICAL PROPERTIES ON THE PERFORMANCE OF MOVING ATTACHED GROWTH SYSTEMS

J. Dias<sup>a</sup>, M. Bellingham<sup>b</sup>, J. Hassan<sup>b</sup>, M. Barrett<sup>b</sup>, M. van Loosdrecht<sup>c</sup>, T. Stephenson<sup>a</sup>, A. Soares<sup>a</sup>

<sup>a</sup> Cranfield University Water Sciences Institute, Cranfield, MK43 0AL, UK.

<sup>b</sup> Warden Biomedica, 31 Sundon Industrial Estate, Dencora Way, Luton, Bedford, LU3 3HP, UK.

<sup>c</sup> Department of Biotechnology, Delft University of Technology, Julianalaan 67, 2628 BC Delft, The Netherlands.

## Abstract

A 2 m<sup>3</sup> pilot plant was used to evaluate the influence of carrier physical properties on the performance of moving attached growth systems. In this study, three spherical shaped carrier media (Media 1, 2 and 3) with protected surface areas of 112-220 m<sup>2</sup>/m<sup>3</sup> and voidage of 95-90%; and two cylindrical shaped media (Media 4 and 5) with a protected surface area of 348-610 m<sup>2</sup>/m<sup>3</sup> and voidage 82.5-80%, were tested. When the pilot plant was operated at steady state, under the similar organic and ammonia loading rates, the average obtainable COD removal efficiency was 89±3, 86±2, 86±3, 85±4 and 86±2%, for Media 1, 2, 3, 4 and 5, respectively. Ammonia removal was higher for the spherical media, achieving values of 70±11, 71±10 and 81±3% compared with the cylindrical media that attained values of 42±6 and 35±12%. Specific activity tests demonstrated that Media 1 achieved the highest rate of organic removals (34.8±2.0 mg sCOD/g TS.h), and the smaller spherical shape, Media 3, achieved the highest rates of nitrification removals (7.2±0.7 mg NH<sub>4</sub><sup>+</sup>-N/g TS.h). The maximum COD utilisation rates ( $U_m$ ) correlated with a carrier media specific surface area, ( $R^2= 0.88$ ) but a stronger correlation was established between  $U_m$  and carrier media physical properties (dimensionality,  $D_i$ , voidage,  $V_{oi}$  and hydraulic efficiency, HE) ( $R^2= 0.92$ ). Correlation between ammonia removal rate and protected surface area was  $R^2= 0.65$  but a stronger correlation was achieved with the media physical properties ( $D_i \times V_{oi}$ )/HE ( $R^2= 0.92$ ). These findings clearly demonstrate, that beside carrier protected surface area, physical parameters such as dimensionality and voidage, play a key role on moving attached growth

systems (e.g.: MBBRs, IFAS and SAFs) and these must be considered towards achieving high reactor performance and effluent quality.

**Keywords:** Biofilm activity, dimensionality, moving bed biofilm reactor, thickness, voidage.

## 5.1 Introduction

The use of moving attached growth systems such as submerged aerated filters (SAF), moving bed biofilm reactors (MBBRs) and integrated fixed film activated sludge (IFAS) is increasing due to their effective removal of pollutants from municipal and industrial wastewater. These processes form a biofilm by relying on microorganisms attached to a carrier media. As a result, long biomass retention times are achieved, maximising the capacity and efficiency of these processes when compared with conventional suspended systems, such as activated sludge processes (ASP). Moving attached growth systems present other advantages such as reduced footprint and low sludge production and have been used in a variety of applications including upgrading, replacing and expanding existing wastewater treatment plants (WWTPs) (Ødegaard, 2006). Furthermore, MBBRs are also frequently applied for tertiary nitrification, due to the capacity of the carrier media to retain and protect slow growing microorganisms such as nitrifiers (Kermani et al., 2008).

A key component of moving attached growth systems, is the carrier media, that is fully submerged within wastewater. Mechanical or diffused aeration promote the mixing of the carrier media, allowing an effective substrate and oxygen distribution over the carrier increasing biochemical reactions and formation of an active biofilm (McQuarrie and Boltz, 2011).

Moving attached growth systems are designed and operated based on the carrier media surface area (area available for biofilm to attach per volume of reactor) and carrier media surface loading rates (Piculell, Welander and Jořsson, 2014). However, not all the area of the carrier media is covered with biofilm due to carrier collision. For this reason, the term protected or specific surface area was defined by Ødegaard, Rusten and Westrum (1994) as the potential area for biofilm growth under a protected environment. Thus, much attention has been given to maximise

the carrier media protected surface area as a means of increasing overall treatment performance. Research has mainly focused on process performance, i.e. investigating the impact of varying organic/nutrient and volumetric loads, carrier media filling ratios (the fraction of volume occupied by the carriers) and aeration rates (Martín-Pascual et al., 2012). Previous studies have also investigated the impact of different carrier media materials, including different plastics and polymeric materials (Sousa et al., 1997). Recently, 3D printing has been used to explore carrier media with complex geometries and high surface area (Elliott, 2017; Tang et al., 2017b). Sponges and electrophilic materials have been added to plastic carriers to improve biofilm development, reducing start-up times and improving organic and nutrient removal (Deng et al., 2016; Mao et al., 2017). Nevertheless, few studies compare the impact of plastic carrier media size and shape on treatment performance. Results on the comparison of different carrier shape and size on MBBR performance, indicated that their performance is primarily dependent on carrier media protected surface area with shape and size being less important given that the protected surface area in the reactor is the same (Ødegaard, Gisvold and Strickland, 2000).

Other studies also demonstrated that shape and size, had little effect on MBBR performance (Bassin et al., 2016; Martín-Pascual et al., 2012; Zinatizadeh and Ghaytooli, 2015). Nevertheless, more recent studies contradict these findings and indicate that carrier media physical properties seem to play an important role on performance. Melcer and Schuler (2014) revealed that when comparing two media with the same surface area (650 and 630 m<sup>2</sup>/m<sup>3</sup>), the larger structure carrier media (Ø22 mm x 17 mm) performed better than the small structure media (Ø12 mm x 14 mm) independent of the protected surface area. The same results were achieved when two different polypropylene media were compared. The cylindrical shape with two helices achieved 12% higher COD removal when compared with the most widely used cylindrical shaped carrier media, with similar protected surface area (950 m<sup>2</sup>/m<sup>3</sup>) (Martínez-Huerta et al., 2009). At high ammonia loadings, two chip shaped media with 900 and 1200 m<sup>2</sup>/m<sup>3</sup> of carrier protected surface area, presented a high tendency to become clogged when compared with cylindrical shaped media and 500 m<sup>2</sup>/m<sup>3</sup> protected surface area

(Forrest, Delatolla and Kennedy, 2016; Young et al., 2016). Results on flow distribution and carrier media orientation emphasise the importance of carrier media shape on biomass distribution and morphology, however the experimental set-up used was a single fixed carrier in a tube (Herrling et al., 2015). Other studies suggested that biofilm activity may not be necessarily linked with carrier media protected surface area (Piculell et al., 2016c).

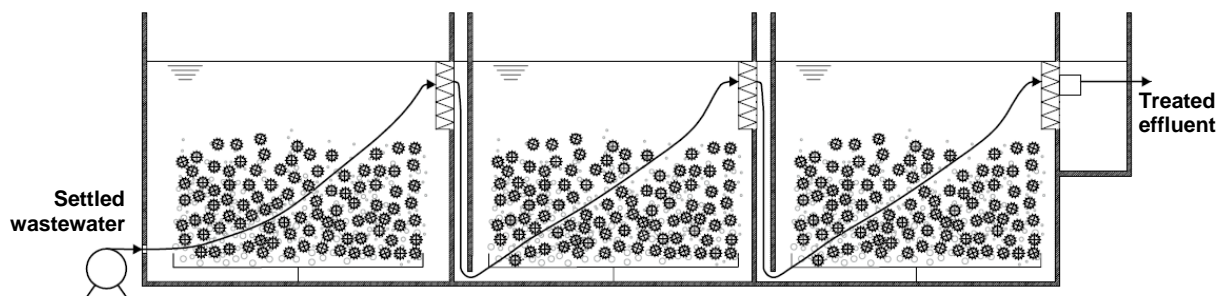
Most of the existing literature has focused on the performance of MBBR systems based on the carrier media protected surface area, not yet identifying the effect of the carrier media shape and size. Thus, the purpose of the study is to investigate the influence of carrier physical properties on substrate utilisation that ultimately influence the overall performance of processes treating municipal wastewater.

## **5.2 Material and methods**

### **5.2.1 Pilot plant setup and operation conditions**

In order to study the effect of carrier media physical properties on moving attached growth system performance, a 2 m<sup>3</sup> pilot plant (1.0 m width x 1.5 m length and 1.3 m height) was designed. The pilot plant was composed of three aerobic cells of equal volume (Figure 5-1). Air and mixing were provided by medium bubble aeration. Three recycled polypropylene spherical shape carrier media (Media 1, 2 and 3) and two recycled polypropylene cylindrical shape carrier media (Media 4 and Media 5) with protected surface area of 112 (Media 1), 148 (Media 2), 220 (Media 3), 348 (Media 4) and 610 m<sup>2</sup>/m<sup>3</sup> (Media 5) were tested (Table 5-1). Carrier media was supplied by Warden Biomedia (Luton, UK). Throughout the experimental period, the pilot plant was continuously fed with settled municipal wastewater from Cranfield University WWTP (Cranfield, UK) (Table 5-2). Organic and nutrient loading rates were kept constant at 6.9±0.4 g COD/m<sup>2</sup>.day and 0.9±0.1 g NH<sub>4</sub><sup>+</sup>-N/m<sup>2</sup>.day, respectively, by fixing the carrier media filling ratio at 60%. The wastewater characterisation is presented in Table 5-2.





**Figure 5-1 Schematic representation of the moving attached growth system pilot plant.**

**Table 5-1 Characteristics of the carrier media tested: Media 1 (Biofil), Media 2 (Bioball), Media 3 (Biomarble), Media 4 (Biopipe) and Media 5 (Biotube). Media was supplied by Warden Biomedica (<http://www.wardenbiomedica.com>).**

Media	Total surface (m <sup>2</sup> /m <sup>3</sup> )	Protected surface area (m <sup>2</sup> /m <sup>3</sup> )	Shape	Dimensions		Voidage (%)	Material	Density (g/cm <sup>3</sup> )
				Length (mm)	Diameter (mm)			
1	135	112	Spherical	65	95	95	Recycled polypropylene (PP)	0.97
2	220	148	Spherical	53	65	92		
3	310	220	Spherical	36	46	90		
4	600	348	Cylindrical	13	21.5	82.5		
5	1000	610	Cylindrical	8	12	80		

**Table 5-2 Influent settled wastewater characterisation for different carrier media (average values measured after star-up until steady state). Media 1 (Biofil), Media 2 (Bioball), Media 3 (Biomarble), Media 4 (Biopipe) and Media 5 (Biotube). Media was supplied by Warden Biomedica (<http://www.wardenbiomedica.com>).**

Parameter	Unit	Media 1	Media 2	Media 3	Media 4	Media 5
Temperature*	°C	19.5±1.5	19.7±1.2	20.1± 0.7	15.8±1.8	15.9±1.5
pH		7.6±0.1	8.0±0.2	7.7±0.2	7.7±0.3	8.1±0.2
Total COD (tCOD)	mg/L	301± 37.1	258± 44	281±34	225±19	242±32
Particulate COD (pCOD)	mg/L	245±74	194±45	204±29	134±20	164±34
Soluble COD (sCOD)	mg/L	55±11	64±12	77±18	92±24	78±18
BOD <sub>5</sub>	mg/L	128±46	107±42	135±27	160±28	138±31

Parameter	Unit	Media 1	Media 2	Media 3	Media 4	Media 5
<b>Soluble BOD<sub>5</sub></b> (sBOD <sub>5</sub> )	mg/L	14±8	18±4	22±6	39±9	28±9
<b>TSS</b>	mg/L	182±48	156±43	171±28	166±34	212±53
<b>Ammonia</b> (NH <sub>4</sub> <sup>+</sup> -N)	mg/L	33±7	33±6	34±7	30±6	34±4

tCOD, pCOD and sCOD – total, particulate and soluble chemical oxygen demand. tBOD<sub>5</sub> and sBOD<sub>5</sub> -total and soluble 5-day carbonaceous biochemical oxygen demand. TSS - total suspended solids.

COD removal efficiencies were evaluated according to Ødegaard (2006). The “obtainable removal rate” was calculated based on 100% solids separation (equation (5-1)).

$$COD = \frac{Q \times [tCOD - sCOD]}{A} \quad (5-1)$$

The detachment coefficient ( $k_{de}$ ) was estimated using the equation described in Patel, Nakhla and Zhu (2005) and (Eldyasti, Nakhla and Zhu, 2012) (equation (5-2)).

$$k_{de} = \frac{Q \times [VSS_{out}]}{A \times M_t} \quad (5-2)$$

Where  $VSS_{out}$  are the solids leaving the pilot plant, Q is the flow rate.  $M_t$  is the biofilm attached per area of carrier media and A is the carrier media protected surface area.

Observed yields were calculated based on Eldyasti, Nakhla and Zhu (2012) using the linear regression between the cumulative production of volatile suspended solids (VSS) in the effluent and the cumulative COD removed ( $tCOD_{in}$ - $sCOD_{out}$ ).

The Stover-Kincannon equation (5-3), was used to analyse the pilot plant performance, based on the COD data obtained during steady state operation for each carrier media studied. Where  $S_0$  is the tCOD influent concentration,  $S_e$  is the sCOD effluent concentration, Q is the wastewater flow, A is the carrier media protected surface area, k is the proportional constant and  $U_m$  is the maximal substrate removal rate (Orantes and González-Martínez, 2004). Maximal substrate removal rate was calculated by the inverse of the organic loading rates plotted against the inverse of organic removal rates.

$$\frac{1}{ds/dt} = \frac{A}{Q(S_0 - S_e)} = \frac{kA}{U_m Q S_0} + \frac{1}{U_m} \quad (5-3)$$

Hydraulic efficiency (HE) was determined through tracer studies using Rhodamine (Rhodamine WT 20%; Fisher Scientific, Loughborough, UK) when the operation reached steady state and the biofilm was fully attached to each media. A volume of 5 ml of Rhodamine was injected instantaneously into the inlet of the reactor. The Rhodamine concentration was then monitored in the effluent using a submersible fluorometer (Cyclops-7; RS Aqua Ltd, Hampshire, UK) and data collected was recorded on a data logger (Databank Handheld Dataloggers; RS Aqua Ltd, Hampshire, UK). Measurements were taken every 30 seconds over a period equivalent to 3 to 4 hydraulic retention times (HRT) to ensure 80-100 % of tracer recovery. All tests were carried out in triplicate. Residence time distribution (RTD) curves were obtained from the tracer concentrations measured at the outlet of the reactor as function of time and parameters for RTD interpretations were calculated following Levenspiel (1999) and Dias et al. (2018).

### 5.2.2 Attached biofilm

The quantity of attached biofilm to the carrier media was measured twice a week after steady state was achieved (between 30 to 90 days of continuous operation, start-up took place during the initial 30 days of operation) following the procedure described in Regmi et al. (2011). Carriers were sampled from the three cells of the pilot plant (at least 10 carriers of Media 1, 2 and 3 and 40 carriers of Media 4 and 5) and dried at 105°C overnight and weighed. The biofilm was removed by placing the carriers in a H<sub>2</sub>SO<sub>4</sub> solution (2 N) which was stirred vigorously for 24 hours. The carriers were washed with tap water then biofilm brushed off and dried at 105°C. The total attached biofilm was calculated based on the difference in media dry weight before and after removing all the attached biofilm. The results were expressed as grams of total solids per metre square of protected surface area of carrier media (g TS/m<sup>2</sup>).

To enable non-destructive measurements of biofilm thickness, biofilm thickness was measured through Optical Coherence Tomography (OCT) using a Thorlabs

Standard (SR-OCT 930nm; Thorlabs. Germany). The obtained signal was multiplied with a factor of 1.33 (refractive index of water) to match the optical depth with the true depth of the biofilm sample. The media was cut into small pieces with a surgical scalpel and placed on a stage under the OCT probe. Two-dimensional cross-sectional images were acquired from different pieces and locations of the carriers. Biofilm thickness was estimated based on 20 OCT images and the average of 60 measurements.

### **5.2.3 Biofilm activity tests**

Biofilm specific activity tests were conducted at steady state using batch experiments. These were performed in a 40 L bioreactor (30 width x 30 length and 45 cm height). Medium bubble aeration, through 4 mm diameter holes, was provided mimicking pilot plant operation. The temperature was maintained at 20°C by using a heater and pH adjusted to 7.5. Dissolved oxygen was always greater than 5 mg/L. The aeration and carrier media filling ratio was 60% and was kept constant to replicate the one used in the pilot plant. The organic batch activity tests were completed according to Nogueira et al. (2015). Endogenous respiration conditions were attained by taking wastewater and carrier media from Cell 1 of the pilot plant and aerating for 12 hours. Sodium acetate ( $C_2H_3NaO_2$ ) (Fisher Scientific, Loughborough, UK) was used as a readily biodegradable organic substrate (150-200 mg/L) and 10 mg/L of allylthiourea (ATU) was added to inhibit nitrification.

The nitrification batch activity tests were completed according to Regmi et al. (2011). The final effluent of Cranfield University WWTP was used and ammonia added as ammonium chloride ( $NH_4Cl$ ) to reach 40-50 mg  $NH_4^+-N$  /L with sodium carbonate ( $Na_2CO_3$ ) for pH control (Fisher Scientific, Loughborough, UK). During the batch tests, samples were collected every 30 minutes for 2 and 3 hours and analysed for sCOD (filtered with a 0.45  $\mu m$  pore size syringe-drive filter units) (Millipore<sup>TM</sup>, Billerica, United States),  $NH_4^+-N$  and nitrate-nitrogen ( $NO_3^- -N$ ) analysis. Attached biofilm were measured at the start of each batch test, as previously described. A sample from the mixed liquor suspended solids was collected before and after the batch tests to consider biofilm detachment. Results

were then expressed as specific organic removal rates (mg sCOD/g TS.day) and specific ammonia removal rates (mg NH<sub>4</sub><sup>+</sup>-N/g TS.day).

#### **5.2.4 Analytical methods**

Temperature, dissolved oxygen (DO) and pH were measured daily on the different cells of the pilot plant using portable meters (HACH HQ40d; Camlab, Cambridge, UK). Influent and effluent quality were monitored three times a week and sBOD<sub>5</sub>, TSS, VSS and alkalinity were measured following Standard Methods for the Examination of Water and Wastewater (APHA, 2005). tCOD and sCOD, NH<sub>4</sub><sup>+</sup>-N and NO<sub>3</sub><sup>-</sup>-N were measured using cell tests (NOVA60 photometer, VWR, UK).

### **5.3 Results and discussion**

#### **5.3.1 Biofilm accumulation**

In Cell 1, average values of biofilm attached to the media were 14.5±1.3, 12.4±0.8, 13.8±1.7, 10.7±2.3 and 8.53±1.6 g TS/m<sup>2</sup> for Media 1, 2, 3, 4 and 5, respectively. Hence, the levels of the attached biofilm were higher in the spherical carrier media (Media 1, 2 and 3) compared to the cylindrical carrier media (Media 4 and 5). An evaluation of biofilm attached to the media across the pilot plant, indicated that, in general, media in Cell 1 and Cell 2 presented higher biofilm attached. The higher organic load reaching Cell 1 promoted the attachment of faster growing heterotrophic bacteria as observed in other studies (Li et al., 2015a). The attached biofilm values were comparable to the ones reported in other studies. Values of 6-8 g TS/m<sup>2</sup> were registered at surface organic loading of 6 g COD/m<sup>2</sup>.day (Siciliano and De Rosa, 2016). Values of 6.1 and 6.6 g TS/m<sup>2</sup> were obtained with organic loading rates of 6.4 g COD/m<sup>2</sup>.day, for a cylindrical shape and a parabolic shape carrier media, respectively (Bassin et al., 2016).

In Cell 3 the attached biofilm was 6.2±0.5, 6.6±0.6, 4.4±0.4, 8.8±0.4 and 6.3±0.5 g TS/m<sup>2</sup> for Media 1, 2, 3, 4 and 5, respectively. Values measured for Media 4 were slightly higher than Media 1, 2, 3 and 5. These are in the same order of magnitude of the 9.3 g TS/m<sup>2</sup> reported as mean high biofilm content and 6.6 g TS/m<sup>2</sup> mean low biofilm content in a tertiary nitrification MBBR (Salveti et al.,

2006). The results are also comparable to those reported in an IFAS reactor, where nitrifying biofilm achieved an average attached biofilm of 6 g TS/m<sup>2</sup> (Regmi et al., 2011).

Biofilm thickness varied for the five carrier media studied. In Cell 1, Media 1, 2 and 3, the biofilm was evenly distributed with average thicknesses of 289±52, 302±41, 282±71 µm, respectively. In Media 4 and 5 the distribution was uneven, varying within the internal areas and edges of the carrier media. Values of 334±71 µm were measured on the flat surface while 634±50 µm were measured on the carrier media ridges. In Media 5 the average thickness on the flat surface was 241±45 and thicknesses of 329±57 and 485±70 µm were measured in the internal ridges and fins of the carrier media. In Cell 3, the biofilm thickness varied with recorded values of 136±44, 124±26, 115±22, 213±35 and 207±22 µm, for Media 1, 2, 3, 4 and 5, respectively. The same behaviour was observed with thicker biofilm being observed at the internal fins and ridges of Media 4 and 5 reaching values of 406±52 µm (Media 4) and 283±70 µm (Media 5).

### **5.3.2 COD and ammonia removal performance**

The process performance was assessed after start-up (between day 30 and 90 of operation) for each carrier media (Table 5-3). The temperatures in different cells were maintained at 20.0±0.5, 19.9±0.2, 20.1±0.1, 15.6±1.0 and 16.0±1.0°C for Media 1, 2, 3, 4 and 5, respectively. Due to wastewater variability, the average surface organic loading rate varied between 6.7±1.8, 7.0±1.3, 7.7±0.9, 6.5±0.6 and 6.8±0.7 g COD/m<sup>2</sup>.day for Media 1, 2, 3, 4 and 5, respectively. The average obtainable COD removal efficiency was 89±3, 86±2, 86±3, 85±4, 86±2%, for Media 1, 2, 3, 4 and 5, respectively, and thus very close to the ideal curve for 100% removal (Figure 5-2a). Soluble BOD removal efficiencies were 82±11, 86±5, 87±4, 70±3, 66±4%, for Media 1, 2, 3, 4 and 5, respectively.

During operation, the ammonia loadings varied from 0.7±0.2, 0.9±0.2, 0.8±0.2, 1.1±0.2 and 0.9±0.1 g NH<sub>4</sub><sup>+</sup>-N/m<sup>2</sup>.day for Media 1, 2, 3, 4 and 5, respectively (Table 5-3). The highest ammonia removal efficiencies were achieved with Media 3 (81±3 %). The mean effluent ammonia concentrations were 3.3±1.0 mg NH<sub>4</sub><sup>+</sup>-N/L and ammonia removal rates of approximately 0.7±0.12 g NH<sub>4</sub><sup>+</sup>-N /m<sup>2</sup>.day

using Media 3. The effluent quality achieved lower values than the 5 mg NH<sub>4</sub><sup>+</sup>-N/L stated in the *Urban Wastewater Treatment Directive 91/271/EEC* (European Parliament. Council of the European Union, 1991).

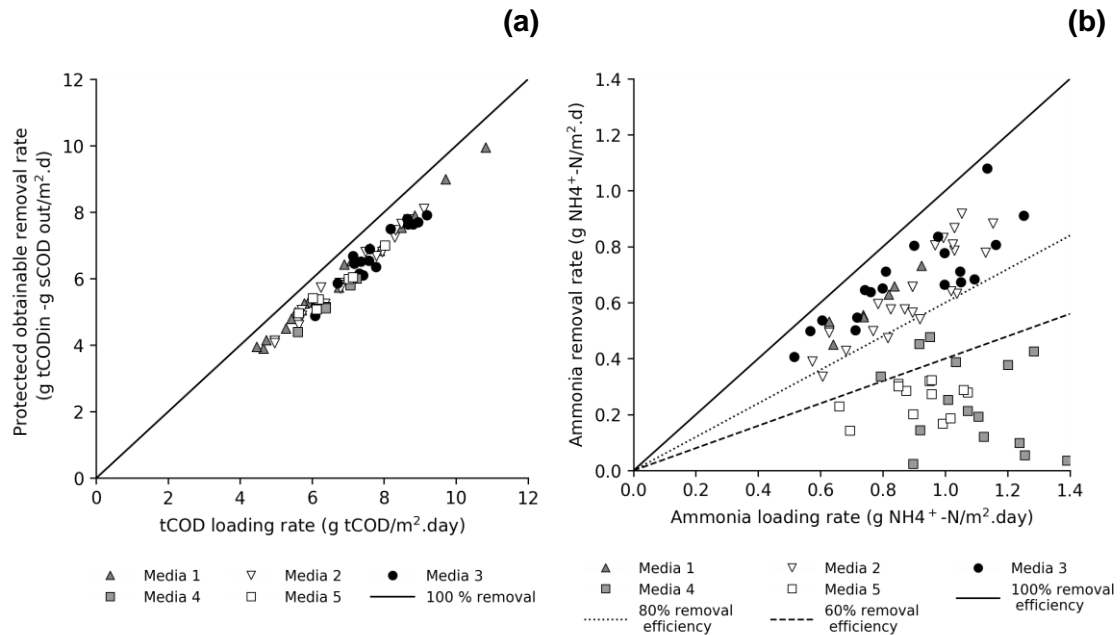
**Table 5-3 Summary of the pilot plant temperature, DO, influent loadings and removals, for the 5 carrier media studied. Media 1 (Biofil), Media 2 (Bioball), Media 3 (Biomarble), Media 4 (Biopipe) and Media 5 (Biotube). Media was supplied by Warden Biomedia (<http://www.wardenbiomedia.com/>).**

	Media 1	Media 2	Media 3	Media 4		Media 5		
Temperature (°C)								
Cell 1	19.6±1.4	19.7±1.4	20.1±0.7	14.7±1.4		15.1±1.4		
Cell 2	20.5±1.0	20.1±0.8	20.2±0.7	15.4±1.5		16.0±0.7		
Cell 3	20.0±1.0	20.0±0.8	20.0±0.7	16.7±1.7*		17.0±1.2*		
DO mg O <sub>2</sub> /L								
Cell 1	3.1±1.1	2.5±1.3	2.0±0.8	3.7±1.1	4.1±1.1	5.4±1.1	5.2±1.0	5.8±0.3
Cell 2	4.5±0.7	4.7±1.36	4.8±1.1	6.0±1.2	6.2±0.6	6.6±0.6	6.7±0.7	6.4±0.5
Cell 3	5.2±0.6	5.5±1.40	6.0±1.2	6.72±1.0	5.9±0.5	6.7±0.5**	6.9±0.5	6.4±0.4
Loading rates								
g COD/m <sup>2</sup> ·d	6.7±1.8***	7.0±1.3	7.7±0.9	6.5±0.6	6.0±0.6	6.6±0.8	6.3±1.9	3.3±0.9
g BOD <sub>5</sub> /m <sup>2</sup> ·d	2.9±1.1	2.9±0.1	3.7±0.7	4.5±0.5	3.5±0.2	4.0±0.6	2.7±0.8	1.7±0.3
g NH <sub>4</sub> <sup>+</sup> -N /m <sup>2</sup> ·d	0.7±0.2	0.9±0.2	0.8±0.2	1.1±0.2	0.7±0.1	0.9±0.1	0.6±0.1	0.4±0.1
Removal rates and removal efficiency								
COD (g COD/m <sup>2</sup> ·d)	6.0±1.7	6.0±1.2	6.6±0.9	5.2±0.5	4.8 ± 0.7	5.7±0.7	5.6±1.9	2.0±0.6
BOD <sub>5</sub> (g BOD <sub>5</sub> /m <sup>2</sup> ·d)	3.2±1.1	1.6±0.6	2.2±0.4	1.7±0.4	1.7 ± 0.3	2.0±0.6	1.2±0.6	0.9±0.2
NH <sub>4</sub> <sup>+</sup> -N (g NH <sub>4</sub> <sup>+</sup> -N/m <sup>2</sup> ·d)	0.5±0.1	0.7±0.2	0.7±0.2	0.3±0.1	0.5±0.1	0.3±0.1	0.4±0.1	0.4±0.1
COD removal (%)	89±3	86±2	86±3	85±4	87±3	86±2	88±2	92±3
BOD <sub>5</sub> and sBOD <sub>5</sub> removal (%)	66±16	56±10	64±11	42±6	46±6	35±12	43±9	50±5
	82±11	86±5	87±4	70±3	93±3	66±4	86±4	94±3
NH <sub>4</sub> <sup>+</sup> -N removal (%)	70±11	71±10	81±3	38±9	81±6	28±7	58±9	84±3
TSS removal (%)	44±17	54±18	51±14	28±5	33±9	47±5	47±13	42±7

\*Due to natural temperature variability, temperature in Cell 3 for Media 4 and 5 were statistically different from other carrier media (p≤0.05). \*\*DO in Media 5 was statistically different from other carrier media (p≤0.05). \*\*\*Due to wastewater natural variability, the total COD loadings during operation with Media 1 were statistically different from the other carrier media (p≤0.05). There was no statistical difference between the ammonia loadings during operation with the different carrier media.

Media 4 and 5 exhibited lower ammonia removals compared to the ones achieved with spherical carrier media (Figure 5-2b). Ammonia removals of 42±6 and 35±12%, were achieved with Media 4 and 5, respectively, at ammonia loadings of 1.1±0.2 and 0.9±0.1 g NH<sub>4</sub><sup>+</sup>-N/m<sup>2</sup>·day (Table 5-3). Temperatures in Cell 3 were slightly lower when the pilot plant was operated with Media 4 and 5, 16.7±1.7 and

17.0±1.2°C, respectively. The range of temperatures in Cell 3 (averages between 16.7-20°C) are not expected to impact nitrification. This is supported by other researchers who have indicated no significant impact on nitrification rate at temperatures of 14, 20 and 27°C with maximum ammonia removal of 1.69, 1.72 and 1.86 g/m<sup>2</sup>.day, respectively (Zhu and Chen, 2002).



**Figure 5-2 Obtainable removal COD (a) and ammonia removal (b) as a function of loading rates for the five media studied.**

Organic loading is one of the most influential parameters on nitrification but often not properly accounted for. Studies on the influence of organic loading on nitrification reported that a BOD<sub>5</sub> load of 1-2 g BOD<sub>5</sub>/m<sup>2</sup>.d in the nitrification zone/cell resulted in nitrification rates between 0.7-1.2 g NH<sub>4</sub><sup>+</sup>-N/m<sup>2</sup>.day. When BOD<sub>5</sub> loadings increased to 2-3 g BOD<sub>5</sub>/m<sup>2</sup>.d, the nitrification rates decreased by 50% to values of 0.3-0.8 g NH<sub>4</sub><sup>+</sup>-N/m<sup>2</sup>.day at a DO concentration of 6 mgO<sub>2</sub>/L (Hem, Rusten and Odegaard, 1994). A 50% reduction on nitrification removal rate was also observed with increased inlet carbon: nitrogen (C/N) ratio in a study completed by Torkaman et al. (2015). Nitrification rate was reduced by 70% using a cylindrical shape carrier media (623 m<sup>2</sup>/m<sup>3</sup>) when C/N ratio was increased from 1 to 2 (Zhu and Chen, 2001). A drop in the nitrifiers' activity was also stated in Piculell (2016) when the C/N ratio was increased to 2 using two carrier media of



a cylindrical ( $800 \text{ m}^2/\text{m}^3$ ) and a saddle shape ( $1280 \text{ m}^2/\text{m}^3$ ), resulting in a reduction from 2.2 and 3 g  $\text{NH}_4^+\text{-N}/\text{m}^2\cdot\text{day}$  to 0.5 and 0.95 g  $\text{NH}_4^+\text{-N}/\text{m}^2\cdot\text{day}$ , respectively.

In this study, the organic load that reached Cell 3 was  $2.8\pm 0.9$  and  $2.9\pm 0.7$  g  $\text{BOD}_5/\text{m}^2\cdot\text{day}$ , corresponding to C/N ratios of 2.8 and 2.7, during operation with Media 4 and 5, respectively. These values were close to the upper range stated in the literature of 2-3 g  $\text{BOD}_5/\text{m}^2\cdot\text{d}$  to ensure effective nitrification (Hem, Rusten and Odegaard, 1994). Presence of biodegradable organic matter affects the competition between heterotrophic and nitrifying bacteria. Heterotrophs have fast growth rates and develop on the external layer of the biofilm, in contact with wastewater, while nitrifiers are formed in the internal layer attached to the surface of the carrier media (Lee, Ong and Ng, 2004). This heterotrophic biofilm layer develops in the presence of biodegradable organic matter, increasing resistance to ammonia diffusion and auto competing with nitrifiers for space and oxygen.

Furthermore, the biofilm in Media 4 and 5 had a thickness of  $406\pm 52 \mu\text{m}$  (Media 4) and  $283\pm 70 \mu\text{m}$  (Media 5) with higher mass of biofilm accumulated at the internal fins and ridges of the carrier media, also characteristic of heterotrophic biofilms (Karizmeh, Delatolla and Narbaitz, 2014). Additionally, the increased thickness may have affected ammonia and oxygen diffusion from the bulk liquid to the core nitrifying biofilm layer. Studies indicated an ammonia penetration depth of less than  $100 \mu\text{m}$  (Ødegaard, 2006; Pfeiffer and Wills, 2011). Other studies indicated that biofilm is partially penetrated by ammonia at about  $200 \mu\text{m}$  (Zhang and Bishop, 1994).

To increase the nitrification rate when Media 4 and 5 were tested, the BOD and  $\text{NH}_4^+\text{-N}$  loadings were reduced to  $3.5\pm 0.2$  and  $0.7\pm 0.1$ ,  $1.7\pm 0.3$  g  $\text{BOD}_5/\text{m}^2\cdot\text{day}$  and  $0.4\pm 0.1$  g  $\text{NH}_4^+\text{-N}/\text{m}^2\cdot\text{day}$ , reaching C/N ratios of  $1.3\pm 0.4$  and  $1.1\pm 0.2$ , for Media 4 and 5, respectively. Air flow rates were also increased on Cell 1 and 2 for Media 4 and 5 (Table 5-3).

Under these conditions, the ammonia removals achieved were  $81\pm 6\%$  with Media 4 and  $84\pm 3\%$  with Media 5, with biofilm thicknesses in Cell 3 of  $185\pm 65$  and  $149\pm 33 \mu\text{m}$ , for Media 4 and 5, respectively. These corresponded to ammonia removal rates of  $0.5\pm 0.1$  and  $0.4\pm 0.1$  g/ $\text{m}^2\cdot\text{day}$ , for Media 4 and 5, respectively.

The decrease in organic loading rate, promoted the increase of ammonia removal efficiencies. To optimise the potential of the carrier media, lower and more conservative BOD loadings should be used in the design process, so that higher nitrification could be achieved in the downstream cells (WEF, 2011). In biofilms, oxygen penetration depth depends on the oxygen bulk liquid concentration. Alternatively, dissolved oxygen concentration could also be further increased to compensate high organic loadings and thicker biofilms. The reduction of oxygen available for nitrification due to heterotrophic activity was found to be approximately 2.5 mg/L when a nitrification reactor was operated at 1.5 g BOD<sub>5</sub>/m<sup>2</sup>.day in Rusten et al. (2006). Other studies stated that values above 6 and 8 mg O<sub>2</sub>/L were required to start and maintain nitrification at 3.5 g BOD<sub>5</sub>/m<sup>2</sup>.day (Ødegaard, 2006; Rusten et al., 2006).

Regarding the amount of suspended solids measured in the pilot plant effluent, values varied between 100.9±29.5, 75.2±30.4, 74.9±14.3, 124.9±23.1, 120.7±18.8 mg TSS/L during operation with Media 1, 2, 3, 4 and 5, respectively. Values of TSS and VSS in the effluent were within the range stated in the literature (150-250 g SS/m<sup>3</sup>) (Bassin et al., 2016). The VSS/TSS ratio was measured with all the carrier media, giving values of 0.86±0.14, 0.87±0.13, 0.96±0.12, 0.94±0.02 and 0.90±0.03 g VSS/g TSS for Media 1, 2, 3, 4 and 5, respectively.

The average biofilm detachment coefficients were calculated during steady state operation. Average values of 0.13±0.1, 0.17±0.1, 0.13±0.1, 0.27±0.1 and 0.31±0.1 1/d were registered for Media 1, 2, 3, 4 and 5, respectively. Furthermore, biofilm yield per COD removal was calculated for each carrier media, and values of 0.28, 0.33, 0.34, 0.52 and 0.43 g VSS/g COD were measured with Media 1, 2, 3, 4 and 5 respectively. A higher biomass yield was observed in the cylindrical carrier media (Media 4 and 5) compared with spherical carrier media (Media 1, 2 and 3). Values were comparable with values reported in the literature 0.5 g SS/g filtered COD (Ødegaard, 2006).

### 5.3.3 Biofilm activity tests

Biofilm activity tests were performed to determine specific organic and nitrification rates of the biofilm attached to each carrier media tested (Table 5-4). The biofilm grown on Media 1 presented a specific organic removal of  $34.8 \pm 2.0$  mg sCOD/g TS.h, compared to Media 2 and 3 that obtained  $26.9 \pm 0.6$  mg sCOD/g TS.h,  $19.2 \pm 1.7$ , respectively. For Media 4 and 5 the specific organic removal was  $13.4 \pm 1.1$  mg sCOD/g TS.h and  $13.4 \pm 0.2$  mg sCOD/g TS.h, respectively. Hence, the specific organic activity was higher in Media 1, demonstrating that oxygen diffusion and substrate mass transfer was greater in Media 1, despite the high attached biofilm measured at  $14.3 \pm 0.2$  g TS/m<sup>2</sup>. Likewise, when the values of specific organic removal were normalised by protected surface area, the highest values were obtained for Media 1,  $11.9 \pm 0.3$  g COD/m<sup>2</sup>.day compared with other carrier media ( $6.4 \pm 0.1$ ,  $9.4 \pm 0.2$ ,  $4.2 \pm 0.8$  and  $2.3 \pm 0.2$  g COD/m<sup>2</sup>.day for Media 2, 3, 4 and 5, respectively). Overall, the spherical carrier media achieved greater specific organic removal rates compared with cylindrical carrier media. The lower heterotrophic activity obtained in Cell 1 with Media 4 and 5, helped to support the observations of high C/N ratio in Cell 3 and reduced nitrification. Other authors have reported a wide range of values for specific organic removal in biofilm systems. For example, a value of 67 mg COD/g TS.h was attained in a system fed with  $1.77$  g COD/m<sup>2</sup>.day and an attached biofilm  $1.1$  g TS/m<sup>2</sup> with a cylindrical  $500$  m<sup>2</sup>/m<sup>3</sup> carrier media (Falletti, Conte and Maestri, 2014). In another study a  $20.5$  mg sCOD/g TS.h was attained in a reactor fed with acetate, with cylindrical shape carrier media of  $680$  m<sup>2</sup>/m<sup>3</sup> surface area (Siciliano and De Rosa, 2016).

Regarding specific nitrification rates, values of  $5.5 \pm 0.9$ ,  $5.2 \pm 0.3$  and  $7.2 \pm 0.7$ ,  $4.9 \pm 0.9$  and  $5.2 \pm 0.5$  mg NH<sub>4</sub><sup>+</sup>-N/g TS.h, were measured with Media 1, 2, 3, 4 and 5, respectively (Table 5-4). Media 3 presented higher specific nitrification rates. However, regarding the specific ammonia removal normalised by protected surface area, the highest values were obtained with Media 1 and 2 ( $1.1$  g NH<sub>4</sub><sup>+</sup>-N/m<sup>2</sup>.day) compared to  $0.8$ ,  $0.6$ ,  $0.7$  g NH<sub>4</sub><sup>+</sup>-N/m<sup>2</sup>.day of Media 3, 4 and 5, respectively. Compared to the ammonia removal rates achieved in the pilot plant, batch scale values were higher with values of  $0.5 \pm 0.1$ ,  $0.7 \pm 0.2$ ,  $0.7 \pm 0.2$ ,  $0.5 \pm 0.1$  and  $0.4 \pm 0.1$  g NH<sub>4</sub><sup>+</sup>-N/m<sup>2</sup>.day for Media 1, 2, 3, 4 and 5 respectively. Other

studies report specific nitrification rates of 15 mg NH<sub>4</sub><sup>+</sup>-N/g TS.h with a 9.3 g TS/m<sup>2</sup> and 18.4 mg NH<sub>4</sub><sup>+</sup>-N/g TS.h with 6.6 g TS/m<sup>2</sup> in a tertiary nitrification MBBR using cylindrical carrier media with 500 m<sup>2</sup>/m<sup>3</sup> at 50% filling ratio (Salvetti et al., 2006). A 10.6 mg NH<sub>4</sub><sup>+</sup>-N/g TS.h with a 3-4 g TS/m<sup>2</sup> was reported in a hybrid MBBR, with cylindrical carrier media with 500m<sup>2</sup>/m<sup>3</sup> protected surface area at 60% filling ratio (Falletti and Conte, 2007). A specific nitrification rate of 5.89 mg NH<sub>4</sub><sup>+</sup>-N/g TS.h and 1.12 g NH<sub>4</sub><sup>+</sup>-N/m<sup>2</sup>.day were reported in an IFAS using cylindrical shape carrier media with 500 m<sup>2</sup>/m<sup>3</sup> protected surface area at a 30% filling ratio (Onnis-Hayden et al., 2011). Values of approximately 4 mg NH<sub>4</sub><sup>+</sup>-N/g VTS.h (volatile total solids, VTS) were achieved for a laboratory scale reactor using a cylindrical shape carrier media with 500 m<sup>2</sup>/m<sup>3</sup> and 8 mg NH<sub>4</sub><sup>+</sup>-N/ g VTS. h using a round parabolic shape carrier media with 3000 m<sup>2</sup>/m<sup>3</sup> at surface organic loading rate of 6 g COD/m<sup>2</sup>.day (Bassin et al., 2016). Other report values of 29.5, 9.2 and 7.5 mg NH<sub>4</sub><sup>+</sup>-N/g TSS.h for a “saddle shaped grid covered surface” carrier media with 50, 200 and 500 μm thickness, with normalised surface area values of approximately 1.8, 1.0 and 1.7 gNH<sub>4</sub><sup>+</sup>-N/m<sup>2</sup>.day (Torresi et al., 2016).

**Table 5-4 Specific organic and nitrification rates obtained during batch tests with the five carrier media studied.**

	Media 1	Media 2	Media 3	Media 4	Media 5
<b>Organic removal</b>					
Attached biofilm (g TS/m <sup>2</sup> )	14.3±1.2	10.0±0.5	14.4±0.7	13.3±0.1	7.2±0.6
Specific COD removal rate (mg sCOD/g TS.h)	34.8±2.0	26.9±0.6	19.2±1.7	13.4±1.1	13.4±0.2
Organic removal rate (g sCOD/m <sup>2</sup> .day)	11.9±0.3	6.4±0.1	9.4±0.2	4.2±0.8	2.3±0.2
<b>Ammonia removal</b>					
Attached biofilm (g TS/m <sup>2</sup> )	8.7±0.2	8.9±0.3	5.2±0.8	7.2±0.7	5.4±0.6
Specific NH <sub>4</sub> <sup>+</sup> removal rate (mg NH <sub>4</sub> <sup>+</sup> -N/g TS.h)	5.5±0.9	5.2±0.3	7.2±0.7	4.9±0.9*	5.2±0.5*
Nitrification rate (g NH <sub>4</sub> <sup>+</sup> -N/m <sup>2</sup> .day)	1.1±0.2	1.1±0.1	0.8±0.1	0.6±0.1	0.7±0.1

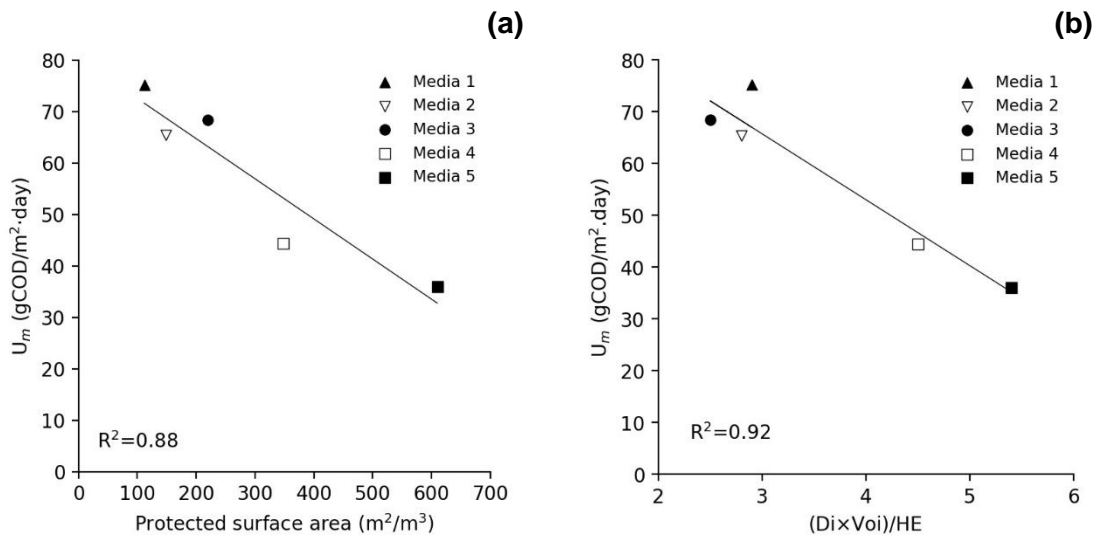
\*After flow reduction

### 5.3.4 Physical carrier media properties and operation performance

When steady state conditions were achieved, maximum COD removal rates were predicted based on the Stover-Kincannon model (equation (5-3)). The maximum substrate utilisation rate per area of carrier ( $U_m$ ) obtained for the different carrier media was 75.2, 65.4, 68.4, 44.4 and 36.0 g COD/m<sup>2</sup>.day, for Media 1, 2, 3, 4 and 5, respectively. Higher substrate utilisation rates were observed with the spherical carrier media compared with cylindrical carrier media. A strong correlation was obtained between  $U_m$  and protected surface area ( $R^2= 0.88$ ) (Figure 5-3a). A decrease in the maximum substrate removal rate was observed with an increase in protected surface area (44.4 and 36.0 g COD/m<sup>2</sup>.day, for Media 4 and 5, with protected surface area of 348 and 610 m<sup>2</sup>/m<sup>3</sup>, respectively). Whereas, an  $U_m$  of 75.2, 65.4, 68.4 g COD/m<sup>2</sup>.day was measured for Media 1 with protected surface area of 112 m<sup>2</sup>/m<sup>3</sup>, Media 2 with 148 m<sup>2</sup>/m<sup>3</sup> and Media 3 with 220 m<sup>2</sup>/m<sup>3</sup>, respectively.

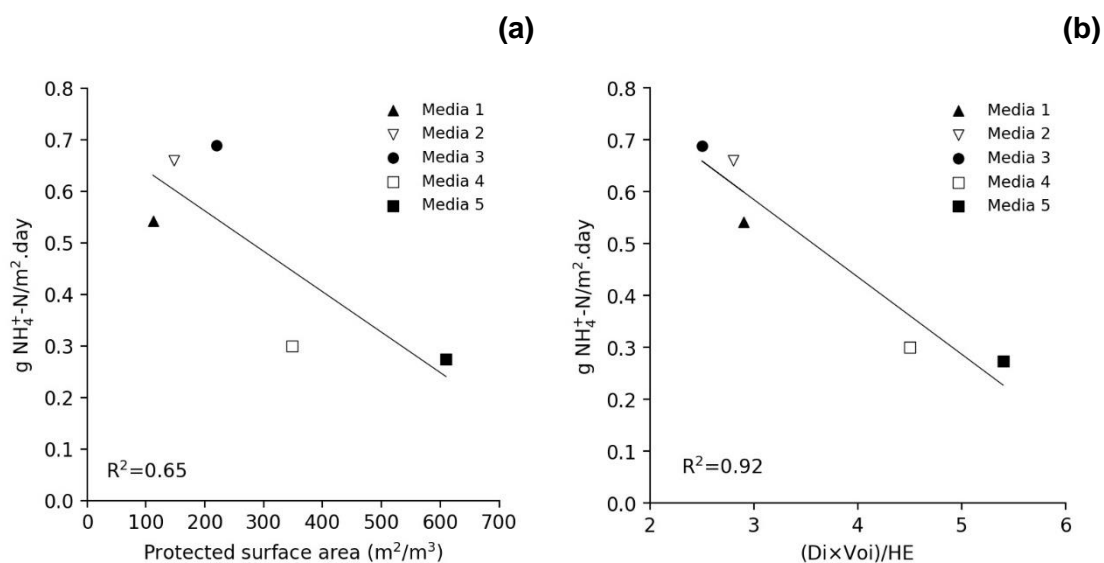
To examine the impact of carrier media physical properties on the pilot plant performance,  $U_m$ , was correlated with different physical parameters (Appendix C). Parameters such as: diameter, length, length to diameter ratio, sphericity, Sauter mean diameter, shape factor and voidage were investigated. Moving attached growth system hydrodynamics and oxygen mass transfer was previously shown to be influenced by carrier media physical properties, dimensionality ( $D_i$ ) and voidage ( $V_{oi}$ ) (Dias et al., 2018). The media dimensionality and voidage influenced the wastewater flow pattern and mixing impacting the reactor hydraulic efficiency. A strong correlation was given between the combination of these two parameters ( $D_i$  and  $V_{oi}$ ) with HE ( $R^2$  of 0.89), and SOTE with HE ( $R^2= 0.88$ ). The influence of dimensionality and voidage on hydraulic efficiency increased with biofilm development. In the cylindrical shape media, an increase in biofilm thickness reduced the internal voids, hindering the contact between the biofilm and the wastewater, thereby affecting the hydraulic and treatment efficiency of the reactor. By contrast, no negative influence was observed on the spherical and higher voidage media at increased biofilm thickness. The maximum substrate utilisation rate per area of carrier ( $U_m$ ) was also correlated with the same combination parameters; physical properties

associated with hydraulic efficiency  $(D_i \times V_{oi})/HE$ . For that voidage was corrected considering the biofilm thickness measured at steady state. Values of  $426 \pm 88$ ,  $375 \pm 45$ ,  $328 \pm 70$ ,  $449 \pm 82$  and  $268 \pm 79$   $\mu\text{m}$  were considered for the biofilm thickness and  $89 \pm 2$ ,  $93 \pm 5$ ,  $100$ ,  $74 \pm 1$  and  $63 \pm 2\%$ , for the hydraulic efficiency measured with each carrier media at steady state in Media 1, 2, 3, 4 and 5, respectively. Comparing statistically the HE results between the media, results were significantly different ( $p < 0.05$ ). A greater degree of association was achieved when comparing the  $U_m$  and  $(D_i \times V_{oi})/HE$  ( $R^2 = 0.92$ ) (Figure 5-3b).



**Figure 5-3 Correlation between  $U_m$  and protected surface area (a) and the combination of parameters  $(D_i \times V_{oi})/HE$  (b).**

Surface ammonia removal rates were correlated with carrier media protected surface area and carrier media physical properties. The correlation obtained between ammonia removal rate and protected surface area was  $R^2$  of 0.65 (Figure 5-4a). The lower ammonia removal rates achieved with Media 4 and 5, the higher protected surface area carrier media, challenges what is currently stated in the literature; that MBBR treatment performance is a function of protected surface area. A higher correlation was obtained when ammonia removal rates were compared with carrier media physical parameters  $(D_i \times V_{oi})/HE$  ( $R^2 = 0.92$ ) (Figure 5-4b).



**Figure 5-4 Correlation between ammonia removal rate and protected surface area (a) and the combination of parameters  $(D_i \times V_{oi})/HE$  (b).**

Despite the high protected surface area, the cylindrical shape and small internal voids of Media 4 and 5 made this carrier media more prone to clogging. The increase in biofilm thickness due to overgrowth of heterotrophic biofilm in the inner areas have limited diffusion. This resulted in a reduction in biofilm activity as was observed by the biofilm activity tests, where organic and ammonia removal rates were lower for Media 4 and 5. The low hydrodynamics efficiencies and low turbulence (dead spaces) inside the voids had also contributed towards the limited ammonia diffusion and oxygen mass transfer (Forrest, Delatolla and Kennedy, 2016). Other studies have identified the importance of increased thickness on the reduction of the protected surface area. A 33% reduction on protected surface area was calculated when the thickness of the biofilm increased from 0.25 mm to 1 mm in a cylindrical shape carrier media (Sen et al., 2007). In Media 4 and 5, the increase in biofilm thickness  $449 \pm 82$  and  $268 \pm 79$   $\mu\text{m}$  led to a reduction in voidage of 6 to 14%, respectively. As stated in other studies, the small internal voids became clogged which in turn affected substrate and oxygen diffusion having a significant impact on nitrification performance (Goode, 2010; Sen et al., 2007). The larger voids of the spherical carrier media, Media 1, 2 and 3, improved the wastewater flow through the media encouraging heterotrophic and nitrifying biofilm to colonise the entire carrier surface (68-83%) resulting in

higher biofilm activity. In Media 4 and 5, biofilm was mainly situated in the internal part of the carrier media (58-61% coverage) that was further reduced due to increased thickness. In the cylindrical shape carrier media biofilm was less exposed to shear when compared with spherical carrier media, hindering biofilm scouring and diffusion of substrates.

Nevertheless, MBBR are still designed and evaluated according to carrier media protected surface area and physical properties have been observed to have a small impact on MBBR performance (Ødegaard, Gisvold and Strickland, 2000). The present findings support that carrier media physical properties play a significant role on biofilm growth and activity and that, carrier media protected surface area is not the only parameter that should be considered. In practice, for some carrier media shapes the estimation/prediction of removal rates can be inaccurate when using protected surface area. This in particular is because nitrification does not take place in all the carrier media protected area, due to increased thickness and carrier media clogging (Piculell et al., 2016c). As such, opting for carrier media with high voidage and open structure, will avoid variations on protected surface area and misleading substrate removal rates estimations while maintaining high treatment performance.

## 5.4 Conclusions

- Average COD removal efficiency of  $89\pm 3$ ,  $86\pm 2$ ,  $86\pm 3$ ,  $85\pm 4$ ,  $86\pm 2\%$  were obtained for Media 1, 2, 3, 4 and 5, respectively.
- Ammonia removal was higher for the spherical Media 1, 2 and 3 achieving values of  $70\pm 11$ ,  $71\pm 10$  and  $81\pm 3\%$  compared with  $42\pm 6$  and  $35\pm 12\%$  achieved with cylindrical carrier media (Media 4 and 5).
- The  $<50\%$  ammonia removal rates obtained with Media 4 and 5 were due to C/N ratios of 2.8 and 2.7 in the nitrification zone of the reactor.
- Heterotrophic and nitrifiers activity tests demonstrated that Media 1 presented the highest specific biofilm activity ( $34.8\pm 2.0$  mg COD/g TS.h) and the smaller spherical shape carrier media (Media 3) achieved the highest specific nitrification activity ( $7.2\pm 0.7$  mg N-NH<sub>4</sub><sup>+</sup>/g TS.h).



- Maximum COD utilisation rates correlated well with carrier media protected surface area, ( $R^2= 0.88$ ). A stronger correlation was obtained between  $U_m$  and carrier media dimensionality ( $D_i$ ), voidage ( $V_{oi}$ ) and hydraulic efficiency (HE) ( $R^2= 0.92$ ).
- Correlation ( $R^2$ ) between ammonia removal rate and protected surface area was 0.65, but a stronger correlation was obtained with the combination of physical parameters and reactor hydrodynamics ( $D_i \times V_{oi}$ )/HE ( $R^2= 0.92$ ).
- These findings support that not only carrier surface area plays an important role on MBBR performance, but size, voidage and carrier media shape can be optimised to improve process performance.
- The spherical shape carrier media with high voidage improved wastewater flow through the carrier media promoting an active biofilm and good process performance.

## Acknowledgements

The authors acknowledge the support from Warden Biomedica and Cranfield University.

## 5.5 References

APHA (2005) *Standard Methods for the Examination of Water and Wastewater*. 21st edn. Washington, D.C.: American Public Health Association.

Bassin, J.P., Dias, I.N., Cao, S.M.S., Senra, E., Laranjeira, Y. and Dezotti, M. (2016) 'Effect of increasing organic loading rates on the performance of moving-bed biofilm reactors filled with different support media: Assessing the activity of suspended and attached biomass fractions', *Process Safety and Environmental Protection*, 100, pp. 131–141.

Deng, L., Guo, W., Ngo, H.H., Zhang, X., Wang, X.C., Zhang, Q. and Chen, R. (2016) 'New functional biocarriers for enhancing the performance of a hybrid moving bed biofilm reactor-membrane bioreactor system', *Bioresource Technology*, 208, pp. 87–93.

Dias, J., Stephenson, T., Bellingham, M., Hassan, J., Barrett, M. and Soares, A. (2018) 'Impact of carrier media on oxygen transfer and wastewater hydrodynamics on a moving attached growth system', *Chemical Engineering Journal*, 351, pp. 399–408.

Eldyasti, A., Nakhla, G. and Zhu, J. (2012) 'Influence of particles properties on biofilm structure and energy consumption in denitrifying fluidized bed bioreactors (DFBBRs)', *Bioresource Technology*, 126, pp. 162–171.

Elliott, O. et al. (2017) 'Design and Manufacturing of High Surface Area 3D-Printed Media for Moving Bed Bioreactors for Wastewater Treatment', *Journal of Contemporary Water Research & Education*, (160), pp. 144–156.

European Parliament. Council of the European Union (1991) *Council Directive concerning urban waste-water treatment (91/271/EEC)*. Available at: <http://eur-lex.europa.eu/legal-content/EN/TXT/?uri=celex%3A31991L0271> (Accessed: 4 October 2015).

Falletti, L. and Conte, L. (2007) 'Upgrading of Activated Sludge Wastewater Treatment Plants with Hybrid Moving-Bed Biofilm Reactors', *Industrial & Engineering Chemistry Research*, 46, pp. 6656–6660.

Falletti, L., Conte, L. and Maestri, A. (2014) 'Upgrading of a wastewater treatment plant with a hybrid moving bed biofilm reactor (MBBR)', *AIMS Environmental Science*, 1(2), pp. 45–52.

Forrest, D., Delatolla, R. and Kennedy, K. (2016) 'Carrier effects on tertiary nitrifying moving bed biofilm reactor: An examination of performance, biofilm and biologically produced solids', *Environmental Technology*, 37(6), pp. 662–671.

Goode, C. (2010) *Understanding biosolids dynamics in a moving bed biofilm reactor*. PhD thesis. University of Toronto. Available at: [https://tspace.library.utoronto.ca/bitstream/1807/24758/6/Goode\\_Christopher\\_J\\_201006\\_PhD\\_Thesis.pdf](https://tspace.library.utoronto.ca/bitstream/1807/24758/6/Goode_Christopher_J_201006_PhD_Thesis.pdf) (Accessed: 18 November 2014).

Hem, L.J., Rusten, B. and Odegaard, H. (1994) 'Nitrification in a moving bed

biofilm reactor', *Water Research*, 28(6), pp. 1425–1433.

Herrling, M.P., Guthausen, G., Wagner, M., Lackner, S. and Horn, H. (2015) 'Determining the flow regime in a biofilm carrier by means of magnetic resonance imaging', *Biotechnology and Bioengineering*, 112(5), pp. 1023–1032.

Karizmeh, M.S., Delatolla, R. and Narbaitz, R.M. (2014) 'Investigation of settleability of biologically produced solids and biofilm morphology in moving bed bioreactors (MBBRs)', *Bioprocess and Biosystems Engineering*, 37(9), pp. 1839–1848.

Kermani, M., Bina, B., Movahedian, H., Amin, M.M. and Nikaein, M. (2008) 'Application of moving bed biofilm process for biological organics and nutrients removal from municipal wastewater', *American Journal of Environmental Sciences*, 6(4), pp. 675–682.

Lee, L.Y., Ong, S.L. and Ng, W.J. (2004) 'Biofilm morphology and nitrification activities: Recovery of nitrifying biofilm particles covered with heterotrophic outgrowth', *Bioresource Technology*, 95(2), pp. 209–214.

Levenspiel, O. (1999) *Chemical Reaction Engineering*. 3rd edn. John Wiley & Sons Inc. (ed.) New York.

Li, H., Zhu, J., Flammig, J.J., O'Connell, J. and Shrader, M. (2015) 'Practical experience with full-scale structured sheet media (SSM) integrated fixed-film activated sludge (IFAS) systems for nitrification', *Water Science and Technology*, 71(4), pp. 545–552.

Mao, Y., Quan, X., Zhao, H., Zhang, Y., Chen, S., Liu, T. and Quan, W. (2017) 'Accelerated startup of moving bed biofilm process with novel electrophilic suspended biofilm carriers', *Chemical Engineering Journal*, 315, pp. 364–372.

Martín-Pascual, J., López-López, C., Cerdá, A., González-López, J., Hontoria, E. and Poyatos, J.M. (2012) 'Comparative kinetic study of carrier type in a moving bed system applied to organic matter removal in urban wastewater treatment', *Water, Air, and Soil Pollution*, 223(4), pp. 1699–1712.

Martínez-Huerta, G., Prendes-Gero, B., Ortega-Fernández, F. and Mesa-Fernández, J.M. (2009) 'Design of a carrier for wastewater treatment using moving bed bioreactor', *Proceedings of the 2nd International Conference on Environmental and Geological Science and Engineering*. Brasov, Romania, pp. 44–49.

McQuarrie, J.P. and Boltz, J.P. (2011) 'Moving Bed Biofilm Reactor Technology: Process Applications, Design, and Performance', *Water Environment Research*, 83(6), pp. 560–575.

Melcer, H. and Schuler, A.J. (2014) *Mass Transfer Characteristics of Floating Media in MBBR and IFAS Fixed-Film Systems*. London, United Kingdom.

Nogueira, B.L., Pérez, J., van Loosdrecht, M.C.M., Secchi, A.R., Dezotti, M. and Biscaia, E.C. (2015) 'Determination of the external mass transfer coefficient and influence of mixing intensity in moving bed biofilm reactors for wastewater treatment', *Water Research*, 80, pp. 90–98.

Ødegaard, H. (2006) 'Innovations in wastewater treatment: The moving bed biofilm process', *Water Science and Technology*, 53(9), pp. 17–33.

Ødegaard, H., Gisvold, B. and Strickland, J. (2000) 'The influence of carrier size and shape in the moving bed biofilm process', *Water Science and Technology*, 41(4–5), pp. 383–391.

Ødegaard, H., Rusten, B. and Westrum, T. (1994) 'A new moving bed biofilm reactor - applications and results', *Water Science & Technology*, 29(10–11), pp. 157–165.

Onnis-Hayden, A., Majed, N., Schramm, A. and Gu, A.Z. (2011) 'Process optimization by decoupled control of key microbial populations: Distribution of activity and abundance of polyphosphate-accumulating organisms and nitrifying populations in a full-scale IFAS-EBPR plant', *Water Research*, 45(13), pp. 3845–3854.

Orantes, J.C. and González-Martínez, S. (2004) 'A new low-cost biofilm carrier

for the treatment of municipal wastewater in a moving bed reactor', *Water Science and Technology*, 48(11–12), pp. 243–250.

Patel, A., Nakhla, G. and Zhu, J. (2005) 'Detachment of multi species biofilm in circulating fluidized bed bioreactor', *Biotechnology and Bioengineering*, 92(4), pp. 427–437.

Pfeiffer, T.J. and Wills, P.S. (2011) 'Evaluation of three types of structured floating plastic media in moving bed biofilters for total ammonia nitrogen removal in a low salinity hatchery recirculating aquaculture system', *Aquacultural Engineering*, 45(2), pp. 51–59.

Piculell, M. (2016) *New Dimensions of Moving Bed Biofilm Carriers. Influence of biofilm thickness and control possibilities*. PhD thesis. Lund University. Available at: [https://lup.lub.lu.se/search/ws/files/7673290/Maria\\_Piculell\\_Webb\\_kappa.pdf](https://lup.lub.lu.se/search/ws/files/7673290/Maria_Piculell_Webb_kappa.pdf) (Accessed: 3 May 2016).

Piculell, M., Welander, P., Jönsson, K. and Welander, T. (2016) 'Evaluating the effect of biofilm thickness on nitrification in moving bed biofilm reactors', *Environmental Technology (United Kingdom)*, 37(6), pp. 732–743.

Piculell, M., Welander, T. and Jönsson, K. (2014) 'Organic removal activity in biofilm and suspended biomass fractions of MBBR systems', *Water Science and Technology*, 69(1), pp. 55–61.

Regmi, P., Thomas, W., Schafran, G., Bott, C., Rutherford, B. and Waltrip, D. (2011) 'Nitrogen removal assessment through nitrification rates and media biofilm accumulation in an IFAS process demonstration study', *Water Research*, 45(20), pp. 6699–6708.

Rusten, B., Eikebrokk, B., Ulgenes, Y. and Lygren, E. (2006) 'Design and operations of the Kaldnes moving bed biofilm reactors', *Aquacultural Engineering*, 34(3), pp. 322–331.

Salveti, R., Azzellino, A., Canziani, R. and Bonomo, L. (2006) 'Effects of temperature on tertiary nitrification in moving-bed biofilm reactors', *Water*

*Research*, 40(15), pp. 2981–2993.

Sen, D., Randall, C.W., Brink, W., Farren, G., Pehrson, D., Flournoy, W. and Copithorn, R.R. (2007) 'Understanding the importance of aerobic mixing, biofilm thickness control and modeling on the success or failure of ifas systems for biological nutrient removal', *Nutrient Removal 2007*. Water Environment Federation, Vol.29, pp. 1098–1126.

Siciliano, A. and De Rosa, S. (2016) 'An experimental model of COD abatement in MBBR based on biofilm growth dynamic and on substrates' removal kinetics', *Environmental Technology (United Kingdom)*, 37(16), pp. 2058–2071.

Sousa, M., Azeredo, J., Feijo, J. and Oliveira, R. (1997) 'Polymeric supports for the adhesion of a consortium of autotrophic nitrifying bacteria', *Biotechnology Techniques*, 11(10), pp. 751–754.

Tang, B., Zhao, Y., Bin, L., Huang, S. and Fu, F. (2017) 'Variation of the characteristics of biofilm on the semi-suspended bio-carrier produced by a 3D printing technique: Investigation of a whole growing cycle', *Bioresource Technology*, 244, pp. 40–47.

Torkaman, M., Borghei, S.M., Tahmasebian, S. and Andalibi, M.R. (2015) 'Nitrogen removal from high organic loading wastewater in modified Ludzack-Ettinger configuration MBBR system', *Water Science and Technology*, 72(8), pp. 1274–1282.

Torresi, E., Fowler, S.J., Poleisel, F., Bester, K., Andersen, H.R., Smets, B.F., Plósz, B.G. and Christensson, M. (2016) 'Biofilm thickness influences biodiversity in nitrifying MBBRs - Implications on micropollutant removal', *Environmental Science and Technology*, 50(17), pp. 9279–9288.

WEF (2011) 'Moving-Bed Biofilm Reactors', in McGraw-Hill (ed.) *Biofilm Reactors* - WEF MoP 35. New York: WEF Press.

Young, B., Banihashemi, B., Forrest, D., Kennedy, K., Stintzi, A. and Delatolla, R. (2016) 'Meso and micro-scale response of post carbon removal nitrifying

MBBR biofilm across carrier type and loading', *Water Research*, 91, pp. 235–243.

Zhang, T.C. and Bishop, P.L. (1994) 'Density, porosity, and pore structure of biofilms', *Water Research*, 28(11), pp. 2267–2277.

Zhu, S. and Chen, S. (2002) 'The impact of temperature on nitrification rate in fixed biofilters', *Aquacultural Engineering*, 26(4), pp. 221–237.

Zhu, S. and Chen, S. (2001) 'Effects of organic carbon on nitrification rate in fixed film biofilters', *Aquacultural Engineering*, 25, pp. 1–11.

Zinatizadeh, A.A.L. and Ghaytooli, E. (2015) 'Simultaneous nitrogen and carbon removal from wastewater at different operating conditions in a moving bed biofilm reactor (MBBR): Process modeling and optimization', *Journal of the Taiwan Institute of Chemical Engineers*, 53, pp. 98–111.





## 6 IMPACT OF CARRIER MEDIA PHYSICAL PROPERTIES ON BOUNDARY LAYER THICKNESS AND EXTERNAL MASS TRANSFER ON MOVING ATTACHED GROWTH SYSTEMS

J. Dias<sup>a</sup>, A. Parsotamo<sup>a</sup>, M. Bellingham<sup>b</sup>, J. Hassan<sup>b</sup>, M. Barrett<sup>b</sup>, T. Stephenson<sup>a</sup>, A. Soares<sup>a</sup>

<sup>a</sup> Cranfield University Water Sciences Institute, Cranfield, MK43 0AL, UK.

<sup>b</sup> Warden Biomedica, 31 Sundon Industrial Estate, Dencora Way, Luton, Bedford, LU3 3HP, UK.

### Abstract

This study aimed at understanding the impact of media of different shape (two spherical and one cylindrical) and voidage on the mass transfer boundary layer (MTBL) thickness and external mass transfer coefficients in a heterotrophic biofilm in a moving attached growth system (e.g.: a moving bed biofilm reactor, MBBRs, or submerged aerated filters, SAFs). Spherical, dimensionality 2.68 and spherical, dimensionality 2.78 media with surface area (SA) of 135 and 310 m<sup>2</sup>/m<sup>3</sup>, respectively. Cylindrical, dimensionality 4.27, a SA of 600 m<sup>2</sup>/m<sup>3</sup>. The MTBL thickness was lower in spherical, dimensionality 2.78 media, varying between 15.5-129.6 µm whereas spherical, dimensionality 2.68 and cylindrical, dimensionality 4.27 presented values of 28.6-172.4 and 39.7-170.5 µm, respectively, dependent on the wastewater mixing velocities. External mass transfer coefficients ranged from 1.0-6.1, 1.3-9.1 and 1.0-4.4 m/day for Media 1, 2 and 3, respectively. The influence of external mass transfer on COD removal were 59, 40 and 30% for spherical, dimensionality 2.68, spherical, dimensionality 2.78 and cylindrical, dimensionality 4.27 media, respectively. A poor correlation was observed between protected surface area and MTBL thickness ( $R^2 = 0.27$ ). A stronger correlation was achieved when comparing carrier media physical properties: dimensionality ( $D_i$ ) and voidage ( $V_{oi}$ ) with MTBL thickness ( $R^2 = 0.86$ ). These high correlations obtained, indicated that other parameters beyond carrier media protected surface area play a role in MBBR/SAF performance. This study clearly signifies the importance of the carrier physical properties on external mass transfer and diffusion within biofilm. Investigating the potential of carrier media physical properties can provide opportunities for capital and operational cost

savings making MBBR processes more competitive and attractive than alternative processes, while also informing the design of new media.

**Keywords:** Biofilm, carrier media, mixing intensities, moving bed biofilm reactors, MTBL, organic removal.

## 6.1 Introduction

The reliability of moving attached growth systems (e.g.: moving bed biofilm reactors, MBBRs, integrated fixed film activated sludge, IFAS, and submerged aerated filters, SAFs) to produce high quality wastewater effluents has been demonstrated in many pilot studies as well as full-scale wastewater treatment plants (WWTPs). MBBRs are implemented to remove organic matter as well as ammonia from municipal and industrial effluents (Ødegaard, Gisvold and Strickland, 2000; Rusten et al., 2006). In these systems, a biofilm grows attached to the surface of a carrier media that is fully submerged and maintained in movement within the wastewater. The continuous movement between the carrier media and the bulk liquid is typically promoted by mechanical mixers (anaerobic and anoxic reactors) or diffuser aeration (aerobic reactors) (McQuarrie and Boltz, 2011). The carrier media is one of the most important components of MBBRs, ensuring a large surface area for biofilm growth and simultaneously exhibiting a geometry that promotes the transport of substrates and oxygen distribution into the biofilm (McQuarrie and Boltz, 2011).

In biofilm processes, as well as in suspended growth, the transfer of substrates and oxygen from the bulk liquid to the interior of the biofilm transpires in three stages: (1) transport from the bulk liquid to stagnant liquid layer commonly designated by a mass transfer boundary layer (MTBL), (2) diffusion within the biofilm matrix and (3) consumption of substrate (Boltz, Morgenroth and Sen, 2010; Wilén, Gapes and Keller, 2004). All the stages are essential for the overall substrate removal efficiency, however the first stage is the most critical. On the other hand, this stage, often expressed as MTBL thickness, is frequently neglected. In most activated sludge process studies, the bulk liquid and aggregate-flocs are assumed to be a single phase (Wilén, Gapes and Keller, 2004). In biofilms, the substrate transfer in the proximity and within the biofilm

occurs mainly by diffusion but the MTBL, assumes a greater importance as it adds an additional resistance to mass transfer (Boltz, Morgenroth and Sen, 2010). Diffusion is commonly the limiting factor for microbial growth and metabolic activity in systems where bacteria do not grow as a single planktonic cell (Herrling et al., 2015). Thus, the thickness of MTBL plays an important role in the performance of moving attached growth systems.

The MTBL is strongly influenced by reactor hydrodynamics, biofilm structure, support structure and substrate diffusivity (Prehn et al., 2012; Wilén, Gapes and Keller, 2004). The hydrodynamic conditions in the biofilm-bulk phase, which are governed by flow velocities and mixing intensities, can significantly affect the boundary layer thickness. Different studies have researched the impact of mixing intensities on MTBL thickness. In these studies the increase in flow velocities and mixing intensities was shown to decrease the MTBL thickness, enhancing mass transport in biofilms (Gapes and Keller, 2009; Hem, Rusten and Odegaard, 1994; Nicoletta, van Loosdrecht and Heijnen, 1998; Nogueira et al., 2015).

The number of studies that have investigated the impact of MTBL and external mass transfer in moving biofilm systems is limited, and most of them are restricted to nitrifying systems. The influence of two different size and shape carrier media (Nat-S1, 310 and K1, 505 m<sup>2</sup>/m<sup>3</sup>) on external mass transfer on a nitrifying biofilm demonstrated that, values of external mass transfer were quite similar between the two carriers Nat-S1 (2.0-5.6 m/d) and K1 (1.3-4.1 m/d) (Gapes and Keller, 2009). Using oxygen microelectrodes to measure the oxygen profile within the biofilm on a flat shaped carrier media, Mašić, Bengtsson and Christensson (2010) demonstrated an increase in MTBL thickness at lower flow rates and a decrease in DO concentration in the boundary layer. Results confirmed the importance of a reduced MTBL thickness for an efficient DO utilisation. However, it is important to emphasise that the study was completed using a fixed flat shaped carrier.

Studies using semi-suspended carrier media also stated the influence of MTBL as an external mass transfer resistance on the DO distribution within the biofilm (Tang et al., 2017a). The effect of mixing, on ammonia utilisation rates, was studied by Melcer and Schuler (2014) and Nogueira et al. (2015) in batch tests.

Melcer and Schuler (2014) compared the effect of two different shape and size media with similar protected surface area on external mass transfer. Higher mixing intensities led to a reduction of MTBL and promoted higher mass transport to the biofilm, thereby increasing reaction rates. Higher nitrifying activity was found on the larger structure carrier media (Ø22 mm x 17 mm) compared to the small structure carrier media (Ø12 mm x 14 mm), despite having an equal protected surface area (Melcer and Schuler, 2014).

An *in-situ* methodology was recently developed to estimate external mass transfer in a moving bed biofilm reactor removing chemical oxygen demand (COD) and ammonia (Nogueira et al., 2015). Results confirmed the importance of mixing towards reducing the MTBL thickness. Moreover, the ammonia removal rate was more impacted by the MTBL thickness, compared with carbon oxidation (Nogueira et al., 2015).

Despite the importance of MTBL thickness on biofilm performance, only the study from Gapes and Keller (2009) assessed the influence of carrier media type on MTBL and external mass transfer in a MBBR operated solely for nitrification and using low carrier media filling ratios (20%).

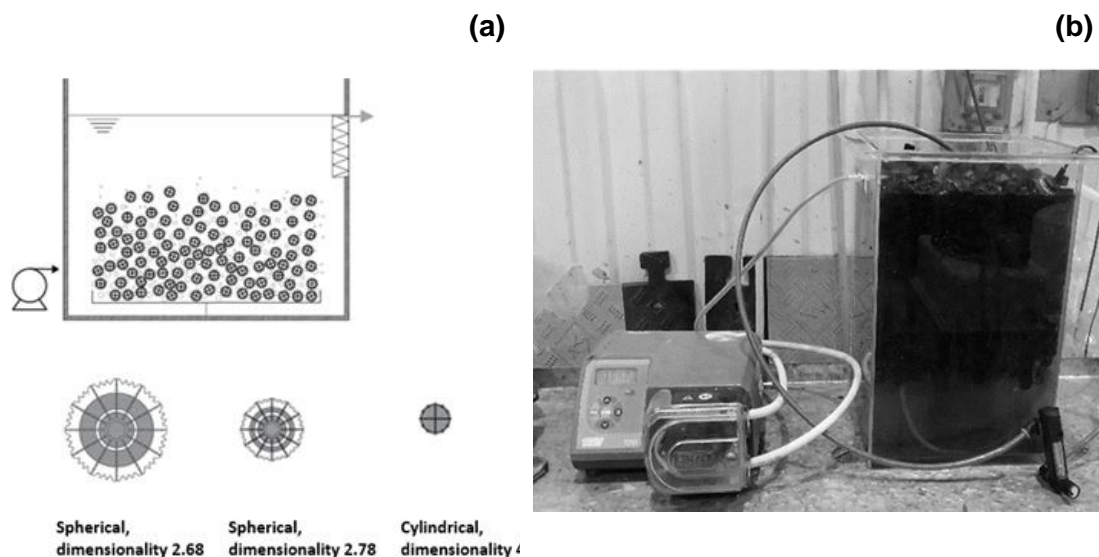
Following the methodology described by Nogueira et al. (2015), the study here presented aimed at understanding the impact of media with different surface area, shape and voidage (two spherical and one cylindrical) on MTBL thickness and external mass transfer in a heterotrophic biofilm (COD removal) in a moving bed biofilm reactor.

## **6.2 Material and methods**

### **6.2.1 Lab scale reactor configuration and experimental process**

A lab scale reactor with a capacity of 40 L (30 cm width x 30 cm length and 45 cm height) was used to determine the MTBL thickness and external mass transfer (Figure 6-1). The reactor was continuously fed with settled municipal wastewater from Cranfield University's wastewater treatment plant treating 2840 population equivalent (PE) (Cranfield, UK). The aeration and mixing were actioned by medium-bubble aeration (air inlet pressure of  $1.01 \times 10^5$  Pa). The carrier media

was supplied by Warden Biomedica (Luton, UK): two recycled polypropylene spherical shape carrier media (spherical, dimensionality 2.68 and spherical, dimensionality 2.78) and one recycled polypropylene cylindrical shape media (cylindrical, dimensionality 4.27). The media total surface area (TSA) varied between 135 (spherical, dimensionality 2.68), 310 (spherical, dimensionality 2.78) and 600  $\text{m}^2/\text{m}^3$  (cylindrical, dimensionality 4.27) and the protected surface area (PSA) was 112, 220 and 348  $\text{m}^2/\text{m}^3$ , respectively. The latter was determined by actually measuring the area of the carrier media that was covered with visible biofilm according to the methodology described by Dias et al. (2018a). All the media were tested at a 60% filling ratio (Table 6-1). The carrier to tank diameter ratio ( $d_p/D_t$ ), for the spherical media with 2.68 of dimensionality was 0.32, the values were comparable with other lab scale reactors that presented ratios of 0.45 and 0.48, where wall effect was minimised (Young et al., 2016).



**Figure 6-1 Schematic of lab scale reactor and media studied (a) cylindrical, dimensionality 4.27 media on the lab scale reactor (b).**

**Table 6-1 Media characteristics and reactor operation conditions. Spherical, dimensionality 2.68 (Biofil), spherical, dimensionality 2.78 (Biomarble), cylindrical, dimensionality 4.27 (Biopipe). Media was supplied by Warden Biomedia (<http://www.wardenbiomedia.com/>)**

Media	Total surface area (m <sup>2</sup> /m <sup>3</sup> )	Protected surface area (m <sup>2</sup> /m <sup>3</sup> )	Shape	Dimensions		Voidage (%)	Material	Density (g/cm <sup>3</sup> )
				Length (mm)	Diameter (mm)			
Spherical, dimensionality 2.68	135	112	Spherical	65	95	95		
Spherical, dimensionality 2.78	310	220	Spherical	36	46	90	Recycled PP	0.97
Cylindrical, dimensionality 4.27	600	348	Cylindrical	13	21.5	82.5		

## 6.2.2 Determination of the external mass transfer

The boundary layer thickness and external mass transfer coefficient were determined following the methodology described by Nogueira et al. (2015). To promote biofilm growth on the media, clean media was placed in a 2 m<sup>3</sup> pilot plant operated in parallel and continuously fed with the same settled municipal wastewater. Once biofilm was fully developed, media was removed from the pilot plant and transferred into the laboratory scale reactor and operated continuously with settled wastewater for 2 to 3 weeks prior to initiating the mass transfer experiments. During the batch tests, temperature was maintained at 20°C using a heater and pH continuously adjusted to a pH=±7.5. Dissolved oxygen was regulated by controlling air and nitrogen flow rate and kept around 2.5-3.5 mg O<sub>2</sub>/L (limiting factor). These batch tests were conducted at varying mixing intensities, according to Nogueira et al. (2015). Mixing intensities were varied based on the airflow rate normalised by the liquid volume inside the reactor (L). Mixing intensities were increased until the COD removal rates stabilised, within a range of 2.5-30 L/min (0.07-0.83 L/L.min).

Before starting each test, the wastewater feed was stopped, and mixed liquor containing the carrier media aerated for 12 hours until the microorganisms reached the endogenous respiration stage. Sodium acetate (C<sub>2</sub>H<sub>3</sub>NaO<sub>2</sub>) (Fisher Scientific, Loughborough, UK) was then added to the reactor as the sole source

of organic carbon at an equivalent COD concentration of 120-150 mg COD/L (150 mg acetate/L). However, in several batch tests the soluble COD concentration values were higher, reaching values of 187 mg COD/L, due to small concentrations of soluble COD presented inside the reactor.

Each test lasted 1h and the wastewater was sampled every 15 min for soluble COD (sCOD) measurements. The linear regression of the sCOD removal (as a function of time) was used to calculate the sCOD removal rate ( $r^{exp}$ ) and expressed as (mg sCOD/L.min).

The calculations used in this study to measure the external mass transfer coefficient followed the methodology described by Nogueira et al. (2015). The external mass transfer coefficient ( $k_{O_2}$ ) and the MTBL thickness ( $\delta$ ) were obtained using equations (6-1) and (6-2), respectively. The limiting substrate in these experiments was oxygen as its concentration was kept constant around 2.5-3.5 mg O<sub>2</sub>/L”

$$k_{O_2} = \frac{V_{bulk}}{A} * \frac{r^{exp} * R^2}{R^2 - (r^{exp})^2} * \frac{\gamma_{O_2/substrate}}{S_{O_2}^{bulk}} \quad (6-1)$$

$$\delta = \frac{D_{O_2}^{water}}{k_{O_2}} \quad (6-2)$$

Where,  $V_{bulk}$  is the liquid volume in the reactor (m<sup>3</sup>),  $A$  is the carrier media protected surface (m<sup>2</sup>/m<sup>3</sup>),  $R$  is the volumetric removal rate where external mass transfer is neglected (mg/L.h),  $y_{O_2/substrate}$  is the ratio of the oxygen to the substrate uptake, and  $S_{O_2}^{bulk}$  is the dissolved oxygen in the liquid phase and  $D_{O_2}^{water}$  is the oxygen diffusivity in water m<sup>2</sup>/day.  $R$  was determined using the average variance of the tests completed at high mixing intensities following equation 6-3. Where,  $\sigma^2$  is the experimental variance of the experiment ( $j$ ) at high mixing intensity (Nogueira et al., 2015).

$$R = \frac{\sum r_j^{exp} / \sigma_j^2}{\sum 1 / \sigma_j^2} \quad (6-3)$$

### **6.2.3 Analytical methods**

Soluble COD was determined by filtering samples using a pore size filter of 0.45  $\mu\text{m}$  (Millipore™, Billerica, United States) and the sCOD concentration determined using Merck cell tests kits (Merck KGaA, Darmstadt, Germany) measured with a NOVA60 photometer (VWR, UK). Temperature, dissolved oxygen (DO) and pH were controlled using portable meters (HACH HQ40d; Camlab, Cambridge, UK). A sample from the mixed liquor suspended solids was collected before and after the batch tests to consider biofilm detachment according and measured following Standard Methods for the Examination of Water and Wastewater (APHA, 2005). The attached biofilm to the carriers was analysed prior to initiating the experiments following the procedure described in Regmi et al. (2011). Carriers were sampled and dried at 105°C overnight and weighed. The biofilm was removed by placing the carriers in a H<sub>2</sub>SO<sub>4</sub> solution (2 N) and stirred vigorously for 24 hours. The carriers were washed with tap water then biofilm brushed off and dried at 105°C. The total attached biofilm was calculated based on the difference in media dry weight before and after removing all biofilm attached. The results were expressed as grams of total solids per metre square of protected surface area of carrier media (g TS/m<sup>2</sup>). Biofilm density measured in the carrier media were obtained by dividing attached biofilm and biofilm thickness.

Biofilm thickness was measured through Optical Coherence Tomography (OCT) using a Thorlabs Standard (SR-OCT 930nm; Thorlabs. Germany), with a refractive index of 1.33 (water). The media was cut into small pieces with a surgical scalpel and images captured in different pieces of the carriers. Biofilm thickness was estimated based on the average measurements.

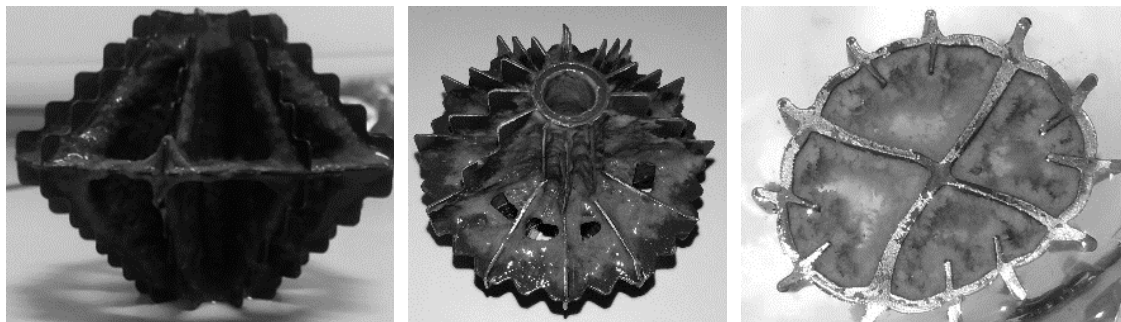
## **6.3 Results and discussion**

### **6.3.1 Attached biofilm and thickness**

Biofilm thickness was measured at the start of the mass transfer determination tests. The average biofilm thickness obtained for spherical, dimensionality 2.68, spherical, dimensionality 2.78 and cylindrical, dimensionality 4.27 media was 363±88, 250±35 and 232±35  $\mu\text{m}$ , respectively. Biofilm was attached all over the



spherical media, and only in the internal surfaces of cylindrical media (Figure 6-2). The attached biofilm was estimated at  $13.4\pm 2.2$ ,  $14.2\pm 2.1$  and  $13.35\pm 2.3$  g TS/m<sup>2</sup> for spherical, dimensionality 2.68, spherical, dimensionality 2.78 and cylindrical, dimensionality 4.27 media, respectively. Biofilm density measured in the carrier media was 36.9, 56.8 and 57.5 g TS/L for spherical, dimensionality 2.68, spherical, dimensionality 2.78 and cylindrical, dimensionality 4.27 media, respectively. No significant biofilm detachment was observed during the different tests.



**Figure 6-2 Biofilm attached to the carrier media: spherical, dimensionality 2.68 (left), spherical, dimensionality 2.78 (centre) and cylindrical, dimensionality 4.27 (right).**

### **6.3.2 External mass transfer**

After the endogenous respiration was achieved in the laboratory scale moving bed biofilm reactor, the sCOD removal was measured over time, at increasing mixing intensities, for the different media tested (Figure 6-3). In general, a significant increase in sCOD removal was observed with the increase in mixing intensities, for all the media (Figure 6-3). At the lowest mixing intensity tested, of 0.07 and 0.10 L/L.m, the sCOD removal was 39, 67.3 and 64.3 mg sCOD/L.h for spherical, dimensionality 2.68, spherical, dimensionality 2.78 and cylindrical, dimensionality 4.27 media, respectively. At the higher mixing intensity tested of 0.69 and 0.83 L/L.min, the sCOD removal rate was 95.8, 111.2 and 99.8 mg /L.h for spherical, dimensionality 2.68, spherical, dimensionality 2.78 and cylindrical, dimensionality 4.27 media, respectively.

Removal rates ( $r^{exp}$ ) were calculated from the slope of sCOD removed for each mixing intensity tested as function of time, according to the methodology by Nogueira et al., 2015 (Table 6-2).

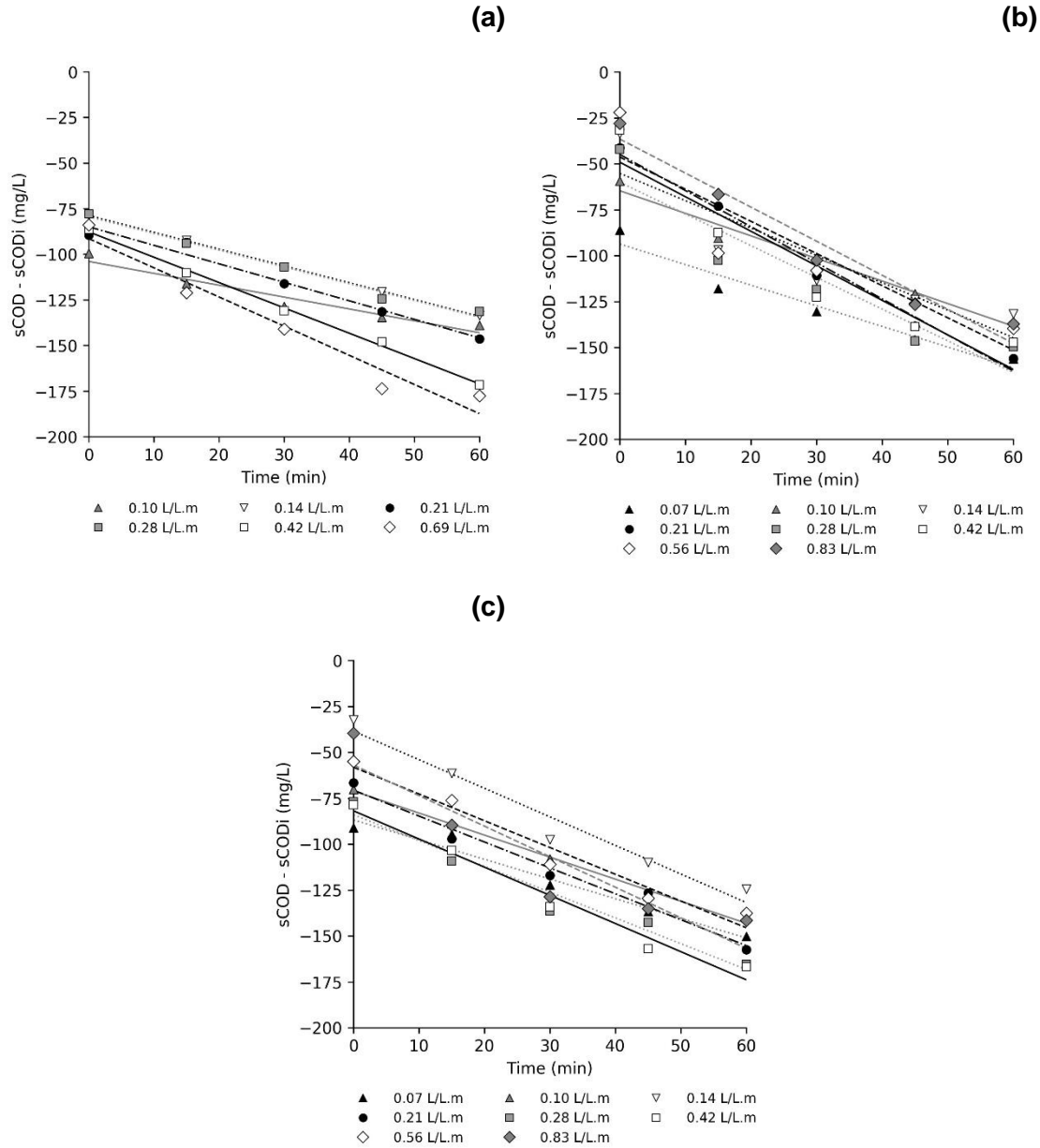


Figure 6-3 Soluble COD removed at different mixing intensities (L/L.min) for spherical, dimensionality 2.68 (a), spherical, dimensionality 2.78 (b) and cylindrical, dimensionality 4.27 (c) as a function of time.

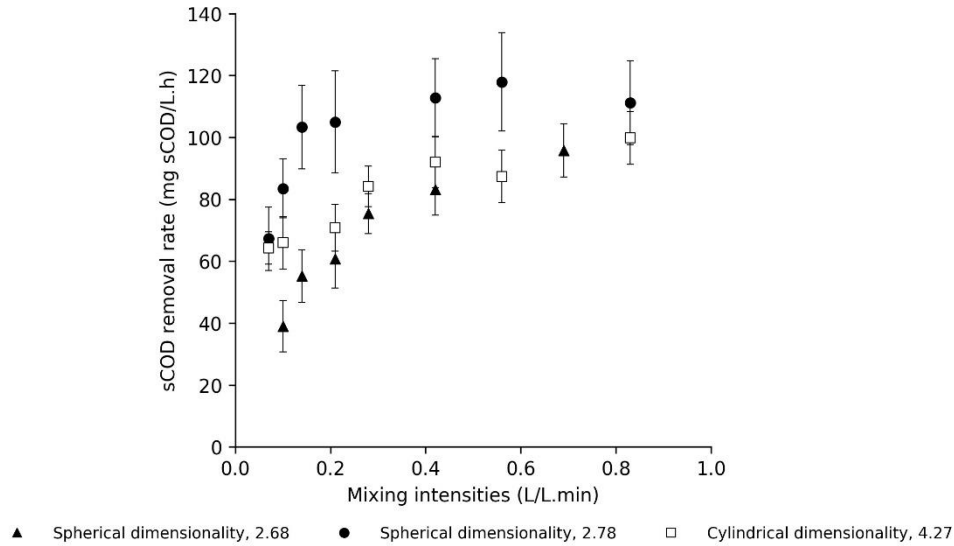
**Table 6-2 Soluble COD removal rates obtained at different mixing intensities for spherical, dimensionality 2.68, spherical, dimensionality 2.78 and cylindrical, dimensionality 4.27 media.**

Gas Flow Rate L/min	Mixing Intensity L/L.min	$r^{exp}$ (mg sCOD/L.h)		
		spherical, dimensionality 2.68	spherical, dimensionality 2.78	cylindrical, dimensionality 4.27
2.5	0.07	-	67.30	64.30
3.5	0.10	39.00	83.50	66.00
5	0.14	55.20	103.40	-
7.5	0.21	60.80	105.10	70.80
10	0.28	75.41	112.80	84.20
15	0.42	83.20	-	92.00
20	0.56		117.90	87.40
25	0.69	95.80	-	-
30	0.83	-	111.20	99.80

The sCOD removal rates presented a typical substrate saturation curve shape (i.e., increasing sCOD removal until maximum value, followed by stabilisation) (Figure 6-4). For spherical, dimensionality 2.78 and cylindrical, dimensionality 4.27 media, the sCOD removal rates stabilised at 0.14 L/L.min and 0.21 L/L.min mixing intensities, respectively (Figure 6-4). For spherical, dimensionality 2.68, the sCOD removal rates increased sharply until 0.42 L/L.min mixing intensity and continued to increase, however at a much slower rate after 0.42 L/L.min (Figure 6-4).

When the sCOD removal rates stabilised, external mass transfer no longer exerted an influence on treatment performance (Nogueira et al., 2015). Comparing COD removal rates over the range of experiments, the difference between the lowest (with influence of external mass transfer) and the highest (without influence of external mass transfer) were approximately 59, 40 and 30% for spherical, dimensionality 2.68, spherical, dimensionality 2.78 and cylindrical,

dimensionality 4.27 media, respectively. An increase in COD removal rates was also observed in Nogueira et al. (2015) when the mixing intensity was increased, the difference between lowest and highest removal rates was approximately 27%.



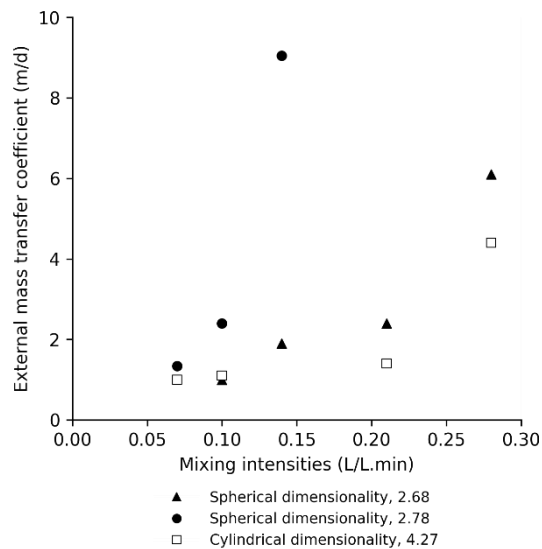
**Figure 6-4 Soluble COD removal rates at different mixing intensities.**

The sCOD removal rates, without external mass transfer influence ( $R$ ), were calculated as per the methodology described by Nogueira et al. (2015), using the average variance of the batch tests completed at high mixing intensities. Values of 95.8, 111.9 and 91.6 mg COD/L.h were obtained for spherical, dimensionality 2.68, spherical, dimensionality 2.78 and cylindrical, dimensionality 4.27 media, respectively. Similar sCOD removal rates were found in Nogueira et al. (2015)  $129.9 \pm 2.0$  mg COD/L.h, when external mass transfer was neglected.

Values of  $R$  were used on the determination of the mass transfer coefficient ( $K_{O_2}$ ) following equation (6-1) for each batch test removal rates ( $r^{exp}$ ), taking into consideration the volume in the reactor, the carrier media protected surface area and the ratio of the oxygen to the substrate uptake  $Y_{O_2/substrate}$  (0.35 g  $O_2$ /g COD) (Mannina et al., 2011; Nogueira et al., 2015).

The estimated external mass transfer coefficients ranged from 1.0-6.1, 1.3-9.1 and 1.0-4.4 m/day for spherical, dimensionality 2.68, spherical, dimensionality 2.78 and cylindrical, dimensionality 4.27 media, respectively (Figure 6-5). These

results indicated that the external mass transfer coefficient increased with mixing intensities. Spherical, dimensionality 2.78 media showed higher external mass transfer (9.1 m/day at 0.14 L/L.min), compared with spherical, dimensionality 2.68 media that achieved an external mass transfer coefficient of 6.1 m/day at 0.28 L/L.min, and cylindrical, dimensionality 4.27 media of 4.4 m/day at 0.28 L/L.min.



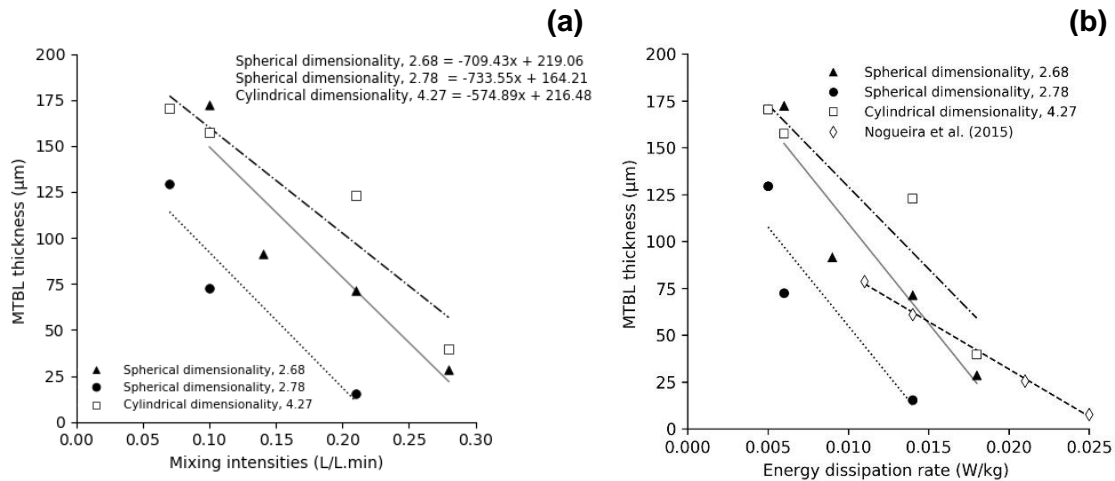
**Figure 6-5 External mass transfer coefficients for spherical, dimensionality 2.68, spherical, dimensionality 2.78 and cylindrical, dimensionality 4.27 media.**

The values of external mass transfer coefficients (1.0-6.1, 1.3-9.1 and 1.0-4.4 m/day for spherical, dimensionality 2.68, spherical, dimensionality 2.78 and cylindrical, dimensionality 4.27 media, respectively) were consistent with the range of the values stated in Nogueira et al. (2015) under comparable hydrodynamic conditions (2.9-6.8 m/d). Other studies, on nitrifying biofilms described external mass transfer values of 1.3 m/d using cylindrical shaped media (Hem, Rusten and Odegaard, 1994) and 3.2-1.5 m/d using a flat shaped carrier media (Mašić, Bengtsson and Christensson, 2010). In an airlift reactor, Nicolella, van Loosdrecht and Heijnen (1998) using spherical solid particle, achieved an external mass transfer of 6.91 m/d. Gapes and Keller (2009) compared two carrier types with cylindrical shape ( Nat-S1, 310 and K1, 505 m<sup>2</sup>/m<sup>3</sup> of protected surface area) operating under high and low ammonium load. Values of external mass transfer were quite similar between the two carriers Nat-S1 (2.0-5.6 m/d) and K1 (1.3-4.1 m/d) and the ones achieved in spherical,

dimensionality 2.68, spherical, dimensionality 2.78 and cylindrical, dimensionality 4.27 media at similar hydrodynamic conditions (Gapes and Keller, 2009).

Values of MTBL thickness were then determined using equation (6-2) for each batch test taking into consideration the diffusivity of oxygen in water ( $D_{O_2}^{water} = 1.74 \times 10^{-4} \text{ m}^2/\text{d}$ ) and the external mass transfer coefficient ( $K_{O_2}$ ). The MTBL thickness values for all the mixing intensities varied between 28.6-172.4, 15.5-129.6 and 39.7-170.5  $\mu\text{m}$  for spherical, dimensionality 2.68, spherical, dimensionality 2.78 and cylindrical, dimensionality 4.27 media, respectively (Figure 6-6a). A reduction in the MTBL thickness was observed with an increase of mixing intensities for all the media. The MTBL thickness values were in agreement with external mass transfer coefficients, decreasing when the MTBL thickness increased.

The influence of the mixing intensity on the estimated MTLB thickness is presented in Figure 6-6a. The higher influence of mixing on sCOD removal was observed to be in spherical, dimensionality 2.78 media where the slope value was higher recorded as 733.6, compared to 709.4 and 574.9 obtained with spherical, dimensionality 2.68 and cylindrical, dimensionality 4.27 media, respectively. Mixing intensities were converted to energy dissipation rates to allow for the comparison of the results with Nogueira et al. (2015) (Figure 6-6b). At similar energy dissipation rates, 0.014 W/kg, MTBL thickness values of 71.4  $\mu\text{m}$  were achieved for spherical, dimensionality 2.68 media, 15.5  $\mu\text{m}$  in spherical, dimensionality 2.78 media and 122.9 with cylindrical, dimensionality 4.27 media compared to 61.1  $\mu\text{m}$  achieved in Nogueira et al. (2015) using a different carrier media and reactor filling ratio (K1 of Anoxkaldnes™ and 40% filling ratio). In agreement with the external mass transfer; that at similar energy dissipation rates, in Nogueira et al. (2015) was lower, 2.9 m/d, compared with 9.1 m/day registered with spherical, dimensionality 2.78 media. Compared with spherical, dimensionality 2.68 media and, cylindrical, dimensionality 4.27 media values achieved by Nogueira et al. (2015) were similar for spherical, dimensionality 2.68 media (2.4 m/d) and slightly higher than cylindrical, dimensionality 4.27 media (1.4 m/d).



**Figure 6-6 MTBL thickness as a function of mixing intensity obtained in the different media tested (a) and comparison between MTBL thickness at different energy dissipation rates identified in this study and in Nogueira et al. (2015) (b).**

Existing literature on MTBL thickness is scarce. The majority of the work published to date focuses on nitrifying reactors, detailing MTBL thicknesses of 40-85 μm, however static carrier media was used (Mašić, Bengtsson and Christensson, 2010).

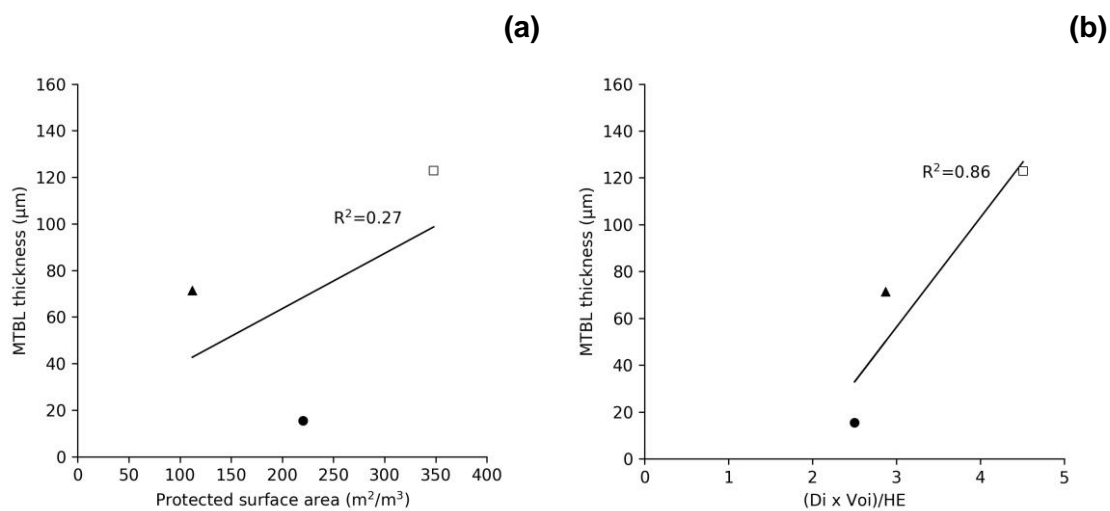
Models have been used to calculate MTBL thicknesses based on the Sherwood and Reynolds numbers, using set values of approximately 100 μm. However this theoretical correlation cannot be used for a particular carrier media geometry (Boltz et al., 2011). Values of MTBL thickness (ranged from 68.9-141 μm) have been estimated using steady-state biofilm models and simulated values, but these are dependent on system hydrodynamics rather than biofilm thickness (Wanner et al., 2006). Other studies, using a semi-suspended carrier media, achieved higher MTBL thickness value compared with results of the presented study. A minimum and a maximum MTBL thickness of 170±20 μm (biofilm thickness 350±10 μm) and 290±40 μm (biofilm thickness 1710± 20 μm) were measured during different biofilm ages, using microelectrode systems to measure DO profile (Tang et al., 2017a).

Regarding biofilm structure, the measured thickness in spherical, dimensionality 2.68 media was higher than in spherical, dimensionality 2.78 media, and cylindrical, dimensionality 4.27 media, 363±88, 250±35 and 232±35 μm,

respectively. An increase in biofilm thickness reduced the biofilm density in spherical, dimensionality 2.68 media of 36.9 g TS/L compared with 56.8 and 57.5 g TS/L for spherical, dimensionality 2.78 media, and cylindrical, dimensionality 4.27 media, respectively. Thin biofilm is expected to produce a denser and more homogeneous structure leading to lower external mass transfer while thick biofilm has more pores and voids producing a less dense and more heterogeneous biofilm (David et al., 2016). Consequently, the thinner biofilm in spherical, dimensionality 2.78 media, and cylindrical, dimensionality 4.27 media was expected to promote greater resistance to mass transfer than the thicker biofilm measured in spherical, dimensionality 2.68. However, results do show that spherical, dimensionality 2.78 media enhanced external mass transfer, indicating that biofilm density was of less influence.

### 6.3.3 Physical carrier media properties and MTBL thickness

The influence of carrier media protected surface area on the MTBL thickness was assessed. A poor correlation was observed between the protected surface area with MTBL thickness, ( $R^2= 0.27$ ) (Figure 6-7a). As opposed to what has been stated in most literature that carrier media protected surface area imparts the most influential role on MBBRs and SAFs performance (Ødegaard, Gisvold and Strickland, 2000), other carrier media properties also seem to play an important role.



**Figure 6-7 Correlation between MTBL thickness and protected surface area (a) and combination of parameters (Di x Voi)/HE (b) at 0.21 L/L.min.**



Other carrier media physical properties were then correlated with MTBL thickness (Appendix D). Weak correlations were observed when MTBL thickness values were correlated with physical properties such as: diameter, length, length to diameter ratio, sphericity, Sauter mean diameter, shape factor and voidage. From previous studies, carrier media physical properties: dimensionality ( $D_i$ ) and voidage ( $V_{oi}$ ), were strongly correlated with MBBRs and SAFs hydrodynamics, oxygen mass transfer, start-up and performance (Dias et al., 2018a, 2018b). Following this study, MTBL thickness was correlated with the physical properties associated with hydraulic efficiency  $(D_i \times V_{oi})/HE$  and a clear correlation was obtained ( $R^2 = 0.86$ ) (Figure 6-7b). The high correlation obtained suggested that other parameters beyond protected surface area do play a role on MBBRs performance. Despite the similar methodology used in this study, the MTBL thickness value stated by Nogueira et al. (2015) at the same energy dissipation rate ( $61.1 \mu\text{m}$ ) did not correlate with  $(D_i \times V_{oi})/HE$ . A possible explanation is the fact that Nogueira et al. (2015) used (i) synthetic wastewater to grow the biofilm (ii) the different carrier media filling ratios used together with the smaller scale reactor and (iii) the lower thickness obtained with the grown biofilm (data not shown in the cited article).

The thicker MTBL registered in cylindrical, dimensionality 4.27 media ( $122.9 \mu\text{m}$ ) compared with spherical, dimensionality 2.68 media ( $71.4 \mu\text{m}$ ) and spherical, dimensionality 2.78 media ( $15.5 \mu\text{m}$ ) might be caused by liquid velocity reduction through the cylindrical carrier media due to biofilm accumulation in the internal parts of cylindrical, dimensionality 4.27 media, resulting in lower biofilm activity and conversion rates.

A clear relationship has been reported between the decrease in MTBL thickness and the increase in reactor performance efficiency, due to higher mass transfer of substrates and products and microbial activity (Mašić, Bengtsson and Christensson, 2010; Wanner et al., 2006). Using biofilm models it was demonstrated that an increase in MTLB thickness from 0 to  $100 \mu\text{m}$  reduced sCOD flux by 19% in a carbon oxidation and nitrification MBBR reactor and 85% in a IFAS configuration (Boltz et al., 2011). In the same study, a decrease in ammonia flux of 16% was revealed when the MTLB thickness increased from 0

to 100  $\mu\text{m}$ . The results corroborated with Zhu and Chen (2001) studies, where in a nitrifying biofilm reactor ammonium flux increased when the MTBL thickness decreased. Sensitivity analyses carried out in studies by Boltz et al. (2011) have presented a strong influence of MTBL thickness on the model results.

The results indicated that cylindrical, dimensionality 4.27 media, with high protected surface area ( $348 \text{ m}^2/\text{m}^3$ ), cylindrical shape and low voidage attained higher MTBL thickness (122.9  $\mu\text{m}$ ) compared with spherical shape and higher voidage media (71.4 and 15.5  $\mu\text{m}$ ). The higher MTBL thickness and external mass transfer resistance compromised substrate and oxygen mass transfer in cylindrical, dimensionality 4.27 media. That was likely related to the obstruction of the internal voids by biofilm growth that hindered wastewater to pass through. Thus, to overcome external mass transfer limitations, in cylindrical, dimensionality 4.27 media will need to be operated at higher mixing intensities (higher airflow rates), that can possibly result in higher energy operating costs. Moreover, high mixing intensities can lead to uncontrolled biofilm detachment that can subsequently have an adverse effect on treatment performance.

This study illustrated the importance of the carrier media physical properties on MTBL thickness and external mass transfer. Studying the potential of carrier media physical properties on the MBBRs/SAFs process optimisation, can provide opportunities for capital and operational cost reduction. This is by means of more compact systems and lower carrier media filling ratio needed due to high carrier media efficiency and improved oxygen utilisation making this process more competitive with alternative technologies.

## 6.4 Conclusions

- MTBL thickness was calculated for 3 different media with varying geometries covered with a mature heterotrophic biofilm using existing methodologies. The MTBL thickness values of 71.4, 15.5 and 122.9  $\mu\text{m}$  were observed for spherical, dimensionality 2.68, spherical, dimensionality 2.78 and cylindrical, dimensionality 4.27 media, respectively at 0.21 L/L.min.

- Soluble COD removal rates of 95.8, 111.9 and 91.6 mg sCOD/L.h were registered for spherical, dimensionality 2.68, spherical, dimensionality 2.78 and cylindrical, dimensionality 4.27 media, respectively, respectively when external mass transfer was negligible.
- Lower external mass transfer values were registered in cylindrical, dimensionality 4.27 media (4.4 m/d) compared with 6.1 and 9.1 m/d of spherical, dimensionality 2.68, spherical, dimensionality 2.78, respectively, resulting in lower conversion rates.
- Strong correlation was attained between MTBL thickness and physical properties of the media associated with hydraulic efficiency ( $(D_i \times V_{oi})/HE$  ( $R^2= 0.86$ )).
- External mass transfer was enhanced with spherical shape and high voidage media, whilst cylindrical shape and low voidage media limited mass transfer. Thus, higher airflow rates will be required to operate cylindrical, dimensionality 4.27 media, that will result in higher operational costs.

## 6.5 References

APHA (2005) *Standard Methods for the Examination of Water and Wastewater*. 21st edn. Washington, D.C.: American Public Health Association.

Boltz, J.P., Morgenroth, E., Brockmann, D., Bott, C., Gellner, W.J. and Vanrolleghem, P.A. (2011) 'Systematic evaluation of biofilm models for engineering practice: Components and critical assumptions', *Water Science and Technology*, 64(4), pp. 930–944.

Boltz, J.P., Morgenroth, E. and Sen, D. (2010) 'Mathematical modelling of biofilms and biofilm reactors for engineering design', *Water Science and Technology*, 62(8), pp. 1821–1836.

David, A., Bons, A., Gabriel, G., Guimera, X., Gabriel, D. and Gamisans, X. (2016) 'Dynamic characterization of external and internal mass transport in heterotrophic biofilms from microsensors measurements', *Water Research*, 102,

pp. 551–560.

Dias, J., Bellingham, M., Hassan, J., Barrett, M., Stephenson, T. and Soares, A. (2018a) 'Influence of carrier media physical properties on start-up of moving attached growth systems', *Bioresource Technology*, 266, pp. 463–471.

Dias, J., Stephenson, T., Bellingham, M., Hassan, J., Barrett, M. and Soares, A. (2018b) 'Impact of carrier media on oxygen transfer and wastewater hydrodynamics on a moving attached growth system', *Chemical Engineering Journal*, 351, pp. 399–408.

Gapes, D.J. and Keller, J. (2009) 'Impact of oxygen mass transfer on nitrification reactions in suspended carrier reactor biofilms', *Process Biochemistry*, 44(1), pp. 43–53.

Hem, L.J., Rusten, B. and Odegaard, H. (1994) 'Nitrification in a moving bed biofilm reactor', *Water Research*, 28(6), pp. 1425–1433.

Herrling, M.P., Guthausen, G., Wagner, M., Lackner, S. and Horn, H. (2015) 'Determining the flow regime in a biofilm carrier by means of magnetic resonance imaging', *Biotechnology and Bioengineering*, 112(5), pp. 1023–1032.

Mannina, G., Trapani, D. Di, Viviani, G. and Ødegaard, H. (2011) 'Modelling and dynamic simulation of hybrid moving bed biofilm reactors: Model concepts and application to a pilot plant', *Biochemical Engineering Journal*, 56(1–2), pp. 23–36.

Mašić, A., Bengtsson, J. and Christensson, M. (2010) 'Measuring and modeling the oxygen profile in a nitrifying Moving Bed Biofilm Reactor', *Mathematical Biosciences*, 227(1), pp. 1–11.

McQuarrie, J.P. and Boltz, J.P. (2011) 'Moving Bed Biofilm Reactor Technology: Process Applications, Design, and Performance', *Water Environment Research*, 83(6), pp. 560–575.

Melcer, H. and Schuler, A.J. (2014) *Mass Transfer Characteristics of Floating Media in MBBR and IFAS Fixed-Film Systems*. London, United Kingdom.

Nicolella, C., van Loosdrecht, M.C.M. and Heijnen, J.J. (1998) 'Mass transfer and reaction in a biofilm airlift suspension reactor', *Chemical Engineering Science*, 53(15), pp. 2743–2753.

Nogueira, B.L., Pérez, J., van Loosdrecht, M.C.M., Secchi, A.R., Dezotti, M. and Biscaia, E.C. (2015) 'Determination of the external mass transfer coefficient and influence of mixing intensity in moving bed biofilm reactors for wastewater treatment', *Water Research*, 80, pp. 90–98.

Ødegaard, H., Gisvold, B. and Strickland, J. (2000) 'The influence of carrier size and shape in the moving bed biofilm process', *Water Science and Technology*, 41(4–5), pp. 383–391.

Prehn, J., Waul, C.K., Pedersen, L.F. and Arvin, E. (2012) 'Impact of water boundary layer diffusion on the nitrification rate of submerged biofilter elements from a recirculating aquaculture system', *Water Research*, 46(11), pp. 3516–3524.

Regmi, P., Thomas, W., Schafran, G., Bott, C., Rutherford, B. and Waltrip, D. (2011) 'Nitrogen removal assessment through nitrification rates and media biofilm accumulation in an IFAS process demonstration study', *Water Research*, 45(20), pp. 6699–6708.

Rusten, B., Eikebrokk, B., Ulgenes, Y. and Lygren, E. (2006) 'Design and operations of the Kaldnes moving bed biofilm reactors', *Aquacultural Engineering*, 34(3), pp. 322–331.

Tang, B., Song, H., Bin, L., Huang, S., Zhang, W., Fu, F., Zhao, Y. and Chen, Q. (2017) 'Determination of the profile of DO and its mass transferring coefficient in a biofilm reactor packed with semi-suspended bio-carriers', *Bioresource Technology*, 241, pp. 54–62.

Wanner, O., Eberl, H.J., Morgenroth, E., Noguera, D.R., Picioreanu, C., Rittmann, B.E. and Loosdrecht, M.C.M. van (2006) *Mathematical Modeling of Biofilms*. IWA Publishing.

Wilén, B.M., Gapes, D. and Keller, J. (2004) 'Determination of external and

internal mass transfer limitation in nitrifying microbial aggregates', *Biotechnology and Bioengineering*, 86(4), pp. 445–457.

Young, B., Banihashemi, B., Forrest, D., Kennedy, K., Stintzi, A. and Delatolla, R. (2016) 'Meso and micro-scale response of post carbon removal nitrifying MBBR biofilm across carrier type and loading', *Water Research*, 91, pp. 235–243.

Zhu, S. and Chen, S. (2001) 'Effects of organic carbon on nitrification rate in fixed film biofilters', *Aquacultural Engineering*, 25, pp. 1–11.

## 7 DISCUSSION

Regulations governing wastewater treatment plants effluent discharge are becoming increasingly stringent. As a consequence compliance with such regulations while trying to maintain low costs using sustainable technologies has become challenging. In the last few decades moving attached growth systems have been widely implemented in WWTPs. Efforts have been made to improve scientific knowledge of moving attached growth systems through research and development and thorough documented case studies. Moving attached growth systems are economic solutions due to smaller reactor volumes, high effluent quality and viability to upgrade and retrofit existing WWTPs in comparison with suspended growth treatment systems. However, further improvements in these technologies (MBBRs, IFAS, SAFs etc) can potentially result in increased capacity and performance thereby further enhancing the economics of the process. The protected surface area of a carrier media has been the conventional parameter used for design, operation and modelling of moving attached growth systems such as MBBRs, SAFs, IFAS etc. Thus, much attention has been given to increasing carrier protected surface area. A variety of carriers are currently being offered in the market. The cylinder-shaped carrier with a cross on the inside and external fins outside is the most used carrier media on MBBRs and investigated within the research community (McQuarrie and Boltz, 2011). Nevertheless, research studies start to question and investigate other parameters that potentially play a role in MBBR performance and should be included in the design criteria. Since Ødegaard's fundamental study in the year 2000 on the influence of carrier media shape and size on MBBR performance, carrier shape and size have not been directly addressed in the literature.

In this PhD thesis, the underpinning science required to understand the influence of carrier media physical properties (e.g.; voidage, shape and size) on oxygen mass transfer, hydraulic efficiency, biofilm attachment, process performance and substrate diffusion on moving attached growth systems is investigated. The outputs of this PhD thesis challenge the use of protected surface area as the sole design parameter in moving attached growth systems. The five media studied in this research varied in shape (cylindrical and spherical), size, voidage and protected surface area (112-610  $\text{m}^2/\text{m}^3$ ). The five media were tested at pilot scale and operated with real wastewater.

## **7.1 The effect of carrier media on oxygen mass transfer and wastewater hydrodynamics**

Biological oxygen requirements and air necessary for the maintenance of media in constant movement conditions make energy consumption a challenge for moving bed biofilm reactors. Dissolved oxygen set points are usually higher than for activated sludge processes, 3-5 mg/L compared to 1-2 mg/L (Jenkins, D. and J. Wanner, 2014). In this study, in Chapter 3, the presence of carrier media enhanced the oxygen transfer efficiency by 23-45%, in a medium bubble aeration system, corroborating with existing literature (Collignon, 2006; Jing, Feng and Li, 2009; Pham, Viswanathan and Kelly, 2008; Sander, Behnisch and Wagner, 2017). Different studies stated that carrier media promoted the shear of bubbles in to smaller ones thereby increasing the gas-liquid interfacial area. However, physical media properties appear to have been overlooked in all these studies. In this study five plastic media, three spherical (Media 1, 2 and 3) and two cylindrical (Media 4 and 5) improved the  $k_{La}$  in clean water by 23-37, 35-45, 36-45, 37-44 and 31-36%, for Media 1, 2, 3,4 and 5, respectively. Achieving values that varied between 3.97-25.57 1/h in comparison with 3.07-15.44 1/h without media. Concurrently, in moving bed biofilm systems the presence of carrier media can impact the hydraulic behaviour of the reactor. Results obtained indicated the presence of hydraulic short circuits or dead zones, in the presence of clean media, reducing the effective volume of the reactor. However, when the media was colonised with biofilm, an increase in residence time in three spherical media studied was achieved and hydraulic efficiencies of 89, 93 and 100% in Media 1, 2 and 3 respectively. On the other side, the presence of biofilm on cylindrical media contributed to a reduction of hydraulic efficiency to 74 and 63% with Media 4 and 5, respectively.

## **7.2 Influence of carrier media on start-up**

The start-up period is crucial to moving attached growth systems, and fast biofilm formation on the carrier media plays a vital role in short commission periods and treatment robustness during steady state (Mao et al., 2017; Tang et al., 2017b). Previously reported studies addressing start-up on moving attached growth systems were performed at the laboratory scale and using strategies to reduce start-up (Bassin et al., 2016; Mao et al., 2017; Tang et al., 2016; Zhu et al., 2015). To the best of the



author's knowledge, Chapter 4 describes the first study that correlated carrier media physical properties and start-up using real wastewater at pilot scale.

Organic removal and nitrification start-up (for each carrier media tested) was completed in a pilot plant operated under the same organic and ammonia loading rates. COD removal start-up was faster 0.50, 0.52, 0.55 g TS/m<sup>2</sup>.day for Media 1, 2 and 3 compared with 0.36 and 0.27 g TS/m<sup>2</sup>.day in Media 4 and 5, respectively. The nitrification biofilm formation rate was also lower in the cylindrical media, 0.18 and 0.17 g TS/m<sup>2</sup>.day (Media 4 and 5) in comparison with spherical media of 0.21, 0.24 and 0.22 g TS/m<sup>2</sup>.day, Media 1, 2 and 3, respectively.

Hence the results clearly demonstrate that start-up (defined as biofilm formation rate) was faster when spherical carrier media was used in comparison with cylindrical media. The potential of spherical media to reduce start-up was attributed to the higher voidage and enhanced air and wastewater distribution leading to increased mass transfer promoting faster adhesion and biofilm growth. This outcome, can be of use as a guidance on MBBRs, SAFs and IFAS start-up. Fast biofilm formation can be considered for the upgrade and retrofit of existing WWTPs as well as in operation conditions modifications (increased flow or loading).

### **7.3 Effect of carrier media on process performance**

Previous studies on process performance have focused their attention on operation conditions such as: organic and nutrient and volumetric loading rates, carrier media filling ratios and aeration. Most of the studies relied on protected surface area as the key factor to design. So far, few studies have focused their attention on the comparison of carrier media size and shape on treatment performance. In this PhD, by fixing the carrier media filling ratio at 60%, organic and ammonia loading rates were kept constant at  $6.9 \pm 0.4$  g COD/m<sup>2</sup>.day and  $0.9 \pm 0.1$  g NH<sub>4</sub><sup>+</sup>-N/m<sup>2</sup>.day for the five media studied. Obtainable COD removals efficiencies very close to the ideal 100% were registered with all the five media tested. However, soluble BOD removal efficiencies were lower when cylindrical shape media was applied ( $70 \pm 3$ ,  $66 \pm 4\%$ , for Media 4 and 5) compared with spherical media,  $82 \pm 11$ ,  $86 \pm 5$ ,  $87 \pm 4\%$  for Media 1, 2 and 3, respectively. Regarding ammonia removal, highest efficiencies were registered with Media 3 ( $81 \pm 3\%$ ), the smaller spherical media investigated in this PhD. Larger spherical media, Media 1 and 2, registered values of  $70 \pm 11$  and  $71 \pm 10\%$ , respectively.

Cylindrical media (Media 4 and 5) registered lower ammonia removals  $42\pm 6$  and  $35\pm 12\%$ , respectively. Lower nitrification efficiencies were mainly attributed to the poor removal of easily biodegradable carbon in Cell 1. The organic loading that reached Cell 3 when pilot was operated with Media 4 and 5 was  $2.8\pm 0.9$  and  $2.9\pm 0.7$  g BOD<sub>5</sub>/m<sup>2</sup>.day, reaching C/N ratios of 2.8 and 2.7, respectively. At this load heterotrophic bacteria will compete and overgrow slow growing nitrifying bacteria. The upper regions of the biofilm was thus occupied by faster growing heterotrophic bacteria where the highest activity occurs, while nitrifiers tended to grow in the internal region of the carrier due to their slower growth rates (Boltz et al., 2011; Herrling et al., 2015). The overgrowth of heterotrophic bacteria and the increased biofilm thickness in the internal fins and ridges of the cylindrical media, in the nitrification zone (Cell 3), negatively influenced the oxygen mass transfer, substrate diffusion and utilisation by nitrifiers. Specific organic and nitrification rates confirmed the higher biofilm activity on the spherical media. Specific organic removal of  $34.8\pm 2.0$ ,  $26.9\pm 0.6$  and  $19.2\pm 1.7$  mg sCOD/g TS.h were obtained with Media 1, 2 and 3, respectively (spherical media) while  $13.4\pm 1.1$  and  $13.4\pm 0.2$  mg sCOD/g TS.h were obtained with Media 4 and 5, respectively (cylindrical media). The cylindrical media had the lowest heterotrophic activity, therefore supporting the argument for poor nitrification achieved in Cell 3. The specific nitrification rates achieved when spherical media was used were  $5.5\pm 0.9$ ,  $5.2\pm 0.3$  and  $7.2\pm 0.7$  mg NH<sub>4</sub><sup>+</sup>-N/g TS.h, with Media 1, 2 and 3, respectively. Values of  $4.9\pm 0.9$  and  $5.2\pm 0.5$  mg NH<sub>4</sub><sup>+</sup>-N/g TS.h, were measured with Media 4 and 5, respectively. However, the specific nitrification rates achieved with Media 4 and 5 were determined following loading reduction. Based on this study it is proposed that moving bed biofilm systems can be operated with mixed media to improve the overall performance and increase effluent quality. Organic removal can be improved by using spherical media in the first stages of the process (Media 1, 2 or 3), complemented with a higher protected surface area media to improve nitrification (Media 4 or 5).

#### **7.4 Boundary layer thickness, external mass transfer and carrier media**

To corroborate the results achieved in previous chapters, the influence of mixing intensity on boundary layer thickness (MTBL) and external mass transfer was tested on three different shape and size media following biofilm development (spherical, dimensionality 2.68, spherical, dimensionality 2.78 and cylindrical, dimensionality 4.27

media) (Chapter 6). Overall results concurred with previous research that external mass transfer is strongly dependent on the system hydrodynamics (Prehn et al., 2012; Wilén, Gapes and Keller, 2004). Through alteration of mixing intensities, MTBL thickness values of 71.4, 15.5 and 122.9  $\mu\text{m}$  were measured for spherical, dimensionality 2.68, spherical, dimensionality 2.78 and cylindrical, dimensionality 4.27 media, respectively at 0.21 L/L.min. Hence, the MTBL thickness was lower in spherical, dimensionality 2.78 (smaller spherical media) and higher external mass transfer coefficients were obtained with this media (9.1 m/d), compared with 6.1 and 4.4 m/day for spherical, dimensionality 2.68 and cylindrical, dimensionality 4.27 media, respectively. Hence, media voidage and shape impacted MTLB and contributed towards reducing mass transfer limitations.

## **7.5 Impact of media physical properties on moving attached growth systems**

Results achieved on the different chapters of this thesis were correlated with protected surface area, the conventional parameter used on moving attached growth system design and operation. From Chapter 3, findings suggested a moderate correlation between oxygen mass transfer efficiency and wastewater hydrodynamics with protected surface area. With HE, a correlation of,  $R^2= 0.67$ , was observed without biofilm and  $R^2= 0.76$  with biofilm. When protected surface area was correlated with SOTE a moderate correlation was achieved ( $R^2= 0.48$ ) without biofilm. However, when biofilm was developed a very high correlation was achieved between SOTE and protected surface area ( $R^2= 0.95$ ). During start-up studies results revealed correlation between protected surface area and biofilm formation rate of,  $R^2$  of 0.83 and 0.76 for COD and ammonia removal, respectively (Chapter 4). On treatment performance (Chapter 5), maximum COD utilisation rates were well correlated with carrier media protected surface area, ( $R^2= 0.88$ ) and a moderate correlation was identified with ammonia removal rate ( $R^2= 0.65$ ). A weak correlation was observed between the protected surface area and the MTBL values attained in Chapter 6 ( $R^2= 0.27$ ).

Within the aims of this PhD is the identification of other physical properties that could potentially play a role alongside carrier protected surface area. Different physical properties of the five media studied were investigated, parameters such as: diameter, length to diameter ratio (L:D), sphericity, Sauter mean diameter, shape factor and

voidage. However, due to the three-dimensional geometric shapes of the carrier media other geometric properties were used to normalise the carrier media shape. Dimensionality ( $D_i$ ) was used and was defined by Jones (2011) as the “*maximum-dimension-normalised sum*”. Dimensionality was then calculated for the 5 media studied; this was 2.68, 2.82 and 2.78 for spherical media, Media 1, 2 and 3, respectively and 4.27 and 4.50 for the cylindrical shaped media, Media 4 and 5, respectively. Besides, dimensionality other carrier media physical properties could simultaneously influence the carrier media performance. Thus, due to the importance of carrier voidage (Dupla et al., 2006) on wastewater circulation and contact with biofilm on the carrier media, a combination of parameters,  $D_i$  and voidage ( $V_{oi}$ ), were considered. A very strong association was achieved between hydraulic efficiency (HE) (Chapter 3) and  $D_i$  and  $V_{oi}$  with and without biofilm attached to the carrier media ( $R^2$  of 0.89 and 0.90) (Figure 7-1). A very strong association was also found when the same combination of physical parameters ( $D_i \times V_{oi}$ ) was used in association with HE, and correlated with oxygen mass transfer efficiency without ( $R^2= 0.92$ ). and with biofilm ( $R^2= 0.88$ ) (Chapter 3).

Along the same line of thought, pilot plant start-up results were correlated with physical parameters ( $D_i \times V_{oi}$ ) associated with HE (Chapter 4). Very strong correlations were achieved between biofilm formation rates and the association of parameters ( $D_i \times V_{oi}$ )/HE,  $R^2= 0.95$  for COD removal (Cell 1) and  $R^2= 0.92$  for ammonia removal (Cell 3). Correlation was also investigated with performance results achieved during steady state operation (Chapter 5). A strong correlation was verified when the maximum COD utilisation rate and ammonia removal rate was compared with association of parameters ( $D_i \times V_{oi}$ )/HE ( $R^2= 0.92$  for both) (Chapter 5). A stronger correlation was also observed between MTBL and ( $D_i \times V_{oi}$ )/HE ( $R^2= 0.86$ ).

Overall, strong correlations were identified between the results achieved in Chapters 3, 4, 5 and 6 of this thesis and the combination of parameter dimensionality, voidage and hydraulic efficiency. These findings support that open structure of spherical media with dimensionality of 2.68, 2.82 and 2.78 and high voidage (95, 92 and 90%) of Media 1, 2 and 3, respectively was associated with good mixing and higher hydraulic efficiencies, higher substrate and oxygen mass transfer in combination with a faster start-up and improved treatment performance (Figure 7-1). In contrast, the cylindrical shaped media with dimensionality of 4.27 and 4.50 and lower voidage 82.5 and 80%

(Media 4 and 5), was associated with poor mixing, lower hydraulic efficiencies and slower start-up. The smaller internal voids were more prone to clogging, hindering the contact between the biofilm and the effluent, thereby affecting treatment efficiencies.

Taking into consideration the results compilation (Figure 7-1) there are clear benefits when the Media had a  $(D_i \times V_{oi})/HE$  lower than 3. A sensitivity analysis was performed to analyse the effects of the individual parameters  $D_i$  and  $V_{oi}$  on a  $(D_i \times V_{oi})$ , as shown in Table 7-1 . The sensitivity analysis was performed by varying each parameter  $D_i$  and  $V_{oi}$  down in value and observing the magnitude of the changes in turn of a  $D_i \times V_{oi}$  equal to 2.4. An extrapolation of the results obtained coupled with the sensitivity analysis indicate that keeping the media spherical shape at a dimensionality between 2.4 and 3, can reduce voidage from 95% up to values of 65% (Table 7-1), without detrimental impact on the factors investigated (on oxygen mass transfer, hydraulic efficiency, biofilm attachment, process performance, substrate diffusion).

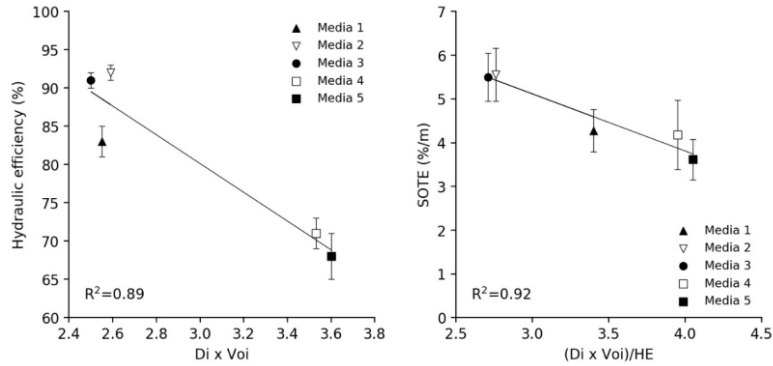
**Table 7-1 Sensitivity analysis for spherical media with a  $D_i \times V_{oi}$  of 2.4.**

		Dimensionality													
		2.4	3	2.95	2.9	2.85	2.8	2.75	2.7	2.65	2.6	2.55	2.5	2.45	2.4
Voidage	0.95	2.38	2.44	2.50	2.57	2.64	2.71	2.79	2.87	2.95	3.05	3.15	3.25	3.36	
	0.90	2.26	2.32	2.38	2.44	2.50	2.57	2.64	2.71	2.79	2.88	2.97	3.06	3.17	
	0.85	2.15	2.20	2.26	2.31	2.37	2.43	2.50	2.57	2.64	2.72	2.80	2.89	2.98	
	0.80	2.05	2.09	2.14	2.20	2.25	2.31	2.37	2.43	2.50	2.57	2.65	2.73	2.81	
	0.75	1.94	1.99	2.03	2.08	2.13	2.19	2.24	2.30	2.36	2.43	2.50	2.57	2.65	
	0.70	1.85	1.89	1.93	1.98	2.02	2.07	2.13	2.18	2.24	2.30	2.36	2.43	2.50	
	0.65	1.76	1.79	1.83	1.88	1.92	1.96	2.01	2.06	2.12	2.17	2.23	2.29	2.36	
	0.60	1.67	1.70	1.74	1.78	1.82	1.86	1.90	1.95	2.00	2.05	2.11	2.16	2.22	
	0.55	1.58	1.61	1.65	1.68	1.72	1.76	1.80	1.85	1.89	1.94	1.99	2.04	2.09	
	0.50	1.50	1.53	1.56	1.60	1.63	1.67	1.70	1.74	1.79	1.83	1.88	1.92	1.97	

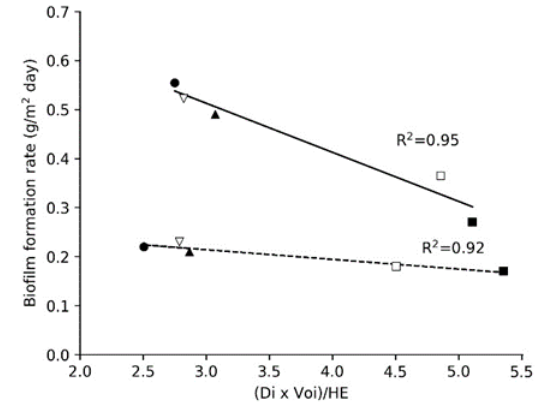
Conversely, for the cylindrical shaped carrier media investigated, the values of  $(D_i \times V_{oi})/HE$  were always higher than 3. By keeping a cylindrical shape and a dimensionality equal or lower than 3, carrier media diameter should be increased and length lowered. However, this media shape is more impacted by voidage due to the small internal voids.

From a process design and modelling standpoint, the use of media surface loading rates as the sole approach can introduce increased uncertainty for the design of full scale plants and in assumptions made during modelling simulations. From this study, suppliers and practitioners should re-evaluate the theory behind carrier media in moving attached growth systems. Removal efficiencies and biofilm activity are not proportional to carrier media protected surface area and to the quantity of biofilm attached. Other factors, such as carrier media physical properties, should be considered. This study proposed an association of parameters  $(D_i \times V_{oi})/HE$  that can be used as drivers for carrier optimisation. Thus, carrier media physical properties should be re-evaluated by manufactures together with a more realistic protected surface area, thus, contributing to both capital and operational savings and in turn a more economically viable solution.

### CHAPTER 3: MIXING AND OXYGEN MASS TRANSFER

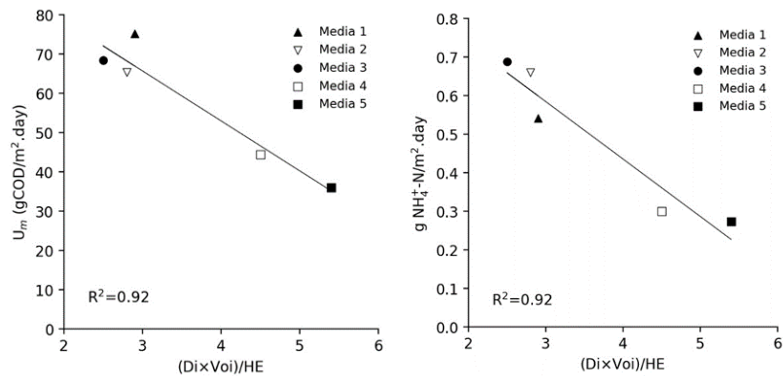


### CHAPTER 4: PROCESS START UP



Drivers for carrier optimisation

### CHAPTER 5: PROCESS PERFORMANCE



### CHAPTER 6: BOUNDARY LAYER THICKNESS

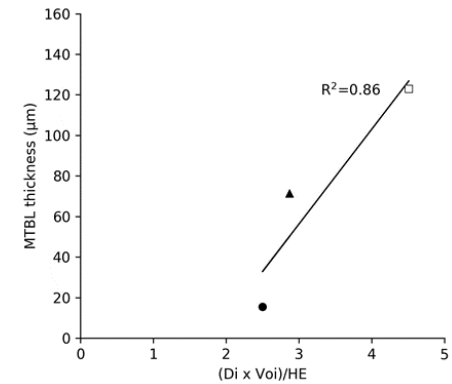


Figure 7-1 Schematic representation of the PhD main results.

## **7.6 Contribution to knowledge**

This work has furthered the understanding of the influence of carrier media physical properties on oxygen mass transfer, reactor hydrodynamics and mixing conditions that are ultimately associated with biofilm attachment rates and overall treatment performance. Table 7-2 summarises the contributions of the research to the current knowledge.



**Table 7-2 Thesis contribution to the current state of knowledge.**

	<b>What has been confirmed?</b>	<b>What has been developed?</b>	<b>What has been found which is brand new?</b>
<b>Theoretical knowledge</b>		Understanding the impact of carrier media physical properties on moving attached growth systems (all chapters).	Chapter 4 and 5 challenge current literature knowledge and commercial strategies (treatment efficiency as a function of carrier media protected surface area).
<b>Empirical evidence</b>	<p>Chapter 3 - Carrier media enhanced the overall oxygen transfer efficiency using medium bubble aeration and hydrodynamic mixing conditions.</p> <p>Chapter 3, 4, 5 and 6 – The increased biofilm thickness promotes voidage reduction (carrier media clogging) and partially penetration of the biofilm conferring a detrimental effect on reactor performance.</p>	Chapter 3, 4, 5 and 6– Understanding the impact of carrier media properties (ex.: geometry, surface area, voidage, shape, size) on: oxygen efficiency, hydrodynamic conditions, start up, performance and mass transfer in a pilot plant treating municipal wastewater.	<p>Chapter 3 - Surface area cannot fully explain oxygen transfer and hydrodynamics, and for the first time, carrier media dimensionality and voidage were identified as the controlling physical parameters.</p> <p>Chapter 4 – Biofilm formation rate is dependent on carrier media physical properties. Findings highlighted the importance of voidage and dimensionality in accelerating initial biofilm growth and maintenance thereby shortening start-up.</p>

	<b>What has been confirmed?</b>	<b>What has been developed?</b>	<b>What has been found which is brand new?</b>
	<p>Chapter 4 and 5 – The dependence of nitrification efficiency on the increase of C/N ratios on the 3<sup>rd</sup> cell.</p> <p>Chapter 6 – A clear relationship between mixing intensity and overall treatment efficiencies.</p>		<p>Chapter 5 – Challenges what is currently known in the literature; that moving attached growth systems' treatment capacity and performance is mainly a function of protected surface area.</p> <p>Chapter 5 – Spherical shape media (lower PSA) presented higher specific organic and nitrification activity in comparison with cylindrical shape media (higher PSA).</p> <p>Chapter 5 – Maximum COD removal rates (<math>U_m</math>) decreased when PSA increased.</p> <p>Chapter 5 – Strong correlation between <math>U_m</math>, ammonia removal rate and the combination of carrier media physical parameters and reactor hydrodynamics (<math>D_i \times V_{oi}</math>)/HE.</p>

	<b>What has been confirmed?</b>	<b>What has been developed?</b>	<b>What has been found which is brand new?</b>
			<p>Chapter 3, 4, 5 and 6 – Physical properties, dimensionality and voidage, should be considered when developing a new carrier media, together with hydrodynamic efficiencies, mixing and mass transfer. Opting for a carrier media with high voidage and open structure is therefore required.</p> <p>Chapter 5 – To Improve the overall treatment process moving bed attached growth systems can be operated with mixed sized Media.</p> <p>Chapter 3, 4, 5 and 6 – Based on this study and sensitivity analysis carrier media with spherical shape and a dimensionality between 2.4 and 3, is preferred. By maintaining a spherical shape, voidage can be reduced from 95% down to values of 65%.</p>

	<b>What has been confirmed?</b>	<b>What has been developed?</b>	<b>What has been found which is brand new?</b>
<b>Methodology</b>	Chapter 6 – Reliable methodology described by Nogueira et al. (2015) on the external mass transfer determination.		Chapter 4 – Biofilm formation rate can be utilised to define start-up, thus, providing guidance for design and commissioning of full scale plants.  Chapter 6 – Assess simultaneously the effect of mixing and carrier media physical properties on mass transfer boundary layer thickness.

## 7.7 References

- Bassin, J.P., Dias, I.N., Cao, S.M.S., Senra, E., Laranjeira, Y. and Dezotti, M. (2016) 'Effect of increasing organic loading rates on the performance of moving-bed biofilm reactors filled with different support media: Assessing the activity of suspended and attached biomass fractions', *Process Safety and Environmental Protection*, 100, pp. 131–141.
- Boltz, J.P., Morgenroth, E., Brockmann, D., Bott, C., Gellner, W.J. and Vanrolleghem, P.A. (2011) 'Systematic evaluation of biofilm models for engineering practice: Components and critical assumptions', *Water Science and Technology*, 64(4), pp. 930–944.
- Collignon, D. (2006) *Insight into oxygen transfer in IFAS processes*. MSc thesis. Cranfield University. Available at: <http://cclibweb-3.central.cranfield.ac.uk/handle/1826.1/2750> (Accessed: 26 August 2015).
- Dupla, M., Comeau, Y., Parent, S., Villemur, R. and Jolicoeur, M. (2006) 'Design optimization of a self-cleaning moving-bed bioreactor for seawater denitrification', *Water Research*, 40(2), pp. 249–258.
- Herrling, M.P., Guthausen, G., Wagner, M., Lackner, S. and Horn, H. (2015) 'Determining the flow regime in a biofilm carrier by means of magnetic resonance imaging', *Biotechnology and Bioengineering*, 112(5), pp. 1023–1032.
- Jenkins, D. and Wanner, J. (eds.) (2014) *Activated Sludge - 100 Years and Counting*. London: IWA Publishing.
- Jing, J.Y., Feng, J. and Li, W.Y. (2009) 'Carrier effects on oxygen mass transfer behavior in a moving bed biofilm reactor', *Asia-Pacific Journal of Chemical Engineering*, 4, pp. 618–623.
- Jones, A. (2011) 'The characterisation of irregularly-shaped particles', *Astronomy & Astrophysics*, 528(15968), p. A98.
- Mao, Y., Quan, X., Zhao, H., Zhang, Y., Chen, S., Liu, T. and Quan, W. (2017) 'Accelerated startup of moving bed biofilm process with novel electrophilic

suspended biofilm carriers', *Chemical Engineering Journal*, 315, pp. 364–372.

McQuarrie, J.P. and Boltz, J.P. (2011) 'Moving Bed Biofilm Reactor Technology: Process Applications, Design, and Performance', *Water Environment Research*, 83(6), pp. 560–575.

Nogueira, B.L., Pérez, J., van Loosdrecht, M.C.M., Secchi, A.R., Dezotti, M. and Biscaia, E.C. (2015) 'Determination of the external mass transfer coefficient and influence of mixing intensity in moving bed biofilm reactors for wastewater treatment', *Water Research*, 80, pp. 90–98.

Pham, H., Viswanathan, S. and Kelly, R.F. (2008) 'Evaluation of Plastic Carrier Media Impact on Oxygen Transfer Efficiency with Coarse and Fine Bubble Diffusers', *WEFTEC 2008*. New Orleans: Water Environment Federation, p. 5069–5079.

Prehn, J., Waul, C.K., Pedersen, L.F. and Arvin, E. (2012) 'Impact of water boundary layer diffusion on the nitrification rate of submerged biofilter elements from a recirculating aquaculture system', *Water Research*, 46(11), pp. 3516–3524.

Sander, S., Behnisch, J. and Wagner, M. (2017) 'Energy, cost and design aspects of coarse and fine bubble aeration systems in the MBBR IFAS process', *Water Science and Technology*, 75(4), pp. 890–897.

Tang, B., Yu, C., Bin, L., Zhao, Y., Feng, X., Huang, S., Fu, F., Ding, J., Chen, C., Li, P. and Chen, Q. (2016) 'Essential factors of an integrated moving bed biofilm reactor-membrane bioreactor: Adhesion characteristics and microbial community of the biofilm', *Bioresource Technology*, 211, pp. 574–583.

Tang, B., Zhao, Y., Bin, L., Huang, S. and Fu, F. (2017) 'Variation of the characteristics of biofilm on the semi-suspended bio-carrier produced by a 3D printing technique: Investigation of a whole growing cycle', *Bioresource Technology*, 244, pp. 40–47.

Wilén, B.M., Gapes, D. and Keller, J. (2004) 'Determination of external and internal mass transfer limitation in nitrifying microbial aggregates', *Biotechnology*

*and Bioengineering*, 86(4), pp. 445–457.

Zhu, Y., Zhang, Y., Ren, H. qiang, Geng, J. ju, Xu, K., Huang, H. and Ding, L. li (2015) 'Physicochemical characteristics and microbial community evolution of biofilms during the start-up period in a moving bed biofilm reactor', *Bioresource Technology*, 180, pp. 345–351.





## 8 CONCLUSIONS

The conclusions are presented in line with the objectives of this thesis:

**Objective 1:** Review scientific literature on the different carrier media designs used at full-scale, pilot-scale and lab-scale studies in moving attached growth systems. Identify the role of carrier shape, size and material surface physical and chemical properties on microorganisms' adhesion, growth and biofilm activity.

- The characteristics of the surface material of the carrier media are vital for the development of the biofilm in it.
- Surface modification, such as an increase in roughness confers protection on the biofilm against shear stresses that cause detachment.
- Protected surface carrier correction appears to be an important factor to consider, with special significance for higher PSA carriers that tend to have smaller internal voids.
- Carrier functionality represents an important parameter; thus, carriers should be linked with treatment application as a way to create distinctive zones for specific biofilm formation and stratification.

**Objective 2:** Identify the key carrier media physical properties that impact oxygen mass transfer and hydraulic efficiency in a moving attached growth system through an understanding of gas-liquid mass transfer, flow hydrodynamics and mixing characteristics with and without biofilm.

- Media enhanced the overall oxygen transfer efficiency by 23-45% and hydraulic efficiency (HE) by 41-53%, compared with operation with no media in clean water tests.
- Spherical media (Media 1, 2 and 3), in the presence of biofilm increased the HE by 89, 93 and 100%, respectively. Conversely, cylindrical media (Media 4 and 5) contributed to a reduction in HE by 74 and 63%, respectively.

- The parameter traditionally selected to design biofilm processes, did not correlate with HE or with oxygen mass transfer efficiency in clean water tests.
- A strong correlation between mixing and media dimensionality and voidage ( $D_i \times V_{oi}$ ) was obtained without and with biofilm ( $R^2$  0.89 and 0.90).
- Carrier media dimensionality and voidage associated with HE ( $(D_i \times V_{oi})/HE$ ) correlated with oxygen mass transfer without and with biofilm (without,  $R^2$  0.92 and with  $R^2$  0.88).
- The combination of parameters: Dimensionality and voidage can potentially be used to improve mixing and oxygen mass transfer contributing to energy savings and higher removal efficiencies.

**Objective 3:** Understand how carrier media physical properties can accelerate bacteria adhesion and biofilm formation rates during wastewater treatment in a moving attached growth system and how they can also influence subsequent reactor performance towards delivering improved effluent quality.

- Carrier media with spherical and lower protected surface area achieved shorter chemical oxygen demand (COD) removal start-up (18, 15 and 17 days for Media 1, 2 and 3), compared to 23 and 24 days required by the cylindrical and high surface area media (Media 4 and 5).
- Ammonia removal start-up was also shorter for Media 1, 2 and 3 (30, 22 and 17 days) when compared with Media 4 and 5 (46 and 47 days).
- During the last days of start-up, the obtainable COD removal efficiencies achieved were similar for all the media ( $88 \pm 4$ ,  $81 \pm 4$ ,  $85 \pm 3$ ,  $80 \pm 3$  and  $86 \pm 4\%$  for Media 1 to 5).
- Media 1, 2 and 3 (spherical media) achieved ammonia removal efficiencies of  $50 \pm 13$ ,  $64 \pm 13$ ,  $63 \pm 7\%$  and Media 4 and 5 (cylindrical media) removal efficiencies of  $32 \pm 17$  and  $34 \pm 5\%$  by the end of start-up.

- A good correlation was observed between protected surface area and biofilm formation rate for COD and ammonia removal ( $R^2$  of 0.83 and 0.76).
- A combination of physical factors, dimensionality ( $D_i$ ) and voidage ( $V_{oi}$ ), and hydraulic efficiency (HE),  $(D_i \times V_{oi})/HE$ , was strongly associated with biofilm formation rates ( $R^2= 0.95$  and  $0.92$ ).
- Physical properties can contribute to enhance biofilm formation, shortening the start-up, contributing to improved removal rates and fast commissioning of the moving attached growth system process.

**Objective 4:** Measure the influence of the carrier media physical properties on organic carbon removal and nitrification through the investigation of biofilm activity and substrate utilisation rates.

- Average obtainable COD removal efficiency was similar for the 5 medias studied,  $89\pm 3$ ,  $86\pm 2$ ,  $86\pm 3$ ,  $85\pm 4$  and  $86\pm 2\%$ , for Media 1, 2, 3, 4 and 5, respectively.
- Ammonia removal was higher for the spherical media, achieving values of  $70\pm 11$ ,  $71\pm 10$  and  $81\pm 3\%$  (Media 1, 2 and 3) compared with the cylindrical media that reached  $42\pm 6$  and  $35\pm 12\%$  (Media 4 and 5).
- Heterotrophic and nitrifiers activity tests demonstrated that Media 1 achieved the highest organic removals ( $34.8\pm 2.0$  mg sCOD/g TS.h), and the smaller spherical shape, Media 3, achieved the highest nitrification removals ( $7.2\pm 0.7$  mg  $NH_4^+-N$ /g TS.h).
- The maximum COD utilisation rates ( $U_m$ ) correlated well with carrier media protected surface area, ( $R^2= 0.88$ ) but a stronger correlation was obtained between  $U_m$  and carrier media physical properties associated with hydraulic efficiency  $(D_i \times V_{oi})/HE$  ( $R^2=0.92$ ).
- Correlation between ammonia removal rate and protected surface area was weak ( $R^2= 0.65$ ) when compared with correlation obtained with the media physical properties  $(D_i \times V_{oi})/HE$  ( $R^2= 0.92$ ).

- These findings clearly demonstrate, that beside carrier protected surface area, physical parameters such as dimensionality and voidage, play a key role on moving attached growth systems design and carrier media selection, towards achieving high reactor performance and effluent quality.

**Objective 5:** Measure the boundary layer thickness to understand the impact of carrier media with different physical properties on biofilm mass transfer limitations, further influencing substrate availability and removal.

- The MTBL thickness was found to be lower in the spherical, dimensionality 2.78 media (smaller spherical media and PSA of 220 m<sup>2</sup>/m<sup>3</sup>), varying between 15.5-129.6 μm whereas spherical, dimensionality 2.68 media (bigger smaller spherical media and PSA of 112 m<sup>2</sup>/m<sup>3</sup>) and cylindrical, dimensionality 4.27 media (cylindrical shape media and PSA of 348 m<sup>2</sup>/m<sup>3</sup>) presented values of 28.6-172.4 and 39.7-170.5 μm, respectively.
- External mass transfer coefficients ranged from 1.0-6.1, 1.3-9.1 and 1.0-4.4 m/day for the spherical, dimensionality 2.68, spherical, dimensionality 2.78 and cylindrical, dimensionality 4.27 media, respectively.
- A poor correlation was observed between protected surface area and MTBL thickness (R<sup>2</sup> 0.27). A stronger correlation was achieved comparing carrier media physical properties: dimensionality (Di) and voidage (Voi) with MTBL thickness (R<sup>2</sup> 0.86).
- Studying the potential of carrier media physical properties can provide opportunities for capital and operational cost savings making the moving attached growth systems process more competitive and attractive than other alternative processes.

## 9 FUTURE WORK

Based on this PhD thesis, the following research efforts should be put within:

- Investigate the impact of carrier media on oxygen mass transfer in clean water using higher tank depth supported with bubble visualisation experiments.
- Further work is required to optimise off-gas monitoring. Analyses were undertaken on a pilot plant and measurements were very sensitive, even if equipment was constantly checked.
- Investigate reactor hydrodynamics and carrier movement at different filling ratios.
- Develop and test new carriers with spherical shape considering dimensionality and voidage and compare with conventional carriers.
- Investigate media performance in biological nutrient removal, e.g. anammox and phosphorus accumulating organisms (PAO) where mass transport limitations are of benefit. This is to create different microbial activity layers within the biofilm permitting different biochemical processes (aerobic, anoxic or anaerobic processes). Investigate media performance on micropollutants removal.
- Create a simple mathematical model using the experimental data including: carrier physical properties (dimensionality and voidage), protected surface, biofilm attached to the carrier media, biofilm thickness and mass transport boundary layer thickness.

## APPENDICES

### Appendix A Correlation between SOTE and HE (with and without biofilm growth) with different carrier media physical properties

Table A-1 Correlation between SOTE and HE (with and without biofilm growth) with different carrier media physical properties.

	Without biofilm growth		With biofilm growth	
	SOTE (%/m)	HE (%)	$\alpha$ SOTE (%/m)	HE (%)
Weight	0.54	0.79	0.88	0.83
Diameter (D)	0.16	0.45	0.86	0.47
Length (L)	0.27	0.59	0.86	0.56
Voidage (Voi)	0.38	0.70	0.85	0.74
Number of carriers (N)	0.53	0.59	0.77	0.75
$(V_{\text{media}}/V_{\text{oi}}) \times N$	0.41	0.73	0.85	0.75
$1/(V_{\text{media}}/V_{\text{oi}})$	0.51	0.77	0.89	0.52
L/D	0.77	0.80	0.14	0.57
$(L/D) \times V_{\text{oi}}$	0.76	0.80	0.41	0.80
Total surface area (TSA)	0.49	0.67	0.91	0.80
Protected surface area (PSA)	0.48	0.67	0.93	0.76
1/D	0.54	0.74	0.89	0.83
Sphericity ( $\phi$ )	0.65	0.76	0.13	0.55
$(TSA_{\text{media}}/N) \times V_{\text{oi}}$	0.11	0.38	0.82	0.36
$(PSA_{\text{media}}/N) \times V_{\text{oi}}$	0.06	0.30	0.82	0.30
Hydraulic diameter ( $D_H$ )	0.16	0.44	0.81	0.45
Volume equivalent diameter ( $d_v$ )	0.19	0.49	0.86	0.77
Sauter mean diameter ( $d_{sv}$ )	0.20	0.50	0.86	0.51
Shape factor ( $\psi$ )	0.65	0.76	0.13	0.55
Dimensionality ( $D_i$ )	0.57	0.87	0.09	0.62
$D_i \times V_{\text{oi}}$	0.61	0.89	0.69	0.90

	Without biofilm growth		With biofilm growth	
	SOTE (%/m)	HE (%)	$\alpha$ SOTE (%/m)	HE (%)
<b>Di x Voi x HE</b>	0.28		0.60	
<b>(Di x Voi)/HE</b>	0.92		0.88	
<b>(Di/Voi) x HE</b>	0.39		0.14	

D - diameter, L – length, Voi – voidage, N - number of carriers,  $V_{media}$  – carrier media volume, TSA - total surface area, PSA - protected surface area,  $\phi$  – sphericity,  $D_H$  – hydraulic diameter,  $d_v$  - volume equivalent diameter,  $d_{sv}$  - Sauter mean diameter,  $\psi$  – shape factor Di – dimensionality, HE – hydraulic efficiency.

Hydraulic diameter

$$D_H = (4 \cdot Voi \cdot V) / (PSA \cdot V) \quad (\text{A-1})$$

Volume equivalent diameter:

$$d_v = (3/2 D^2 \cdot L)^{1/3} \quad (\text{A-2})$$

Sphericity

$$\phi = d_v^2 / (0.5 D^2 + D \cdot L) \quad (\text{A-3})$$

Sauter mean diameter ( $d_{sv}$ )

$$d_{sv} = d_v \cdot \phi \quad (\text{A-4})$$

Shape factor

$$\psi = (1/36 \cdot \pi) \cdot (d_{sv}/D) \quad (\text{A-5})$$

Dimensionality sphere

$$Di = (L_x + L_y + L_z) / \max(L_x, L_y, L_z) \quad (\text{A-6})$$

Dimensionality cylinder

$$Di = 1 + (4 \cdot r \cdot L / [2r^2 + L^2]) + \left( 2r / \left[ \sqrt{4r^2 + L^2} \right] \right) \quad (\text{A-7})$$

r - radius





## Appendix B Correlation between rate of biofilm with different carrier media physical properties during COD and ammonia removal start-up

Table B-1 Correlation between rate of biofilm with different carrier media physical properties during COD and ammonia removal start-up

	Start-up	
	COD removal	Ammonia removal
Weight	0.73	0.81
Diameter (D)	0.47	0.49
Length (L)	0.59	0.64
Voidage (Voi)	0.71	0.71
Number of carriers (N)	0.49	0.59
$(V_{\text{media}}/V_{\text{oi}}) \times N$	0.73	0.73
$1/(V_{\text{media}}/V_{\text{oi}})$	0.72	0.78
L/D	0.76	0.77
$(L/D) \times \text{Voi}$	0.91	0.90
Total surface area (TSA)	0.65	0.73
Protected surface area (PSA)	0.61	0.75
1/D	0.67	0.78
Sphericity ( $\phi$ )	0.78	0.71
$(TSA_{\text{media}}/N) \times \text{Voi}$	0.39	0.45
$(PSA_{\text{media}}/N) \times \text{Voi}$	0.40	0.42
Hydraulic diameter ( $D_H$ )	0.38	0.38
Volume equivalent diameter ( $d_v$ )	0.51	0.54
Sauter mean diameter ( $d_{sv}$ )	0.52	0.55
Shape factor ( $\psi$ )	0.78	0.71
Dimensionality ( $D_i$ )	0.90	0.83
$D_i \times \text{Voi}$	0.94	0.90
$D_i \times \text{Voi} \times \text{HE}$	0.04	0.04

<b>Start-up</b>		
	<b>COD removal</b>	<b>Ammonia removal</b>
<b>(Di x Voi)/HE</b>	0.96	0.92
<b>(Di/Voi) x HE</b>	0.81	0.82

D - diameter, L – length, Voi – voidage, N - number of carriers,  $V_{media}$  – carrier media volume, TSA - total surface area, PSA - protected surface area,  $\phi$  – sphericity,  $D_H$  – hydraulic diameter,  $d_v$  - volume equivalent diameter,  $d_{sv}$  - Sauter mean diameter,  $\psi$  – shape factor Di – dimensionality, HE – hydraulic efficiency.

## Appendix C Correlation between $U_m$ and ammonia removal rate with different carrier media physical properties.

Table C-1 Correlation between  $U_m$  and ammonia removal rate with different carrier media physical properties.

	Performance	
	COD removal	Ammonia removal
Weight	0.93	0.76
Diameter (D)	0.84	0.45
Length (L)	0.87	0.58
Voidage (Voi)	0.96	0.70
Number of carriers (N)	0.70	0.55
$(V_{media}/Voi) \times N$	0.97	0.30
$1/(V_{media}/Voi)$	0.94	0.75
L/D	0.35	0.78
$(L/D) \times Voi$	0.66	0.93
Total surface area (TSA)	0.92	0.69
Protected surface area (PSA)	0.87	0.65
1/D	0.90	0.72
Sphericity ( $\phi$ )	0.38	0.77
$(TSA_{media}/N) \times Voi$	0.74	0.38
$(PSA_{media}/N) \times Voi$	0.75	0.30
Hydraulic diameter ( $D_H$ )	0.78	0.35
Volume equivalent diameter ( $d_v$ )	0.85	0.49
Sauter mean diameter ( $d_{sv}$ )	0.86	0.50
Shape factor ( $\psi$ )	0.38	0.77
Dimensionality (Di)	0.96	0.72
Di x Voi	0.93	0.84
Di x Voi x HE	0.14	0.26

<b>Performance</b>		
	<b>COD removal</b>	<b>Ammonia removal</b>
<b>(Di x Voi)/HE</b>	0.91	0.92
<b>(Di/Voi) x HE</b>	0.85	0.82

D - diameter, L – length, Voi – voidage, N - number of carriers,  $V_{media}$  – carrier media volume, TSA - total surface area, PSA - protected surface area,  $\phi$  – sphericity,  $D_H$  – hydraulic diameter,  $d_v$  - volume equivalent diameter,  $d_{SV}$  - Sauter mean diameter,  $\psi$  – shape factor Di – dimensionality, HE – hydraulic efficiency.

## Appendix D Correlation between MTBL thickness and media physical properties.

Table D-1 Correlation between MTBL thickness and physical properties.

	<b>MTBL thickness</b>
<b>Weight</b>	0.44
<b>Diameter (D)</b>	0.09
<b>Length (L)</b>	0.17
<b>Voidage (Voi)</b>	0.33
<b>Number of carriers (N)</b>	0.65
<b>(V<sub>media</sub>/Voi) x N</b>	0.36
<b>1/(V<sub>media</sub>/Voi)</b>	0.40
<b>Total surface area (TSA)</b>	0.35
<b>Protected surface area (PSA)</b>	0.27
<b>1/D</b>	0.44
<b>Sphericity (φ)</b>	0.99
<b>(TSA<sub>media</sub>/N) x Voi</b>	0.05
<b>(PSA<sub>media</sub>/N) x Voi</b>	0.05
<b>Hydraulic diameter (D<sub>H</sub>)</b>	0.05
<b>Volume equivalent diameter (d<sub>v</sub>)</b>	0.11
<b>Sauter mean diameter (d<sub>sv</sub>)</b>	0.12
<b>Shape factor (ψ)</b>	0.99
<b>Dimensionality (Di)</b>	0.76
<b>Di x Voi</b>	0.76
<b>Di x Voi x HE</b>	0.07
<b>(Di x Voi)/HE</b>	0.86
<b>(Di/Voi) x HE</b>	0.74

D - diameter, L – length, Voi – voidage, N - number of carriers, V<sub>media</sub> – carrier media volume, TSA - total surface area, PSA - protected surface area, φ – sphericity, D<sub>H</sub> – hydraulic diameter, d<sub>v</sub> - volume equivalent diameter, d<sub>sv</sub> - Sauter mean diameter, ψ – shape factor Di – dimensionality, HE – hydraulic efficiency.